Examination of cytotoxicity of *Crotalus adamanteus* and *Crotalus scutulatus scutulatus* venom on human skin melanoma and ovarian carcinoma cell lines.

A thesis submitted to the Faculty of Science of the University of Strathclyde in fulfilment of the requirements for the degree of PhD.

By

Sajjad Khan

2016

Strathclyde Institute of Pharmacy and Biomedical Sciences

The John Arbuthnott Building University

of Strathclyde

27 Taylor Street

Glasgow, G4 0NR.

Copyright

Dedication

To my dear Dad and sweet mum....

i

Acknowledgement

I am truly grateful to my supervisors, Dr. Edward Rowan and Valerie Ferro, for their guidance, support and patience. They both have been flawless mentors. Eddie has always been very kind to me and has always encouraged me to come up new ideas. I cannot thank Val enough for her eternal support and for always been there for me when I felt totally dishearted. I really appreciate her bearing with all those emergency meetings and round the clock emails.

I also owe thanks to Louise Young, Dr. Dima Semaan, Dr. Rothwell Rate, Dr. Sukrut Somani, Dr. Ed Chan for helping me out with my project from time to time.

I am thankful to Abdul Wali Khan University Mardan, Pakistan, for financing my studies which gave me a great opportunity to come to University of Strathclyde, to work with fine researchers in this amazing research environment.

My family, including my brothers, sisters and my uncle, Sohail Khan, is the best family to have. Regardless of the distance, they have been here with me to make sure I was ok and help me get through difficult situations.

My office-mates and friends, Majid, Noor, Roua, Joan, Ibtisam, Louise and Rubab provided me with a very nice office environment and good laughs to feel fresh and release all the stress at the end of the day. Also, thanks to Dr. Laura Hutchison for making the lab such a fun place to work with all the laughter and songs.

There are few people whom I feel blessed to know and proudly call them my dear friends. They have always been there for me when I was feeling low and would hear out me problems and, at least, pretend to care. So thanks a lot Sukrut, Serge and Molly. You guys have been a great sport.

Abstract

Cancer is global health problem that is responsible for the highest number of human mortalities worldwide. Cancers originates from aberrations in genes that are responsible for maintaining tissue homeostasis. These genetic aberrations render some unique qualities to cancer cells, such as uncontrolled proliferation, apoptosis evasion, angiogenesis, insensitivity to growth signals and metastasis to other parts of the body, which make the condition challenging for the current medical practices. Efforts for eradication of cancer have been made since the dawn of civilisation and have resulted in some promising outcomes such as complete cure of a few types of cancer, improvement in patient's quality of life and increasing survival rates but the adverse effects associated with cancer treatment are mostly life threatening in the form of initiation of other tumours, effects on the vital body organs and anxiety. In order to introduce better treatment options in terms of less adverse effects, cost effectiveness and cancer specificity, the pursuit of a satisfactory cancer cure is still ongoing. Nature has always been a source of some important remedies such as antimalarial, antibiotics and neuromuscular agents which were used to successfully cope with contemporary health challenges and that is why scientists have always turned to nature to find answers to the existing medical problems. Snakes have held a fascination for mankind since early civilisation, probably because they are responsible for substantial mortality and morbidity around the world. Snake venom mainly comprises of a cocktail of a large number of enzymatic and nonenzymatic proteins,

which affect the vital physiological systems. Due to their biological consequences, efforts are being made to translate snake venom toxins into potential therapeutics for various medical conditions. Since the emergence of captopril, the classic example of a venom based drug, various components of the venom have been isolated, identified, characterised and their associated pharmacology is established and have been used a platform for development of pro/anti-coagulants, analgesics and anti-cancer entities. In addition to other enzymes, L-amino acid oxidases (LAAO) are present in significant amounts in snake venom. They are a group of flavoenzymes, known to catalyse oxidative deamination of L-amino acid substrates, in order to form α-keto acids, hydrogen peroxide and ammonia.

The aim of this study was to evaluate the cytotoxic effects of *Crotalas adamanteus* (Cad) and *Crotalus scutulatus scutulatus* (Css) snake venom on a human skin melanoma cell line (A375) and human ovarian cancer cell line and to establish the mode of cell death along with isolation and identification the active components. In order to determine the enzymatic activity of the whole venom, substrate solution containing 250 µM L-leucine (L-Leu) was incubated with 20 µg/mL of Cad and Css whole venom for 4 hours (h) at 37 °C. Both the venom samples were then fractionated using size exclusion chromatography and the fractions were lyophilised. Fractionation resulted in 5 peaks from each venom. As previously reported, LAAO are inactivated under high pH or low temperature as consequence of conformational changes in prosthetic group of the enzyme. Therefore, the

fractions obtained were heated at pH 5 for 30 minutes (min) for reactivation and the enzyme activity assay was repeated to identify the fraction containing LAAO. Fraction 1 from Cad, called as Cad F1, whereas, fraction 2 of Css whole venom (Css F2) showed LAAO activity which indicated by the significant (P=0.005) metabolism of L-Leu. Cad F1 and Css F2 were further fractionated using cation exchange chromatography (CEC), producing 4 and 6 peaks, respectively. The reactivation step and LAAO activity assay were repeated to identify the LAAO in both the separated fractions. Sodium dodecyl sulphatepolyacrylamide gel electrophoresis (SDS-PAGE) was used to establish the purity and estimate the molecular weights (MW) of the purified enzymes. The presence of single band on the gel, after SDS-PAGE, indicated the purity of the extracted components. LAAO purified from Cad was designates as Lcad and had MW of 75 kDa, and the LAAO purified from Css had MW of 50 kDa and was designated as

CsL. MW determined for Lcad and CsL are similar to MW reported for LAAO of Cad and Css by other researchers. Michaelis-Menten equation used to determine the maximum velocity of the reaction (v_{max}) and Michaelis-Menten constant (K_M) which shows the substrate turn over for the enzymes. v_{max} for Cad (0.8911±.023 $\mu M.min^{-1}.mg^{-1}$), Cad F1 (0.8163±0.026 $\mu M.min^{-1}.mg^{-1}$) and Lcad (0.7897±0.023 $\mu M.min^{-1}.mg^{-1}$) showed a gradual decrease which was also observed in K_M values for Cad (137.7±19.9 µM), Cad F1 (124.2±19.19.1µM) and Lcad (131.4±20.7 µM). Similarly, decrease in v_{max} values which were 0.9630±0.034, 0.7841±0.018,

0.07051±0.011 µM.min^{-1}.mg^{-1} for Css, Css F2 and CsL, respectively, and K_M values (221±31.1, 204.6±18.8 and 210.8±13.2 µM for Css, Css F2 and CsL, respectively) was also observed. These observations referred to the fact that LAAO partially and gradually lose their enzymatic activity when reactivated after every

lyophilisation step.

LAAO are of great interest in pharmacological research because of their reputed therapeutic properties, including apoptotic-inducing activities. The mechanism underlying the cytotoxicity has been mainly attributed to reactive oxygen species (ROS) production, which culminates in apoptosis via either caspase-dependent or apoptosis inducing factor (AIF) pathway. In order to confirm the cytotoxicity of Lcad/CsL and further elaborate on pharmacology underlying their cytotoxicity induced in human melanoma (A375) and human ovarian carcinoma (A2780) cell lines, several cell bases assays were carried out. For this purpose, cells of both cell lines were incubated with 20 µg/mL of Lcad and CsL at 37 °C for 4 h. Cell viability was measured by using CellTiter Blue® assay by incubating the cells treated with 0.15-20 µg/mL Lcad/CsL for 4 hours (h) with the dye at 37 °C and measuring the fluorescence at excitation/emisstion (ex/em) 560/590 nm. The potency of the separated proteins was determined by treating the cells with 0.15-20 µg/mL of cisplatin for 4 h at 37 °C. The cancer specificity of Lcad and CsL was established by incubating human non-cancer epithelial cell line (PNT2a) at 37 °C with 0.15-20 µg/mL of Lcad and CsL for 4 h. Morphological changes in the cells after Lcad/CsL

treatment were observed under light upright microscope using 40X objective lens. Autophagy was evaluated by measuring the increase in acidic vesicular organelles (AVOs) by staining the Lcad/CsL treated cells with 100 µg/mL acridine orange (AO) and measuring the fluorescence at (ex/em) 490/650 nm with a microplate reader. Necrosis was evaluated by observing the morphological changes in the cells after Lcad/CsL treatment and, also, effect of the specific necrosis inhibitor, IM-54, on the cell death of by incubating cells with 10 µM of IM-54 prior to treating the cells with Lcad and CsL. Role of reactive oxygen species (ROS) was also investigated. In order to confirm the extracellular generation of ROS, the catalytic effect of Lcad and CsL on the growth medium Lamino acids was determine with/without additional L-Leu. Intracellular ROS production was measured with the help of cell permeant ROS stain 2,7dichlorodihydrofluorescein diacetate (DCDHF) (10 µM). To establish whether cell death pathway initiated by Lcad/CsL proceeded through mitochondria, the effect of Lcad and CsL on the mitochondrial metabolic function and outer mitochondria membrane (OMM) integrity were determined. Mitochondrial function was determined by incubated the cells with 20 % (v/v) 3-(4,5-dimethylthiazol-2-yl)2,5-diphenyltetrazolium bromide (MTT) and measuring the absorbance at 560 nm. Tetramethylerhodamine ethyl ester (TMRE), to a final concentration 500 nm was incubated with the cells after Lcad/CsL treatment and the fluorescence was measured (ex/em: 545/590). Fluorescent substrate assay for caspase-3/7 was exploited to establish the activation of the effector caspases-3/7 in response to mitochondrial signalling. In order to have insight into the molecular

mechanisms involved in the progression of cell death in response to Lcad and CsL treatment, western blotting was used to confirm the activation of caspase-8, Bid, apoptosis inducing factor (AIF) and poly-(ADP ribose)-polymerase (PARP).

The cell viability assays showed that Lcad is cytotoxic as indicated by IC_{50} values 1.1±0.1 µg/mL and 1.95±0.2 µg/mL of Lcad on A375 and A2780 cell lines, respectively. Similarly, CsL cytotoxicity is denoted by the IC_{50} values of 2.46±0.2 µg/mL and 3.6±0.6 µg/mL on A375 and A2780, respectively. Cisplatin did not show any cytotoxic effect on both cancer cell lines after 4 h of incubation whereas Lcad and CsL did not affect the viability of PNT2a cells. Compared with the negative control, no significant increase in the increase of AO was observed which implied that intracellular acidity did not increase and there was basal level of AVOs. IM-54 did not delay cell death in the cells incubated with Lcad and CsL which proved that necrotic pathways were not activated by Lcad/CsL which is also supported by the loss in cellular volume rather than fragmentation of the treated cells, a hallmark of apoptosis. In addition, no extracellular or intracellular ROS generation was observed. Although there was significant ($P<0.05$) reduction in the mitochondrial metabolic activity was shown compared with the negative control, mitochondria were not uncoupled. The fluorescent substrate assay established that effector caspase-3/7 were not activated, suggesting that cell induced by Lcad/CsL is independent of effector caspases. Western blot confirmed the activation of caspase-8, translocation of Bid to mitochondria, translocation of AIF to nucleus and activation of PARP.

This study concluded that Lcad/CsL are highly cytotoxic to human melanoma and human ovarian cancer cells lines, and are more potent than cisplatin. Lcad and CsL seem to be cancer-selective as inferred by the lack of cytotoxicity on PNT2a cell lines. It was established Lcad/CsL activate apoptotic pathway which is executed in caspase-independent way. It would appear that Lcad/CsL activates caspase-8, which was supposedly via activation of cell death receptors as there was no ROS production. Activated caspase-8 in turn signalled the translocation of Bid to mitochondria which resulted in the translocation of AIF to nucleus. However, mitochondria were not uncoupled in order for AIF to be released. The translocated AIF activates PARP, an enzyme responsible for DNA damage during cell death.

The ROS-independent cell death and release of AIF without affecting the mitochondrial membrane integrity are rarely reported facts for snake venom LAAO which needs further investigation to understand variability of mechanism of action of LAAO from different resources which could be exploited in future for medical uses.

List of abbreviations

Ach	acetylcholine
AchE	acetylcholine esterase
AEC	anion-exchange chromatography
AIF	apoptosis inducing factor
AO	acridine orange
Apaf-1	apoptosis activating factor-1
Atg	autophagy-related genes
AVO	acidic vesicular organelles
BSA	bovine serum albumin
Cad	*Crotalus adamanteus*
CDK	cyclin-dependent kinase
CEC	cation-exchange chromatography
cm	centimetre
conc	concentration
CsL *scutulatus*	L-amino acid oxidases extracted from *Crotalus scutulatus*
Css	*Crotalus scutulatus scutulatus*
Cyt.C	cytochrome c
DID	death inducing domain
DMSO	dimethyl sulfoxide
DNA	deoxyribonucleic acid
ER	endoplasmic reticulum
et al	and others

ex/em:	excitation/emission
FADD	Fas associated death domain
Fas	first apoptotic signals
h	hours
IEC	ion- exchange chromatography
IM-54	indolylmaleimide-54
JNK	c-Jun N-terminal kinase 1
kDa	kilo Daltons
Lcad	LAAO extracted from Cad
L-Ile	L-isoleucine
L-Leu	L-leucine
L-Met	L-methionine
L-Phe	L-phenylalanine
LPS	lipopolysaccharide
M	Molar
mg	milligram
min	minutes
mL	millilitre
mm	millimetre
mM	millimolar
MMP	mitochondrial membrane potential
MTT	3-(4,5-dimethylthiazol-2-yl)-2,5-diphenyltetrazolium bromide
NADPH	nicotinamide adenine dinucleotide phosphate
NEMO	Nk-Kβ essential modulator

Nox	NADPH oxidase
OMMP	outer mitochondrial membrane potential
OPD	o-phenylenediamine dihydrochloride
PARP	poly-(ADP ribose)-polymerase
PBS	phosphate buffer saline
RIP	Receptor interacting protein
ROS	reactive oxygen species
SDS-PAGE	Sodium dodecyl sulphate-polyacrylamide gel electrophoresis
SEC	size-exclusion chromatography
SV40	Simian virus 40 T antigen
SVMP	snake venom metalloproteinases
TGF-β	transforming growth factor-beta
TNF	tissue necrosis factor
TRAIL	TNF-related apoptosis inducing ligand
TRL-3	Toll-like receptor-3
UK	United Kingdom
USA	United States of America
VEGF	vascular endothelial growth factor
WHO	World Health Organisation

Contents

2. Isolation, identification and characterisation of the active component from whole venom

List of Figures

List of Tables

1. Introduction

1.1 Cancer: a global challenge

Cancer is a major health challenge in every part of the world and is the leading cause of death worldwide (Seigal *et al*., 2014). It is responsible for one in four deaths in the United States (American Cancer Society, 2014) and United Kingdom (Cancer Research, UK). Facts and concepts regarding the mortality/morbidity rates and prevalence of this lethal disease have changed over time. Until recently, cancer was considered to be second to cardiovascular diseases in causing the highest number of deaths (WHO, 2008), but according to the latest World Health Organization (WHO) report, cancer is now responsible for more deaths than any other disease globally (Ferlay *et al*., 2015). Previously, it was reported to be more common in developed countries rather than the developing countries; westernised lifestyle (poor food, smoking, physical inactivity and industrial exposure) being the main reason given for this difference in prevalence (Jemal *et al*., 2011; Kanavos, 2006). However, according to recent studies, cancer is now a universal disease, equally common in all parts of the world regardless of the socio-economic status of the residing population, mainly because of the overwhelming westernised life style throughout the world (Torre *et al*., 2015; Ferlay *et al*., 2015). The role of life style in the causation of cancer was affirmed by studying the frequency of cancer in migrated communities in the western world (Jemal *et al*., 2010).

Despite advancement in health technologies, statistics, related to cancer incidence and number of death produced in the last 15 years, reveal the seriousness of this challenge (Figure 1.1). In 2000, 10.1 million new cases of cancer and 6.1 million deaths

were estimated worldwide (Parkin, 2001). These figures rose to 10.9 and 6.7 for incidence and mortality, respectively, in the following two years (Parkin *et al*., 2005). Cancer incidence was projected to be almost 14 million in the year 2006, however, the number of cancer related deaths reduced to 5.7 million (Jemal *et al*., 2006). In the following couple of years, 14.34 million cases of cancer were diagnosed, reflecting a decrease in the progression of the disease whereas the death toll remained at 5.67 million, the same as 2006 (Jemal *et al*., 2008). In 2008, 12.7 million cancer cases were detected causing 7.6 deaths worldwide, with 56 % of morbidity and 64 % mortality taking in economically developing countries (Jemal *et al*., 2011). As it takes 3-4 years for the data to be collected and compiled, the last cancer statistics available is for the year 2012 (Seigel *et al*., 2012). For the year 2012, 14.1 million incidences and 8.1 million deaths were estimated to have occurred worldwide (Ferlay *et al*., 2015).

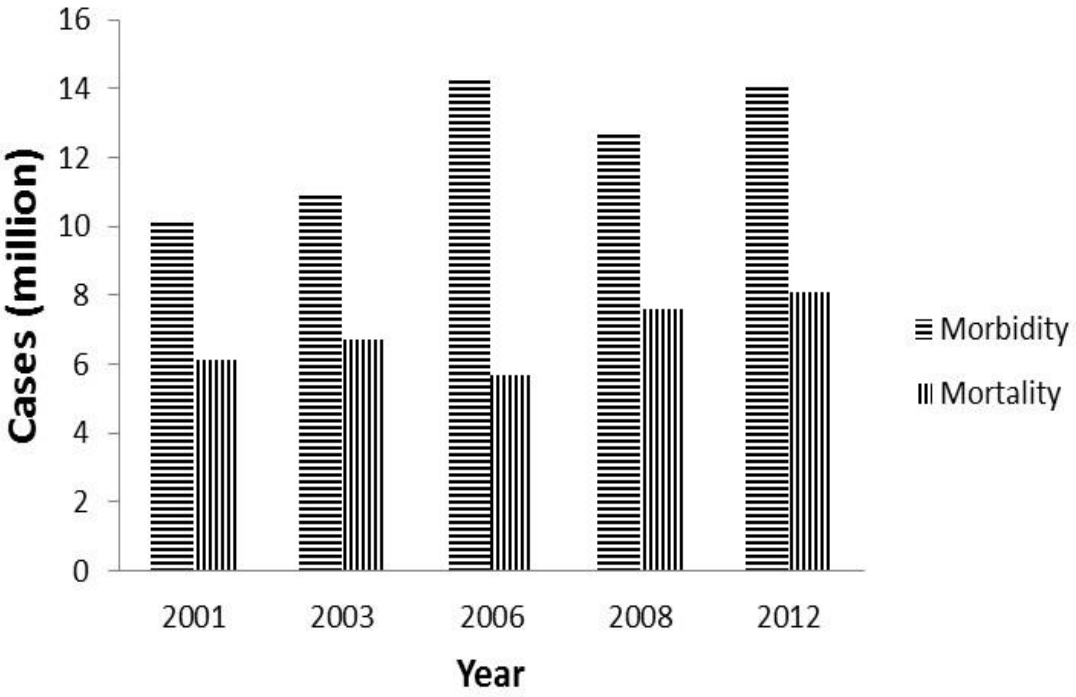

Figure 1.1: Worldwide cancer morbidity and mortality statistics: Number (millions) of cancer cases diagnosed and deaths due to cancer estimated worldwide during 2001-2012.

Cancer is not only a life crisis for the patient but the economic aspects associated with cancer treatment impact the whole family in particular, and the society in general. For instance, the total cost of cancer treatment in European Union for the year 2009 was €129 billion (Luengo-Fernandez *et al*., 2013). In 2010, the total expenses of cancer treatment in USA was estimated to be $124.57 billion which is expected to rise by as much as 39% by the year 2020 (Mariotto *et al*., 2011).

Therefore, cancer is a global medical and social challenge which needs even more attention from researchers to work on finding effective treatments in order to improve quality of patients' lives and eradicate cancer which has been the case with other global health challenges faced by mankind.

1.2 Defining Cancer

Cancer refers to a condition in which cells acquire the ability to deregulate proliferation and have the capacity to invade distant body tissues (Lucena *et al*., 2011). Normal tissue mass is maintained through a balance between cell division and cell death; both of which are controlled by tightly regulated processes. Alteration in genes, which govern these complex processes is considered to be the reason for this altered behaviour of cells that can be a result of either deoxyribose nucleic acid (DNA) aberrations during cell division or genetic mutations later on in life (Tomlinson *et al*., 2002). By virtue of such genetic instability, cells autonomously divide and multiply uncontrollably and can escape controlled cell death processes such as apoptosis

(Lahtz and Pfeifer, 2011). Consequently, an abnormal mass of cells is produced which is known as a tumour; the process being referred to as carcinogenesis or oncogenesis. In addition to unregulated growth, cancer cells are able to invade other tissues of the body using the cardiovascular or lymphatic system as their transportation medium by a process known as metastasis (Harlozinska, 2005). In 90% of the cases, cancer becomes fatal because of spread of the tumour (primary tumour) to distant tissue sites where numerous other tumours (secondary tumours) are produced (O'Flaherty *et al*., 2012).

1.3 Characteristics of cancer cells

Cancer is mainly a disease of unregulated tissue growth induced by deletion, amplification or alteration of genes. These genetic changes render some unique features to cancer cells which, taken together, characterise initiation of tumorigenesis and progression. However, it has been established that the degree of mutation and therefore, its outcome may vary form one type of cancer to another (Boland and Ricciardiello, 1999). Examples of such hallmarks of cancer, common to most of the tumour types, are briefly discussed below:

1.3.1 Independence on growth signals

In order to switch from a passive state to an actively dividing state, normal cells require mitogenic growth signals, which are mediated by transmembrane receptors (Hanahan and Weinberg, 2000). Genetic mutations that lead to division of cells to become independent of these signals will cause the cells to adopt uncontrolled

proliferation (Li and Neaves, 2006). By deregulating growth signals, cancer cells sustain a chronic division resulting in tumorigenesis (Hanahan and Weinberg, 2011).

1.3.2 Insensitivity to anti-growth signals

Tissue homeostasis is maintained by a balance between mitogenic growth signals and anti-growth signals (Giancotti, 2014; Hanahan and Weinberg, 2000). The most important of the signals that control tissue growth are tissue necrosis factor-alpha (TNF-α), a cytokine (Horssen *et al*., 2006), and a peptide called transforming growth factor-beta (TGF-β) (Massague, 2008;Pardali and Moustakas, 2007) (see section 1.4.6). Both of these are considered to be the major tumour suppressors because of their role in growth arrest and apoptosis. In many types of cancers, these signalling pathways have been found to be inactivated either by means of biallelic (involving both the alleles) deletions or mutations of the genes responsible for these receptors, resulting in failure to halt the cell division process (Giancotti, 2014).

1.3.3 Apoptosis evasion

Apoptosis is a well-orchestrated mode of cell death, which underlies programmed cell death upon the receipt of specific stimuli (Wong, 2011). Cancer cells manage to suppress apoptotic death programme by adapting different mechanisms in order to continue proliferation (Giancotti, 2014; Igney, 2002). These mechanisms include disruption of first apoptotic signals (FAS) by mutations of FAS receptors (Ghavami *et al*., 2009), deregulation of inhibitors of apoptosis (LaCasse *et al*., 2008; Mesri *et al*., 2001; Ambrosini *et al*., 1997), reduced caspase activity due to caspase gene polymorphism (Ghavami, 2009; Son *et al*., 2006) and overexpression of antiapoptotic

genes such as Bcl-2 (Iqbal *et al*., 2004) (apoptotic cell death discussed in details in section 1.9.7).

1.3.4 Uncontrolled and unlimited cell division

Hanahan and Weinberg (2011) described cell division behaviour in detail and the factors that limit cell division. According to their study, the division of cells are limited by two barriers, senescence and crisis. Senescence is the stage where the cell stops dividing, but is still viable whereas crisis results in cell death. When a cell manages to circumvent these two barriers by evading apoptosis, they achieve a state termed as immortalisation, where the cell escapes death and proliferates continuously (Hanahan and Weinberg, 2011), which occurs with cancer cells

(Falzacappa *et al*., 2012).

1.3.5 Angiogenesis; arrangement of blood vessels

One of the consequences of increased cell growth is that tumour cells need nutrients for their non-stop growth and oxygen for respiration and, also, there is a need to remove metabolic waste (Hanahan and Weinberg, 2011; Nishida *et al*., 2006). Therefore, angiogenesis, the formation of new blood vessels, plays an important role in the survival of cancer cells, in the growth of tumours and even metastasis (Dimova *et al*., 2014). The primary signals for angiogenesis are hypoxia, low glucose levels and low extracellular pH (Raghunand *et al*., 2014) in the vicinity of the tumour, which leads to the secretion of various pro-angiogenic factors, mainly vascular endothelial growth factor (VEGF) (Oliveira *et al*., 2011). VEGF normally promotes angiogenesis during embryonic development and helps in wound healing in adults, but in the case

of cancer, it is a key factor in promoting angiogenesis in tumorous areas as it is up-regulated by gene expression in response to hypoxia (Carmeliet, 2006).

1.3.6 Metastasis; invading other tissues

Metastasis refers to the dissemination of cancer cells from the primary tumour site to invade anatomically distant normal tissues of the body where they seed and grow to produce secondary tumours (Mendoza and Khanna, 2008; Montavani, 2009). Metastasis is agreed to be the phenomenon that makes cancer the second leading cause of death in the world as the outcome of metastatic deposits of secondary tumours in the vital organs of the body causes 90% of cancer-related deaths worldwide (Yilmaz *et al*., 2007; Peindo *et al*., 2011; Shao *et al*., 2014). The process of cancer cells entering into a malignant state involves a number of discrete steps, collectively known as the metastatic cascade (Geiger and Peeper, 2012), which includes bringing about extensive phenotypical changes, such as epithelial-tomesenchymal shift, and remodelling of the extracellular matrix using a number of factors, for example, cancer associated fibroblasts (Peitras and Ostman, 2011, Patel *et* al., 2011; Sleeman *et al*., 2012). For the purpose of physical translocation, cancer cells first relocate to the draining lymph nodes through lymphatic vessels (AlixPanabieres and Pantel, 2013) from where the blood stream is used as a transportation medium to reach peripheral tissues (Geiger and Peeper, 2009). The new microenvironment as well as therapeutic stress form the many challenges tumour cells have to cope with in order to succeed in metastasis (Klemm and Joyce, 2015; Seguin *et al*., 2015).

1.4 Mechanism of cell cycle and cell death; correlation to cancer

The development of new cells, that is, the cell cycle and the mechanism of cell death are two well-orchestrated processes which are very closely monitored and regulated by the responsible proteins at different stages. These processes are routine components of general tissue development and a balance is maintained between cell production and cell death by virtue of proteins/enzymes that strictly regulate these processes, deregulation of either of the processes pave the way for oncogenesis. The key proteins in these processes serve as targets for cancer therapy, inhibition/activation of which either leads to blockade of the cell cycle or activation of cell death pathways.

The following sections highlight the main events and the key players of these processes.

1.4.1 Cell cycle

The cell cycle, generally referred to as cell proliferation, encompasses a set of sequential events taking place between the appearance of a new cell and division of the same cell into two new daughter cells. This is a process that results in the increase of the tissue mass, but more importantly, it ensures that the daughter cells obtain error-free DNA. The majority of cells in the human body, such as functional cells, e.g., neurons, epithelial cells of the skin, do not enter the cell cycling process and instead reside in a quiescent state, while other cells reversibly withdraw from the cell proliferation process, for instance, glial cells and hepatocytes. There are only a few types of cells that are present in a state of active division. These types of cells are

exemplified by epithelial cells and cells in the bone marrow (Potten and Loeffler, 1990).

The cell cycle has four successive stages (Figure 1.1), most important of which are the S phase, when DNA is replicated, and the mitosis (M) phase, when two new cells emerge. Two gap phases, G_1 and G_2, separate the S and M phases. G_1 is the phase after M phase and is sensitive to positive/negative cues from the growth signals, whereas G_2 follows on from S phase and the cells gets ready for M phase (Murray and Hunt, 1993). G_0 is the quiescent state of cells where the cell cycle has reversibly stopped in response to a high number of cells in the vicinity or deprivation of mitogenic signals (Zetterberg and Larsson, 1985; Collar and Sang, 2006).

Coordination between these phases and progression in the cell cycle is thought to be achieved by phase transitions in serine/threonine kinases, known as cyclindependent kinases (CDK) (Malumbres and Barbacid, 2006). These enzymes are a complex of at least two proteins, kinase and cyclin, changes in the composition of which are thought to drive cells from one phase into the next (Hartwell and Kastan., 1994). Cyclin A-CDK2 initiates S phase, whereas, cyclin B-CDK1 drives the cell cycle progression through G_2 and facilitates cells' entry into mitosis (Nigg, 2001). Cyclin DCDK4, cyclin E-CDK2 and cyclin D-CDK6 regulate G_1 progression and help the cell complete the cycle (Planas-Silva and Weinberg, 1997). Progression of the cells through the cycle and correct order of succession between the phases are regulated by certain sensor mechanisms called checkpoints (Hartwell and Weinert, 1989). In cases of any aberrations or DNA damage, a signal is carried by the checkpoint pathways to the

effectors (CDK inhibitors) that trigger the blockade of the cell cycle until the problem is rectified (Bartek *et al*., 2004). For example, CDK inhibitors (CDKIs), belonging to Ink4 family, arrest cell cycle at G_1 in response to growth inhibitory signals (Malumbres and Barbacid, 2009). Deregulation of these checkpoints of the cell cycle release the brakes on the division of cells which underlies uncontrolled proliferation of cells, a characteristic of the cancer phenotype.

The four phases of cell cycle are briefly discussed in the following sections.

1.4.2 G_1 phase

G_1 phase, which separates mitosis and DNA formation, has the most variable and uncertain length among all the phases of the cell cycle. It depends upon the availability of nutrients and reception of proliferative/anti-proliferative signals (Davis *et al*., 2001). At this stage, the progression can be delayed or the cell can exit the cycle altogether and enter into G_0 or apoptosis is signalled, depending on the extent of aberration (Pardee, 1989; Hartwell and Kastan, 1994). G_1 progression is monitored by a checkpoint on the integrity of DNA and once this checkpoint is cleared, the cell engages in proliferative cycle without further stopping (Lundblad and Szostak, 1990; Levy *et al*., 1992). The checkpoint at G_1 includes cyclin A, D and E, the loss of which leads to genomic instability, survival of genetically damaged cells and the evolutionary pathway of cells to enter malignancy (Malumbres and Barbacid, 2009). Moreover, the “authorisation” or “licensing” for the replication of DNA, is granted to the cells during this phase by expression of six proteins collectively known as mini-chromosomes maintenance proteins (MCM2-7) (Sclafani and Holzen, 2007), overexpression of which has also been found to be oncogenic (Arentson *et al*., 2002).

Furthermore, genes and some of the components associated with the enzymes that regulate the nucleotides synthesis (dihydrofolate reductase, thymidylate synthase) and DNA replication (polymerases and topoisomerases) are activated during G_1 (Lozano and Elledge, 2000).

1.9.1 S phase

S phase is the stage of DNA replication, which is simultaneously initiated on different sites of the DNA, called origins of replications (Aparicio *et al*., 1997). Each of the newly replicated DNA molecules from a given site are called replicons, which are stable small DNA units, similar to the origin of DNA replication (Jackson and Pombo, 1998).

1.9.2 G_2 phase

During the G_2 phase, the newly synthesized DNA is double checked for any errors and corrections are made wherever necessary, before the cell can commit to the M phase. A series of protein kinases and checkpoints regulate progression through the G_2 phase. Checkpoints on this phase include cycline A, B, and CDC2 (Jiang *et al*., 1993). The G_2-M transition is prohibited by incomplete replication and DNA damage and also, the segregation of chromosomes is prevented if they are not intact (Weinert and Hartwell, 1993; Weinert *et al*., 1994).

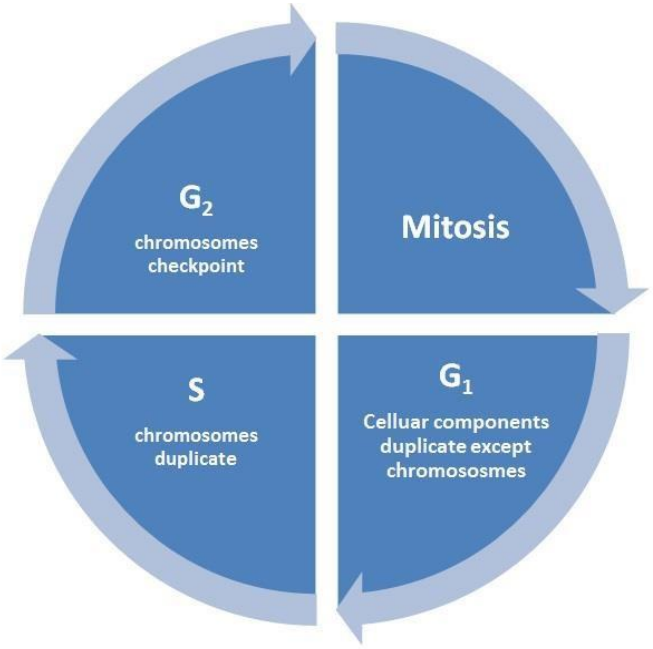

Figure 1.2: **The Cell cycle**: schematic representation of the four phases of the cell cycle and pattern of succession.

1.9.3 M phase

After clearance from the checkpoints in G_2 phase, the cell cycle proceeds to the mitosis phase or M phase. M phase is comprised of 5 sub-phases, namely, propase, metaphase, anaphase, telophase and cytokinesis, all of which lead to the division of chromosomes and cytoplasm into two to form two distinct daughter cells. The five sub-phases of M phase and the main events taking places in each of these phases are summarized in Figure 1.2.

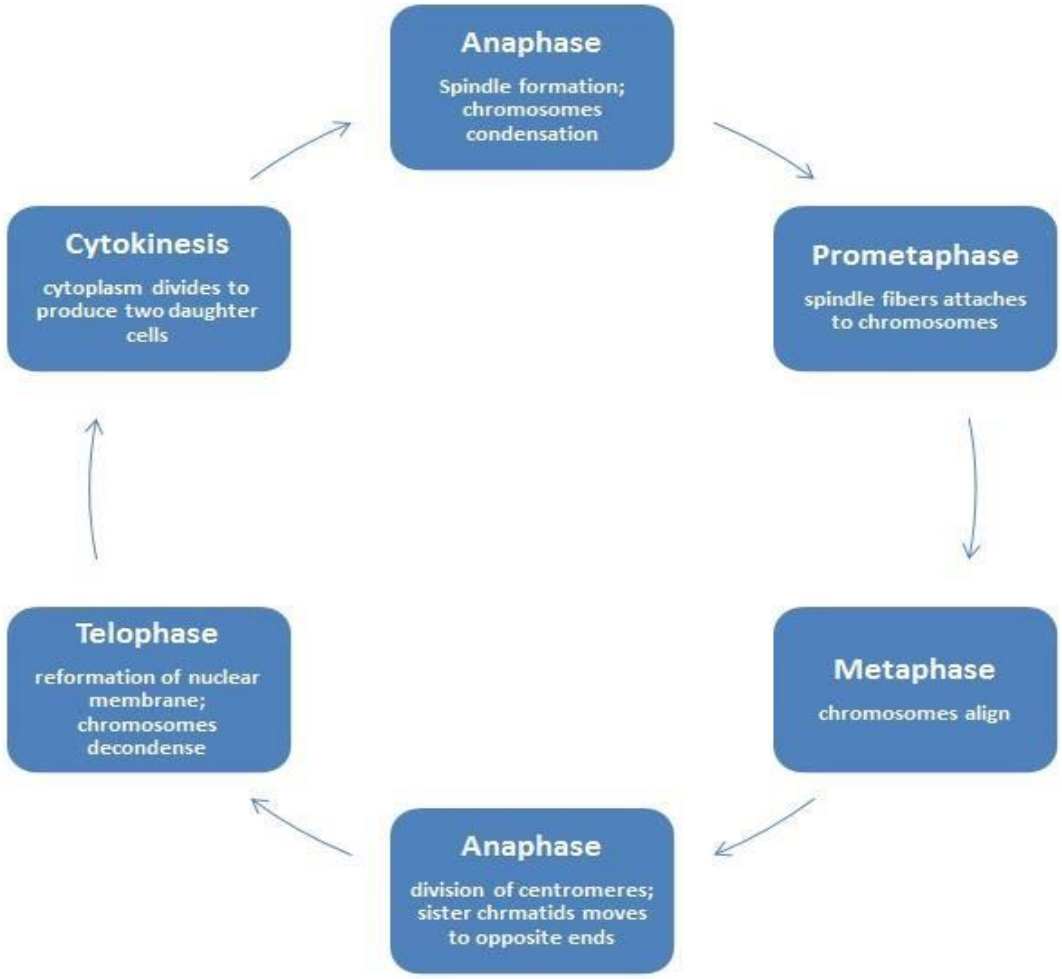

Figure 1.3: **M Phase and its sub-phase**: diagrammatic representation of the subphases of mitosis and highlights of the main events occurring during these phases as the cell cycle progresses through M phase.

1.9.4 Mechanism of cell death

Cell death has been briefly described as the rupture of the plasma membrane resulting in fragmentation of cellular components (Kromoer *et al.*, 2005). The Nomenclature Committee on Cell Death has proposed unified criteria for defining cell death and different morphologies related to death processes. Based on its recommendation, there are three well-established modes of cell death, namely, apoptosis, necrosis and autophagy (Kroemer *et al*., 2009). Majno and Joris (1995) reviewed apoptosis and necrosis and put forward the idea that both of these

processes are two steps of the same mechanism that bring about the demise of a cell. In their opinion, apoptosis is the mechanism of cell death whereas necrosis describes the post-death changes in a cell. However, in the same year their contemporary scientists (Bonfoco *et al.*, 1995) claimed that apoptosis and necrosis were two distinct mechanisms of cell death. A fact that draws a distinction between these two processes is that necrosis ends up in local inflammation in the vicinity of the necrotic cells which is attributed to the release of cellular fragments (Zitvogel *et al.*, 2004), whereas due to shrinkage of the cellular body in apoptosis, these apoptotic bodies are engulfed by neighbouring cells which prevents the release of cellular contents from the dying cells and therefore, there is no after-effects such as inflammation (Krysko *et al.*, 2006). Furthermore, after identifying the role of caspases in apoptosis, their inhibitors were introduced to elaborate their role in initiating apoptosis (reviewed by Lockshin and Zakeri, 2004). It was found that cells would still die if cell death is triggered with TNF-α, despite the presence of nonspecific inhibitors of caspases like zVAD-fmk, or anti-apoptotic agents such as BclXL. This observation further strengthens the idea that necrosis is another type of cell death which is distinct from apoptosis and is caspase independent.

The following sections review the three main types of cell death in terms of initiation, progression, related morphology and the key proteins critical to these processes.

1.9.5 Necrosis

In morphological terms, necrosis can be described as a type of caspase-independent cell death involving swelling of the cell (oncosis) at the onset of the process, rupture

of the plasma membrane and other membrane bound organelles, resulting in release of fragments of cellular bodies which triggers inflammation (Kroemer *et al*., 2005). Figure 1.3 illustrates the morphological changes, that is, rupture of cells into irregular fragments, in human skin melanoma cells (A375) treated with 500 µM H_2O_2 for 24 h to induce necrosis.

(A)

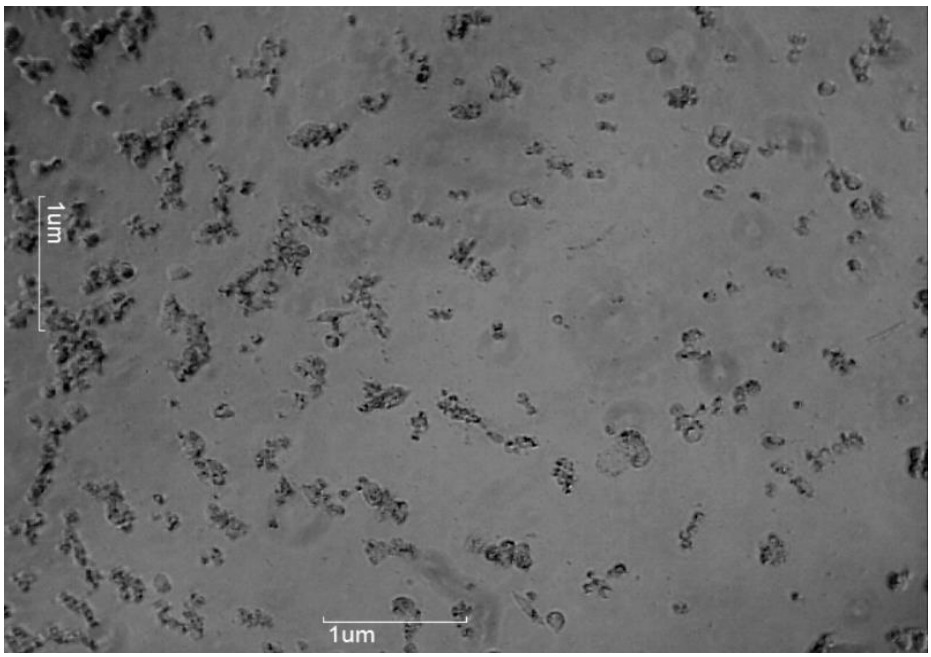

(B)

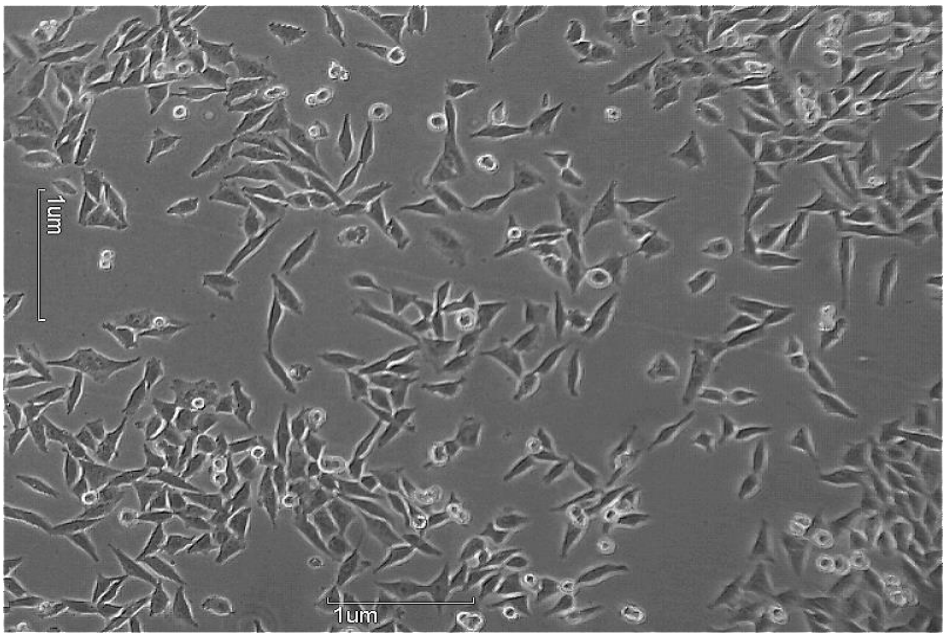

Figure 1.4: Morphology of necrotic cells: A375 cells (A) were incubated with H_2O_2 (500 µM) for 24 h and photomicrophs were with a 10X lens to compare the morphological changes with viable A375 cells (B). The irregular fragmentation of the cells is a consequence of necrotic cell death culminating in cell rupture.

Previously, necrosis was considered to be accidental and uncontrolled, but more recent findings suggest that it can be controlled both in terms of onset and duration

(Golstein and Kroemor, 2006). The onset and duration of necrosis depends on the nature of factors initiating this process. It can be slow and well-programmed as in the case of tissue development, for instance, death of chrondrocytes in the cartilage of bones in order to regulate their longitudinal growth (Roach *et al.*, 2000). On the other hand it can be accomplished in matters of minutes as in the case of neuronal cells exposed to N-methyl-D-aspartate (NMDA) (Bonfoco *et al.*, 1995) or H_2O_2 (Saberi *et al*., 2008).

1.9.6 Mechanisms underlying necrosis

Necrosis does not occur as a result of one well-established signalling pathway. A number of intracellular and extracellular events, which can initiate necrosis include excessive cytotoxicity, freeze-thawing, excessive heat, trauma, ischemia and accumulation of free radicals inside the cells (Golstein and Kroemer, 2006). Various enzymes and chemical entities are involved in this process, however, a serine/threonine kinase known as receptor-interacting protein 1 kinase (RIP1), calcium ions and reactive oxygen species (ROS) are thought to be the main players at molecular level in provoking necrosis (Festjens *et al*., 2006). Among the receptors, the activation of which leads to the initiation of necrosis, the best studied are TNF receptor, Fas receptor (FasR) and TNF-related apoptosis-inducing ligand **(**TRAIL) receptors. The activation of these receptors leads to the activation of an adaptor molecule, Fas receptor associated death domain (FADD), which is at the crossroads of apoptosis and necrosis. This molecule contains both a death effector domain (DED) and death domain (DD). Normally, FADD leads to apoptosis upon activation of DED

which triggers caspase-8, however, when this mechanism fails (by gene alterationsor by caspase inhibitors), DD initiates necrosis by activating RIP1 (Festjens *et al.*, 2006). However, caspases have the ability to cleave RIP1, which leads to suppression of necrosis and the cell can die by apoptosis, which also indicates that the full length of RIP1 is necessary for triggering necrosis directly or indirectly (Chan *et al*., 2003).

The direct mechanism involves the action of RIP1 on mitochondria where it blocks the generation of adenosine triphospate (ATP) molecules, thus leading to ATP deficiency and ultimately cell death (Temkin *et al.*, 2006). The indirect mechanism involves the triggering of nicotinamide adenine dinucleotide phosphate (NADPH) oxidase (Nox), which is responsible for the generation of ROS, especially superoxide (O_2^-). ROS are essential mediators of TNF-induced necrosis because inhibition of ROS brings necrosis to a halt. Another important factor in this pathway is a mitogenactivated protein (MAP) kinase, c-Jun N-terminal kinase or JNK, which exerts the same effect on mitochondria as the direct effect of RIP1 on mitochondria. JNK is also important for this pathway because its inhibition also results in the blockade of necrosis (Kim *et al.*, 2007). Besides death-receptors, RIP1 is also activated by tolllike receptors (TLR) such as TLR3 and TLR4 when triggered by lipopolysaccharide (LPS) that ultimately leads to necrosis. This pathway has been observed in macrophages (Ma *et al.*, 2005). The following figure summarises various necrotic pathways.

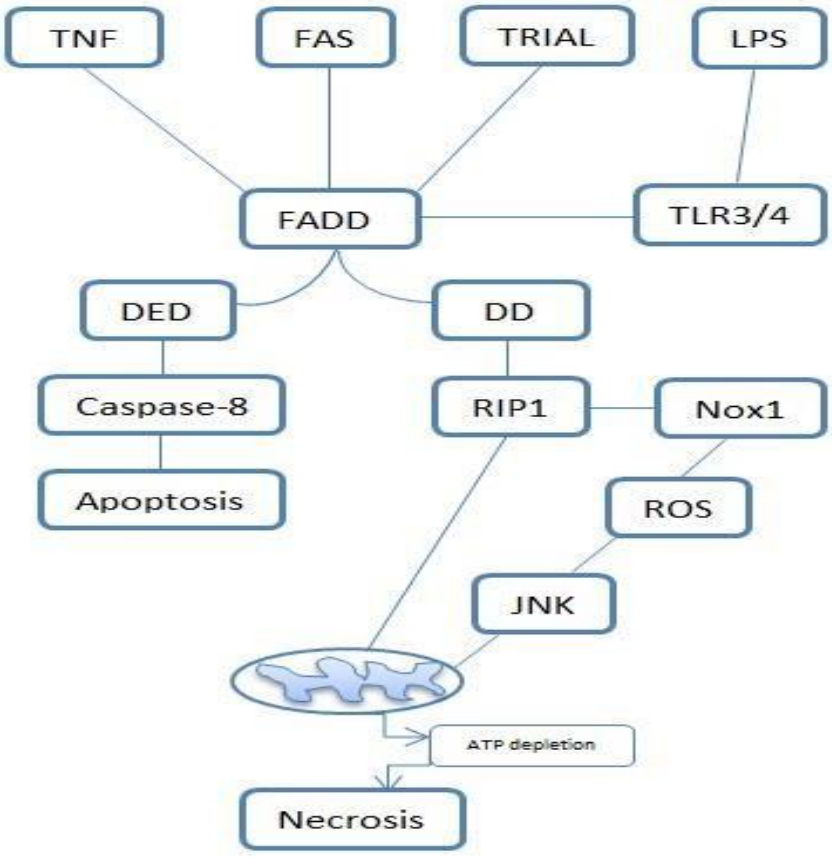

Figure 1.5: Enzymatic and signalling pathways regulating necrosis: A flow diagram which shows the mode of cell death downstream from the activation of different death receptor.

1.9.7 Apoptosis

The word 'apoptosis' was coined by Kerr *et al.* in 1972. This is the principle mechanism of cell death which is characterised by condensation of chromatin material (pyknosis), fragmentation of chromatin (karyorrhexis) and finally the dissolution of the nucleus (karyolysis). Morphologically it is manifested by reduction in cell volume, the cell becomes almost round in shape (Figure 1.5), and in the last stages, disintegration of cellular bodies form small globules or bubbles (blebbing) which are engulfed *in vivo* by resident phagocytes (Kroemer *et al.*, 2009) or by neighbouring cells in *in vivo* systems, which is the main reason for absence of inflammation in apoptosis, unlike

necrosis. The integrity of the cell membrane as well as the membranes surrounding the organelles is unaffected until the intervention of phagocytosis in order to safely seal the contents of the dying cell and that is why apoptosis is sometimes referred to as “death with dignity” (Bonfoco *et al.*, 1995). DNA is broken down into fragments that are multiples of 185 bp due to cleavage between nucleosomes (Majno and Joris, 1995) or fragments of 200 bp, which is considered to be characteristic of apoptosis and is, therefore, used as a biomarker for apoptosis (Edinger and Thompson, 2004).

(A)

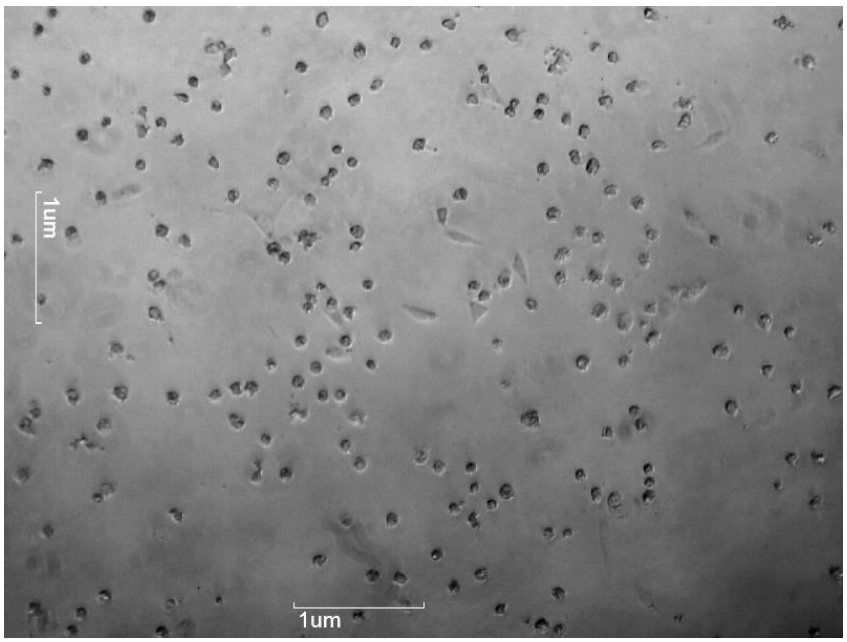

(B)

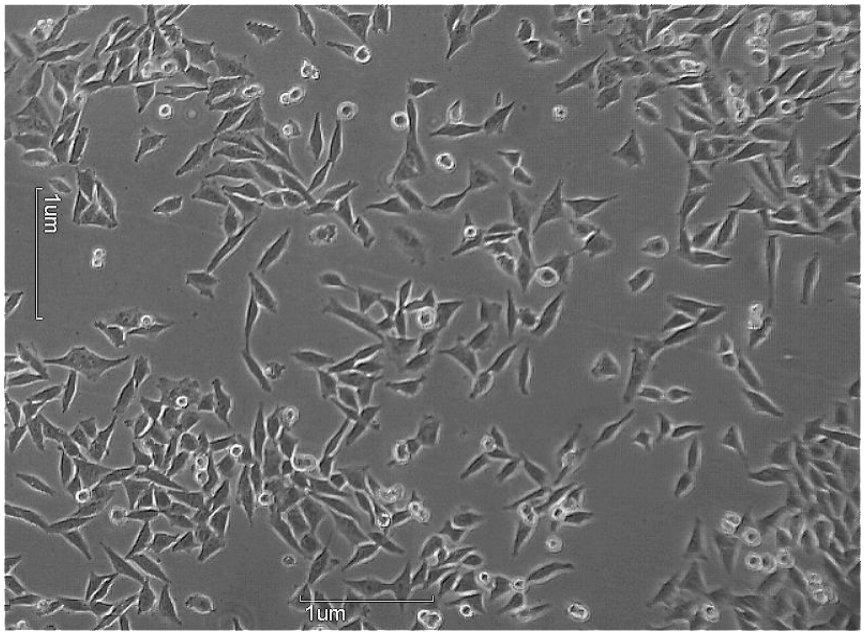

Figure 1.6: Morphology of apoptotic cells: A375 cells treated with (A) 300 µM of cisplatin for 24 h. The rounding of the cells and reduction in cellular volume, compared with (B) negative control, is noticeable.

1.9.8 Apoptotic Pathways

The mechanism of apoptosis has been well studied and documented since 1972, especially in the last decade. Caspases are the driving force of apoptosis and based

on the nature of their role in apoptosis, caspases are broadly classified into signalling/initiator caspases and effector caspases (Wong, 2011). Signalling caspases are those that associate with adaptor molecules in order to facilitate the activation of downstream caspases. Examples of signalling caspases include caspase-8 for FADD or caspase-9 that associates with Apaf-1. Those caspases that are involved in the breakdown of proteins to execute apoptosis are referred to as effector caspases, exemplified by caspase-3, caspase-6 and caspase-7 (Thornberry and Lazebmik, 1998). It is widely reported that there are two pathways for the activation of caspases to initiate apoptosis, namely the intrinsic pathway and extrinsic pathway as reviewed by Lowe and Lin, 2000, and Kominami *et al.*, 2012.

Both of these pathways are briefly discussed below and illustrated in Figure 1.6.

1.9.9 Intrinsic pathway

Some internal stimuli, such as irreversible genetic damage or hypoxia, constitute the internal pathway for the onset of apoptosis which leads to increase in mitochondrial permeability, that results in the release of pro-apoptotic proteins, mainly cytochrome-c (Danial and Korsmeyer, 2004) through proposed channels known as permeability transition pores (PTP). PTP are thought to be made up projections of mitochondrial membrane and are thought to form following apoptotic signals (Green and Reed, 1998). The intrinsic pathway is closely regulated by two groups of proteins that belong to the Bcl-2 family of proteins. One group, called pro-apoptotic proteins including Bax, Bak, Bad, Bid, Bik, Bim, Bcl-X_S, and Hrk, favour apoptosis by promoting the release of cytochrome-c from mitochondria. The second group is known as anti-

apoptotic proteins, represented by Bcl-X_L, Bcl-W, Bfl1 and Mcl-1. As the name implies, these proteins prevent apoptosis by inhibiting mitochondrial release of cytochrome-c (Reed, 1997). Cytochrome-c interacts with caspase-9 and Apaf-1 to form a complex, which is known as an apoptosome, which leads to the activation of the effector caspase-12 and eventually apoptosis (Kroemer *et al.*, 2007).

1.9.10 Extrinsic pathway

This pathway is triggered by external stimuli and is mediated by certain receptors on the cell surface, which are collectively known as death receptors (Reuter *et al*., 2008). The best studied among these receptors are Fas and TNF receptor-1 (TNFR1) (Thorburn, 2004). Fas ligand (FasL) and TNF are ligands for these receptors respectively which lead to the activation of these receptors. These receptors are intracellularly associated with death domains such as TNF receptor-associated death domain (TRADD) and Fas-associated death domain (FADD) (Schneider and Tschopp, 2000). Binding of a death ligand to its respective death domain opens a binding site for an adaptor molecule to form a ligand-receptor-adaptor protein complex (DISC). DISC transforms pro-caspase-8 into caspase-8, which is an effector caspase (O'Broem and Kirby, 2008).

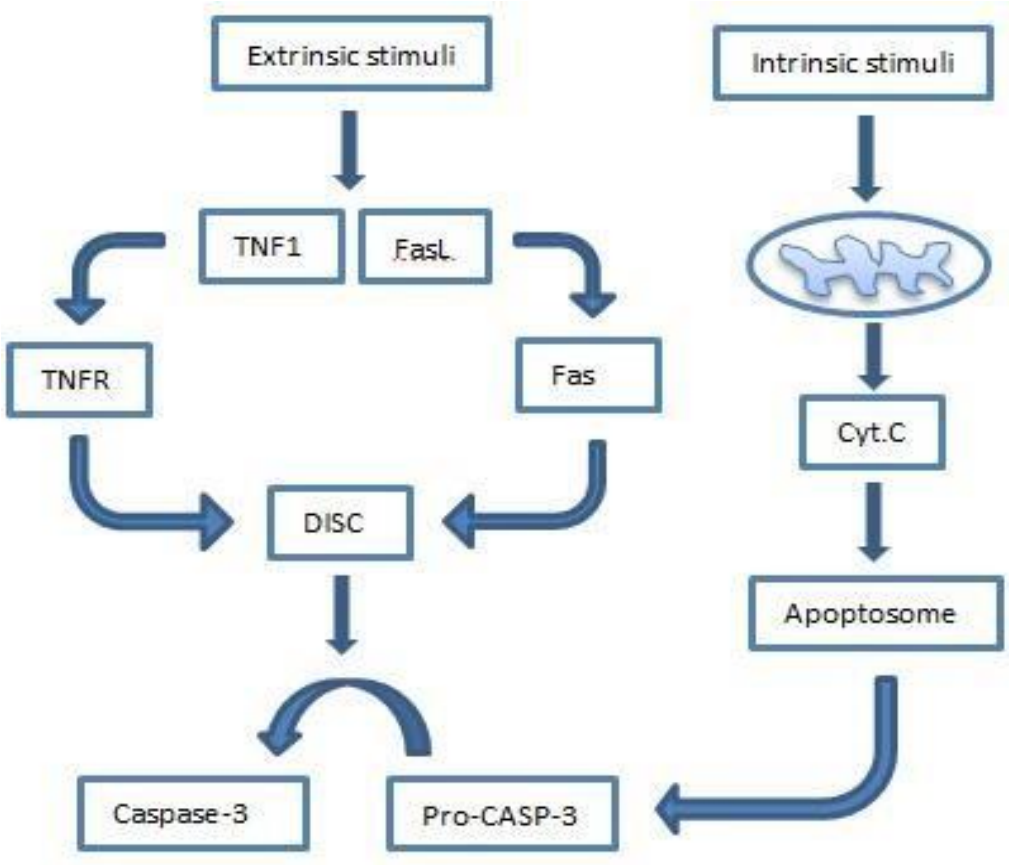

Figure 1.7: Activation pathways of apoptosis: Summary of the three pathways that result in apoptotic cell death.

1.9.11 Caspase-independent apoptosis; role of AIF

Caspases are thought to be the key players in bringing about the characteristic morphological manifestations of apoptosis. However, other proteins released from mitochondria have been described that induce apoptosis with all the characteristics in place except for the involvement of effector caspases in the process.

Apoptosis-inducing factor (AIF) is a 67 kDa flavoprotein having NADH oxidase activity attached to the inner mitochondrial membrane (IMM), catalysing localised redox metabolism for the optimum processes of oxidative phosphorylation and anti-oxidation under normal conditions (Susin *et al*., 1999; Modjtahedi *et al*., 2006;

Orrenius and Zhivotovsky, 2010). This protein was identified and characterized for the first time by Susin *et al*. (1996), and was shown to trigger chromatin condensation in isolated nuclei of a human cervical cell line (HeLa) upon apoptotic stimulus. It was further demonstrated that the apoptosis induced by this soluble factor is caspase independent (Susin *et al*., 1999). AIF is released from mitochondria in response to both extrinsic and intrinsic stimuli. As discussed in the sections above, death receptors, upon activation, recruit the adaptor FADD which has two protein domains, DD and DED. In case of caspase-dependant apoptosis, FADD binds to pro-caspase 8 via DED interactions to create DISC, which down the pathway activates the effector caspases. Whereas in the other case, activated caspase-8 leads to the cleavage of Bid, a BH3-only protein, and its translocation to mitochondria (Lou *et al*., 1998). Translocation of Bid to mitochondria triggers the release of AIF from mitochondria and its translocation to nuclei where it promotes

DNA damage and DNA fragmentation into ~50 kbp (Hanahan *et* al., 2000; Thorburn, 2004). The translocated AIF (tAIF) is believed to be ~57 kDa (Susin *et* al., 1999), nonetheless, three other isoforms of AIF (57, 62 and 67 kDa) have also been reported in apoptotic cells (Otera *et al*., 2005).

Mitochondria contain a number of apoptogenic proteins such as cytochrome C and AIF (Loo *et al*., 2002). The role of mitochondrial outer membrane potential (MOMP) to release these apoptogenic proteins is a subject of extensive debate and still remains unclear and controversial. MOMP is primarily managed by a group of proteins belonging to the Bcl-2 family of proteins, namely, Bax, Bad and Bid.

Bax/Bad, form pores or channels in the outer membrane of mitochondria, thus causing the release of pro-apoptotic proteins including cytochrome C (Martinou and Green, 2001). Release of cytochrome C in this manner takes place as a result of oligomerization of Bax/Bad induced by Bid (Wei *et al*., 2001). Loss of MOMP is necessary for the release of cytochrome C and is considered essential for the translocation of AIF (Hong *et* al., 2004; Norberg *et al*., 2010). Arnoult *et al*. (2003), through a series of experiments, proved that release of AIF is independent of Bax/Bad and it can be released at unaltered MOMP. Abundant evidence is found in the published literature that MOMP does not have to drop in order to leak AIF into cytosol. Due to its solubility in the intermembrane space and low molecular weight, MOMP is sufficient for AIF to be released (Susin *et al*., 1999; Daugas *et al*., 2000). In other apoptotic models, AIF was found to be released prior to cytochrome C where the MOMP was high, which further strengthens the hypothesis that AIF release is not dependant on MOMP (Ferri *et al*., 2000a; Ferri *et al*., 2000b; Genini *et al*., 2001).

A number of factors are considered responsible for the activation and translocation of AIF to nuclei. Calcium ions (Ca^{2+}) are also known to play an important role in the release of AIF through two indirect ways. Firstly, Ca^{2+} is required for the activation and catalytic properties of enzymes known as calpains. This is a group of proteases, represented by two isoforms, calpain-I (μ-calpain) and calpain-II (m-calpain), differing only in the amount of Ca^{2+}, that is required, μM and mM respectively, for their optimal activity (Norberg *et al*., 2010a). A number of studies have concluded that these

enzymes play a key role in cleavage of AIF from IMM (Polster *et al*., 2005; Cao *et al*., 2007; Liu *et al*., 2009). The second role of Ca^{2+} is the generation of ROS.

Increased influx of Ca^{2+} leads to the generation of ROS within mitochondria resulting in the oxidative modification of AIF and its release and thus is regarded as an important regulator of the activation and release of AIF from mitochondria (Kim *et* al., 2003; Norberg *et al*., 2010b). Cathepsins are peptidases found in lysosomes and are thought to contribute to the release of AIF (Bidere *et al*., 2003). However, the part of these enzymes in the modification of AIF is questionable as these enzymes are stable only in the acidic environment of lysosomes (pH <6) and it is not certain how of their activity is retained in the soluble cytosol where the pH is close to 7 (Pillay *et al*., 2002).

Another protein called poly(ADP-ribose) polymerase 1 (PARP-1) is an abundant nuclear protein which is part of the DNA repair system and belongs to a broad family of proteins that includes PARP-2, PARP-3 and vault PARP (Hong *et al*., 2004).

It is a 116 kDa enzyme that can recognise both single and double-strand breaks in DNA (Lindahl *et al*., 1995). PARP-1 is present in the nucleus, mending mild damages and errors as a normal repair process of DNA-base-excision (Smulson *et al*., 2000). In cases of excessive DNA damage, PARP-1 is unregulated up to 500-fold, which leads to the transduction of cell death signals to mitochondria and AIF is released in response (Yu *et al*., 2002) (Figure. 1.7). Therefore, PARP-1 activation is regarded as a key factor to determine whether the cell lives by repairing DNA or dies by inducing release of AIF from mitochondria.

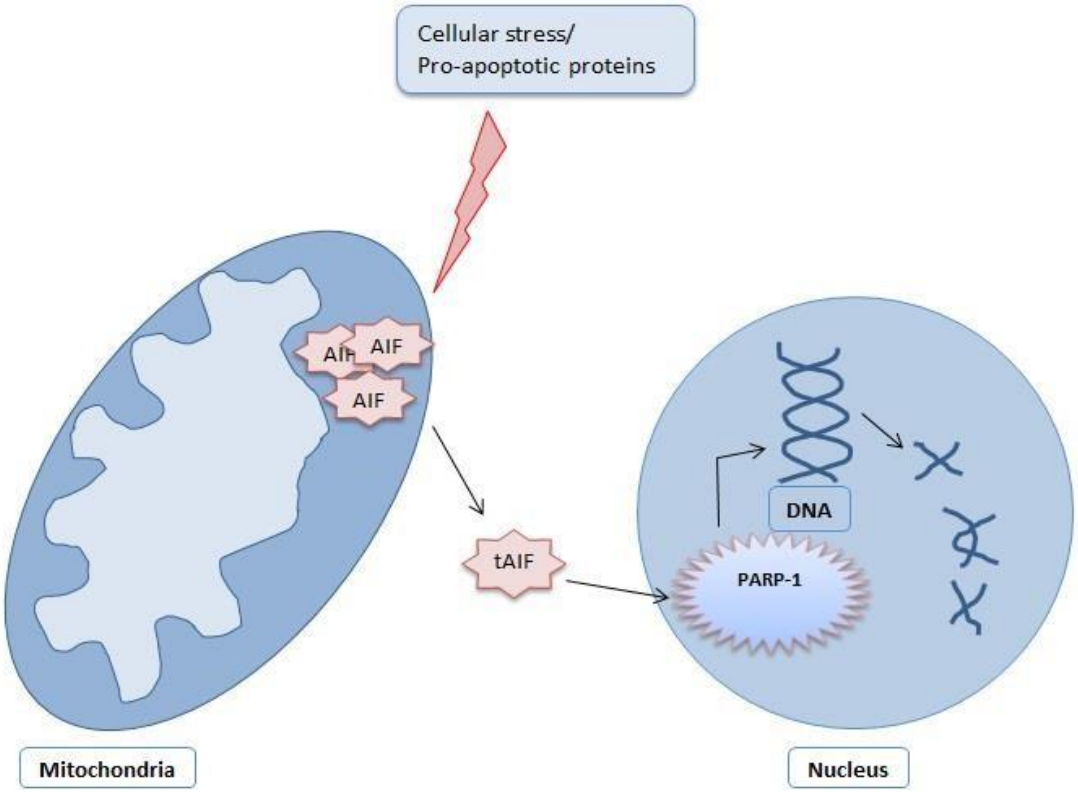

Figure 1.8: Release of PARP-1: The release of PARP-1 in response to various mechanisms that induce DNA damage. After mild damages, PARP-1 repairs DNA, however, in severe cases, it signals the release of AIF from mitochondria to initiate a caspase-independent cell death process.

1.9.12 Autophagy

The term 'autophagy' means 'eating of self' and was coined by Christian de Duve over four decades ago after observing the self-digestion of mitochondria within rat liver lysosomes (Deter and de Duve, 1967). Autophagy can be defined as a process by which cytoplasmic components are transported to and engulfed by lysosomes for degradation (Levine and Kroemer, 2008; Mizushima *et al*., 2008). Morphologically autophagy is defined as the type of cell death that proceeds through the excessive vacuolisation of the cytoplasm and without chromatin condensation (Kroemer *et al*.,

2009). Basal autophagy plays a critical role in cell survival by maintaining cellular homeostasis as well as genomic integrity by breaking down malfunctioning and damaged proteins to avoid the accumulation of defective cellular substructures, on the other hand, it also leads to cell death in severe conditions like oxidative stress, starvation, high temperature and excessive organelle damage (Levine, 2007). Depending on the mechanism of transportation of the cargo, that is the organelle or cellular proteins to be degraded, to the lysosomes, autophagy has three defined types known as macro-autophagy, microautophagy and chaperone-mediated autophagy (Glick *et al*., 2012; Mizushima, 2007; Shintani and Klionsky, 2004). Macro-autophagy proceeds through the formation of a double membrane (phagophore) around the cargo, the whole complex is referred to as autophagosome, which is then transported to lysosomes to form autolysosome where the degradation of proteins takes place whereas mirco-autophagy involves the direct take up of the cargo by lysosomes via by lysosomal membrane invagination. Both of these types of autophagy can engulf cytoplasmic components through selective (e.g., defective proteins) and nonselective (e.g., during starvation) mechanisms (Glick *et al*., 2012). As the name indicates, chaperone-mediated autophagy involved the labelling of cargo with other proteins, for instance heat shock cognate 70 (Hsc70), which is identified by lysosomal membrane receptors, such as lysosomal-associated membrane protein 2A (LAMP-2A), and are taken up for degradation.

Autophagy has a multifunctional role in cancer. It appears to suppress cancer during the initiation of cancer by digesting the malformed DNA (Rouschop and Wouters, 2009). However, during the later stages, autophagy prolongs the survival of cancer

cells by meeting the metabolic need of rapidly proliferation cancer cells (Amaravdi *et al*., 2011; Mathew *et al*., 2007).

1.9.13 Mechanism of autophagy

The process of autophagy commences with the formation of a phagophore around the cargo for which multiple origins have been suggested. Endoplasmic reticulum (ER) has been suggested to be the primary source of phagophore (Hayashi-Nishino *et al*., 2009; Yla-Anttila *et al*., 2009). One of the processes that initiate the formation of the phagophore is the binding of Beclin-1 with Vps34 (vesicular protein sorting 34). Vps34 is involved in different membrane-sorting processes within the cells but when it is coupled with Beclin-1, it is specifically involved in activation of autophagy (Backer, 2008). A checkpoint at this stage is the interaction of Bcl-2 with Beclin-1 which prevents the binding of Vps37 to Beclin-1, thus halting autophagy (Pattingre *et al*., 2005). However, upon the receipt of autophagic signals, for instance starvation, JNK1 (c-Jun N-terminal kinase 1) mediates the phosphorylation of Bcl-2, thereby, allowing autophagy to take place (Wei *et al*., 2008). Also, the mammalian target of rapamcyin (mTOR), a serine/threonine kinase, blocks autophagy at the stage of phagophore formation (Tang *et al*., 2014). Rapamycin inhibits mTOR and therefore, is used as an antiproliferative agent and to induce autophagy in experimental conditions (Li *et al*., 2014).

Another trigger for the initiation of phagophore formation is autophagy related genes (Atg) which are a group of 32 genes, originally described in yeast (Nakatogawa *et al*., 2009). However in mammals, ubiquitin homologues of Atg are involved in the process

of autophagy by forming two types of systems which are critical for the progression of the phagophore (Kirkin *et al.,* 2009). Firstly, the formation of Atg5-Atg12 complex - for this purpose, Atg12 is activated by partial binding of Agt7 to carboxy-terminal gylcin residue of Agt12 in an ATP-dependant manner followed by conjugation with Atg5 facilitated by a transporting protein, Atg10. This complex is further paired with a diametric Atg16 to form a multimeric system (Atg5-Atg12-Atg16-Atg-16) which supposedly induces curvature into the extending phagophore. Moreover, Atg5 is strictly involved in crosstalk between autophagy and apoptosis. Autophagy is blocked as consequence of Atg5 cleavage, mediated by calpains, followed by translocation of the truncated Atg5 to mitochondria where its interaction with Bcl-X_L triggers the release of Cyt.C and caspase activation (Aredia *et* al., 2012; Yousefi *et al*., 2006). Atg3, Atg4 and Atg7 is the other ubiquitin-like system that is involved with autophagy by facilitating the processing of light chain 3B (LC3B) which is a microtubule associated protein. LC3B is a full length protein that is expressed in the cytosol of most the cell types and is encoded by Atg8 mammalian homologue. On the onset of autophagy, the LC3B is cleaved by a cysteine protease, Atg4, (Yang *et al*., 2015) and is activated by Atg7 in

the same manner as Atg12 to give LC3B-I (Jong-Ok *et al*., 2012). Phosphatidylethanolamine is conjugated with LC3B-I to generate an activated LC3BII and is transferred to a carrier protein Atg3 followed by integration of the LC3B-II into the developing phagophore (Rockenfeller *et al*., 2015). LC3B-II is found on both the inner and outer surfaces of phagophore membranes. LC3B-II also acts as a receptor on the phagophore outer membrane for adaptor molecules expressed on the target

proteins for their selective autophagy, for example, Atg32 is an identified adaptor for the selective uptake of mitochondria (Sakakibara *et al*., 2015). The cargo at this stage, where it is fully enveloped in phagophore, is known as autophagosome. The next step is the fusion of autophagosomes with lysosomes to form autolysosomes, a process known as maturation. However, there is evidence of fusion of endosomes to autophasomes prior to maturation as a result of which the pH of autophagomes drops before the fusion of lysosomal enzymes (Glick *et al*., 2010). Cytoskeleton has an unidentified role in the formation of autolysosomes which is inferred by finding out the rearrangement of both actin and tubulin in the cytoskeleton consistently with the formation of autophagosomes (Gama *et al*., 2014). Moreover, microtubule poisons, e.g. nocadazole, block the fusion of lysosomes with autophagosomes, which also confirms the role of the cytoskeleton in autolysosomes (Webb *et al*., 2004). In autolysosomes the degradation of the engulfed proteins takes place. Atg5-Atg12-Atg16-Atg-16 complex detaches from the membrane and the proteins are recycled after autophagosome formation, thus making this complex a poor marker for the detection of autophagy, whereas, LC3BII is preserved until the formation and maturation of autolysosomes and is, therefore, a reliable indicator of autophagy (Barth *et al*., 2010).

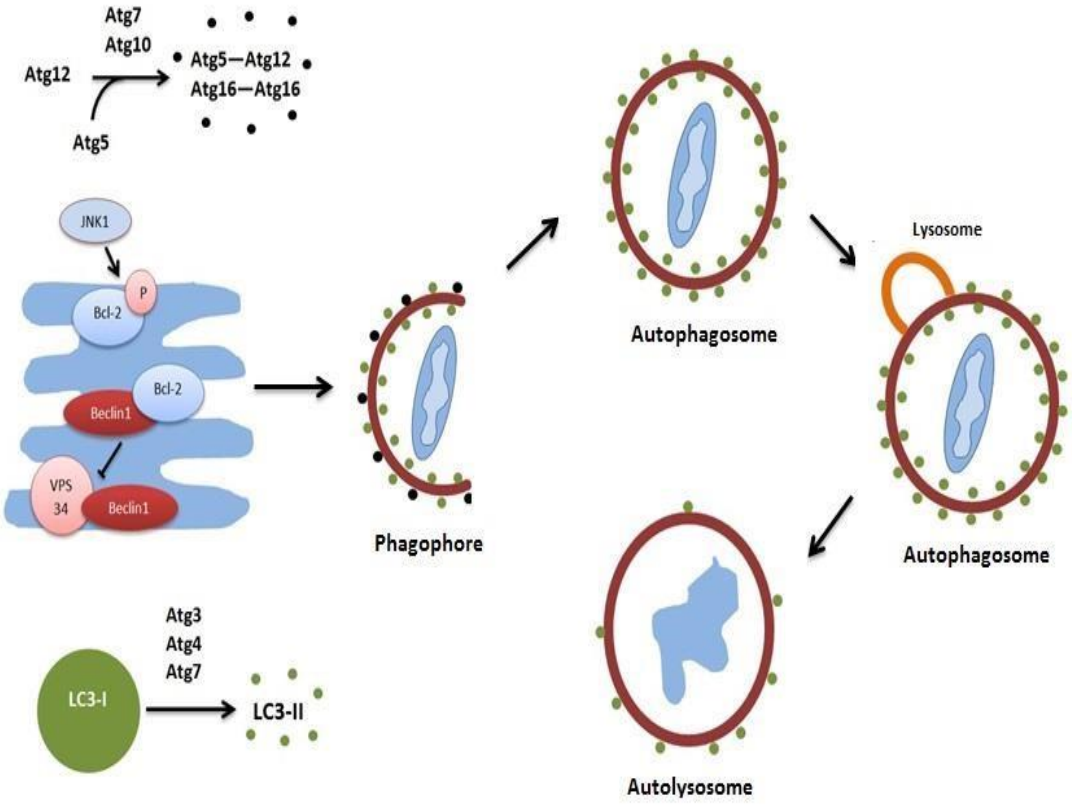

Figure 1.9: Mechanism of autophagy: A flow diagram highlighting the main events in the progression of autophagic cell death from the formation of phagophore until the maturation of autolysosomes.

1.5 Treatment of cancer

The ultimate goal in the treatment of cancer is to control the progression of the tumours and prevent their spread to other tissues of the body. Despite the considerable progress in understanding of the patho-physiology and various treatment options, cures for most types of this disease have not yet been found. The current main treatment options are surgical removal of the tumour, radiotherapy and chemotherapy. Due the complex nature of cancer, a single treatment approach is insufficient in most cases and therefore a combination of these options is often used to cope with this disease. Various considerations are taken into account for selecting

the treatment of choice for a particular case such performance status of the patient (that is general wellbeing and daily activities), any other coexisting medical conditions, patient compliance and risk to benefit ratio (Greenhalgh and Symonds, 2014). Moreover, the treatment strategy depends on the site and degree of metastasis.

1.5.1 Radiotherapy

Radiotherapy involves exposure of tumorous area with high-energy ionising radiations. Various particles such as protons, heavy ions and X-rays are used as ionising radiations (Newhauser and Durante, 2011). These radiations produce free radicals and charged particles which lead to breakage of single or double stranded DNA or cluster damage that halt the DNA repair system and thus culminates in cell demise (Nikjoo *et* al., 1999; Greenhalgh and Symonds, 2014). Various imaging techniques are used for this purpose, such as positron emission tomography (Bradley *et al*., 2004), magnetic resonance imaging (Flores-Tapia *et al.,* 2008), magnetic resonance spectroscopy (Payne and Leach 2006) and ultrasound (Berrang *et al*., 2009). Radiotherapy is a productive treatment approach for a variety of solid tumours and according to one estimate, approximately 17,000 cancer patients are administered radiotherapy every year (West *et al*., 2009). Radiotherapy is a common practice to the pelvic area for gynaecological cancers and cancers of prostate, rectum, anus and bladder (Adams *et al*., 2014). Radiotherapy has also been effective against tumours in the head and neck, but under strict precautionary measures because of the anatomical complexity of the region (Grégoire *et* al., 2012;

Schwartz *et al*., 2013). In some cases, for example ovarian cancer, the role of radiotherapy is controversial and the choice of treatment is chemotherapy only (Rai *et al*., 2014), whereas, in other cases, like human skin malignant melanoma, radiotherapy is coupled with chemotherapy (platinum drugs) to increase treatment efficacy (Xie *et al*., 2014).

1.5.2 Surgery

Surgical removal, or resection, of whole or a part of the tissue harbouring solid tumours is a common practice to provide long lasting cancer-free survival (Khong *et al.,* 2014) and is regarded as the treatment of choice for a number of solid tumours such as testicular cancer (Leonhartsberger *et al*., 2014), lung cancer (Nakada *et al*., 2014) and carotid body tumour (Ma *et al*., 2014). Surgery is helpful in removing the primary tumour, but it fails to control or treat metastasis or micro tumours and that is why it used as an adjuvant therapy along with chemo or radiotherapies, for example, chemotherapy along with surgery has shown promising results in colorectal cancer (Carrto, 2008); survival rates of breast cancer patients receiving postoperative radiotherapy have also been claimed to increase (Early Breast Cancer Trialists' Collaborative Group, 2005).

1.5.3 Chemotherapy

Chemotherapeutic drugs work by inducing cell death through halting the division of cells via various mechanisms (discussed in detail in the following sections) and therefore, they are more active against rapidly dividing cells, that is, cancer cells, relative to quiescent non-cancer cells. The era of usage of chemotherapeutic agents,

such as nitrogen mustard and antifolate agents, can be traced back to the 1940s and since then a lot of transformations have been observed in chemotherapy, but the early findings, in terms of working principles of the drugs and limitation of the therapy, still apply (Chabner and Roberts, 2005). However, in the last two decades the approach of chemotherapy has changed from broadspectrum cytotoxic agents to mechanism-based therapy (Vanneman and Dranoff, 2012).

Various classes of chemotherapeutic agents, according to the British National Formulary, BNF (2015), their clinical indications and mechanism of action (MOA) are mentioned below:

Alkylating agents

Alkylating agents include cyclophosphamide, ifosfamide, cholrambucil, melphalan, busulfan, lomustine, bendamustine and Temozolomide. Drugs in this class have the reputation of the frontline chemotherapeutic agents that induce cytotoxic effects by DNA damage (Fu *et al*., 2012). The principle underlying their mechanism of action (MOA) is binding an alkyl group covalently to DNA which leads to DNA damage and apoptosis (Makin, 2014). Alkylating agents have been used, alone or in combination, in solid tumours (Sartorelli, 1998; Radhakrishnan *et al*., 2015). Cholrambucil has a limited role in ovarian carcinoma treatment whereas cyclophosphamide and ifosfamide are highly effective in ovarian cancer and other gynaecological cancer such as carcinomas of the cervix and vulva (Greenhalgh and

Symonds, 2014). Temozolomide has been used in cases of malignant melanoma

(Sanjiv and Kirkwood, 2000).

Anthracyclines

This is a class of drugs with similar structures showing anticancer properties. Daunorubicin, doxorubicin, epirubicin, idarubicin and mitoxantrone (anthracycline derivative) are members of this class. Daunorubicin, the first drug to be described from this category, as well as doxorubicin were both initially isolated from a bacterium *Streptomyces peucetius* (Arcamone *et al*., 1969; Marco *et al*., 1969). Despite extensive investigation over the last several decades the exact MAO of these agents that leads to apoptotic death of the cells is still controversial. However, a number of concepts have been put forward (Yang *et al*., 2014). Disruption of chromatin structure which most probably interferes with

transcriptional and replication process (Rabbani *et al.*, 2005), production of reactive oxygen species through a redox reaction which results in loss of mitochondrial membrane potential (Mizutani *et al*., 2005), inhibition of topoisomerase II through intercalating DNA (Zunino and Capranico, 1990; Yang *et al*, 2015) are prevailing models for the MOA of anthracyclines. Anthracyclines are being used in solid tumours like cancers of the breast (Tew *et al*., 2014) and ovaries (Markman *et al*., 2004), and in other cases of cancer such as leukaemia, Hodgkin lymphoma and nonHodgkin lymphoma (Fernandaz *et al*., 2009, Makin 2014). The role of anthracyclines in treatment of melanoma has also been recently investigated (Hannai *et al*., 2014).

Antimetabolites

Antimetabolites account for 20% of all anti-cancer drugs currently in practice

(Casorelly *et al*., 2012). Methotrexate, mercaptopurine, thioguanine and cytarabine are included in this group. These drugs are structural analogues of natural compounds that are intermediate in synthesis of proteins and nucleic acids, for example, purines and pyramidines (Makin, 2014). These drugs are enzymatically activated to nucleotide metabolites, which results in the formation of faulty DNA when incorporated into nucleic acid during the synthesis process causing cell death or exert inhibitory effects directly on enzymes essential for DNA synthesis. For instance, depletion of cellular tetrahydrofolate due to inhibition of dihyderofolate reductase by methotrexate results in halting DNA synthesis (Casorelly *et al*., 2012; Hess and Khasawneh, 2014). Antimetabolites are being used in a number of haematological cancers such as acute leukaemia and lymphoma (Makin, 2014). Due to their antimetabolite activity, these drugs have been reported to be very productive in both platinum-sensitive and platinum-resistant ovarian cancers

(Walters *et al*., 2013).

Vinca alkaloids

This group of anticancer comprises of vinblastine**,** vincristine, vindesine and vinorelbine (a semi-synthetic vinca alkaloid). Vinblastine and vincristine were first extracted from the leaves of the Madagascar periwinkle (*Catharanthus roseus*) and were initially used as anti-diabetic agents (Noble, 1990). Vinca alkaloids are stated to disrupt microtubule dynamics, arresting cell division at metaphase of mitosis, subsequently causing cell death (Jordan *et al*., 1991; Mukhtar *et al*., 2014). These agents have been shown to be active against gynaecological-like breast and ovarian cancer (Rocha *et al*., 2001). Childhood cancers, retinoblastoma, Hodgkin's disease as

well as brain tumour are some examples of other types of cancer that vinca alkaloids are used to treat (Makin, 2014).

Miscellaneous anti-cancer drugs

There are a number of drugs mentioned in the BNF (2015) under the heading of 'other anti-neoplastic drugs' which includes the following names:

Aflibercept, Arsenic trioxide, Bevacizumab, Bexarotene, Bortezomib, Brentuximab vedotin, Catumaxomab, Cetuximab, Crisantaspase, Dacarbazine, Temozolomide, Eribulin, Hydroxycarbamide, Ipilimumab, Mitotane, Panitumumab, Pentostatin, Pertuzumab, Platinum compounds, Porfimer sodium, Temoporfin, Procarbazine, Protein kinase inhibitors, Taxanes, Topoisomerase inhibitors, Trabectedin, Trastuzumab, Trastuzumab, Emtansine Tretinoin and Vismodegib.

Platinum compounds, especially cisplatin, are of prime importance because they are widely used in a number of cancer types (Deborah *et al*., 1995; Trimmer and Essigmann, 1999; Kelland, 2007, Koizumi *et al*., 2008; Basak *et al*., 2014). Platinum compounds induce cell deaths in cancer cells by interaction with DNA to form adduct which activate signalling pathways to initiate apoptosis (Siddik, 2003)

1.6 Problems with current cancer therapies

The ultimate goal of cancer therapy is to eliminate the disease, increase chances of survival and improve quality of life of patients, but unfortunately despite all the advancements, cancer treatment has failed in its goal in most cases (Segel *et al*., 2012). Conventional cancer strategies have several limitations including low efficacy, life-threatening adverse effects as well as occurrence of drug resistance

(Assaraf *et al*., 2014).

Chemotherapy is the preferred treatment approach for metastatic diseases, but it is not absolutely curative and in some cases prolongs life expectancy only by weeks or months (Glimelius *et al*., 1994; de Gramont *et al*., 2000; NSCLC Meta-Analyses Collaborative Group, 2008). Among several other factors that determine the response of a tumour to a particular treatment modality, the risk of developing multidrug resistance (MDR) to chemotherapeutic agents in cancer patients is a major clinical concern as it limits the efficacy of the therapy (Solyanik, 2010; Bock and Lengauer, 2012). Generally, the efficacy of chemotherapy is determined by the tolerance of a patient to the dose of a particular drug because of the potential nonspecific toxicities at higher doses (Lyman, 2012). Therefore, to avoid toxicities, a subtherapeutic dose is administered which could lead to development of MDR as it allows the cells to gradually adapt to the changing microenvironment (Peetla *et al*., 2013). This defence system is a complex phenomenon, which is either intrinsic (Li *et al*., 2008) or acquired (Wiliting and Dannenberg, 2012), and is based on mechanisms which can be broadly grouped into two types, mechanisms that lead to decreased intracellular level of anti-cancer agents and mechanisms that prevent cell death.

Decreased anti-cancer drugs influx, increased efflux of anti-cancer agents, higher DNA repair rate, epigenetic changes, increasing drug metabolism and detoxification, alteration in drug targets and signal transduction pathways contribute to MDR (Gillet *et al*., 2010; Al-Lazikani *et al*., 2012). Cancer cells decrease intracellular accumulation of the drug in intracellular vesicles by increasing drug efflux via permeability glycoprotein (P-gp), MDR protein 1 and extrusion pumps. Drug resistance against

platinum-drugs is attributed to over expression of excision repair cross-complementation group 1 (ERRC1) activity that promotes DNA repair (Vilmar and Sorensen, 2009). Furthermore, genetic changes in cancer cells such as mutation in p53 genes promotes MDR as mutated p53 genes play a role in survival, growth and evasion of apoptosis in cancer cells (Knappskog and Lonning, 2012).

There are a number of adverse effects related to cancer therapies. Severe nausea and vomiting is a major side effect associated with chemotherapeutic agents, jeopardizing patients' quality of life (Hilarius *et al*., 2012). The extent of nausea and vomiting depends on the type of cancer being treated and the type of chemotherapeutic agent, for example, cisplatin has proved to be severely emotegenic when used in treatment of tumours of gastrointestinal and genitourinary tracts (Okines *et al*., 2010). Other chemotherapeutic agents such as anthracyclines, cyclophosphamide, methotrexate, ifosfamide and carboplatin are also known to induce severe nausea and vomiting (Apro *et al*., 2013). In about 70% of the cases, vomiting is controlled with antiemetics, but the management for nausea still needs further work (Fernandez-Ortega *et al*., 2012). Bone marrow suppression is another life threatening condition associated with chemotherapy and radiotherapy. Bone marrow is a complex and well-regulated microenvironment, which hosts mesenchymal and haematopoietic stem cells. The high proliferative capability of these cells leaves them vulnerable to anti-cancer therapies (Georgiou *et al*., 2012). Suppression of bone marrow is a common toxicity of platinum drugs, antimetabolites, alkylating agents and anthracyclines (Wang *et al*., 2006; Hassett *et al*., 2006; Reis *et*

al., 2007). Haematological disorders resulting from bone marrow suppression in response to chemotherapy have been a limiting factor in cancer treatment, and have eventually led to treatment discontinuation and deaths in severe cases (Muss *et al*., 2007). Alopecia is another distressing side effect of cancer chemotherapy that impacts on the patient's body image, self-confidence and therefore, quality of life (Lyons, 2004; van den Hurk *et al*., 2015). Alopecia is associated with several chemotherapeutic agents, but with some chemotherapeutic agents, for instance doxorubicin, its chances are 80-100% (Trueb, 2009). Chemotherapeutic agents target the anagen phase (growth phase) of hair production because of the rapid multiplication of the cells, thus weakening hair bases which is followed by hair loss (Trueb, 2007). Permanent gonadal failure appears to be caused by alkylating agents in women (Greenhalgh and Symonds,

2014). Heart-related problems (Yeh *et al*., 2004), pulmonary toxicity (Gale *et al*., 2012), neurotoxicity (Grisold *et al*., 2012) are other well-established major side effects of chemotherapeutic agents.

Untoward effects associated with radiotherapy mainly arise for two reasons, firstly, the accidental irradiation of the organs found near the tumorous area and secondly, genetic aberrations as a consequence of irradiation. Women receiving radiotherapy for breast cancer are at higher risk of developing ischemic heart diseases (Darby *et al*., 2013). Similarly, patients treated with malignancies of the pelvic regions end up with malfunctions associated with bowel moments, bladder or genitalia (Adams *et al*., 2014). Genetic aberrations caused by radiotherapy is exemplified by ataxia which

is a syndrome developed by radiation-induced mutation of ataxia telangiectasia mutated (*ATM*) gene (11q22- 23) (Kerns *et al*., 2014). Radiotherapy is also associated with development of secondary cancers, such as leukaemia, which is found commonly in women treated with radiotherapy for cancer of the cervix (Travis *et al*., 2012). Although surgery is helpful in eradiating solid tumours, it has limitations when it comes to cancer metastasis and tumours at anatomically complex sites. Primary tumours in the breast and the surrounding tissues are removed with the help of surgery, however, the undetected tumour deposits in the chest wall and regional lymph nodes are left untreated and a critical recurrence could develop (Early Breast Cancer Trialists' Collaborative Group, 2005). Moreover, extreme precautionary measures are taken during oesophagectomy due the high risk of paralysis of vocal cords, and chances of cardiorespiratory complications have been reported to be high (Mariette *et al*., 2007). The addition of chemotherapy or radiotherapy to surgery to cope with metastasis of the disease not only adds more side effects to the treatment regimen, but also increases the cost of the therapy (Smith and Hilner, 2011).

The above discussion implies the need for new therapeutic compounds with certain characteristics such as high efficacy and target oriented towards cancer cells. The higher the efficacy, the lower the dose and subsequently the reduction in the adverse effects associated with the drug. If cancer cells remain the only targets of the therapeutic agent, the side effects that arise from the general distribution and interaction with normal tissue could be minimised.

Due to diverse biological activities and potential medicines, the contribution of natural products, including both plants and animals, to our health and medicine has been enormous throughout our history. Natural products have been the first choice for drug development since millennia until the last few decades when the drug development became the prime focus of scientist because of the advancements in molecular biology and chemistry to synthesise target oriented molecules. The few years, however, the better understanding of biology and its integration with chemistry has renewed the interest of scientists in natural products. Among natural product, snake venom has become a centre of focus for scientists for the majority of the venom components have evolved to affect physiological systems such as neurological and haemostatic systems as well as local tissues. In addition, the snake venom proteins have more structural stability because of cross-linked cysteines (discussed in detail in section 1.8) and are also target specific (reviewed by Fry *et al*., 2009). Keeping in view these unique properties of snake venom, the following section elaborates on the reasons for why exploration of snake venom for anticancer drugs is an important and evolving approach.

1.7 Rational for exploring snake venom for anticancer drugs

Snake venom is a collection of proteins and peptides, collectively known as toxins (discussed in detail below in section 1.8), which has evolved primarily to immobilise and capture prey as well as to defend against predators (Koh and Kinj, 2012). Envenomation has severe effects on the nervous system, respiratory system, cardiovascular system (CVS), muscles and viability of cells especially of the bitten area

(Casewella *et al*., 2014). The initial interest in snake venom was to understand the mechanism of toxicity in order to develop anti-venom to combat the harmful effects of snakebites, however, due to their physiological effects, the idea of using snake venom in therapeutics emerged in the early 20th century. Although, crude snake venoms have been used in the traditional medicine for centuries, the classic example of drug development on the basis of an understanding of the mechanism of action of a purified toxin was reported in 1975 in the form of captopril, an antihypertensive agent. Since then, many drugs have been in development, utilising isolated snake venom proteins either as a source or as prototypes. The following sections give examples of various snake venom toxins which lead to the development of drugs used in different fields of medicine for various purposes.

1.7.1 Anti-hypertensive agents

It is a well-known fact that bites of some snakes drastically lower blood pressure (BP) in human victims as well as experimental animals (reviewed in Joseph, 2014; de Mesquita *et al*., 1991; Marsh and Whaler, 1978). This effect can be a direct result of the hypotensive agents present in the snake venom or can arise due to coronary ischaemia and pulmonary vascular obstruction (Tibballs, 1998). The direct hypotensive agents in the snake venom are of particular interest because of potential drug development for the treatment of hypertension. One example includes bradykinin-potentiating peptides (BPPs). BPPs mediate the hypotensive effect through vasodilation. The presence of BPPs in snake venom was reported in *Bothrops jararaca* venom (Ferreira, 1965). A series of BPPs analogues were studied and

ultimately a pentapeptide was selected as the lead compound (Cushman *et al*., 1973). A final substitution of sulfhdryl on the molecule resulted in captopril (Cushman and Ondetti, 1999) which was previously regarded as the first choice antihypertensive agent (Smith and Ashiya, 2007). Natriuretic peptides (peptides that induce secretion of sodium in urine; NP) belong to another group of widely used antihypertensive agents. NPs are hormones that are released from the cells in the myocardium in response to myocardial mechanical stress and decrease BP by inducing diuresis (Kinnunen *et al*., 1993). Snake venom is one of the main sources of NPs. The first venom source for NP was reported to be *Dendraospis angusticeps*, a green mamba, and was called Dendroaspis NP (DNP) (Schweitz *et al*., 1992). Later on, NPs from many different snakes were reported, such as *Micrurus corallinus* (Hoet al., 1997), *Pseudocerastes persicus* (Amininasab *et al*., 2004), *Crotalus durissus cascavella* (Evangelista *et al*., 2008) and *Bungarus flaviceps* (Siang *et al*., 2010).

1.7.2 Hemostasis related agents

The flow of blood to essential organs is necessary for survival, however, in the case of blood vessel rupture, spontaneous arrest of blood flow is required in order to stop blood loss; a process referred to as hemostasis (Jackson and Nemerson, 1980). Hemostasis is a complex cascade involving several processes including vasoconstriction, platelet activation/aggregation, fibrinolysis and blood coagulation. When the blood vessels are ruptured, platelets are activated by certain factors including collagen, ADP and thrombin (Shenkman *et al*., 2000; Connolly *et al*., 1992). The platelet aggregation occurs as a result of interaction between fibrinogen and

integrin on the platelet surface (D'Souza *et al*., 1991). However, functional aberrations in platelets can lead to various thrombotic disorders such as stroke and myocardial infarction (Witt *et al*., 2014; Wilson and Ferguson, 1999). Therefore, antiplatelet agents, especially disintegrins, gained reputation as the cornerstone for the clinical management of cases related to arterial thrombosis (Eikelboom and Hirsh, 2007; Packham and Mustard, 1986). Disintegrins are a group of low molecular weight and cysteine-rich proteins (discussed in detail below in section 1.8.6). These proteins were initially extracted from vipers venom that typically contain arginine-glycine-aspartic acid (RGD) motif for binding to integrins (Gan *et al*., 1988; Shebuski *et al*., 1989; Scarborough *et al*., 1991), however, motifs of different peptide sequences including lysine-glycine-aspartic acid (KGD), glutamic acid-cysteine-aspartic acid (ECD), methionine-leucine-aspartic acid (MLD) were also reported in later studies (McLane *et al*., 2004; Calvete *et al*, 2005). Two antiplatelet agents, Tirofiban and Eptifibatide, available in the market under the name Aggrastat® and Integrillin®, respectively, were developed based on disintegrins isolated from snake venom. Tirofiban was designed according to the RGD motif of a disintegrin, echistatin, purified from the venom of *Echis carinatus* (Saudek *et al*., 1991). Eptifibatide was designed on the basis of barbourin, a $\alpha_{IIb}\beta_3$-specific integrin from *Sistrurus miliarius barbouri* (Scarborough *et al*., 1991).

In addition, snake venoms abundantly contain proteins that play a role in blood coagulation and can be potentially used as pro- and anti-coagulants agents. Enzymes present in snake venom that activate some of the coagulation factors through proteolysis are regarded as pro-coagulants. Snake venom pro-coagulants are

classified functionally, such as thrombin-like enzymes (TLE), factor X activating agents and factor V activators (reviewed in Lu *et al*., 2005). However, both enzymes (phospholipases, serine proteinases, metalloproteinases) and non-enzymes proteins (e.g., lectin-like proteins) comprise the anti-coagulant agents (reviewed in Kini, 2006). Regardless of the anti-coagulant effects of TLE, a combination of TLE with thromboplastin-like enzyme, from the venom of *Bothrops atrox*, forms a product known as Haemocoagulase® is used for the treatment of haemorrhage (Koh and Kini, 2012; Koh *et al*., 2006).

1.7.3 Analgesics

Chronic pain management is a challenging field of medicine as the currently available drug options failed to produce satisfactory outcome in many patients. The investigation of snake venom toxins can be traced back to 1937 where cobra venom was used as an analgesic in treatment of cancer associated pain (Macht *et al*., 1937) and since then snake venom has been thoroughly examined for potential analgesics. A unique characteristic observed in venom-based analgesics is the ability to block essential factors of the pain pathway, such as ion channels (Gazerani and Caris, 2014). One example of snake venom based lead analgesic is Prohanin, the design of which is based on a peptide from the venom of king cobra (*O. hannah*) (Pu *et al*., 1995) and was pursued by Theralpha SAS company as a potential pain treatment (Harvey, 2014). A 3 kDa component from the venom of *Crotalus durissus terrificus* was isolated and was shown to induce analgesia in mice by acting on the opioid receptors and K^+ channels (Giorgi *et al*., 1993). A product known as crotalphine has

been developed on the basis of this peptide and is currently under study and has some advantages over opioids such as development of tolerance, dependence and lack of withdrawal symptoms upon cessation of therapy (Machado *et al*., 2014).

Keeping in view the fact that snake venom, and peptides derived from it, have proved to have pharmacological activities, it is pertinent to further explore the components of snake venom and elaborate the pharmacology associated with them to have some insight into their potential anti-cancer uses as indicated in many studies. Disintegrins derived from snake venom have shown anticancer potential against certain cancer cells characteristics such as proliferation, cancer associated angiogenesis and metastasis (revieved by Koh and Kini, 2012). Examples of such snake venom disintegrins include contortrostatin, extracted from *Agkistrodon contortrix contortrix* venom which binds to integrins, for examples, $\alpha_{IIb}\beta_3$, $\alpha_v\beta_3$, $\alpha_5\beta_1$ and effectively inhibited metastasis and angiogenesis in a human melanoma cell line, M24 (Trikha *et al*., 1994) as well as in ovarian (Markland *et al*., 2001) and breast cancer cell lines (Swenson *et al*., 2004). The cytotoxic effects of snake venom proteins and peptides in various human cancer cell lines is also well documented (reviewed in Vyas *et al*., 2013; Souza *et al*., 1999; Suhr and Kim, 1996), which further supports the concept of examining snake venom for possible drug leads.

1.8 Characterized snake venom components

Snake venom is a rich source of pharmacologically active compounds. It is difficult to predict the actual number of pharmacologically active compounds produced by snakes (Georgieva *et al.,* 2010), but according to an estimate there are around 90,000

proteins/peptides found in the venom of about 2,200 different species of snakes (King, 2011). Generally, snake venom contains up to 90-95% proteins and peptides, while the remaining portion is a mixture of compounds attached to these proteins, for example, amino acids, nucleotides, lipids, carbohydrates and some metallic elements (Lima *et al.,* 2005). The protein part of the venom is a mixture of enzymatic and non-enzymatic components (Kang *et al*., 2011).

The following sections highlight the enzymatic proteins, their structures and mechanism of substrate metabolism.

1.8.1 Acetylcholine esterases (AChEs)

The biological role of AChE in the venom involves acetylcholine metabolism by hydrolysing the ester linkage in the ACh structure producing choline and an acetate group, resulting in the termination of cholinergic neurotransmission at neuronal as well as neuromuscular synapses and prey paralysis (Silman and Sussman, 2008).

AChE was reported for the first time in cobra venom by Lyenger *et al.* in 1938. Copious amounts of AChE are found in the venom of most snakes, but it is particularly abundant in the venom of the species of the Elapidae family [e.g., *Naja haje* (Egyptian cobra)]. However, AChE is present to a lesser extent in the venom of snakes belonging to the Viperdae [*Agkistrodon contortrix* (Southern copperhead)] and Crotalidae [*Crotalus scutulatus scutulatus* (Mojave rattlesnake)] families (Frobert *et al.*, 1997).

1.8.2 Structure of AChE

The structure of AChE purified from the venom of *Bungarus fasciatus* (Banded krait) has been elaborated by Frobert *et al.*, in 1997. There is a cleft in the catalytic site of

the AChE molecule, which is 20 angstroms deep and is lined by 14 aromatic residues. The active site of the cleft consists of an anionic site to bind quaternary ammonium groups and an esteric site to bind acyl-groups (Figure. 1.9).

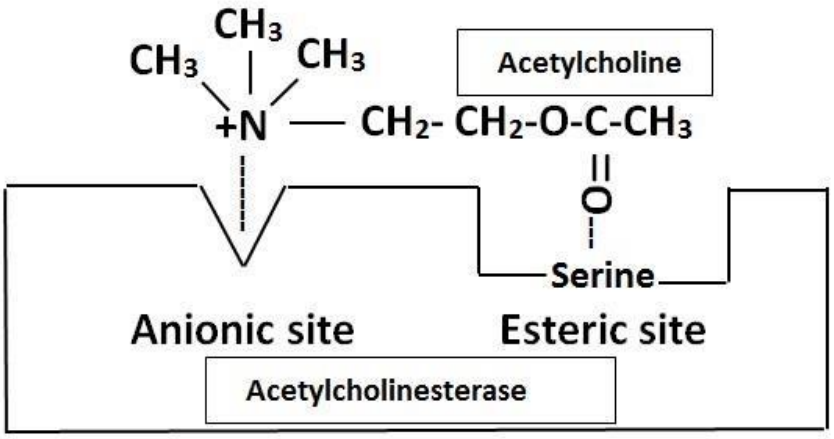

Figure 1.10: AchE structure: structure of AChE, showing the anionic site for quaternary ammonium group binding and an esteric site to attach to the acyl group of Ach.

1.8.2.1 Mechanism of action of AChEs

This catalysis of AChE is brought about in the cleft of the catalytic site of the enzyme. The aromatic residues linning the cleft play an important role in pushing the substrate of AChE into the cleft where it is hydrolysed (Felder *et al*., 1997). This chemical reaction is summarised in the following Figure 1.10.

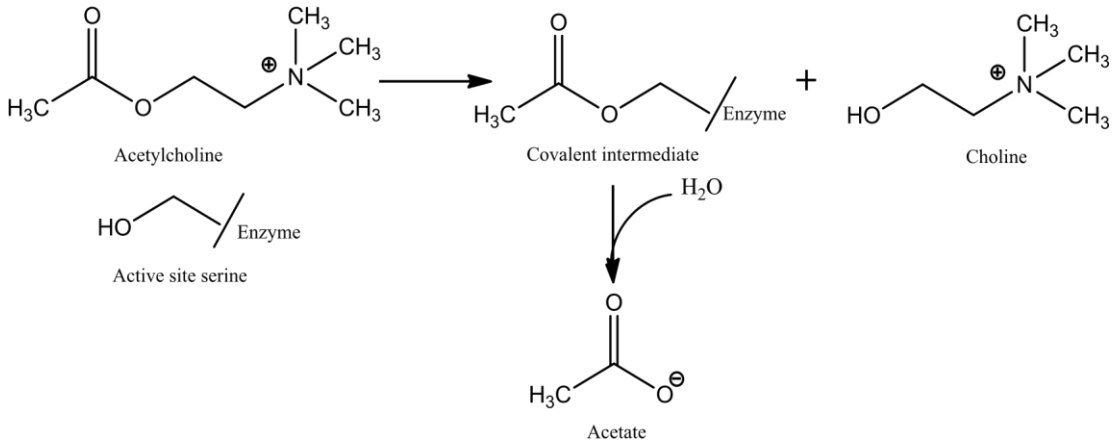

Figure 1.11: Catalytic action of AchE: A chemical reaction showing the catalysis of Ach by AchE, producing an intermediate and consequently the final products of the reaction.

1.8.3 L-amino acid oxidases (LAAOs)

LAAOs are flavoenzymes that are responsible for removal of the amino group from L-amino acids through stereospecific oxidation in order to produce the respective αketo acid and ammonia. These enzymes account for the yellow colour of the venom and contribute to the cytotoxicity at the bite site and inhibition of collagen/ADPdependant platelet aggregation (Wei *et al*., 2002). These enzymes are found abundantly in nature, but snakes are considered to be a highly productive source.

LAAO has been isolated from various species of snakes, e.g., *Bothrops pauloensis* (Rodrigues *et al*., 2009), *Phiophagus hannah* (Jin *et al*., 2007), *Calloselasma rhodostoma* (Ponnudurai *et al*., 1994) and *Crotalus adamamanteus* (Massey and Curti, 1966). These enzymes usually constitute about 1-4% of the weight of dried snake venom. Among the snake species, *Calloselasma rhodostom*, the Malayan pit viper, is thought to be the richest source of LAAO where it is present in 30% by weight of the dried venom (Tan, 1998). Biological effects associated with snake venom LAAO

upon envenomation includes excessive edema along with slight haemorrhage (Tan and Choy, 1994) which was later on claimed to be in response to the inflammatory reaction activated by H_2O_2 (Izidoro *et al*., 2006). Snake venom LAAO has a complex role in platelet aggregation because there are reports showing that snake venom LAAO induce platelet aggregation (Stábeli *et* al., 2004; Lu *et* al., 2002) but the inhibitory effects of LAAO on platelet aggregation has been claimed by other research groups (Takatsuka *et* al., 2001; Sakurai *et* al., 2001). Apoptotic activity has also been associated with LAAO which is evident by tissue damage at the bite site. Most of the snake venom LAAO induced biological effects are attributed to H_2O_2 production, however, the role of H_2O_2 in apoptosis induction in response to LAAO is not well understood as in some cases ROS scavenger inhibits cell death (Torii *et al*., 1997) whereas apoptosis in cells has also been observed regardless of the presence of ROS scavenger, catalase, suggesting the LAAO related apoptotic activity is not solely H_2O_2 dependant (Ande *et al*., 2006; Suhr and Kim, 1999; Suhr and Kim, 1996).

1.8.3.1 Structure of LAAO

The 3-D structure of LAAO was first reported by Pawelek *et al.* (2000). They elucidated the structure of LAAO from *Calloselasma rhodostom,* providing evidence for the sites of substrate binding and catalytic sites of the enzyme. Their data suggest that functionally this enzyme is a dimer formed by two protomers, each of 55 kDa and consisting of 15 α-helices and 22 β-helices all of which are folded to give three well-defined domains; flavin adenine dinucleotide (FAD) domain (responsible for the yellow colour of the venom), substrate binding domain and a helical domain.

Stabeli *et al*., 2004, isolated and characterised an isoform of LAAO from *Bothrops alternatus* (crossed pit viper). However, the amino acid sequencing of this isoform was found to be substantially the same to the amino acid sequencing of the reported LAAO from other snake venom.

1.8.3.2 Mechanism of LAAO activity

The oxidation of L-amino acids can chemically be divided into two half reactions, reductive half reaction and hydrolysis. In the first step, FAD reduces L-amino acid to produce an intermediate α-imino acid. The second reaction is the hydrolysis of the intermediate to give the respective α-keto acid and ammonia. This reaction can be summarised as follows (Kang *et al.*, 2011).

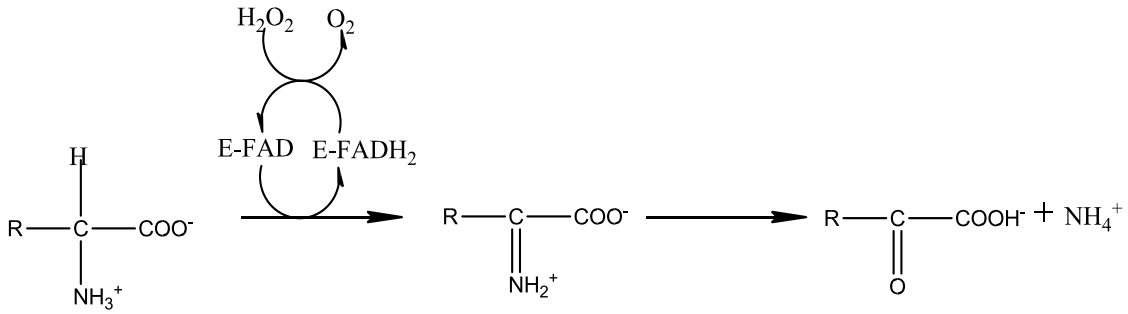

Figure 1.12: **metabolism of L-amino acid by LAAO**. A general chemical reaction of the enzymatic activity of LAAO to give the intermediate α-imno acid which goes on to produce α-keto acid and ammonia.

1.8.4 Phospholipases (PLA_2)

PLA_2s are lypolytic enzymes belonging to a superfamily of enzymes, which catalyse the hydrolysis of the ester bond in glycerophospholipids, resulting in the generation of fatty acids and lysophospholipids (Funk, 2001). These enzymes are responsible for

a variety of biological outcomes in the case of snake bite such edema, tissue necrosis, neurotoxicity and myotoxicity (Kanashiro *et al*., 2002).

Snake venom PLA_2s are a vast superfamily of enzymes, which is divided further into many different groups on the basis of different enzyme structures. Broadly, they are classified into 2 groups, Group-I and Group-II, which are further subdivided into many subgroups according to their functional and structural characteristics (reviewed by Kang *et al*., 2011). Group-I consists of enzymes from elapid and colubrid snakes, and mammalian pancreas. PLA_2s belonging to this group have 115120 amino acids. Group-II enzymes typically have 120-125 amino acids in their structures and mainly comprise PLA_2 from Viperidae snakes. These groups have subgroups based on the number of amino acids and difference in catalytic sites. Another classification of the PLA_2 is division of the enzymes into classes such as secreted PLA_2, cytosolic PLA_2, Ca^{2+} independent and lipoproteins-associated PLA_2 (Burke and Dennis, 2009).

1.8.4.1 Structure of PLA_2

Generally, snake venom PLA_2s are found as either a single chain polypeptide of approximately 115-125 amino acids or a combination of 2-5 complementary polypeptides. Generally, their structures contain seven disulphide bonds between cysteine 11-72, 27-119, 29-45, 44-100, 51-93, 61-86 and 79-91. The crystal structures of venom PLA_2s show three helices, H1 (helix 1) at residues 2-12, H2 at 40-55 and H3 86-103 and two 3_{10} short helices at 19-22 and 108-110. Venom PLA_2s also have two short antiparallel β-strands at 70-74 and 76-79. Two oxygen atoms in the carboxylate molecule of Asp49, three oxygen atoms of Tyr28, Gly30 and Gly32 and oxygen atoms

in the water molecules form pentagonal coordinates that balance the Ca^{2+} in the structure of PLA_2s. The site that binds to the ligand of the substrate consists of residues Leu2, Phe5, I1e9, Ala23, Tyr65, Phe22, Gly30 and

Ala23, while His48, Asp49, Asp94 and Try52 form the active site of the enzyme

(Kang *et al*., 2011).

1.8.4.2 Mechanism of PLA_2 action

The overall catalytic action of PLA_2 on glycerophospholipids, e.g., tridecanoic acid, is the production of arachidonic acid and lysophospholipid. The glycerol backbone of a phospholipid is hydrolysed at the sn-2 position to produce these products and the conserved water molecule acts as a nucleophile to hydrolyse the main bond of its substrate (Koh *et al.*, 2006). The complete chemical reaction is shown in the below.

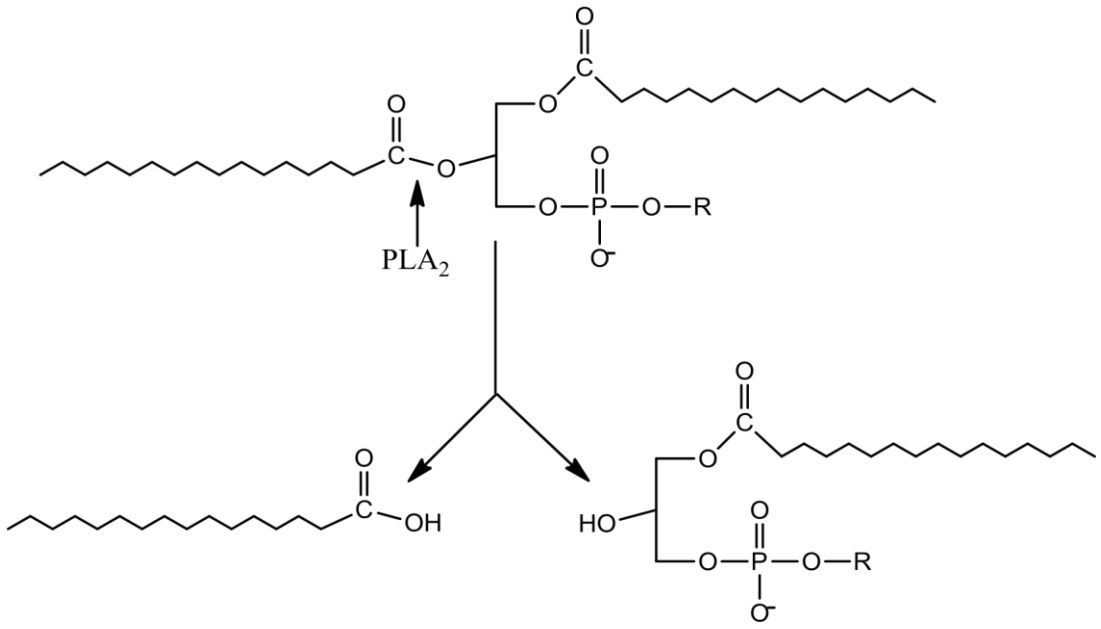

Figure 1.13: Catalysis of glycerophospholipids by PLA_2.

1.8.5 Snake venom metalloproteinase (SVMP)

These enzymes are basically responsible for haemorrhagic activities. They not only induce local and systemic bleeding, but also interfere with the haemostasis mediated by procoagulant effects or platelet aggregation and pro-inflammatory activities (Kang *et al,* 2010).

1.8.5.1 Structure of SVMP

SVMPs range in size from 20-100 kDa. On the basis of their domain organisation they are grouped into three classes, P-I, P-II and P-III. P-I SVMPs contain only a metalloproteinase domain (M domain), while P-II contains a disintegrin domain (D domain) along with a M domain; whereas P-III contains an additional cysteine-rich (C) domain to M and D domains (Fox and Serrano, 2008).

There are 200-210 residues in the catalytic M domain of SVMPs (Fox and Serrano, 2005). On the flat side of the M domain there is a notch that separates the lower domain from the upper molecular body. There is another cleft in the active site of these enzymes which is a peptide substrate binding site and also possesses a catalytically active zinc ion (Takeda *et al*., 2012).

1.8.5.2 Mechanism of action of SVMP

The mechanism through which SVMPs bring about their action is being investigated at gross and molecular levels, but the exact molecular and cellular events taking place in this process has not been fully elucidated (Markland and Swenson, 2013). However, it has been proposed that these enzymes degrade the basement membrane of the vasculature to initiate the disruption of capillaries. This is achieved

by hydrolysing the four basic components of the basement membrane, namely type IV collagen, perlecan, nidogen and laminin that provides structural support to the vasculature. This hypothesis is supported by *in vitro* degradation of these components of the vascular basement membrane by SVMPs (Barramova *et al.*, 1986).

1.8.6 Pharmacologically active non-enzymatic snake venom proteins

Disintegrins comprise the non-enzymatic part of snake venom proteins which are low molecular weight proteins found in the venom of many snakes. Their molecular weights range from 4-15 kDa (Galan *et al.*, 2008). Distintegrins are found abundantly in the venoms of snakes from four families, Atractaspididae (mole vipers), Elapidae (family of King Cobra), Viperidae (vipers) and Colubridae (Sanchez *et al*., 2008).

1.8.6.1 General structure

The disintegrins family includes a vast group of cysteine-rich small polypeptides (40100 amino acids) produced by the proteolysis of PII SVMPs (Kini and Evans, 1992). Disintegrins have disulphide linkages, which confer them their 3-D structure. Most disintegrins have RGD as their binding motif near the C-terminal, however, KGD has also been reported in many cases (Okuda *et al*., 2002).

On the basis of the number of amino acid residues and number of cysteines, disintegrins are classified into three classes (Kim *et al*., 2005):

i) Short disintegrins: 41-51 amino acids and 8 cysteines.

ii) Medium disintegrins: up to 70 disintegrins and 12 cysteines.

iii) Long disintegrins: usually have up to 84 amino acids and 14 cysteines.

Examples of disintegrins include:

1.8.6.2 Crotatroxin 2

Crotatroxin 2 is a 7384 kDa protein having 71 amino acids. It is found in the venom of *Crotalus atrox,* a snake commonly known as Western diamondback rattlesnake. It has been shown by Galan *et al*. (2008), that it blocks platelet aggregation by an ADP-induced mechanism. It has also been shown to inhibit migration of murine cells. This disintegrin seems to bind to integrins β_1, α_v and α_{IIb} which are expressed by murine cells and are thought to be involved in cell migration (Raso *et al*., 2001; Trikha *et al*., 2002).

1.8.6.3 r-mojastin 1

This disintegrin is obtained from the venom of Mohave rattlesnake, *Crotalus scutulatus scutulatus,* from southwestern U.S. It has shown inhibitory effects on adhesion, migration and cancer cell invasion by binding to integrins $\alpha_1\beta_1$ and $\alpha_5\beta_{1;}$ $\alpha_3\beta_{1;}$ and $\alpha_v\beta_{5,}$ respectively (Lucena *et al*., 2011).

1.8.6.4 Colombistatin

Colombistatin is a distintegrin found in the venom of *Bothrops colombiensis*, Mapanre, which is the largest snake found in the forests of Venezuela. Its molecular mass is 7.8 kDa. Colombistatin stops cell-cell interaction, cell-matirx interaction and cell signal transduction (Sanchez *et al*., 2009). Markland and Zhou (2002) have shown that colombistatin blocks the metastasis of human urinary bladder cells (T24) by blocking integrins $\alpha_v\beta_3$ and $\alpha_v\beta_5$ which are expressed on these cells. Older studies

indicate that other integrin subunits such as α_2, α_3, α_5, α_6, α_v, β_1, β_3 and β_4 could be targets of colombistatin (karuda *et al*., 1993).

1.8.6.5 Contortrostatin

Contortrostatin is a disintegrin found in the venom of *Agkistrodon contortrix contortrix,* a snake commonly known as Southern copperheaded snake, from United States. It is a protein of molecular mass 13500 kDa and has the RGD sequence in its active site (Trikha et al., 1994). Several studies indicate that it is a potent inhibitor of angiogenesis. It was shown earlier that VEGF initiates angiogenesis by activating various integrins including $\alpha_2\beta_1$, $\alpha_5\beta_1$, $\alpha_v\beta_5$, and, $\alpha_v\beta_3$, the most important and active of which is $\alpha_v\beta_3$, making it the primary target for the inhibition of angiogenesis (Byzova *et al*., 2000). Zhou *et al*., (2000), proved that contortrostatin blocked tube formation of human umbilical vein endothelial cells.

1.9 Project aims

This project aims to elaborate anti-cancer properties of rattlesnake venoms with a view to identifying suitable candidates for drug discovery. Venom from *Crotalus adamanteus* (Cad, eastern diamondback rattle snake), and *Crotalus scutulatus scutulatus* (Css, mojave snake) were examined against two types of cancer cell lines, namely, human skin melanoma (A375) and human ovarian carcinoma (A2780), compared with a human non-cancer prostate epithelial cell line (PNT2a) to determine the selectivity of the venom between cancer and non-cancer cells. The potency of the venom was also compared with the anti-cancer drug cisplatin.

Cad/Css were selected because the venom of the snakes are well characterised in terms of biology, chemistry and pharmacology. Amino acid sequencing and structures of the active sites are well established. Despite the evidence of the presence of many pharmacologically active proteins in Cad/Css venom, this project focused on LAAO because, as indicated by the literature and the yellow colour,

LAAO apparently constitutes a larger part of the Cad/Css venom and so the biology and Cad/Css associated pharmacological activities can be attributed to these enzymes. Secondly, compared with other venoms, fractionation of the venom is easier and the conventional methods of fractionation suffice to separate the components of the Cad/Css venom to a high degree of purity. Although the pharmacology associated with the LAAO from Cad/Css is well reported, some more research is required to further elaborate the mechanism underlyjng the LAAO related pharmacology. For instance, to establish the mode of LAAO induced cytotoxicity, pathways of cell death progression and role of H_2O_2, are controversial and need more detailed insight into these processes. Therefore, the objective of this project was to further elaborate the LAAO pharmacology. Similarly, the cell lines used in this project also have well-established morphological, genetic and biochemical profiles. All the cell lines have a doubling time of 24 h which suited the time scale of the experiments. Also, the cell lines are adherent to polystyrene assay plates and no plate-coating for cellular adhesion was required which was very convenient. From a pharmacology point of view, these cell lines have been used in numerous cancer researches and have been shown to demonstrate apoptosis, necrosis and autophagy. Initially the pathway of cell death induced by Cad/Css was unknown and cell lines that have

expressed the three main types of cell death were required for this project. Cisplatin was chosen because of its wide clinical use in cancer and research. Also, the handling of the drug is easy and can be stored in an amber bottle on a shelf at room temperature as compared to other formulations which require specific temperatures and light conditions for storage.

The following points highlight the overall aims of this project:

- To determine cytotoxicity of crude venom against A375 and A2780 (ovarian) cell lines.
- To determine the selectivity of cytotoxicity of the crude venoms against PNT2a non-cancer cells.
- To compare the potency of both venoms with the anti-cancer drug, cisplastin.
- To fractionate the venom and characterise the active components in the venom by:
    - SDS-PAGE
    - Gel filtration chromatography ○ Ion-exchange chromatography ○ Amino acid sequencing
- To establish the mechanism of cell death induced using various techniques such as:
    - Microscopy ○ Sytox® Green assay, ○ Caspase3/7 assay, ○ Mitochondrial membrane potential

determination, ○ Confirmation of DNA damage ○

Western blotting

2. Isolation, Identification, and characterisation of the active component from whole venom

2.1 Introduction

Snake venom consists of a mixture of hundreds of pharmacologically active enzymatic/non-enzymatic proteins with different pharmacological implications. In order to understand and evaluate the role of specific components, separation, isolation and concentration of the components to an appropriate working concentration is necessary. Different techniques are used to purify the components which can be broadly classified into two types: conventional methods and secondgeneration sequencing technologies. Conventional methods include size exclusion chromatography, ion-exchange chromatography, reverse-phase chromatography and electrophoresis. These conventional bioprospecting methods rely on bioactivity-guided fractionation of the venom. Despite the fact that these techniques are time consuming and usually require large amounts of venom samples, the conventional procedures still remain successful and are widely used. The more recent second-generation analytical techniques are used for better understanding of molecular properties of venom components and help in structural elucidation of the proteins. Mass spectroscopy (MS) is the method of choice for analysis of the complexity of venom. Various MS approaches such as liquid chromatography-mass spectroscopy (LC-MS), matrix-assisted laser desorptionionization (MALDI) and electrospray ionisation (ESI) are exploited to further elucidate the complex molecular properties of the venom proteins. For structure elucidation, the main technique used is nuclear magnetic resonance (NMR). This technique is utilised to determine the

nature and number of atoms present in a compound and their influence on the surrounding chemical environment.

The techniques used in this study for isolation and functional characterisation are briefly discussed below:

2.1.1 LAAO activity assay

As discussed previously, LAAO are enzymes that are responsible for stereospecific metabolism of L-isomers of amino acids. L-leucine (L-Leu) is broadly used in assays to establish LAAO activity of a sample in an enzyme coupled reaction (Naumann *et al*., 2010; Izidoro *et al*., 2006). The underlying principle of the assay is that the byproduct, H_2O_2, which is produced from L-Leu metabolism by LAAO, catalyses the metabolism of o-phenylenediamine (OPD) by peroxidases from horseradish (HRP) to produce a fluorescent substrate (Figure 2.1).

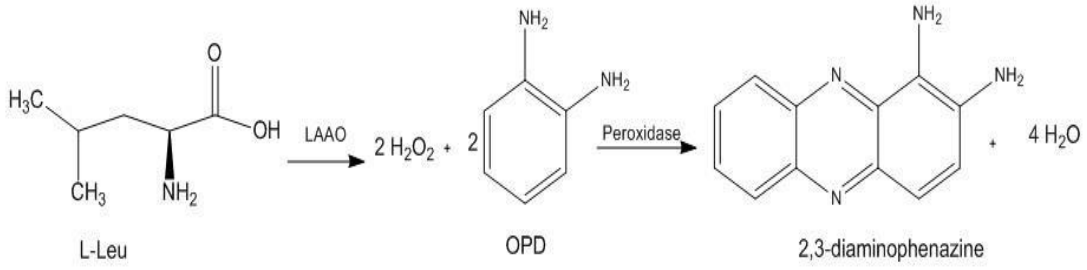

Figure 2.1: Catalysis of L-leucine and OPD: The metabolism of OPD catalysed by H_2O_2 produced by LAAO action on L-leucine, the principle used to determine LAAO activity of venom samples.

2.1.2 Determination protein concentration

Determination of protein content of samples obtained from fractionation of venom is necessary in order to accurately establish the therapeutic activity of the sample in

terms of bioactivity of the protein per unit weight of the protein. The Bradford protein assay, originally developed by Bradford (1976), is a widely used technique for the determination of the protein concentration in a sample, binding of proteins to a dye through formation of ionic linkages (Zor and Selinger, 1996). The Bradford reagent includes Coomassie G-250 dye which exists in anionic, cationic and neutral form. When the dye binds to proteins, it converts to a stable form (blue) which is spectrophotometrically detected at 595 nm. This assay is sensitive enough determine 50 ng of BSA in 0.25 mL assay solution in a microplate (Zor and Selinger, 1996).

2.1.3 Fractionation of whole venom

Size exclusion chromatography was used to separate the major fractions present in the Cad and Css whole venom.

Size exclusion/gel filtration chromatography (SEC) separates molecules according to the variation in their sizes as the sample passes through the separation mesh provided by the gel packed in a column. The gel is formed by beads bearing pores of different size distribution. Different materials are used to provide the separation medium, for example, silica, agarose, polyacrylamide and the most widely used sephadex. Ideally, the separating medium has no interaction with the proteins that are separated. Depending upon the pore size distribution, there are different types of sephadex which are used for separation of different range of molecular sizes such as G10 (100-800 Da), G50 (1,500-30,000 Da), G75 (3,000-80,000 Da), G100 (4,000150,000 Da). An elution profile or chromatogram that shows the difference in concentration of chromophores present in the components, based on UV absorption

($\lambda_{280\ nm}$), as they are eluted from the column in order of decreasing molecular sizes. The gel in the column forms a matrix of various pore sizes. Large components cannot enter the matrix and elute almost with the void volume, whereas components that have partial or full access to the matrix are released from the column in decreasing order of molecular sizes as the mobile phase passes through the column. The separated components are then collected either at regular time intervals or peaks as they appear on the chromatogram.

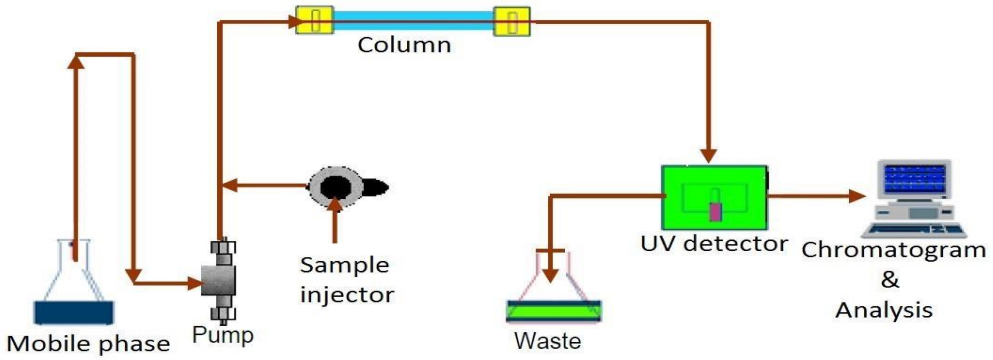

Figure 2.2: Gel chromatography flowchart: A schematic representation of chromatography showing the functional sequence and interconnection of the various parts of the system.

2.1.4 Ion exchange chromatography

Ion exchange chromatography (IEC) is a widely used binary gradient separation technique for the purification of charged molecules. The difference in the net surface charge of the molecules is the underlying principle of IEC separation. For IEC, the separating medium present in the column has a net charge which is opposite to the charge of the sample that engages in a reversible interaction with the charged molecules of the sample. To have optimal binding of the charged molecules, the mobile phase changes from low to high salt concentration which accordingly changes

the conductivity from low to high. The separating medium facilitates adsorption of the sample molecules bearing opposite charge by the interaction between the ionic groups on the sample molecule and the separating medium. The strength of these ionic interactions is determined by location as well as the number of the charges on both the sample molecules and separating medium. By applying a linear salt gradient to the column, molecules with the weakest charge elute first, whereas molecules with a stronger interaction with the separating medium require relatively higher salt concentration and elute gradually as the gradient increases.

There are two types of IEC based on the type of charge that the separating medium bears. If the separating medium is negative and thus attracts positively charged moieties, the IEC is referred to as cation exchange chromatography (CEC) and in contrast, if the medium offers positive charge to attract negatively charged sample molecules, it is known as anion exchange chromatography (AEC).

2.1.5 Sodium dodecyl sulphate-polyacrylamide gel electrophoresis

Gel electrophoresis is a useful technique to provide some insight into the purity as well as the range of molecular weights of the protein samples. The word electrophoresis refers to the separation of charged molecules as a result of their movement in an electric field. In order to separate proteins only on the basis of their sizes, they must have a uniform charge to respond equally to the applied electric field. For this purpose, they are denatured by removing their secondary, tertiary or quaternary structure which is achieved by introducing sodium dodecyl sulphate (SDS)

to the medium. Therefore, the native charge of the proteins is masked by the negative charge of SDS and all the proteins in the system express the same charge. When the denatured proteins are subjected to a gel system of various pore sizes and an electric field is applied, the gel serves as a molecular sieve, hindering the movement of the proteins depending on their sizes as they move towards the anode. When this process is carried out on a polymerised acrylamide gel, the system is known as SDS-polyacrylamide electrophoresis or SDS-PAGE. The size of the protein can be estimated by comparing the distance covered by the protein to that of a marker of known molecular weight, which is subjected to the gel along with the sample proteins whereas purity of the sample is reflected by the number of bands appeared on the gel.

2.2 Aims and objectives

This chapter deals with the isolation and identification of the active proteins in venom from Cad and Css, as well as the reactivation and preservation of the activities of the isolated active components and later on, the characterisation of the active components.

Since LAAO are present in abundance in snake venom, firstly the LAAO activity of Cad and Css whole venom was determined to confirm the presence of these enzymes. As opposed to the traditional approach, the fractionation was then based on the enzymatic activity detection rather than the cytotoxicity of the fractions.

Conventional separation techniques were used to fractionate the venom first until the enzymatically active fraction was purified and the purity was confirmed by

electrophoresis. Protein concentration of all the fractions was determined before the enzyme activity assay and electrophoresis to ensure that equal amounts of proteins were assayed. The molecular ranges as well as the purity of the fractions and subfractions were established with help of electrophoresis. The last step was amino acid sequencing of the active fraction to identify the protein.

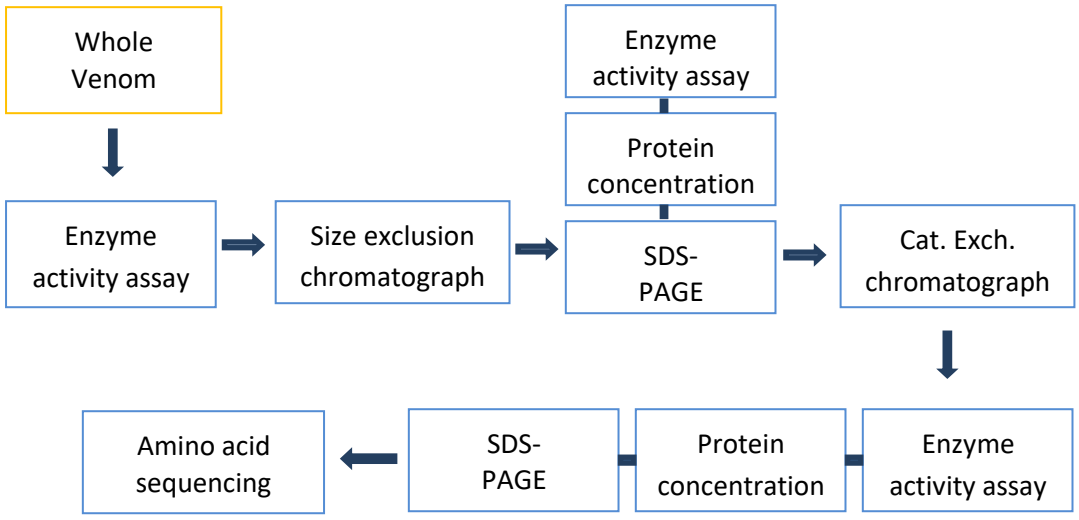

Figure 2.3: Isolation of the active component: A flow chart showing a combination of subsequent techniques that were used to isolate and characterize the active components from Cad and Css venom.

2.3 Materials

The following materials were used in isolation and purification of LAAO from whole venom.

Table 2.1: List of material: Table enlisting all the material used along with details of the supplier and product batch number.

Product	Supplier	Batch No
Ammonium Acetate (AmAc)	Calbiochem, UK	A1542-500G
Bio-safe Coomassie G250 stain	Bio-Rad Laboratories Incorporation	161-0786
Cad whole venom	National Natural Research Centre, Kingsville, Texas, USA	AVID # 011-544-607
CM Sephadex™ C-50	GE Healthcare Life sciences	17-0220-01
criterion TGX stain-free precast any-kDa gels	Bio-Rad Laboratories Incorporation	567-8124
Css whole venom	National Natural Research Centre, Kingsville, Texas, USA	AVID # 010-374-583
NuPAGE LDS buffer	Invitrogen	NP0007
o-phenylenediamine dihydrochloride (OPD)	Sigma-Aldrich Company Ltd	P9029-50G
peroxidase from horseradish	Sigma-Aldrich Company Ltd	777332-100MG
Precision Plus Protein® Dual Colour Standard	Bio-Rad Laboratories Incorporation	161-0394
Quick Start™ Bradford assay kit	Bio-Rad Laboratories Incorporation	500-0205
Sephadex G-75	Sigma-Aldrich Company Ltd	G7550-50G
Sodium azide	Sigma-Aldrich Company Ltd	S-2002
Sodium chloride (NaCl)	VWR Chemicals, UK	2145
Tris/Glysin/SDS buffer (10x)	Bio-Rad Laboratories Incorporation	161-0732
trizma base	Sigma-Aldrich Company Ltd	T-1503

2.4 Fractionation of whole venom

2.4.1 Size exclusion chromatography

The chromatographic assembly consisted of a Shimadzu LC-6A liquid chromatography pump controller, Shimadzu SCL-6B system controller, Rheodyne model 7725 injector with a 1ml loading loop, Shimadzu SPD-6A UV spectrophotometric detector and Pharmacia LKB.FRAC.100 fraction collector and a desktop computer running Microsoft XP operating system for fraction detection and generation of chromatogram.

Sephadex G-75 gel for the column was prepared by soaking 13.3 g of sephadex G-75 in 200 mL 0.1 ammonium acetate (AmAc) and left overnight for the beads to swell. The gel was autoclaved at 121 ˚C for 20 min under 15 psi to achieve sterilisation. The gel was then loaded on to an Omni column of 1000 mm length and 20 mm internal diameter. Precautions were taken to avoid trapping air bubbles as that would interfere with the movement pattern of the samples through the column. After loading, the gel was allowed to settle in the column. The column was then equilibrated with 3 column volumes (CV) of the mobile phase at a flow rate of 0.3 mL/min.

2.4.2 Preparation, fractionation and collection of venom for SEC

The venom was prepared by dissolving 100 mg of the whole venom in 1 mL of the mobile phase and vortexed (WhirliMixer) for at least one minute. This step was followed by centrifugation (Micro Centaur, Sanyo) at 7000 x g for 1 minute and filtering through 0.22 µM (Milliex® GC, Millipore) to remove any insoluble

components. The injecting loop was first washed with 1 ml mobile phase to clean traces of previous samples after which samples were loaded and injected onto the column. Fractions were eluted at a flow rate of 0.3 mL/min of the mobile phase. The output of the spectrophotometer, detecting various peaks at λ_{280nm}, was digitised every 10 millisecond via a National Instruments analogue to digital PC-1200 convertor and displayed using Chart V.4.9 (John Dempster, University of Strathclyde) programme. The sample collector was set to collect 3 mL of the fraction in each 15 mL tube. The factions obtained were then lyophilised using an Edward Freeze Dryer Modulyo®. A total of 1000 mg of each of Cad and Css venoms were fractionated.

After identification of the fractions with LAAO activity, as described in section 2.8, the fractions of interest obtained from both venoms were then subjected to CEC.

2.4.3 Cation-exchange chromatography (CEC)

The gel for CEC was prepared by dissolving 334 mg CM Sephadex C-50 in 10 mL 0.1 M AmAc. The gel was left overnight to make sure that the beads were fully swollen up. The gel was sterilised by autoclaving at 121 °C for 20 min. The gel was then carefully poured into a Pharmacia XK-16/40 column (length 40mm, internal diameter 16 mm), avoiding air bubbles. After the gel had settled in the column, the column was equilibrated with 3 CV of 0.1 M AmAc before loading the sample on the column.

2.4.4 Preparation, fractionation and collection of sample for CEC

The sample for CEC was prepared by dissolving 50 mg of the active component obtained from gel filtration of each venom. The sample solution was vortexed and

passed through a 0.22 µm filter unit (Milliex® GC, Millipore) to remove undissolved debris. The sample was then loaded and injected onto the column. A stepwise gradient was set between solution A (0.1 M AmAc) and solution B (1 M AmAc) which changed in a time-dependant manner as shown in Table 2.2 at a flow rate of 0.3 mL/min.

Time (min.)	Solution	Conc. (%)
10	**B**	**0**
600	**B**	**75**
610	**B**	**75**
620	**B**	**100**
650	**B**	**0**

Table 2.2: Binary gradient of CEC: The gradient set for CEC between solution A (0.01 M AmAc) and solution B (0.1 M AmAc). The pH of the mobile phase increased from less basic to more basic with increase in concentration (Conc.) of B which stepwise increased from 0-75-100 % and then dropped back to 0% over a period of 650 minutes.

The fractionation assembly used was the same as SEC (section 2.5.1). Fractions from CEC were collected in 15 mL tubes at rate of 3 mL/tube. The fractions were then lyophilised and analysed further.

2.5 Reactivation of the fractions

As discussed previously, LAAO are comprised of two FAD-subunits. When these enyzmes are exposed to certain conditions such as basic pH, elevation of temperature up to 50°C or freezing, conformational changes in the flavin group takes place in the LAAO structure culminating in the inactivation of the enzyme. This inactivation phenomenon is, however, reversible and these enzymes can be reactivated by heating at 30° C at slightly acidic conditions (pH 5). The fractions obtained from SEC and CEC were initially resuspended in 1 mL 0.1 M Tris-HCl pH 8, but no enzymatic activity was observed. However, resuspension in acidic Tris-HCl (pH 5), followed by heating at 37 °C for 30 min allowed LAAO activity to be determined.

2.6 Bradford protein assay

Protein concentration was determined using a Quick Start™ Bradford assay kit following the manufacturer's instructions.

Briefly, 1X reagent was removed from 4 °C and was warmed at 37° C in a water bath for 30 min. Samples were prepared by dissolving fractions from Cad and Css in *d*H_2O to a final concentration of 1 mg/mL. After a gentle mix, 250 µL of the 1X reagent was transferred to each well of a 96-well flat bottom, black plate and 5 µL of the venom sample was added to designated wells. A blank was prepared by adding 5 µL of *d*H_2O to the 1X reagent. The plate was then incubated for 15 min at room temperature and the absorbance read at 595 nm on a M5 microplate reader (Molecular Devices, UK). A standard curve was set up using BSA at a concentration range of 7.5-1000 µg/mL.

The results were expressed as mean±SEM of triplicate readings, compared to a negative control which was only *d*H_2O..

2.7 Functional characterisation of LAAO in whole venom and fractions In order to confirm the LAAO activity of whole venom of Cad and Css, and fractions obtained from these venoms, a fluorogenic substrate assay was carried out using L(Leu), a substrate specific for LAAO.

2.7.1 Preparation of reaction mixtures

Substrate solution was prepared by dissolving 0.3 mg L-leu (250 µM) in 10 mL 0.1 M Tris-HCl (prepared from a stock solution of 100 mL 1.21 g of Trizma® base to deionised water (dH_2O) and pH adjusted to 8. The stock was stored at room temperature (25 °C). To this solution, 2.14 mg of OPD was added to a final concentration of 2 mM. Just before the assay, HRP to a final concentration of 0.8 U/mL was added. The substrate solution was prepared fresh for every assay.

Sample solution was prepared by dissolving 1 mg of whole venom in 1 mL 0.1 M Tris-HCl (pH 5).

2.7.2 LAAO assay method

Before starting the assay, HRP was added to the substrate solution and both the reaction mixtures (substrate and sample solution) were preheated to 37 °C for 30 min. To each well of a 96-well black flat bottom plate, 100 µL of the substrate solution was added. The reaction was started by adding 2 µL of whole venom (final concentration 20 µg/mL). The plate was wrapped in aluminium foil to protect from

direct light and incubated at 37 °C for 1 h. The absorbance was read at 436 nm on a M5 microplate reader, preheated to 37 °C. Increase in absorbance, compared to the negative control, expressed the enzymatic activity of the whole venom and fractions. Substrate solution, without the addition of the sample, was used as a negative control while the sample solution alone was used as a blank to take into account for absorbance of the venoms. The increase in absorbance of the treatment wells compared with the negative control indicated the LAAO activity. Results are shown in RFU calculated as mean±SEM of triplicate readings compared to the untreated control. For enzymes kinetics studies, substrate solutions containing a concentration of L-Leu ranging from 7.5-3000 µM were used. The following parameters were statistically determined for each sample using Michaelis-Menten equation and non-linear regression.

V_{max}: Maximum rate of reaction attained by the enzymes in a medium containing saturating substrate concentrations. It is represented in units of concentration of substrate converted per unit time per unit of enzyme ($\mu M.min^{-1}.mg^{-1}$).

K_M or Michaelis constant represents the substrate concentration at which the rate of the reaction is 50 % of V_{max}. It is constant for a particular reaction and is independent of Vmax or substrate concentration. It has the same units as substrate concentration (µM).

kcat represents product turnover per unit of enzymes. It is represented as concentration of substrate converted per unit of enzyme ($\mu M. mg^{-1}$)

2.7.3 SDS-PAGE preparation of sample and buffer

SDS buffer (1X) was prepared by diluting the 10X SDS 1:10 just before use. SDS buffer was prepared fresh every time. Coomassie blue G-250 (10X) and NuPAGE stains were used in the concentrated form.

Sample solutions (whole venom of Cad, Css or the obtained fractions) were prepared by dissolving venom in *d*H_2O to make 1mg/mL solution.

2.7.4 SDS-PAGE procedure

Loading solution was prepared by mixing 15 µL of the sample solution with 5 µL NuPAGE stain and vortexed to ensure a good mix. Molecular weight markers (Precision Plus Protein® Standard) (20 µL) and the loading solution (samples + LDS buffer) were heated at 70 °C for 15 min to decrease viscosity and facilitate loading, and were loaded on the gel plate. Electrophoresis was carried out at 200 V for 40 min. The gel was removed from the plate and washed with *d*H_2O for 5 min three times. Coomassie blue G-250 stain (50 mL) was then added to the gel for an hour and was placed on a rocker (Mini Orbital Shaker, Stuart) for continuous gentle rocking . The gel was again washed three times after removing the stain and was transferred to an Odyssey infrared visualizer (Li-COR®) for imaging.

2.8 Results

2.8.1 Size exclusion chromatography

The separation profile of Cad whole venom on Sephadex G-75 gel showed five distinct peaks (Figure 2.4 A). The obtained peaks were designated as fraction 1-5 (F1-F5)

according to the retention time. The percentage yield obtained from the chromatography of Cad whole venom was 98.02%. The weight of F3 and F4 of Cad venom was too low to be detected, whereas the weights of the rest of the fractions are shown in Table 2.3. Similarly, chromatography of Css whole venom, with the same technique, also resulted in 5 fractions (F1-F5) (Figure 2.4 B). Separation of Css whole venom produced a percentage yield of 81.48% (Table 2.3). Fraction 2 of Css whole venom is represented by a broad peak, which shows the presence of many proteins in F2 of Css venom, that was also confirmed by SDS-PAGE (section 2.9.6).

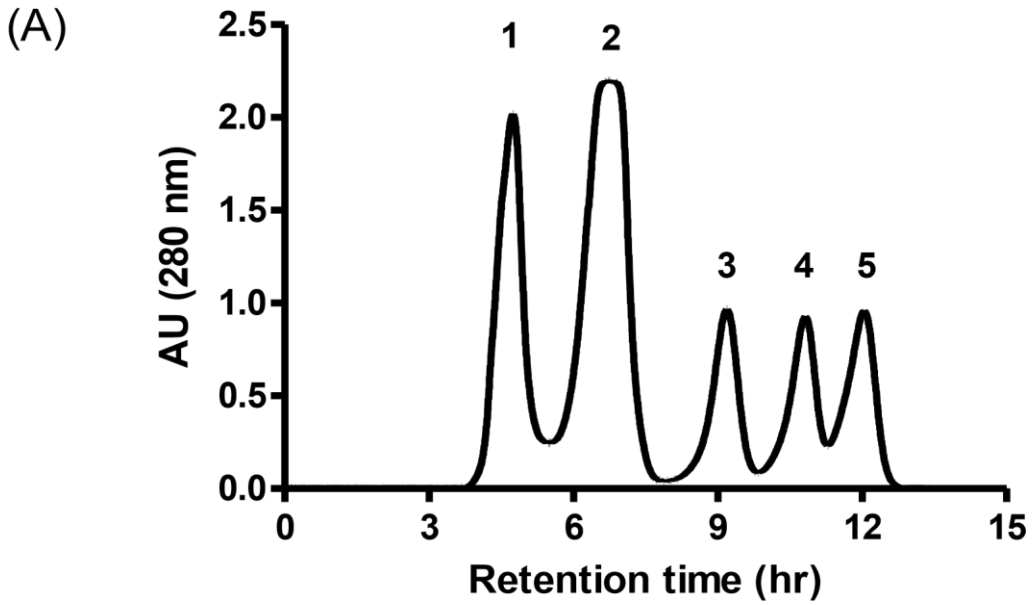

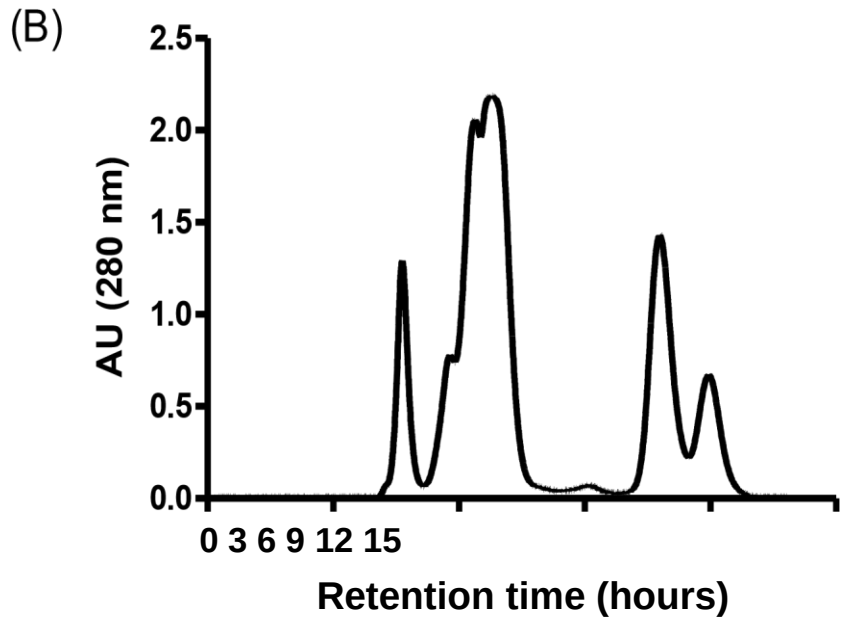

Figure 2.4: Sephadex G-75 Chromatograms of Cad and Css: Chromatograms, representative of three, showing the five peaks obtained from the separation of Cad whole venom (A) and Css whole venom (B) on SEC.

Table 2.3: Yield from gel filtration chromatography: Weights (mg) of all the fractions obtained from separating 500 mg of Cad and Css venom.

Venom sample	Fraction	Quantity (mg)
Crotalus adamanteus	1	448.5
	2	37.5
	3	Negligible
	4	Negligible
	5	4.1
	Total yield	490.1
Crotalus s.scutulatus	1	19.4

	2	310
	3	24.9
	4	40
	5	13.1
	Total yield	407.4

In terms of the protein content of the active fractions, the percentage yield was 44.5 % and 55 % for Cad and Css, respectively.

2.8.2 Cation exchange chromatography

The active fractions from the whole venom, Cad1 from Cad and Css2 from Css obtained from SEC, were then subjected to CEC for further purification. Separation of Cad1 resulted in four fractions (Figure 2.5 A). Fraction 4, had a retention time of 3 h, showed LAAO activity and was designated Lcad. In terms of protein content, the percentage yield of the active protein after CES was 19.8%. Similarly, Css2, was separated into 6 fractions (Figure 2.5 B), but only F3 showed LAAO activity which had a retention time of 2.36 h . The percentage yield of active protein was 18.4%.

This fraction was designated CsL.

(A)

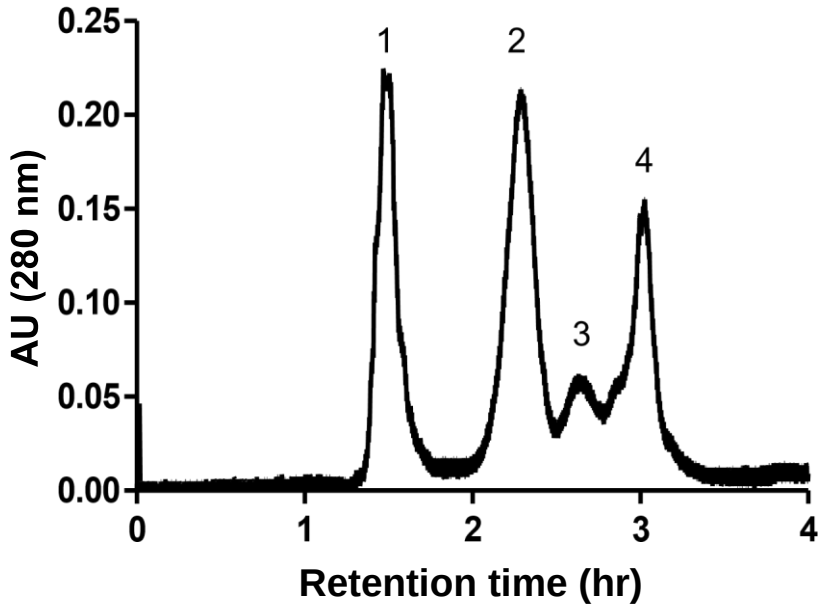

(B)

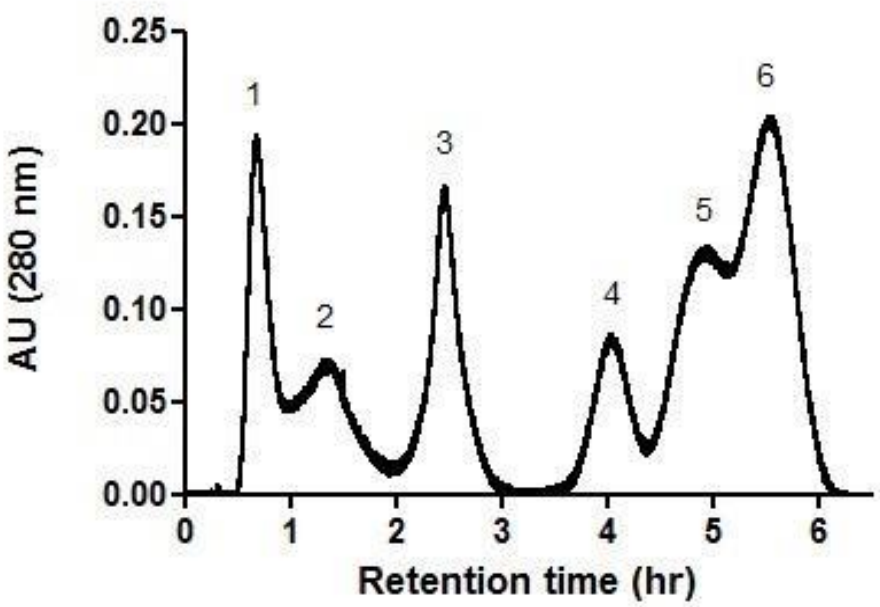

Figure 2.5: CEC chromatogram: A chromatogram, typical of three, showing the separation of Cad 1 (A) and Css 2 (B) into four and six fractions, respectively, after loading 50 mg of each sample on CEC gel.

2.8.3 Protein content of the fractions and subfractions

The concentration of proteins present in the fractions obtained from SEC and CEC, was determined using a standard curve constructed with BSA (7.5-1000 mg/mL). A typical BSA calibration curve is shown in Figure 2.6.

Where Y is the absorbance, m is the slope of the calibration curve (0.0008 for this experiment), x is the concentration (mg/mL) of the sample and c is the Y-intercept (0.1094). Table 2.4 shows the concentration of protein present in each sample as compared to the concentration of BSA.

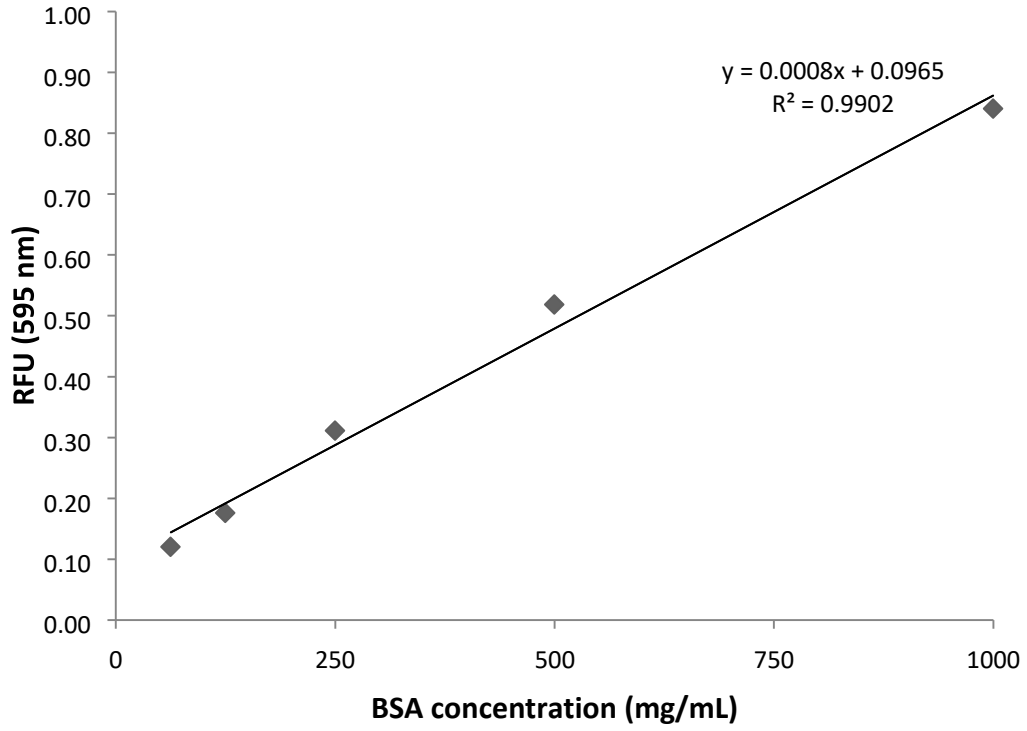

Figure 2.6: BSA calibration curve: The calibration curve was plotted against increasing concentrations of BSA (7.5-1000 mg/mL). The values shown are the mean of triplicate readings±SEM (SEM bars too small to be seen).

Table 2.4: Protein concentration of the separated fractions: RFU values (mean of three experiments ± SEM), obtained from samples solutions of 20 µg/mL, were put in the equation of straight line to determine their protein concentration in comparison to standard BSA of known concentration (7.5-1000 µg/mL).

Fraction	RFU±SEM (595 nm)	BSA concentration (mg/mL)
Cad F1	0.46±0.02	443.22

Lcad	0.27±0.01	198.05
Css F[1]	0.58±0.01	590.55
CsL	0.26±0.02	184.39

[1] **.8.4 Reactivation of the fractions after lyophilisation**

The fractions showed no significant LAAO activity when the samples were dissolved in basic buffer after lyophilisation. On the other hand, when the samples were dissolved in Tris-HCl pH 5, the samples showed significant (*P*=0.001) effect on the metabolism of L-Leu. The effect of pH on the enzymatic activity of the fractions is shown in Figure 2.7.

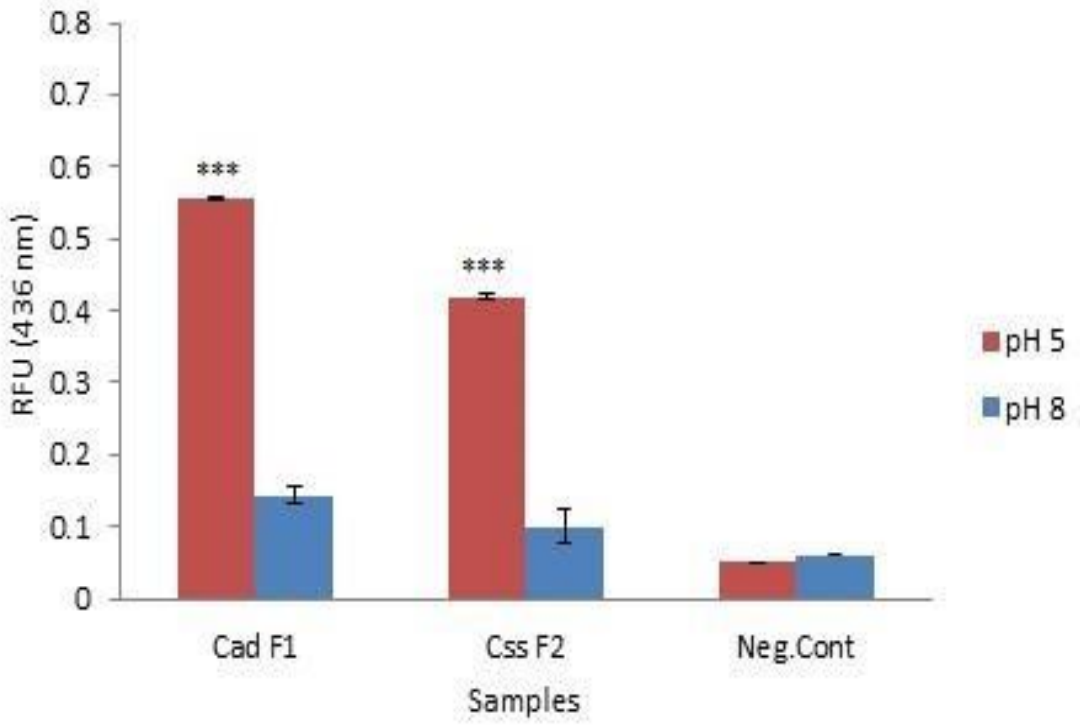

Figure 2.7: Effect of pH on LAAO of fractions: Fractions obtained from the SEC of Cad and Css did not have LAAO activity when dissolved in pH 8 buffer. *** shows significant (P=0.001) increase in the fluorescence , compared with negative control, shows that samples obtained from SEC were active only in acidic medium. Each data point represents mean±SEM of triplicate values compared with untreated control.

2.8.5 LAAO detection

Cad and Css whole venom showed metabolism of L-Leu, confirming the presence of LAAO activity in abundance in the whole venom. Figure 2.8 shows the significant (*P*=0.005) increase in L-Leu metabolism by Cad and Css whole venom. The rate of the reaction in terms of the product formed per minute was also calculated for Cad and Css venom using various concentrations of L-Leu (7.5-3000 µM) which further indicates the high LAAO activity of the venom samples (Figure 2.8).

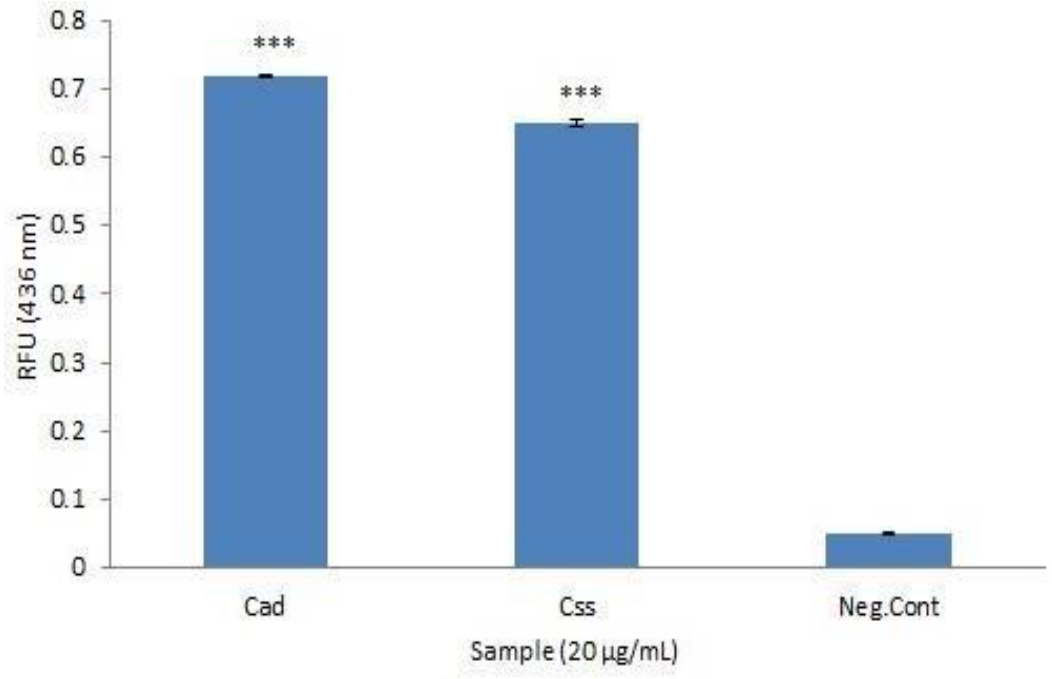

Figure 2.8: LAAO activity of Cad and Css whole venom: 20 µg/mL of Cad and Css venom was incubated with 250 µM of L-Leu for 1 hour. Each point represents the mean±SEM of three readings. *** represents the significant (*P*=0.005) increase in fluorescence enzyme activity of the samples compared with the negative control.

Cad whole venom was then subjected to SEC and CEC, the fractions were activated and their LAAO activity was determined. Fraction Cad 1, obtained from SEC, was identified with the same assay and was further purified by running it on a CEC column and the LAAO activity of the active component, Lcad, was determined. Figure 2.9 (A) shows the metabolism of L-Leu by the fractions. Cad whole venom was used as a positive control to which the activity of the active components was compared. Cad 1 and Lcad showed significant (*P*=0.001) increase in fluorescence , referring to the metabolism of Leu by these fractions. A subsequent decrease in the

LAAO activity was observed in the fractions obtained from Cad whole venom. As compared to whole venom, there was a 22% decrease in LAAO activity after SEC and a 44% loss in enzymatic activity in Cad 1 and Lcad, respectively.

Similarly, the Css fractions, Css 2 and CsL, obtained from SEC and CEC respectively, exhibited LAAO activity (Figure 2.9 B). Css 2 showed a 35 % decrease, whereas CsL showed a 55 % decrease in LAAO activity compared with Css whole venom.

(A)

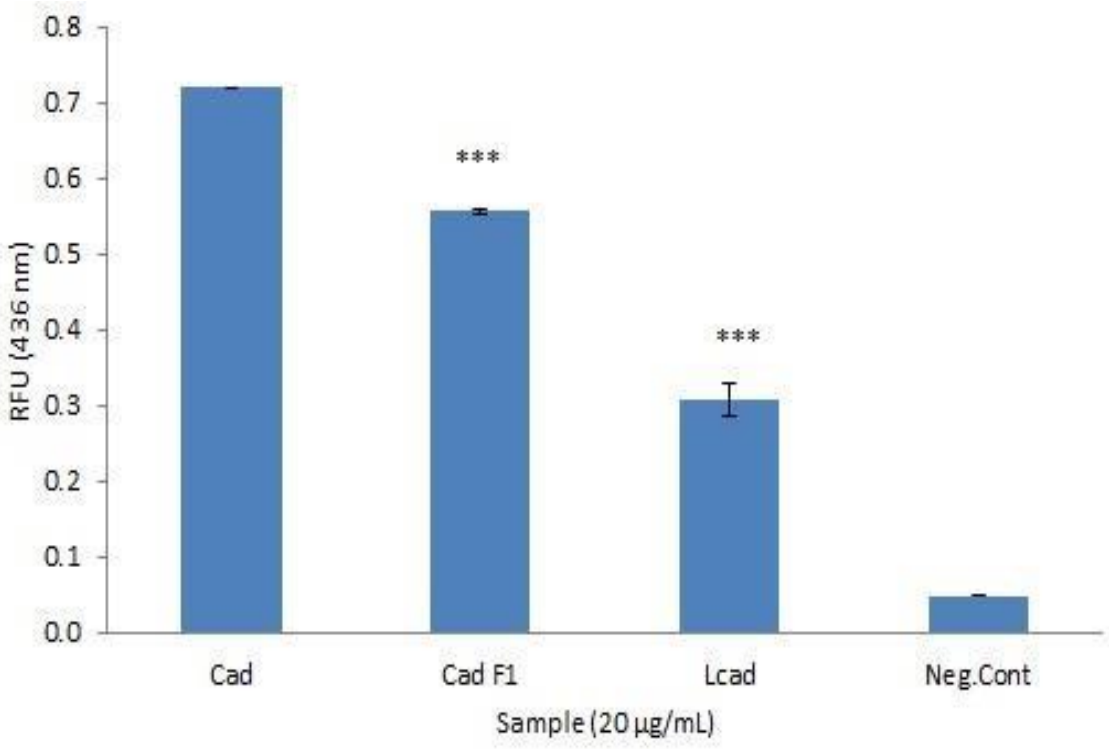

(B)

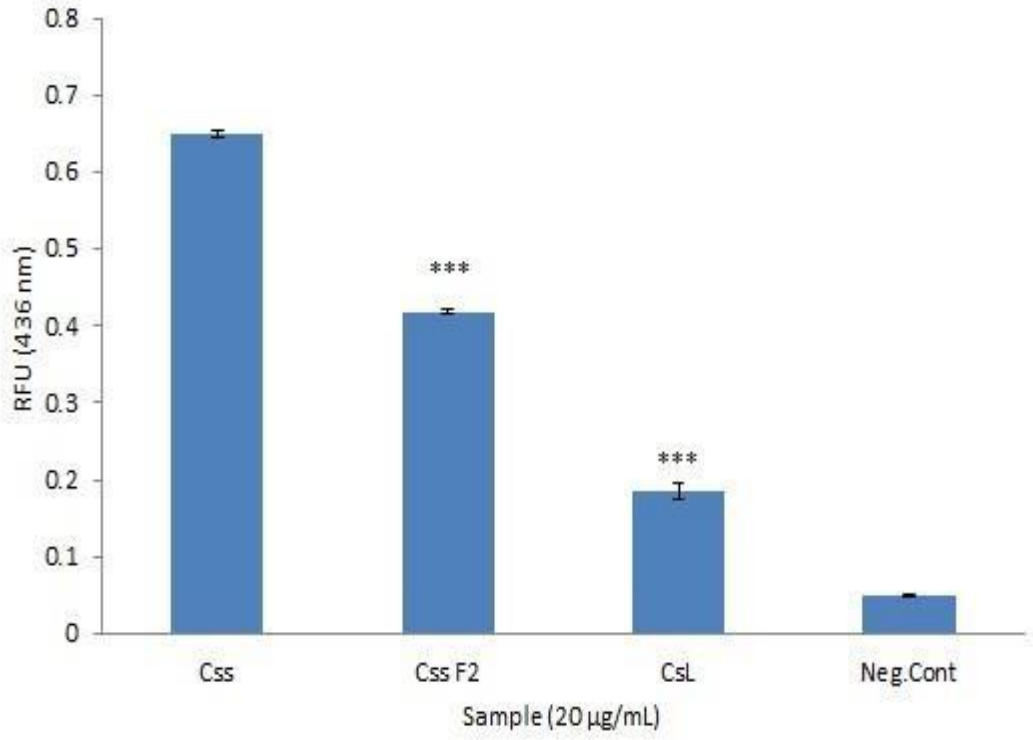

Figure 2.9: LAAO activity of Cad and Css venom fractions: Fractions obtained from Cad (A) and Css (B) were incubated at a concentration of 20 µg/mL with 250 µM of Leu for one hour at 37 °C. An Increase in fluourescence showed the LAAO activity of both fractions. ****P* 0.001 shows significance in L-Leu metablism. Data shown is mean±SEM of triplicate values compared with negative control.

After solving Michaelis-Menten equation, v_{max} values for Cad, Cad F1 and Lcad are 0.89±0.023, 0.8163±0.026, 0.7897±0.023 µM.min^{-1}.mg^{-1}, respectively. The substrate turnout for Cad, Cad F1 and Lcad represented by kcat is 99.59±2.9, 99.15±9.1 and 98.95±2.7 µM.min^{-1}, respectively.

A similar desending pattern in both v_{max} and kcat (Table 2.5) values was observed in Css, Css F2 and CsL (Figure 2.10). These results imply a gradual loss of enzymatic activity in both types of venom samples with each separation step.

(A)

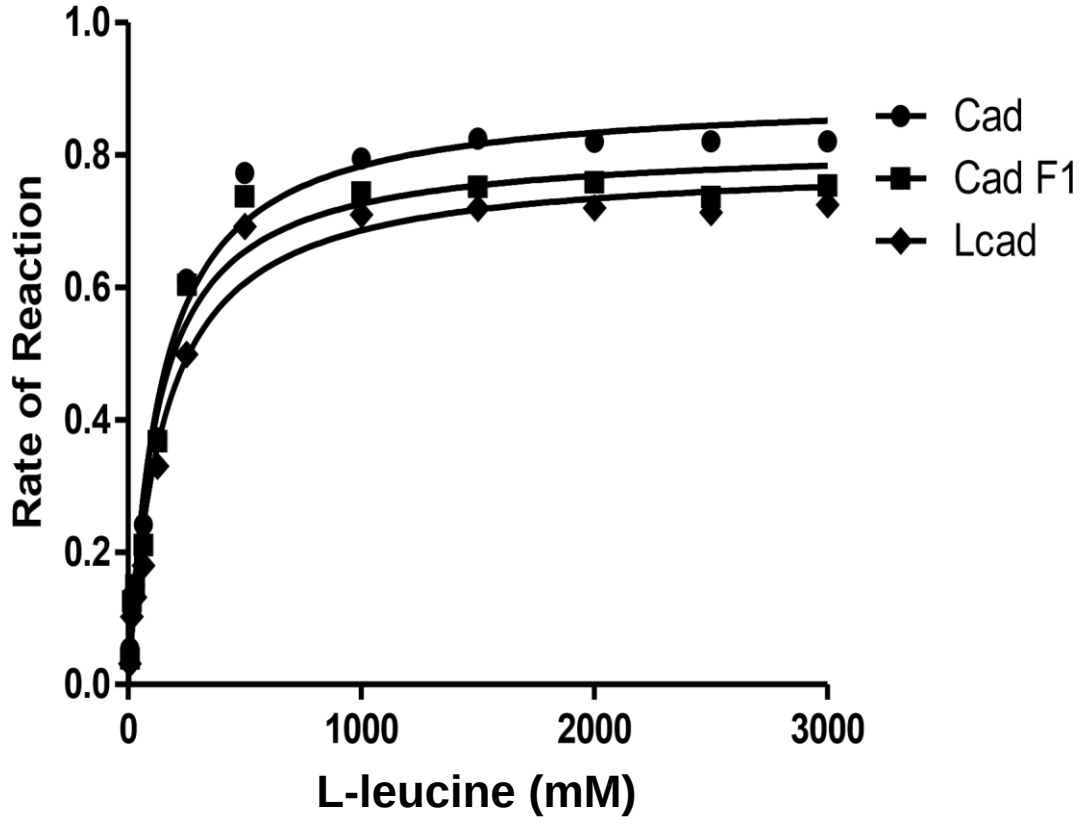

(B)

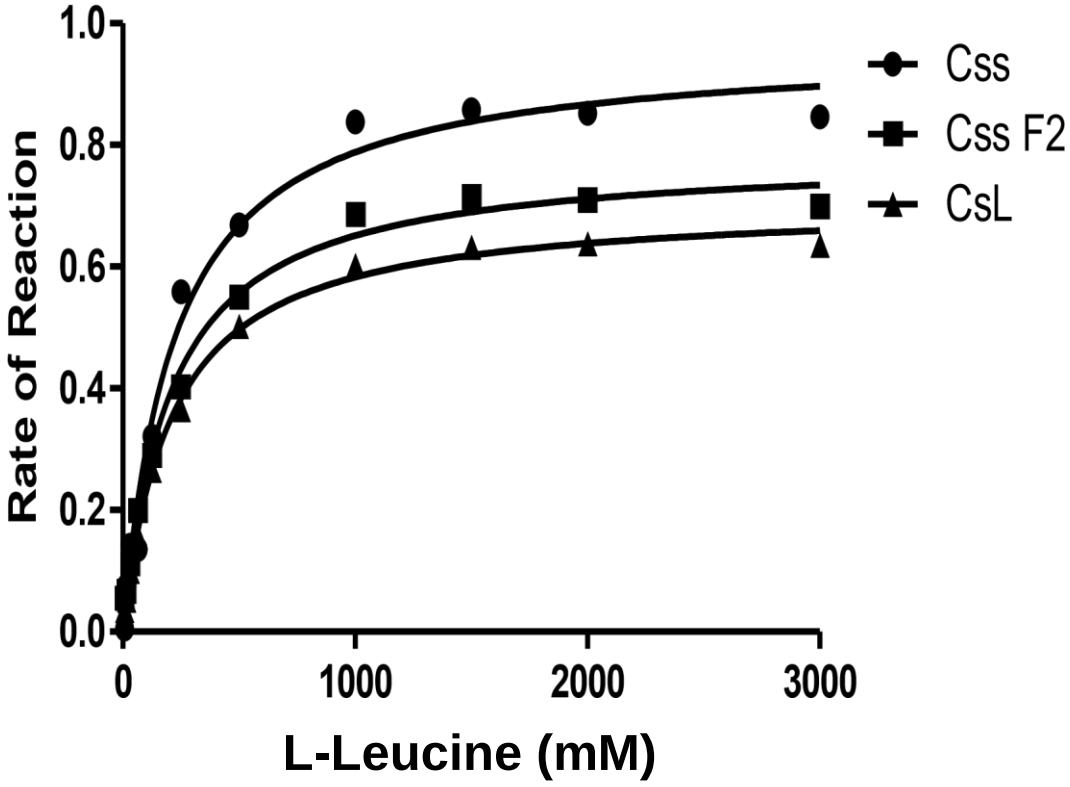

Figure 2.10: Enzyme Kinetics: Effect of various concentrations (7.5-3000 µM) of LLeu of LAAO activity of (A) Cad and (B) Css samples. Each data point represents mean±SEM of triplicate results.

Table 2.5: Enzyme kinetic statistics: statistical values for various Vmax, kcat and K_M derived from Michaelis-Menten equation.

Sample	V_{max} (μM.min^{-1}.mg^{-1})	kcat (μM.min^{-1})	K_M (μM)
Cad	0.8911±.023	99.59±2.9	137.7±19.9
Cad F1	0.8163±0.026	99.15±9.1	124.2±19.19.1
Lcad	0.7897±0.023	98.95±2.7	131.4±20.7
Css	0.9630±0.034	101.9±9.7	221±31.1
Css F2	0.7841±0.018	99.89±8.9	204.6±18.8
CsL	0.07051±0.011	98.93±8.1	210.8±13.2

2.8.6 Sodium dodecyl sulphate-polyacrylamide gel electrophoresis

SDS-PAGE was used to evaluate the purity of the fractions as well as the range of molecular weights present.

SDS-PAGE of Cad whole venom showed five bands having protein molecular weights ranging from 10-150 kDa. Cad F1, the enzymatically active fraction, showed three bands after SEC, referring to the presence of at least three different of proteins in that fraction the molecular weights of which were in the range of 20-100 kDa. CEC resulted in Cad 1 being purified to a single protein, Lcad, evident by the single band shown on the gel, having molecular weight in the range of 70 kDa. Figure 2.11 (A) shows the stepwise purification and molecular weights of the purified proteins. Due to the denaturing properties of electrophoresis, the dimeric molecule of LAAO

dissociates and the weight represented is of the single monomer only. Css whole venom is comprised of proteins distributed over a wide range of molecular weights ranging from 10-150 kDa (Figure 2.11 B). Css 2 is a complex fraction, having proteins of molecular weights ranging from 30 to 100 kDa. CsL, however, is the purified active protein of 50-70 kDa.

(A)

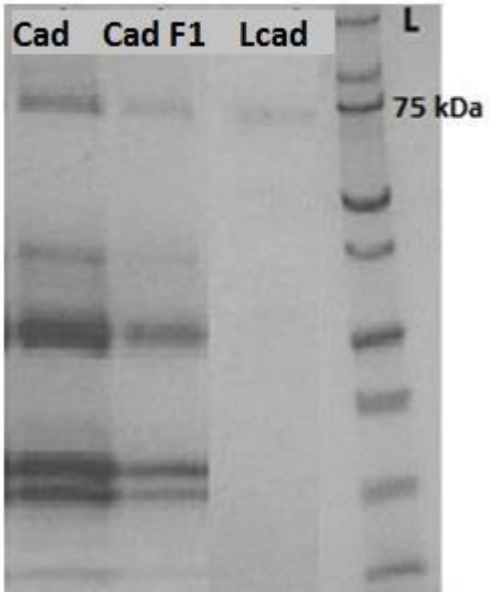

(B)

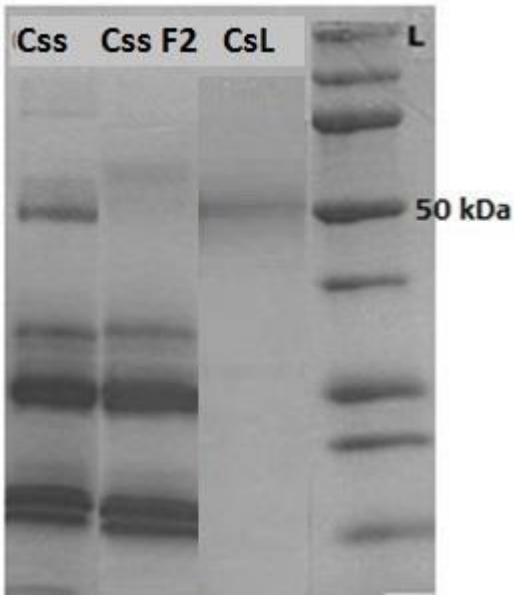

Figure 2.11: SDS-PAGE of whole venom and subsequent fractions: Images, typical of three, showing the purification and molecular weights of whole venom (Cad/Css) and fractions obtained from SEC (Cad F1/Css F2) and CEC (Lcad/CsL). The molecular weight of Lcad and CsL is approximately 75 and 50 kDa, respectively, which is equal to the weight of one subunit of LAAO. L is the molecular ladder.

2.9 Discussion

LAAO are enzymes that are highly specific for the catalysis of L-amino acids and are found in a wide range of snake venoms, especially in venom of snakes from Crotalinae, Viperidae and Elapidae subfamily/families. LAAO are flavo-proteins and consist of two identical subunits, each of 57-68 kDa. LAAOs have been studied since 1960 and their molecular, biological and enzymatic profiles are the subject to increasing interest due to the unusual pharmacological effects of these proteins. The purification method used for the separation of these enzymes were first described in the 1960s which mainly included SEC and CEC and are still considered efficient to obtain LAAO of high purity from whole venom.

In this study, LAAO from two rattlesnakes, Cad and Css were isolated using two chromatographic steps, SEC and CEC. The purified enzymes were stable only in acidic pH and had FAD as a co-factor as indicated by the yellow colour of the lyophilised proteins. The physical properties and the elution pattern of the active fractions obtained from SEC and CEC similar to the data previously reported for LAAO from different sources (Alves *et al*., 2008; Tõnismägi *et al*., 2006; Toyama *et al*., 2006). The chromatogram of Cad fractionation on SEC, showed 5 distinct peaks, indicating five types of proteins which are distinct from one other in molecular sizes. All the separated fractions were then subjected to LAAO assay for identification of the active fraction. Fraction 1, having yellow colour, showed significant ($P<0.001$) metabolism of L-Leu and was designated as Cad F1. Cad F1 had a retention time of 5 h and was further fractionated and purified by CEC. The last fraction which was released at 4 h

time point showed LAAO activity and was called Lcad. Similarly, the fractionation of the Css whole venom resulted in five fractions. SDS-PAGE revealed that the active fraction, Css F2, is comprised of many different proteins, apparently very similar in molecular sizes. However, the active protein was further purified using CEC to isolate LAAO and the purified proteins were designated as CsL. SDS-PAGE analysis was used to determine the MW of the LAAO obtained from both the venoms, which turned out to be in the range of 75 and 50 kDA for Lcad and CsL, respectively. The MW of the LAAO in this study correlates with the MW being reported for LAAO purified from Cad (68.7 kDa) (Du and Clemetson, 2002) and Css (56 kDa) (Massey *et al*., 2012). The active site of the LAAO has been reported to be very sensitive to low temperature and high pH. For example, the Cad LAAO are shown to undergo reversible inactivation at

temperature ≤ -5 °C or pH >7 (Curti *et al*., 1968). It occurs because of either increase in pH or low temperature which brings about limited conformational changes in the enzyme prosthetic group, flavin (Soltysik *et al*., 1987; Massey and Zmudka, 1967), however, FAD cofactor remains bound to enzyme (Wellner, 1966). This inactivation phenomenon is accompanied by shifts in absorption spectrum. The reactivation of the enzymes restores the conformational changes and the enzyme activity. The inactivation caused by shift of pH to the basic range can be reversed by introduction of monovalent anions, addition of substrate/substrate analogue and requires high energy (42.5 kcal.mole^{-1}) for reactivation (Coles *et al*., 1977). On the other hand, the freezing inactivation of LAAO is not prevented by monovalent anions and the reactivation requires heating the enzymes at 38°C at mildly acidic pH, ideally pH 5

(Curti *et al*., 1967; Wellner, 1966). Although, the enzymes are reactivated, loss of enzymes activity has been reported (Curti *et al*., 1968). The reversible inaction by freezing has been observed in LAAO from different snake sources especially the Crotalus species, however, LAAO purified from the venom of *Ophiophagus hanna* are not inactivated by freezing (Tan and Saifuddin, 1989). Interestingly, there is a homology of high degree in the N-terminal sequence of the LAAO from the Crotalus species (Table 2.6) which are considerably different from N-terminal sequence of LAAO from *O. hanna*, implying the co-dependency of the stability and amino acids present in the protein's structure.

Table 2.6: N-terminal sequence of LAAO from different snake venom.

LAAO source	N-terminal sequence	Reference
Cad	AHDRNPLEECFRETDYEEFL	Raibekas and Massey, 1998
Css	AHDRNPLEECFRETDYEEFL	Massey *et al*., 2012
Crotalus atrox	AHDRNPLEECFRETDYEEFL	Torii *et al*., 1997
Calloselasma rhodostoma	ADDRNPLAEEFQENNYEEFL	Ponnudurai *et al*., 1994
Crotalus durissus cumanensis	ADDRNPLEECFRETDYEEFL	Vargas *et al*., 2013
Ophiophagus hanna	SVINLEESFQEPEYENHLA	Ahn *et al*., 1997
Bangarus fasciatus	DDRRSALEECFREADYE	Wei *et al*., 2009

Another exception to the reversible inactivation of LAAO is demonstrated by LAAO from *Calloselasma rhodostoma*. Despite having homology in the N-terminal sequence with Crotalus species, LAAO from *C. rhodostoma* are not inactivated by freezing. LAAO from this source have FMN instead of FAD as prosthetic group (Ponnudurai *et al*., 1994), which also shows the relationship between the structure and stability of proteins. This property was demonstrated by Lcad and CsL. Both of the fractions did not show any significant metabolism of L-leu at the basic pH, whereas, at pH 5 statistical significance ($P<0.001$) in the results was observed, which demonstrates the reversible inactivation due to freezing.

Specificity for L-amino acids is common among all LAAO of different snake origins. Comparison of enzymatic activities of different LAAO towards various types of Lamino acids shows relative high specificity for aromatic and hydrophobic substrates such as L-Leu, L-Ile, L-Phe and L-Met (Silva *et al*., 2007; Wei *et al*., 2007; Du and Clemetson, 2002). However, some of the snake venom LAAO have higher enzymatic activity towards specific L-amino acids, for example, *O. hannah* shows specificity towards L-Lys, whereas *Bangarus fasciatus* LAAO are more active against L-Glu (Wei *et al*., 2009). These catalytic preferences in substrate selection are attributed to the difference in the side chain binding sites of LAAO (for details see section 1.8.3.1). For example, most of the LAAO have 3-4 hydrophobic binding sites; *O. hannah* has an additional binding site for the ε-amino group of the L-Lys, making it a suitable substrate for *O. hannah* LAAO (Nget-Hong and Saifuddin, 1991). The specificity of LAAO from Crotalus species towards L-Leu is well established (Vargas *et al*., 2013; Toyama *et al*., 2006; Torii *et al*., 1997; Massey and Curti, 1967) and therefore, L-Leu was used to determine the enzymatic activity of Lcad and CsL in this study. Lcad and CsL proved to have high enzymatic activity towards L-Leu as is suggested by K_M values, that is, 131.4±20.7 and 210.8±13.2 µM respectively. Comparing K_M values determined for Lcad and CsL in this study with K_M values reported for LAAO from other resources such as *C. durissus cascavella* (K_M=46.7 µM) (Toyama *et al*., 2006), Apoxin-1 (K_M=4.7 µM) (Torii *et al*., 1997) and *C. durissus cumanensis* (K_M=9.23 µM (Vargas *et al*., 2013), shows that Lcad and CsL are more active. However, LAAO from
O. hannah, having a KM of 2.2 mM (Jin *et al*., 2007), are more active than Lcad and

CsL which is due to more binding sites on the catalytic site on *O. hannah* LAAO. This observation suggests the structural similarity of Lcad and CsL with the LAAO from the Crotalus family.

The purified samples were sent to Prof. Dr. Igor Križaj, Department of Molecular and Biomedical Sciences, Jožef Stefan Institute, Ljubljana, Slovenia, for molecular characterisation and amino acid sequence analysis, but due to severe desiccation of the samples during transportation, the samples became water insoluble, which was the limiting factor to further analysis. It will interesting to see the amino acid sequence of Lcad and CsL for confirmation of their enzyme family and further elaborate on the differences in their enzymatic activities compared with their counterparts from other resources. However, given the physicochemical properties of the isolated proteins as well as the elution pattern and catalysis of L-Leu, it is safe to presume that the active fractions obtained from both venoms are LAAO.

3. *In vitro* investigation of Lcad and CsL induced cytotoxicity in human cancer cell lines.

3.1 Introduction

Investigation of different types of cell death has evolved as a vital area of research in biomedical sciences and several modes of cell death have been characterised on a morphological and biochemical basis. Among the best described forms of cell death are apoptosis, necrosis and autophagy. The mechanisms underlying cell death processes are distinct and biochemically unique, however, the main organelles and proteins, such as mitochondria, caspases and FADD, are supposedly at the crossroads of these processes and are thought to play a crucial role in the cross-talk between these cell death pathways (outlined in section 1.4). This chapter deals with elaboration of the biochemical cascades triggered by Lcad and CsL culminating in cell death. In this study, two human cancer cell lines, human skin melanoma (A375) and human ovarian carcinoma (A2780), were used to determine the cytotoxic effects of the proteins extracted from Cad and Css. Initially, a CellTiter Blue® assay was carried out to confirm the cytotoxicity effects of Lcad and CsL (section 3.1.2). After morphological evaluation of the treated cells (3.1.3), further assays were accordingly carried out to elucidate the mode of cell death. Autophagy was evaluated by looking at the formation of AVOs (section 3.1.6) and to assess necrosis, the inhibitory effect of necrosis inhibitor 2-(1*H*-Indol-3-yl)-3-pentylaminomaleimide (IM-54) on cell death was investigated (section 3.1.5). In order to have further insight into the cell death

pathway triggered by Lcad and CsL, the role of ROS (section 3.1.7), mitochondria (section 3.1.8), caspases (3.1.9), Ca^{2+} (section

3.1.10) and other pro-apoptotic proteins, such as AIF and Bid, were evaluated (section 3.1.11). DNA damage was evaluated by examining the activation of PARP (section 3.1.11). Furthermore, the effect of Lcad and CsL on the two cancer cell lines was compared with a human non-cancer cell line (PNT2a) and the potency of these compounds was compared with the chemotherapeutic drug, cisplatin (section 3.3.3). The following sections give a brief introduction to various approaches used in this study. Despite the limitations and disadvantages, the advantages related to the following techniques were in best interest of the project and that is why these techniques were exploited to elaborate the pharmacology associated with Lcad and CsL.

3.1.1 Cell lines used

A375 is an adherent cell line derived from human skin tissue of a female having a malignant melanoma cancer phenotype (Welch *et al*., 1991). Morphologically these are epithelial cells, which grow as a monolayer on flat surfaces like that of a flask (Figure 3.1).

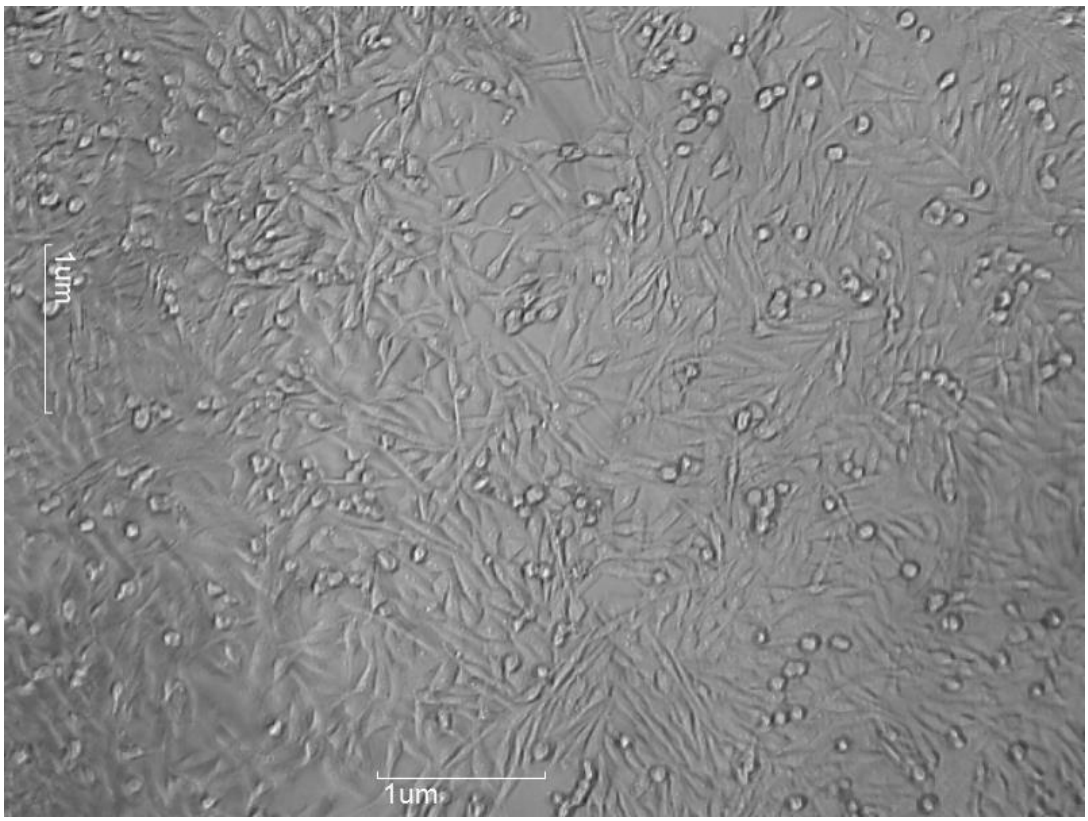

Figure 3.1: A375 growth pattern: Photomicrograph, taken with a 10X objective lens, showing a continuous and monolayer growth pattern after 72 h of seeding in a 75 cm^2 flask.

A2780 is an epithelial cell line extracted from tumors from ovaries of an untreated female patient. These cells grow as a monolayer in the form of small patches or islands on the surface rather than in a continuous layer (Behrens *et al*., 1987) (Figure 3.2).

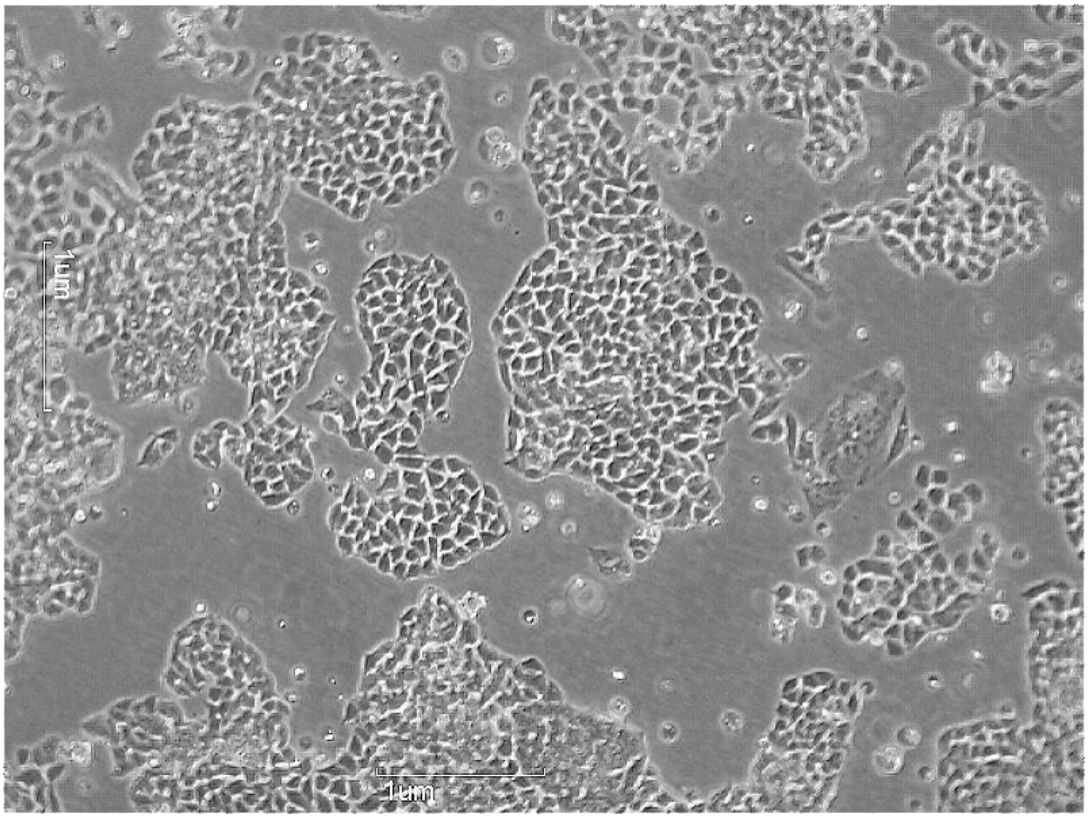

Figure 3.2: A2780 growth pattern: A2780 cells seeded and grown for 72 h in a 75 cm^2 flask. This photomicrograph, taken with 10X objective lens, shows the growth of the A2780 cells in the form of patches.

The A2780 cell line used in this project was cisplatin sensitive. The cytotoxicity of the Lcad and CsL on the cancer cell lines was compared to a non-cancer cell line PNT2a which have an epithelial morphology and are extracted from non-cancer human prostate tissue. This cell line was obtained in immortalised form achieved by transfection with a SV40 plasmid with an aberrant replication origin. PNT2a cells form a continuous layer, as shown in Figure 3.3, while proliferating as a monolayer on the growth surface (Berthon *et al*., 1995).

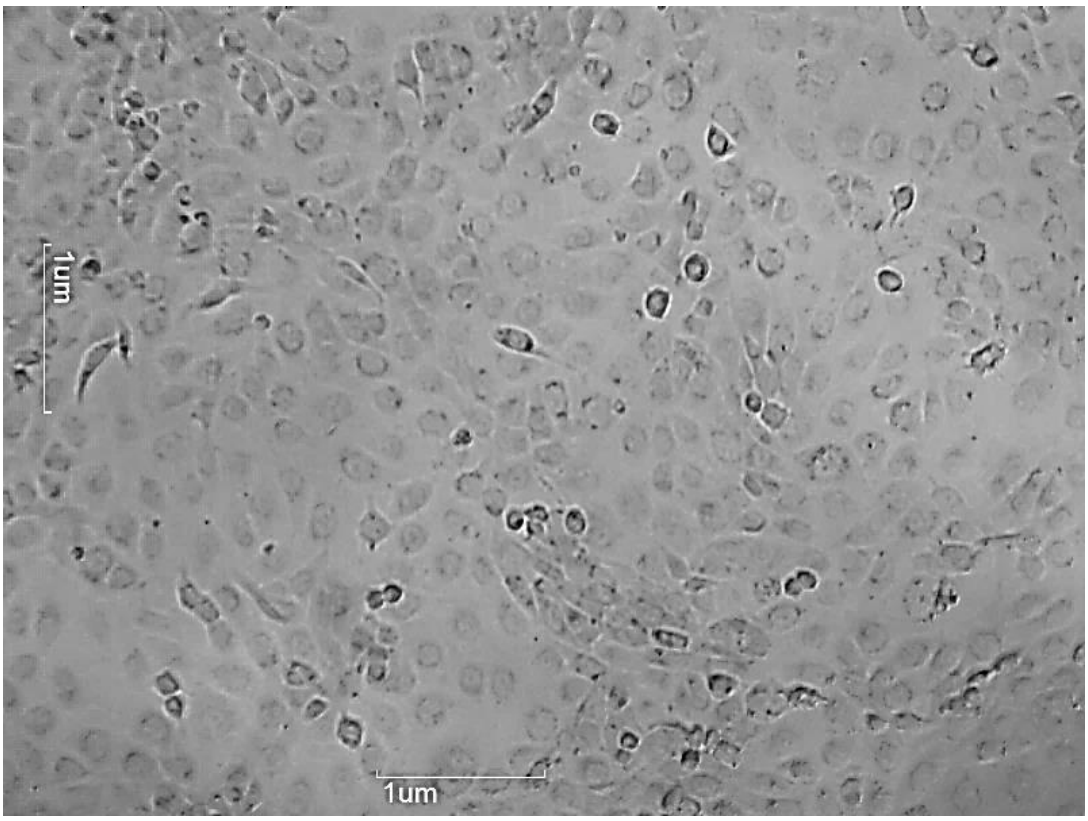

Figure 3.3: PNT2a growth pattern: Photomicrograph taken with a 10X objective lens showing a monolayer growth pattern

3.1.2 Cell viability assay

The effect of external factors on a cell population can be determined by numerous *in vitro* assays with the cell viability measurement being the mainstay following exposure to a chemical entity. CellTiter Blue® has been widely used over 5 decades to evaluate cell viability and screening of cytotoxicity of compounds (Rampersad, 2012). The CellTiter Blue® assay is based on the ability of viable cells to convert resazurin, a redox dye, into a fluorescent product, resorufin. The metabolic capacity of nonviable cells come to a halt and therefore, cannot produce a fluorescence signal. The strength of the fluorescence signal, compared with a control, indicates cell viability. Resazurin is a cell permeant, cell culture media stable, water soluble and

nontoxic dye that detects the reducing environment of cells. It is originally a blue non-fluorescent dye. It acts as a temporary electron acceptor in the presence of NADPH/FADH and is reduced to a highly fluorescent pink product, resofurin. The reduced form can be fluorometrically detected (ex/em: 560/590 nm) (Goegan *et al.,* 1995). Resorufin can freely cross the cell membrane of the cells to diffuse back to the surrounding medium and therefore, the pink colour can be seen in the medium surrounding the viable cells. Figure 3.4 summarises the chemical reduction of resazurin taking place inside the cells.

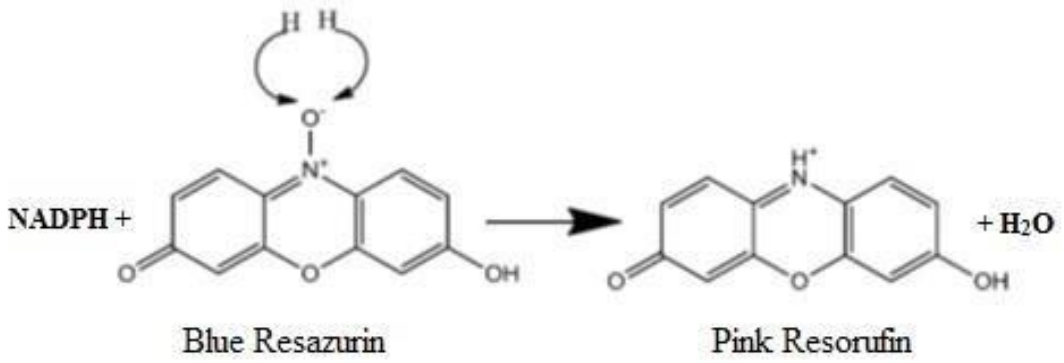

Figure 3.4: Chemical reaction underlying CellTiter Blue® assay: Conversion of blue resazurin into fluorometrically active pink resorufin.

This assay is useful to determine cell viability in a 96-well plate for upto 20,000 cells/well which is the limitation of the CellTiter Blue assay®. It has fewer steps compared with other assays such as the MTT assay and the fluorescence is recorded using a microplate plate reader as opposed to complex equipment such flow cytometer used to Annexinv/propidium iodide assay for the detection of cell viability.

3.1.3 Morphologic evaluation

The morphology of cells during the death process is an important tool for characterising the type of cell death, as all types of cell death are morphologically distinct (reviewed in Galluzzi *et al*., 2012). Microscopy is very helpful to differentiate between necrosis and other forms of cell death such as apoptosis (Darzynkiewicz and Gong, 1994). Necrosis is characterised by swelling and finally rupturing of the plasma membrane and breakdown of the cellular organelles and ultimately, release of cellular debris (discussed in detail in section 1.9.5). On the other hand, apoptosis is a cell death process which is brought about by a number of mechanisms that morphologically manifests in cellular volume reduction (outlined in section 1.9.7). Generally, light microscopy is used for observing and recording these morphological changes to support other evidence to establish the mode of cell death induced by cytotoxic agents.

3.1.4 Cell membrane integrity

The disruption of cell membrane integrity also reveals the mechanism of cellular toxicity. In apoptosis, the integrity of the cell membrane is maintained till the end of the cell death process whereas permeabilisation of the cell membrane and, later on, cell membrane rupture is the key feature of necrosis. Sytox® Green is an intercalating nucleic acid stain that is usually used to determine the integrity of cell membranes under stress (Jones and Singer, 2001). This dye can only penetrate compromised cell membranes while intact cell membranes are impermeable to Sytox® Green. After crossing the cell membrane, it intercalates with DNA and becomes fluorescent

(ex/em: 504/523) which can be quantified using a microplate reader and can also be visualised by fluorescent microscopy (Catala and Parthuisot, 1998). Sytox® Green is an easy and quick way of quantifying cell membrane integrity by producing height fluorescence signal. The disadvantage of the assay is that it does not give any information regarding the mechanism causing damage to the cell membrane.

3.1.5 Necrosis evaluation using necrosis inhibitors

Oxidative stress induced by the intracellular accumulation of ROS is one of the potent mechanisms to induce cell death. ROS accumulation in cells perturbs the anti-oxidant machinery of the cells and results in disturbances of the organelles as well as production of intracellular macromolecules such as proteins, carbohydrates and nucleic acids, all of which culminates in acute cell death, that is, necrosis (Klaunig *et* al., 1998; Nathanand Cunningham-Bussel, 2013) IM-54 is a selective inhibitor of oxidative stress induced necrosis, but has no effect on apoptosis (Sedokeok and Dodo, 2010). Normally, as a positive control, H_2O_2 is used to demonstrate the blocking effect of IM-54 on ROS induced necrosis.

3.1.6 AVOs detection, evaluating autophagy

The formation of AVOs characterises the autophagic type of cell death (for details see section 1.9.12). AVOs contain enzymes that degrade intracellular proteins, which is the hallmark of autophagy. Other than that, the acidic compartments also contain enzymes involved in activating other cell death pathways, for example cathepsins, that are supposed to play a role in the release of AIF from mitochondria and induce caspase-independent apoptosis (section 1.9.11). Acridine orange (AO) is a stain used

for the detection of AVOs in living cells. AO freely crosses the plasma membrane. In acidic environments, AO is protonated where it fluoresces bright red (ex/em: 490/650 nm), which can be detected fluorometrically. The protonated form of the stain consequently hinders its escape from the acidic compartments and therefore, AO accumulates in AVOs (Pierzynska-Mach *et al*., 2014). AO is very easy, quick and economical to use. In addition, it can be used to produce both qualitative as well as quantitative data to evaluate intracellular acidity. However, the fluorescence signal produced is weak and sometimes, recording of the signal is a challenge. Therefore, the microscope lamp is recommended to be changed

frequently, which can be costly.

3.1.7 ROS detection

ROS are vitally important biological intermediates which have multiple physiological essential roles including initiation/progression of cell death. At the mitochondrial level, ROS is responsible for initiation of DNA mutations, alteration in inner MMP to facilitate the release of pro-apoptotic proteins and collapse of MMP to activate cell death pathways. The cell permeable dye, 2,7-dichlorodihydrofluorescein diacetate (DCDHF), is used to detect ROS in cells. After it is taken up by the cells, the diacetate groups are removed from DCDHF by cytosolic esterases and the intermediate is oxidised by ROS to dichlorofluorescein (DCF), which is highly fluorescent (ex/em:

504/523 nm) and is detected using a microplate reader (Brubacher and Bols, 2001). The intracellular conversion DCDHF to DCF is shown below in Figure 3.5.

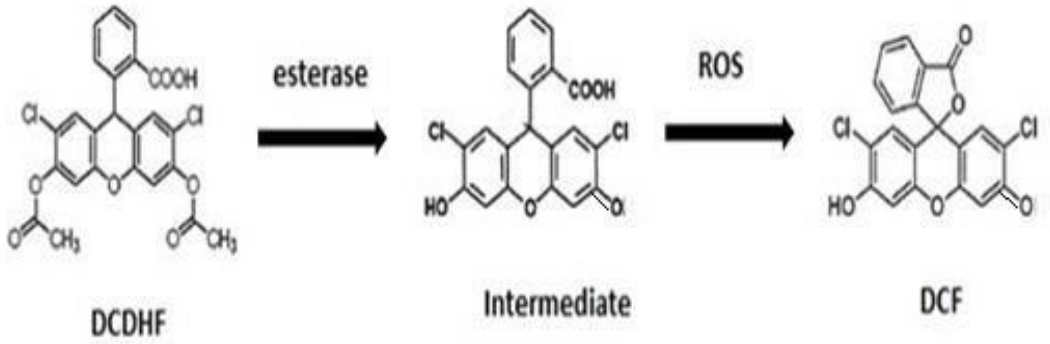

Figure 3.5: DCDHF conversion to fluorescent DCF: A chemical reaction showing the removal of ester groups from DCDHF by esterases and then oxidation of the intermediate by ROS to produce the fluorescent DCF.

The limitation to DCDHF is that the intermediate produced during this process can react with oxygen (O_2) to produce superoxide, the dismutation of which leads to the production of further H_2O_2 and therefore, false amplification of signal (Kalyanaraman *et al*., 2012).

3.1.8 Mitochondrial membrane permeabilisation

A crucial step in the execution of apoptosis is the translocation of proteins from the mitochondrial intermembrane space to the cytosol that can ultimately lead to the demise of the cell, either directly, with AIF, or indirectly by activation of caspases (by Cyt. C). Although still a matter of debate, the widely accepted hypothesis is that in response to an apoptotic stimulus (ROS or pro-apoptotic proteins), the MMP drops in order to enhance the permeability of the mitochondrial outer membrane for the translocation of apoptogenic proteins. Therefore, evaluating the changes in MMP is important to establish the role of mitochondria in cell death. Tetramethylerhodamine ethyl ester (TMRE) is a cell permeant orange dye bearing a

positive charge. It is used to label active mitochondria in which TMRE accumulates due to a relative negative charged environment and fluoresces red-orange light (ex/em: 549/575 nm). However, in case of mitochondrial membrane depolarisation, it leaks out and the fluorescence signal decreases (Farkas *et al*., 1989; Nicholls and Ward, 2000). Using TMRE is a quick assay to assess MMP both qualitatively and quantitatively and is very useful for time-dependant measurements. The length of exposure of the dye to light is critical, especially during imaging, as long exposure of the dye to the microscope lamp light leads to quick bleaching of the dye and termination of the fluorescence signal.

3.1.9 Caspase 3/7 activity

Caspases, a family of proteases, are the main regulators of apoptosis and are broadly classified into initiator caspases (caspase 8, 10) and the effector or executioner caspases (caspase 3, 7) which are the downstream caspases that carry out the apoptotic cell death. One of the most commonly used methods for detection of caspase activity is the measurement of substrate cleavage by caspases present in the lysate of treated cells. Caspase substrates are synthetically prepared which possess amino acid sequences that mimic the cleavage sites for different caspases. These synthetic substrates are conjugated either to a chromophore *p*nitroanilide (*p*NA) or fluorochrome 7-amino-4-methylcoumarin (AMC). Upon cleavage by caspases, pNA (450nm) or AMC (ex/em: 360/460) is

spectrophotometrically detected (Kohler *et al*., 2002; Timmerand Salvesen, 2007). Using the synthetic substrates according to the above technique is a one-step assay

which can be carried out in a 96-well plateand therefore, a large number of samples can be analysed at one time. This method is cheaper and easier compared to the available assay kits. The lysis of the treated cells, however, is an important step in the assay. As caspases are intracellular enzymes, selection of the appropriate lysis buffer and working concentration is important to make sure that the cells are properly lysed, failing of which leads to false negative results.

3.1.10 Ca^{2+} imaging

It has long been established that Ca^{2+} ions play a crucial role in, at least, the three best characterised modes of cell death (reviewed by Orrenius *et* al., 2015; Fraber in 1981). Ca^{2+} can downregulate MMP as a result of which apoptogenic proteins are released to bring about the distant apoptotic processes (Zhivotovsky and Orrenius, 2011). In addition, Ca^{2+} ions are indirectly involved in the cleavage of AIF from the intermembrane space of mitochondria by activating enzymes, calpains) (Norberg *et al*., 2008). Along with influencing other autophagic pathways, the formation of autophagosomes has also been claimed to be Ca^{2+}-dependent (reviewed by HoyerHansen *et al*., 2007). Therefore it is important to evaluate intracellular Ca^{2+} levels to determine the role of Ca^{2+} in Lcad/CsL induced cell death. Fluorescent dyes such as FLuo-2, Fluo-3 and Fluo-4 are widely used for Ca^{2+} imaging (Assinger *et al*., 2015;).

These dyes are used in a non-fluorescent acetoxymethyl ester (Fluo-2 AM) form. Upon entry into living cells, the ester complex breaks to generate free fluorescent dye (Fluo-2). Binding to Ca^{2+} leads to a 40-fold increase in fluorescence which is detected

at ex/em: 488/535 nm (Minta *et al*., 1989). Although, they are useful to measure cytosolic $Ca^{2+,}$ these are single wavelength dyes and cannot be used for ratio-metric studies, such as Fura-2. However, AM dyes are easy to passively load into cells as these are hydrophilic dyes and cross the cell membrane easily (Paredes *et al*., 2008). Fluo-2 is the brightest of all these single wavelength dyes, which is partly attributed to higher intracellular accumulation (Minta *et al*., 1989).

3.1.11 Western blotting

Western blotting or immunoblotting is an important technique that is able to separate and identify proteins in a cell lysate containing a mixture of proteins. This technique involves three basic steps. The first step is electrophoresis which separates and therefore identifies proteins in terms of molecular weights. SDSPAGE is the widely used method. SDS buffer is used to obtain the linear structure of proteins through denaturation and masks the native charge of the proteins with a common negative charge. The separated proteins are then transferred to a membrane for solid support, generally polyvinylidene difluorideor nitrocellulose membranes are used. The membrane is then treated with fat-free dried milk or bovine serume albumin (BSA) in order to block the binding of antibodies to nonspecific sites. The last step involves the detection of the protein band on the membrane. Protein detection is achieved by incubating the membrane with primary antibodies that are specific for the targeted protein, and are visualised by recording images on X-ray film. The detection of antibody marked protein is broadly classified into direct and indirect methods. In the direct method, the antibody is labelled with an enzyme that is active

against a chemiluminescent substrate. When the substrate is exposed to the enzyme/antibody complex, the substrate is degraded by the enzyme and light is produced as a by-product which is recorded on a film or a phosphorimager that is suitable for chemiluminescence detection. The secondary method for detection of the primary antibody is the use of a fluorescent secondary antibody that targets the primary antibody. The secondary antibody is directly detected on X-ray film using fluorescent imaging systems. Due to the ease of detection and signal amplification, the indirect method is widely used for protein detection in Western blotting. The presence of a band refers to the presence of the protein of interest in the protein mixture whereas the band width indicates the concentration of that protein.

This technique has several advantages and disadvantages. The techniques allow a better separation and detection of proteins in a mixture on the basis of size, charge as well as conformation. Due to the option of stripping of the primary antibodies from the proteins of interest, many different proteins can be detected in one assay. As SDS-PAGE is part of the process, the molecular weight of the proteins is determined as well. With the necessary level of expertise, antibodies for most of the proteins can be developed in the lab, if not available on the market. The main disadvantage of western blotting is that it is time consuming as it takes 2-4 days. In order to get precise results, both the theoretical and practical knowledge of the process, the role of the involved material and the properties of the protein of interest are very important. The antibodies used in this technique are expensive, and most are consumed in optimisation studies, which escalates the total cost of the experiments. Also, the non-

specific binding of the antibodies to other proteins sometimes produces confusing results. It is very important to confirm that equal amounts of proteins are loaded in all the lanes of the gel, compared with the control, as differences in the loading interferes with the results. In order to normalise the amount of proteins across the gel, other protein quantification assays are needed to be coupled with western blotting.

3.2 Materials

The following materials were used in this research.

Table 3.1: List of materials: Table enlisting various materials along with the suppliers and batch number/product code used in this part of the project.

Product	Supplier	Batch Number
12-well plates	Corning	3512
25/75 cm^2 Flasks	Corning	26414015
6-well plates	Corning	3506
96-well plates	Corning	3799
A2780	Lab cryostore	Passag No. 12
A375	Lab cryotstore	Passag No. 18
AO	Sigma-Aldrich Company Ltd	A6014-10G
Aprotinin	Sigma-Aldrich Company Ltd	A1153
Calcium chloride ($CaCl_2$)	Sigma-Aldrich Company Ltd	21114-1L
CellTiter-Blue®	Promega	304416
CHAPS	Sigma-Aldrich Company Ltd	C5070
DCDHF	Sigma	5153
DEVD-AMC	BD Biosciences	556449
Dimethyle sulfoxide (DMSO)	Thermoscientific.	20688
Dithiothrietol (DTT)	Sigma-Aldrich Company Ltd.	D9779
Dried Milk	Tesco stores, UK	3024249
Ethylene glycol tetra acetic acid (EGTA)	Sigma-Aldrich Company Ltd.	E8145
Foetal bovine serum (FBS)	Invitrogen	10270-098
FCCP	Sigma-Aldrich Company Ltd	C2920-10MG
FLUO-2	TEFlabs	0229
L-glutamine	Sigma-Aldrich Company Ltd	G-7513
Glycerol	Sigma-Aldrich Company Ltd	G7893-1L

H_2O_2	Sigma-Aldrich Company Ltd	H1009-5ML
Haemocytometer	Mausser, USA	
Hepes	Sigma-Aldrich Company Ltd	H7523
IM-54	Sigma-Aldrich Company Ltd	SM40412-5ML
Potassium Chloride (KCl)	Sigma-Aldrich Company Ltd	P9333
Leupeptin	Sigma-Aldrich Company Ltd	9783-25MG
Methanol	VWR chemicals	15D270505
Magnesium chloride ($MgCl_2$)	Sigma-Aldrich Company Ltd	M1028
MTT (3-[4,5-dimethylthiazol-22-yl])-2,5 diphenyl tetrazolium bromide)	Calbiochem	4759-89
Sodium chloride (NaCl)	VWR chemicals	7647-14-5
Non-essential amino acids (NEAA)	Invitrogen	11140-050
Needles	BD Microlance	BD300800
Nitrocellulose membrane	GE Healthcare	10600002
Phosphate buffer saline (PBS)	Sigma-Aldrich Company Ltd	P4417-50TAB
p-Coumaric acid	Sigma-Aldrich Company Ltd	C9008-10G
Phenylemethanesulfonyle floride (PMSF)	Sigma-Aldrich Company Ltd	P7626
PNT2a cells	Lab cryostore	(Passag No.) 12
Polyacrylamide gel	Sigma-Aldrich Company Ltd	A3574-10ML
Roswell Park Memorial Institute medium 1640 (RPMI 1640)	Lonza	BE12-167F
SDS	Sigma-Aldrich Company Ltd	L4501
Sodium orthovanadate	Sigma-Aldrich Company Ltd	S6508-250G
Sodium Puruvate	Invitrogen	11360-09
Staurosporine from ***Streptomuces* specie**	Calbiochem	S-69397
Penicillin /streptomycin	Sigma-Aldrich Company Ltd	P4408-100ML
Sucrose	Sigma-Aldrich Company Ltd	S5016
5 mL Syringes	Terumo	95H14X3
Sytox® Green	Life technologies	16205

Tetramethylrhodamine ethyl ester (TMRE)	Sigma-Aldrich Company Ltd	87917-25MG
Tris-base	Sigma-Aldrich Company Ltd	T-1503
Triton X-100	Sigma-Aldrich Company Ltd	103H0421
TrypLE Express	Invitrogen	12604-013
Hank's balanced salt solution (HBSS)	Invitrogen	14175-057
o-Phenylenediamine dihydrochloride	Sigma-Aldrich Company Ltd	P9029-50G
Peroxidase from horseradish	Sigma-Aldrich Company Ltd	777332-100MG
Cisplatin (*cis*-Diammineplatinum(II)dichloride)	Sigma-Aldrich Company Ltd.	P4394

3.3 Methods

3.3.1 Cell lines; seeding, culture and storage

Two human cancer cell lines, A375 and A2780, and human non-cancer cell line, PNT2a, were used for the evaluation of the cytotoxicity effects of Lcad and CsL.

The cells were cultured in complete growth medium, that is, Roswell Park Memorial Institute (RPMI) 1640 growth medium supplemented with 10% (v/v) foetal bovine serum, 1% (v/v) non-essential amino acids, 1% (v/v) sodium pyruvate and 1% (v/v) streptomycin/penicillin. For culturing, cells were removed from a cryo-bank (liquid N_2, -210 °C) and thawed slowly to equilibrate at 37 °C in a water bath and were then transferred to a 25 cm^2 flask to which 5 mL of pre-warmed (at 37 °C) medium was added. The cells were incubated in humidified air containing 5% CO_2 at 37 °C for 3-5

days and the medium was changed every 24 hours. After the initial growth phase, all cell lines were then transferred to 75 cm^2 flasks. In order to harvest them, cells were incubated with TripLE Express® for 3 minutes at 37 °C. An equal volume of complete growth medium was added to deactivate the TripLE Express® followed by transfer to a 15 mL centrifuge tube and centrifugation at 600 x g for 2.5 minutes. The supernatant was removed and the cell pellet resuspended in 10 mL growth medium. The cell suspension was transferred to a 75 cm^2 flask, and the final volume was made up to 20 mL with growth medium and the flask was incubated in humidified air containing 5% CO_2 and at 37 °C. In order to seed the cells in a 12/24/96 well plate, cells were harvested according to the above procedure and counted using a haemocytometer. The volume of the cell suspension containing the pre-determined number of cells for each assay and plate type was transferred to the wells in the plate and incubated at 37 °C in a humidified atmosphere containing 5% CO_2. Cells were allowed to adhere to the plates for 24h. For cryopreservation, cells were harvested from the flasks and resuspended in FBS containing 10% (v/v) DMSO to a final concentration of 10^6 cells/mL. The cell suspension was transferred to cryovials (1ml/vial), placed at -80 °C overnight after which the vials were transferred to liquid N_2 for long term storage.

3.3.2 Effect of Lcad/CsL on amino acids present in growth media

Cell culture media, RPMI 1640, contains a number of essential and non-essential amino acids including L-glutamic acid, L-arginine hydrochloride, L-aspartic acid, Lserine, L-threonine, L-isoleucine and L-leucine. In order to evaluate the catalytic effect of the venom samples on these amino acids, a LAAO assay was carried out

with/without the presence of additional L-Leu according to the procedure mentioned in section 2.8.2. RPMI 1640 (RPMI) and complete RPMI 1640 (RPMI.C) growth medium were used as negative controls. Data were represented as mean±SEM of triplicate readings compared with the respective negative control.

3.3.3 Cell morphology

Cells were seeded at a concentration of 5,000 cells/well (A375) and 10,000 cells/well (A2780 and PNT2a) in 96-well plates and incubated overnight at 37 °C in a cell culture incubator having humidified atmosphere with 5% CO_2 for adhesion to the plates. The next day the cells were exposed to 20 µg/mL of Lcad and CsL for 4h.

A Nikon TMS inverted phase contrast microscope was used to visualise the cells with a 10X objective lens to observe changes in the morphology of the treated cells as well as the positive control (staurosporine, 5 µM) and negative control (growth medium only). The morphological changes were recorded as digital photomicrographs with the aid of a microscope mounted digital camera (Moticam) 1000; Motic Germany), using Motic Images Plus 2.0 and were stored on a desktop computer running Microsoft Windows XP.

3.3.4 CellTiter-Blue® cell viability assay

Cell viability was determined using a CellTiter-Blue® assay kit according to the manufacturer's instructions. A375 (5,000 cells/well), A2780 (10,000 cells/well) or PNT2a (10,000 cells/well) were seeded in 96-well plates in a final volume of 100 µL of growth medium per well. The plates were then incubated at 37 °C overnight in order to allow cell adhesion. Dose-response curves were constructed by incubating the cells

with increasing concentrations (0.15-20 µg/mL) of Lcad or CsL for 4h in a cell culture incubator. Staurosporine at a final concentration of 5 µM was used as a positive control for apoptosis. The negative control consisted of the same number of cells in growth medium only. Cells were further incubated for 4h at 37 °C in humidified air containing 5% CO_2 after adding 20 µL of the CellTiter-Blue® reagent. The fluorescence (ex/em: 560/590 nm) of the resofurin was then measured. The potency of the venom samples was compared with the chemotherapeutic drug, cisplatin (20 µg/mL). The sensitivity of the cancer cell lines used were determined by carrying out the same procedure after incubating A375 and A2780 cells to 0.1520 µg/mL of cisplatin for 24 h. The viability of the cells was expressed as a percentage of the untreated (negative) control. The experiment was carried out three times and the percentage calculated from the mean ± SEM of the triplicate values. $P \leq 0.05$ was considered as significant.

3.3.5 Cell membrane integrity

For quantitative analysis of cell membrane integrity, A375 and A2780 cells were seeded in 96-well plates at a concentration of 5,000 cells/well and 10,000 cells/well, respectively. After 24h, cells were incubated with 20 µg/mL of Lcad and CsL for 4h at 37 °C. Sytox® Green working solution (5 µM) was prepared by diluting with prewarmed growth medium. The medium containing venom samples was replaced with Sytox® Green working solution and the plates were incubated for 10 min at 37 °C in humidified air containing 5% CO_2. Fluorescence was then measured at 504 nm excitation and 523 nm emission using a microplate reader (M5, Molecular Devices).

As a positive control, cell membrane integrity of the cells was compromised with ROS by treating cells with 1 mM of H_2O_2 for the same amount of time as venom . Cells exposed to growth medium were used as a negative control to which the treated wells were compared. The experiment was repeated three times and results were expressed as mean ± SEM compared to the negative control.

For fluorescence imaging of Sytox® Green, cells were grown on cover slips. Cell suspension containing A375 and A2780 cells at a concentration of 5 x 10^5 cells/well and 1 x 10^6 cells/well, respectively, were transferred to 12-well plates containing cover slips (12 mm) pre-sterilised by soaking in 70% (v/v) ethanol overnight. The cells were allowed to adhere to the cover slips for 24h in an incubator providing an atmosphere containing 5% CO_2 and constant temperature of 37 °C. Cells were then treated with 20 μg/mL of Lcad and CsL for 4h under the same conditions. The media was removed, cells adhered to the cover slips were washed twice with sterile PBS and then transferred to a petri-dish containing 1 mL of PBS. The petri-dish was placed on the stage of a fluorescent microscope (Ziess, Germany) and the fluorescence was visualised using a filter set 9 (ex/em: 450-490/515 nm). Images were taken using a camera (Hamamatsu multi format CCD camera) attached to the microscope and stored on a desktop computer with a XP operation system using WinFluor V3.8.2 (University of Strathclyde).

3.3.6 Necrosis Inhibition with IM-54

A375 and A2780 cells were seeded in 96-well plates as described above. The cells were exposed to a final concentration of 10 μM of IM-54 for 2 h. The media was

replaced with fresh media containing 20 µg/mL of Lcad and CsL. H_2O_2 at a final concentration of 1 mM was used as a positive control, while the negative control consisted of untreated cells grown growth medium only. The cells were incubated at 37 °C for 4 h with these different treatments after which the viability of the cells was assessed with CellTIter Blue® assay according to the procedure in section 3.3.2. The results were expressed as the mean ± SEM of triplicate readings as a percentage of the negative control.

3.3.7 AO staining

AO staining was used to detect increases in AVOs formation in the cells. In order to quantify AVOs in the venom treated cells, A375 and A2780 cells were grown in 6well plates at a concentration of 5 x 10^5 and 10^6 cells/well, respectively, and were incubated overnight at 37 °C in an incubator having humidified atmosphere of 5% CO_2. The cells were then exposed to 20 µg/mL of Lcad and CsL for 4 h. The cells were harvested using Triple Express® , and were suspended in fresh growth medium containing AO to a final concentration of 100 µg/mL. The cell suspension was incubated with the stain solution for 20 min at 37 °C. Excess dye was washed by pelleting the cells at 7000 x g for 3 min which were then resuspended in prewarmed PBS. The washing step was repeated twice. Fluorescence (ex/em: 490/650 nm) of the AO was measured by transferring 100 µL of the cell suspension in a 96well plate and measuring the absorbance at (ex/em) 490/650 nm. Rapamycin, autophagy inhibitor (MOA explained in section 1.9.8), to final a concentration of 100 µM was used as a

positive control, while cells incubated with growth medium were used as a negative control.

3.3.8 ROS measurement

The level of ROS generation in response to Lcad and CsL treatments in A375 and A2780 cells was determined with DCDHF. DCDHF stock solution of 100 µM concentration was prepared in DMSO. A375 (5 x 10^5/well) and A2780 (1 x 10^6) were seeded in a 6 well plate. After 24 h from seeding, Lcad and CsL were added to designated wells to get a final concentration of 20 µg/mL. The positive control consisted of cells treated with 100 µM of H_2O_2. ALL the cells were then incubated for 4 h at 37 °C in an incubator containing 5% CO_2. After the treatments, the media was removed and fresh media was added to the wells containing DCDHF to a final concentration of 10 µM. The cells were incubated with the dye at 37 °C for 30 min. Cells were washed twice with sterile PBS to wash out the excess dye. Cells were harvested using TripLE Express® and 100 µL of each treatment was transferred to different wells of a 96-well plate. Fluorescence of the cells was measured (ex/em: 495/525 nm). Untreated cells grown in RPMI 1640 were used as the negative control. The experiment was carried out in triplicate wells and results expressed as mean ± SEM compared to the negative control.

3.3.9 Evaluation of mitochondrial membrane potential and function The MMP was quantitatively and qualitatively evaluated using TMRE.

For quantitative evaluation of MMP, A375 (5 x 10^3/well) and A2780 (1 x 10^4/well) cells were seeded in 96-well plates. After 24 h fresh media containing Lcad and CsL to a final concentration of 20 µg/mL was added to designated wells and incubated at 37 °C for 4 h. At the end of the treatment, TMRE solution was added to obtain a final concentration of 500 nM in each well. Carbonyl cyanide 4-(trifluoromethoxy)phenylhydrazone (FCCP), at a final concentration of 100 nM, was used as a positive control and was added to the control wells at the same time as TMRE. The plates were incubated at 37 °C for 40 min with the probe, after which the fluorescence (ex/em: 545/590) was measured using a microplate reader.

For fluorescent imaging, cells at a concentrations of 5 x 10^5 /well (A375) and 1 x 10^6/well were grown on coverslips. Solutions of Lcad and CsL to a final concentration of 20 µg/mL were prepared in fresh growth media and incubated with the cells at 37 °C in humidified air containing 5% CO_2. After venom treatment, the cells were further incubated with 500 nM TMRE for 40 min and were washed twice with pre-warmed PBS to wash off the excess dye. The coverslips were transferred to a petri-dish (60 x 15 mm) containing 1 mL of PBS and visualised with a Zeiss fluorescent microscope using filter set 09 (Ex 450-490/ Em 515).

To further investigate the effect of these venom samples on mitochondrial function, a MTT assay was carried out. A375 (5,000 cells/well) and A2780 (10,000 cells/well) were seeded in 96-well plates in a final volume of 100 µL of growth medium per well. The plates were then incubated at 37 °C overnight in order to allow cell adhesion to the bottom of the wells. A dose-response was constructed by incubating the cells with

increasing concentrations (0.15-20 μg/mL) of Lcad and CsL for 4 h in a cell culture incubator. Staurosporine at a final concentration of 5 μM was used as a positive control. The negative control consisted of untreated cells, grown in growth medium only. The medium in the plate was then replaced with fresh cell growth medium containing 20% (v/v) MTT and was further incubated for 4 h at 37 °C in humidified air containing 5% CO_2. The metabolite formazan was then solubilised by adding DMSO to the cells and incubating at room temperature for 10 min. The absorbance was measured at 560 nm with a microplate reader. The metabolic activity of the cells was expressed as a percentage of the untreated control. The experiment was carried out in triplicate and the results calculated from their mean ± SEM compared to the untreated control.

3.3.10 Caspase 3/7 activity

Caspase 3/7 activity was detected using the fluorogenic substrate N-acetyl- Asp-GluVal-Asp-7-amino-4-methlycoumarin (DEVD-AMC). Assay buffer (3X) was prepared by mixing 150mM HEPES, 450mM NaCl, 150mM KCl, 1.2 mM EGTA, 1.5 % (v/v) triton, 0.3 % (w/v) CHAPS and 30 % (w/v) sucrose and the pH was adjusted to 7.4. Substrate solution was freshly prepared just before the assay by adding 21 μL of DEVD-AMC (10mM), 50 μL of PMSF (3 mM) and 300 μL of DTT (30 mM) to 3.1 mL of the assay buffer. A375 and A2780 cells were seeded at a concentration of 5,000 cells/well and 10,000 cells/well, respectively, in 96-well plates. After 24 h, 60 μL of growth medium containing 20 μg/mL of Lcad and CsL were added to designated wells and incubated for 4 h at 37 °C in humidified air containing 5% of CO_2. A total of 30 μL of substrate

solution was added to the wells and the plates were further incubated at 37 ° for an hour. The fluorescence was measured using a microplate reader (ex/em: 360/460 nm). The experiment was repeated three times and results were represented as mean ± SEM of the triplicate experiments compared to the untreated control.

3.3.11 Ca^{2+} imaging assay

The Ca^{2+} flux was measured with the help of Fluo-2. A375 (5,000 cells/well) and A2780 (10,000 cells/well) were seeded in 96-well plates. After 24 h, Lcad and CsL were added to designated wells to a final concentration of 20 µg/mL and the plates were incubated at 37 °C for 4 h. $CaCl_2$ at a final concentration of 1mM was used as the positive control. The negative control consisted of cells in growth medium only. After aspiration of the media, fresh media containing 4 µM Flou-2 was added to the wells followed by 30 min incubation. The cells were washed with pre-warmed sterile PBS. Fresh 100 µL PBS was added to the wells and the fluorescence was measured using a microplate reader (ex/em: 488/535). The experiment was carried out in triplicate and the results were expressed as their mean ± SEM of the three experiments compared to the negative control.

For qualitative analysis, A375 and A2780 cells at a concentration of 5 x 10^5 and 10^6 cells/ well, respectively, were grown on coverslips and, after 24 h, were incubated with 20 µg/mL of Lcad and CsL for 4 h. $CaCl_2$ (1 mM) and growth media were used as positive and negative controls, respectively. The cells were then incubated with 4 µM of Fluo-2 for 30 min at 37 °C. Excess dye was washed with pre-warmed PBS and the

coverslips were then transferred to a petridish containing 1 mL of PBS for imaging using a Ziess microscope with filter set 9 (ex/em: 450-490/515 nm).

3.3.12 Western blotting

For Western blotting, A375 and A2780 cells were seeded at a concentration of 10^6 and 2 x 10^6 cells/well in 6-well plates and were allowed to adhere to bottom of the plate for 24 h. Lcad and CsL were added to the wells to a final concentration of 20 µg/mL. Staurosporine (5 µM) was used as the positive control. The cells were incubated for 4 h at 37 °C. The plates were placed on ice and washed twice with ice cold PBS. PBS was aspirated and 250 µL of 1X lysis buffer (137 mM NaCl, 2.7 mM KCl , 1 mM $MgCl_2$, 1 mM $CaCl_2$, 1% nonidet P-40, 20 mM Tris-base 10% (v/v) glycerol, 0.5 mM sodium orthovanadate, 0.2 mM PMSF, Leupeptin 10 µl, Aprotinin 10 µL) was added to the wells. A cell scraper was used to detach cells from the bottom of the plate. The cell lysate was homogenised by passing the cell suspension through a 0.5 mm (gauge 21) syringe needle at least 3 times. The cell lysate was analysed on the same day or stored at -80 °C. The cell lysate was then separated using SDS-PAGE using a 10 % polyacrylamide gel and SDS buffer (glycine 0.14 % (w/v) g, SDS 0.01 %(w/v), Tris-Base 0.030 % (w/v) for 1 hour at 100 V. Protein from the gel was then transferred to a nitrocellulose membrane by electrophoresis at 120 V for an hour in transfer buffer (glycine 0.01% (w/v), Tris-Base 0.3 % (w/v), *d*H2O 80 % (v/v), methanol 20 % (v/v). The nitrocellulose paper with the blotted proteins was then left on a rocker for an hour in blocking solution [3 % (w/v) dried milk in TBST (Tris(hydroxymethyl)aminomethane (Tris)]. Primary antibody solution was prepared

by diluting primary antibodies (AIF, Bid, Casp-8, PARP, GAPDH) 1:1,000 in TBST further supplemented with 1 % (v/v) BSA and 5 % (v/v) penicillinstreptomycin. The nitrocellulose paper was incubated in the primary antibody solution overnight at 4°C. The paper was then washed three times with TBST for 5 min and incubated at room temperature with secondary antibody diluted 1:40,000 in TBST containing 1 % (v/v) BSA for an hour. The washing step was repeated and the fluorescence of the proteins was then recorded on X-ray film using two enhanced chemiluminescence (ECL) solutions, ECL 1 [2.5 mL (250 mM in DMSO, 1.1 mL of p-coumaric acid (250 mM in DMSO), Tris-Base (1 M; pH 8.5)] and ECL 2 [165 µL of H_2O_2, Tris-Base (1 M; pH 8.5), 225 mL of *d*H2O].

3.3.13 Statistical analysis

Excel 2010 was used to calculate the mean ± SEM of the triplicate results. Graphs were plotte with Excel 2010 whereas dose-response curves were plotted using Biograph. Statistical significance was calculated using Prism V5 by analysis of variance (ANOVA) and Dunnett Test, where applicable and a P value less than 0.05 was considered as significant.

3.4 Results

3.4.1 Oxidation of growth medium L-amino acids by Lcad/CsL

The depletion of amino acids present in the cell culture medium was determined by exposing growth medium to 20 µg/mL of Lcad and CsL for 4 h. The results showed that both the venom samples did not induce the cataylsis of the amino acids present in the cell culture medium. Significant (P=0.001) LAAO activity was observed only in

treatments containing additional L-Leu (250 µM). RPMI and RMPI.C, without L-Leu, did not demonstrate any LAAO activity when treated with Lcad (Figure 3.6 A) and CsL (Figure 3.6 B).

(A)

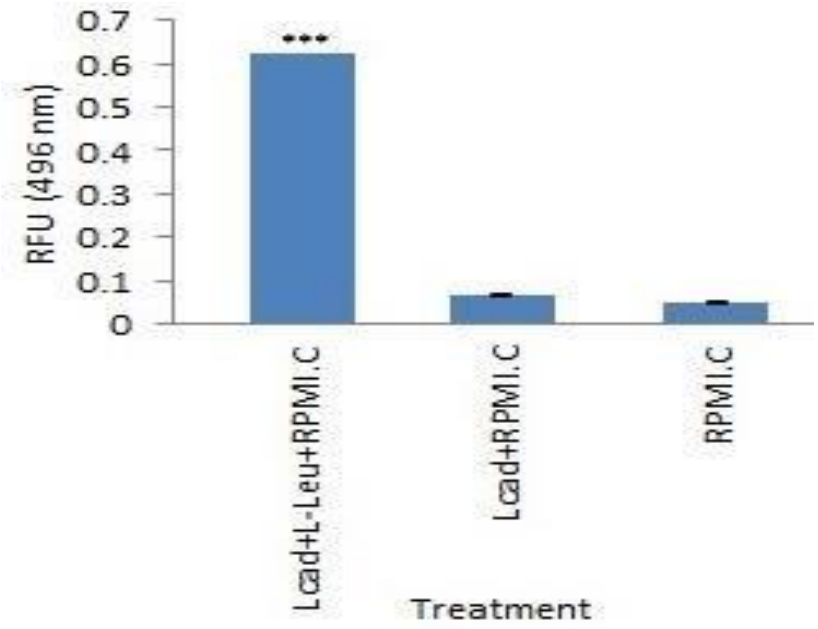

(B)

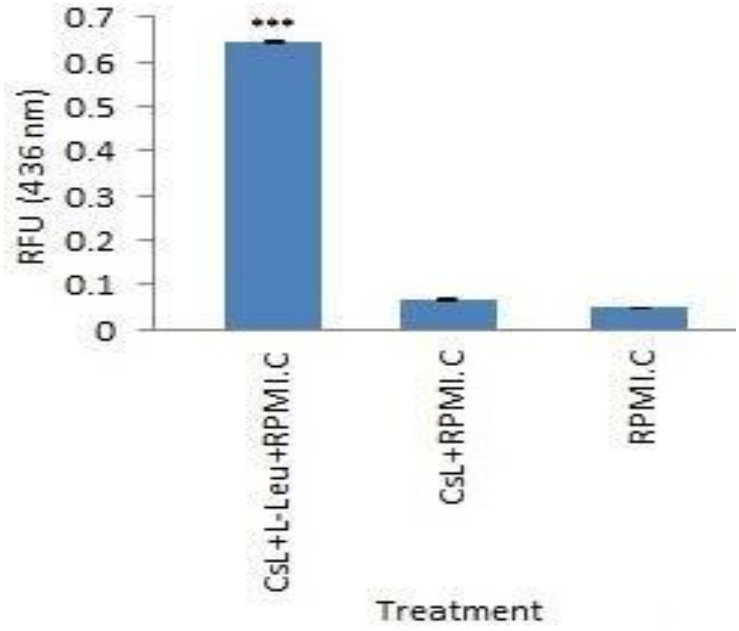

Figure 3.6: Effect of Lcad/CsL on growth medium amino acids: Complete RMPI (RPMI.C) was incubated with 20 µg/mL of Lcad and CsL without or without L-Leu to a final concentration of 250 µM. ***P=0.001 significant rise in L-Leu metabolism, compared with RPMI only. Each data point represents mean±SEM of triplicate readings compared with negative control. (n=3)

3.4.2 Cell Morphology

After 4 h treatment of A375 and A2780 cells with 20 µg/mL of Lcad and CsL, photomicrographs were taken to assess the morphological changes in the cells. Notable reduction in the cellular volume in cells of both cell lines was observed which was similar to the effect of apoptosis-inducer Staurosporine on the morphology of A375 and A2780 cells. Figures 3.7 and 3.8 compare the morphological changes in the cells treated with Lcad and CsL with Staurosporine and negative control.

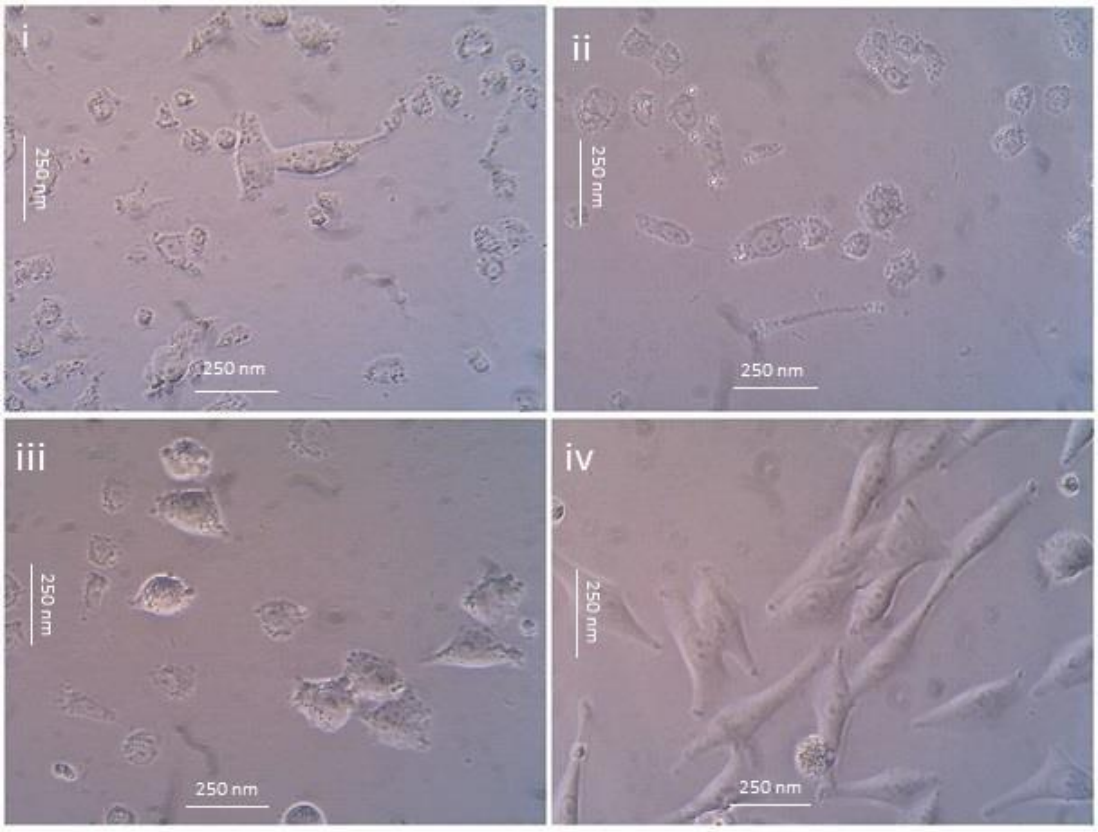

Figure 3.7: Morphological evaluation of Lcad/CsL treated A375 cells: A375 cells were seeded at a concentration of 5,000 cells/well and treated with 20 µg/mL of Lcad and CsL for 4 hours. 40X objective lens was used to observe and record images of the treated and untreated cells. A clear reduction in volume can be seen in (i) Lcad, (ii) CsL, (iii) staurosporine (5 µM) treated cells compared to (iv) untreated controls.

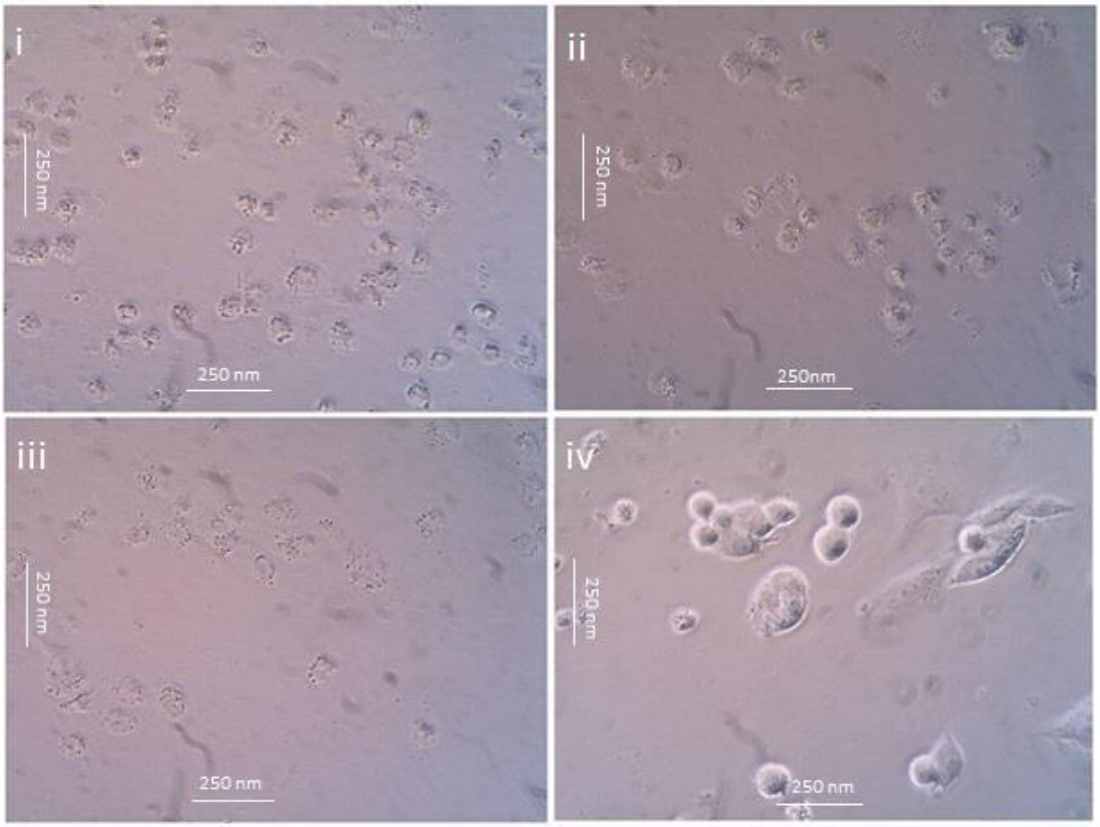

Figure 3.8: Morphological evaluation of Lcad/CsL treated A2780 cells: A2780 cells were seeded at concentration of 10,000 cells/well in 96-well plate and treated with 20 µg/mL of Lcad and CsL for 4 h. Staurosporine to a final concentration of 5 µM was used as a positive control. 40X objective lens was used to observe and record images. A clear reduction in volume can be seen in (i) Lcad, (ii) CsL, Staurosporine (5 µM) treated cells compared to (iv) untreated controls.

3.4.3 Cell viability

The effect of Lcad and CsL on the viability of A375, A2780 and PNT2a was determined with a CellTiter-Blue® assay kit. Dose-response curves were plotted and the IC_{50} for Lcad on A375 and A2780 was 1.1±0.1 µg/mL (Figure 3.9 A) and 1.95±0.2 µg/mL (Figure 3.9 B), respectively. Similarly, treatment with CsL on A375 and A2780 cells showed an IC_{50} of 2.46±0.2 µg/mL (Figure 3.9 C) and 3.6±0.6 µg/mL (Figure 3.9 D), respectively.

(A)

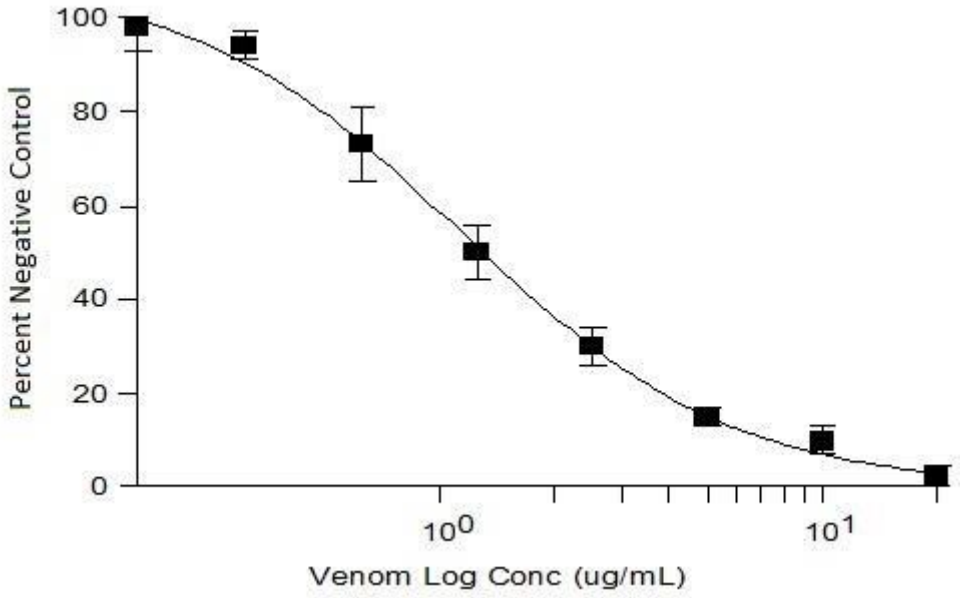
100
80
60
40
20
0
Percent Negative Control
10^0
10^1
Venom Log Conc (ug/mL)

(B)

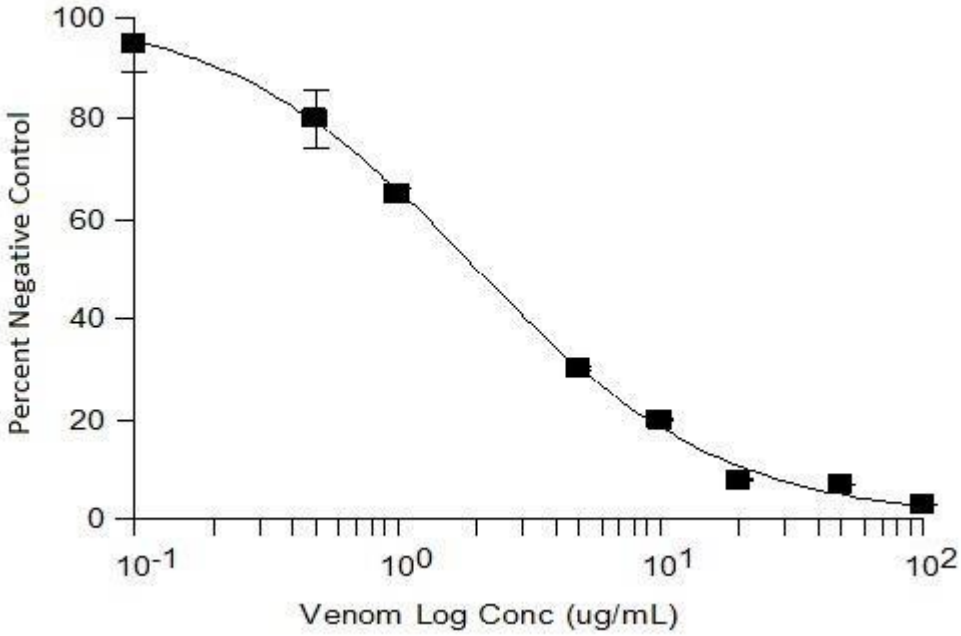
100
80
60
40
20
0
Percent Negative Control
10^{-1}
10^0
10^1
10^2
Venom Log Conc (ug/mL)

(C)

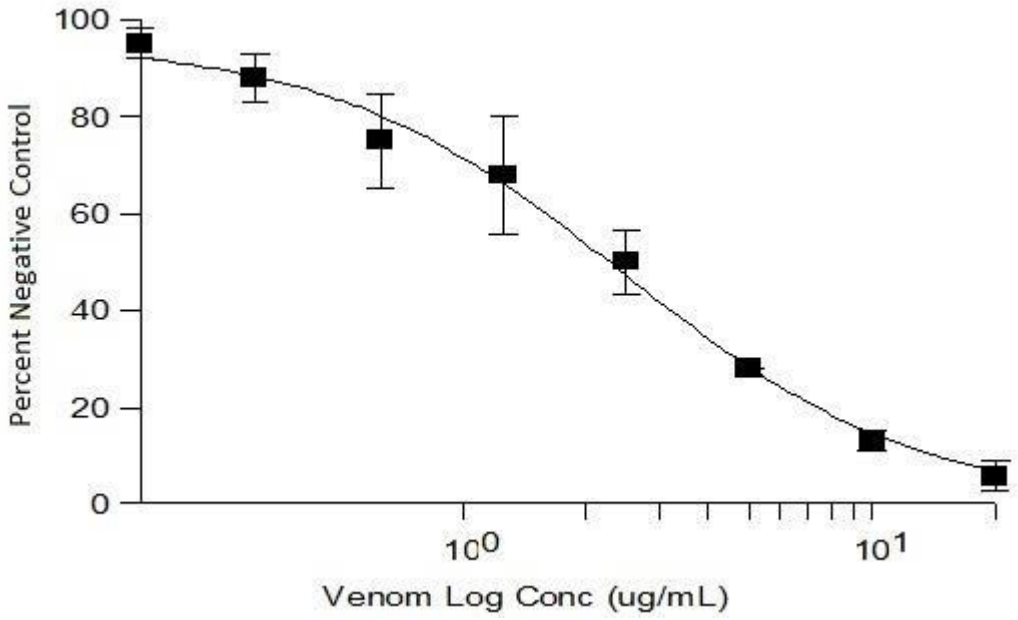

(D)

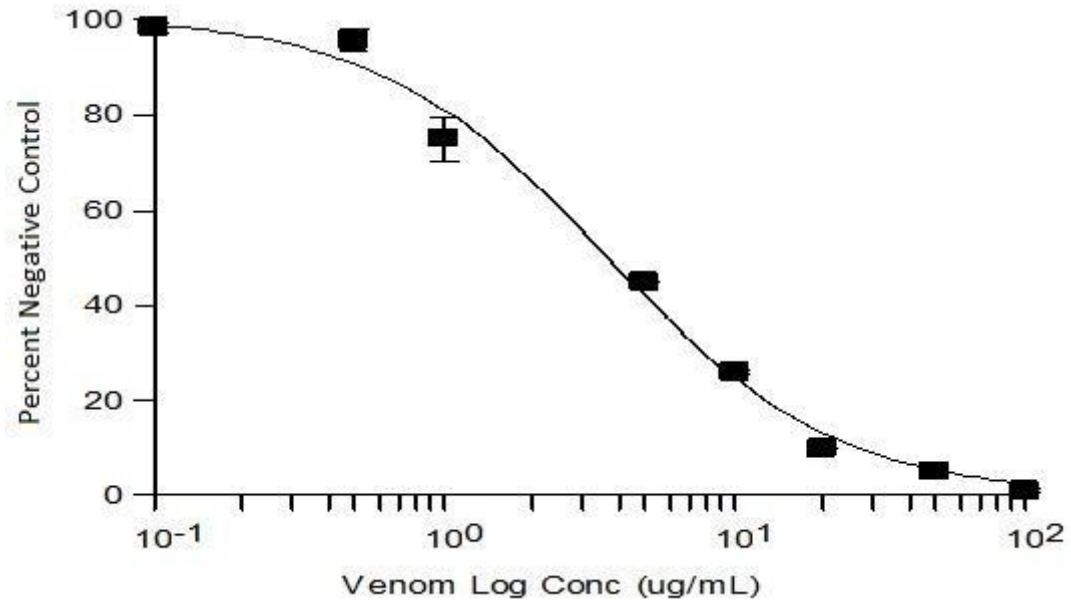

Figure 3.9: Dose-response curves: Effect of Lcad and CsL at various concentrations (0.15-20 µg/mL) on (A)/(C) A375 and (B)/(D) A2780 cells after 4 h of incubation at 37 °C. Each point represents cell viability as the mean±SEM of the untreated controls, carried out in triplicate wells (n=3).

The cancer selectivity of Lcad and CsL was determined by treating the cancer cell lines and a non-cancer cell line (PNT2a) with 20 µg/mL of Lcad and CsL for 4 h. The results revealed that Lcad and CsL significantly (*P*=0.001) (Figure 3.10) affected the viability of A375 and A2780 cells, whereas, a non-significant decrease in the viability of PNT2a cells was observed after Lcad and CsL treatment.

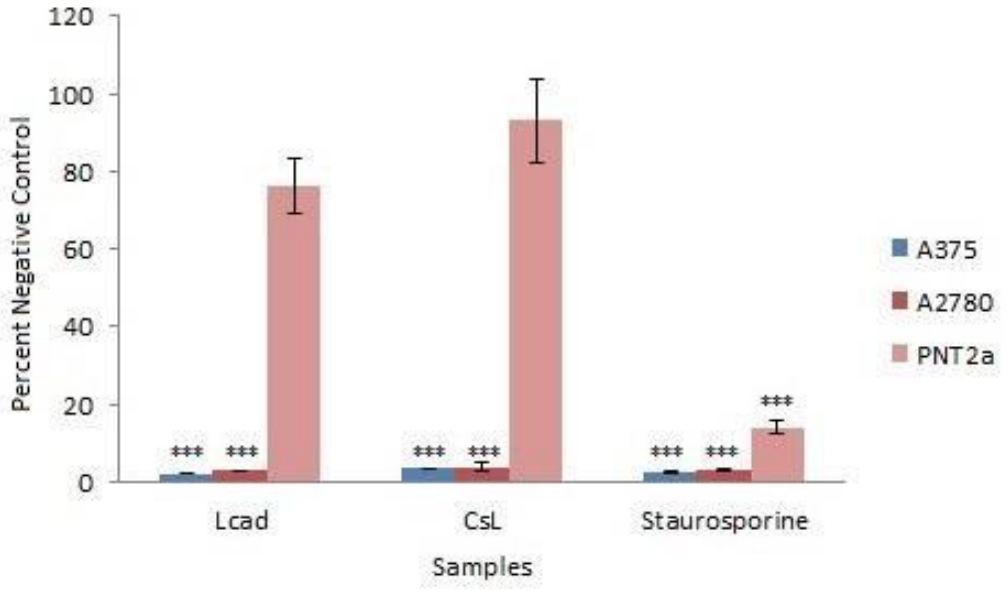

Figure 3.10: Cancer selectivity of Lcad and CsL: Lcad and CsL (20 µg/mL) were incubated for 4 h with cancer cell lines (A375 and A2780) and a non-cancer cell line (PNT2a). ****P*= 0.001 indicates significant decrease in viability, compared with negative control. Stuarosporine (5 µM) was used as a positive control. Each bar represents the mean of triplicate values ± SEM, compared with untreated control cells. (n=3)

The sensitivity of both the cancer cell lines used in this project was confirmed before comparing the potency of Lcad and CsL to cisplatin. The dose-response curve of cisplatin on A375 (Figure 3.11 A) showed IC50 of 1.01±0.11 µg/mL, whereas, the cisplatin showed IC 50 2.55±0.1 µg/mL of on A2780 (Figure 3.11 B), which proves the cytotoxic effect of cisplatin on both cells lines. (A)

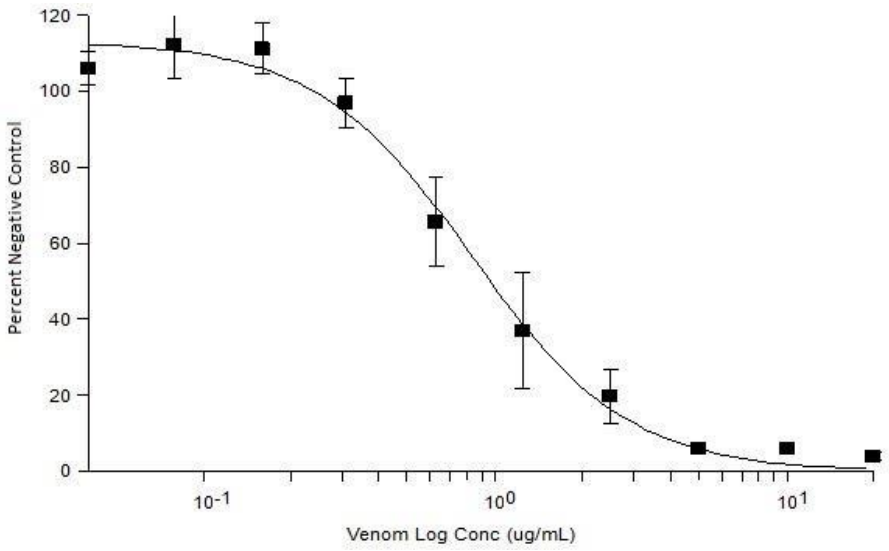

(B)

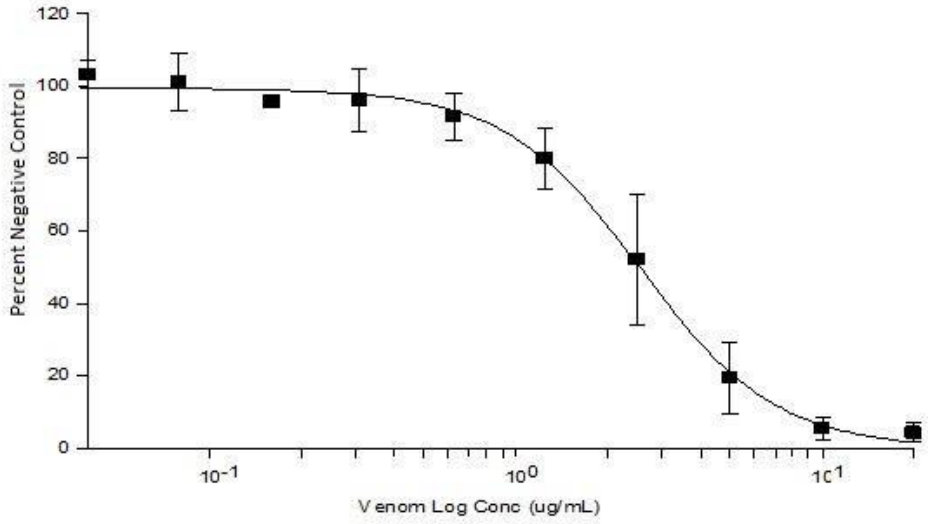

Figure 3.11: Dose response curve of cisplatin on A375 and A2780 cell lines: Effect of cisplatin (0.15-20 µg/mL) on the viability of (A) A375 and (B) A2780 cells after 24 h incubation. Each point represents cell viability as the mean±SEM of the untreated controls, carried out in triplicate wells (n=3).

The potency of the Lcad and CsL was compared to cisplatin. The data suggests that incubation of 20 µg/mL of cisplatin has no significant effect on the viability of A375

and A2780 cells. Figure 3.12 compares potency of 20 µg/mL of Lcad and CsL to the same concentration of cisplatin after 4 h of incubation with the cancer cell lines.

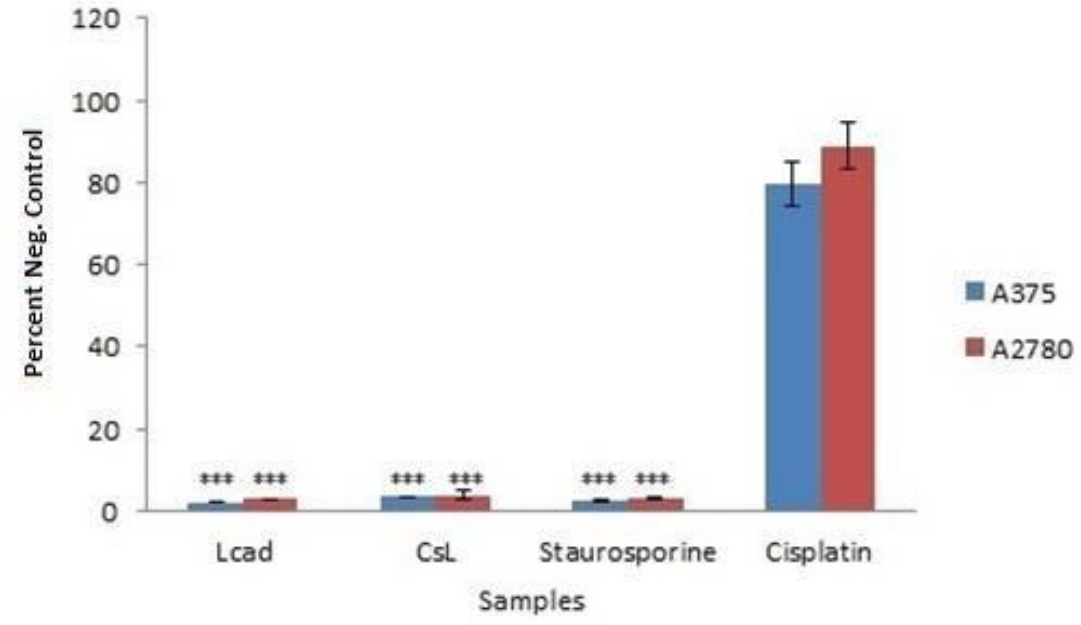

Figure 3.12: Comparison of potency of Lcad and CsL to cisplatin: Cells from A375 and A2780 cell lines were seeded at concentration of 5,000 cells/well and 10,000 cells/well, respectively and treated with Lcad, CsL and cisplatin to a final concentration of 20 µg/mL for 4 h. ****P*=0.001 significant decrease in cell viability, compared with untreated control. Staurosporine (5 µM) was used as a positive control. Each bar represents the mean ± SEM of triplicate results, compared with untreated control cells (n=3).

3.4.4 Cell membrane integrity

The Sytox® Green assay results indicated that the integrity of the cell membrane of the treated cells was retained during the process of cell death. Figure 3.13 shows a signifcant (*P*=0.001) increase of the fluorescence of Sytox® Green in the H_2O_2 (1 mM) treated cells (the positive control). Compared with the untreated control cells, there was no increase in the fluorescence in the Lcad and CsL treated cells which indicates the intact cell membranes of the A375 and A2780 cells after 4 h of treatment with 20

µg/mL of the venom. These results are further supported by the fluorescence imaging. The bright fluorescence from H_2O_2 treated cells (Figure 3.14 Ci A375; Figure 3.15 Ci A2780) confirms the loss of the cell membrane integrity in both the cells lines in the positive controls only, whereas there is no increase in the Sytox® Green fluorescence in A375 (Figure 3.14) and A2780 (Figure 3.15) cells treated with Lcad and CsL confirming that the cell membrane integrity is not compromised.

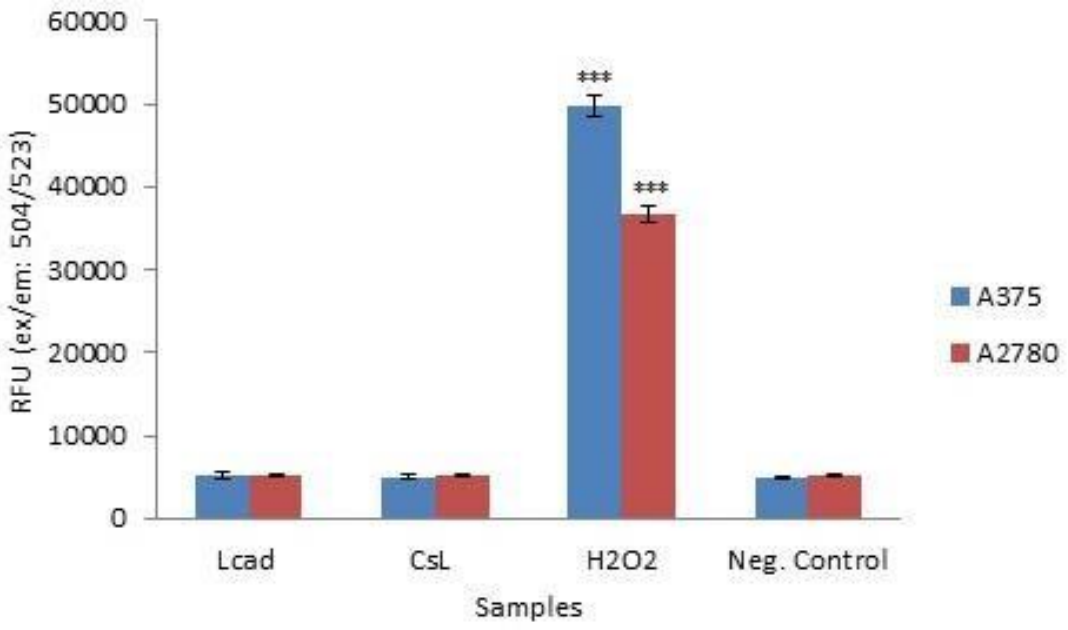

Figure 3.13: Effect of Lcad/CsL on cell membrane integrity: A375 (5,000 cells/well) and A2780 (10,000 cells/well) were seeded in 96-well plates and treated with Lcad and CsL (20 µg/mL) for 4 h. H_2O_2 (1mM) was used as a postive control. *** *P*=0.001 shows a significant effect on the cell membrane integrity, compared with negative control. Each represents mean ± SEM of triplicate readings (n=3).

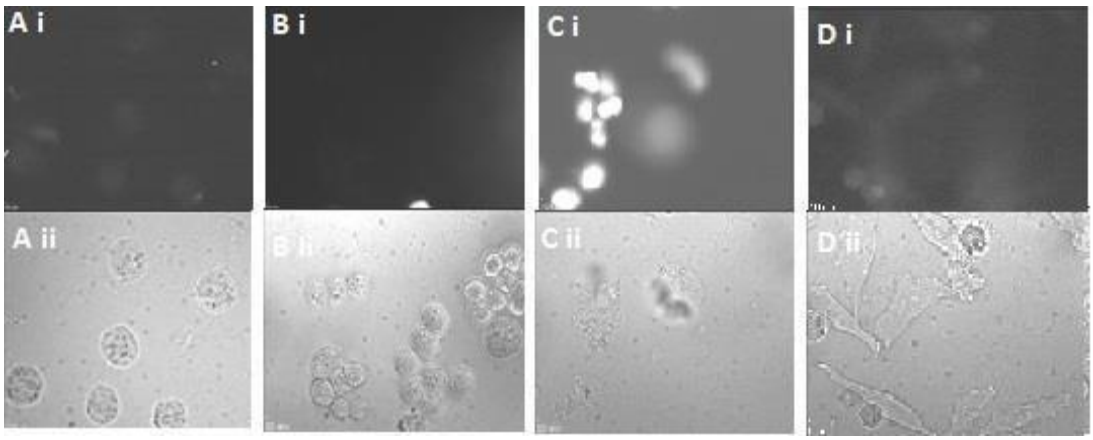

Figure 3.14: Sytox Green® fluorescence/bright field images of A375 cells: A375 cells (5×10^5) were grown on cover-slips and exposed to 20 µg/mL of (Ai) Lcad, (Bi) CsL and (Ci) 1mM of H_2O_2 for 4 h. Fluorescence images were taken at 40X objective lens. Increase in the fluorescence of Sytox Green® is observed in H_2O_2 cells compared to the (Di) negative control. Aii, Bii, Cii and Dii are the respective bright field images.

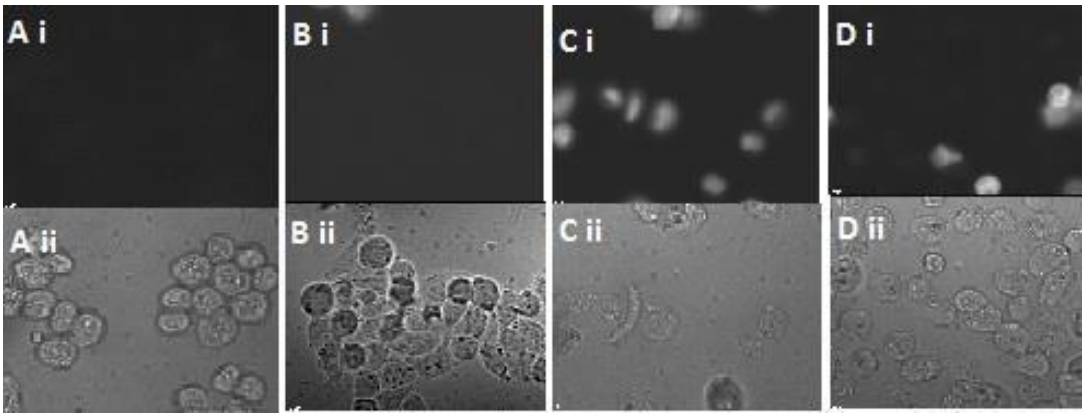

Figure 3.15: Sytox Green® fluorescence/bright field images of A2780 cells: A2780 (10^6) were grown on cover-slips and treated with (Ai) Lcad and (Bi) CsL to a final concentration of 20 µg/mL. (Ci) H2O2 (1 mM) was used a positive control. Increase in the fluorescence in the positive control cells is clear compared to the (Di) untreated cells. Aii, Bii, Cii and Dii are the bright field images of the treated cells, respectively, to verify the presence of cells on the cover-slips.

3.4.5 Inhibition of necrosis

A375 (5,000 cells/well) and A2780 (10,000 cells/well) were seeded in 96-well plates pre-treated with IM-54 (10 µM) and then exposed to 20 µg/mL of Lcad and CsL to determine cell death. Cell death induced by H_2O_2 was delayed by IM-54 in A375 cells (Figure 3.16 A) by as much as 22 % and in A2780 cells (Figure 3.16 B) by 28 %, compared with the untreated controls cells. There was no effect of IM-54 on cell death in A375/A2780 cells treated with Lcad/CsL.

(A)

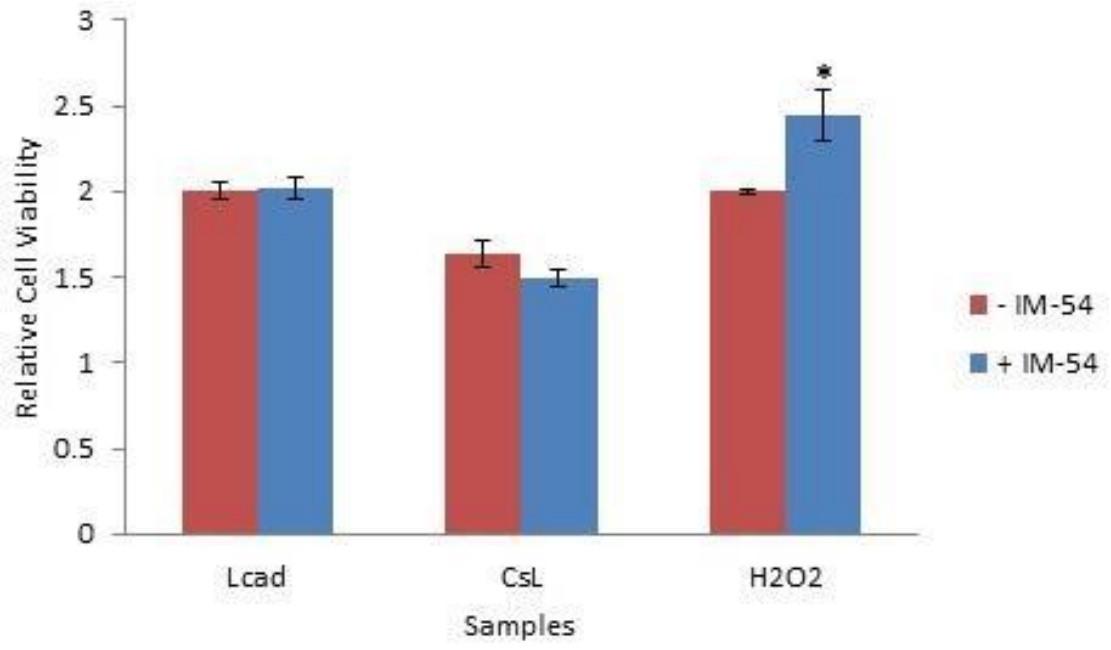

(B)

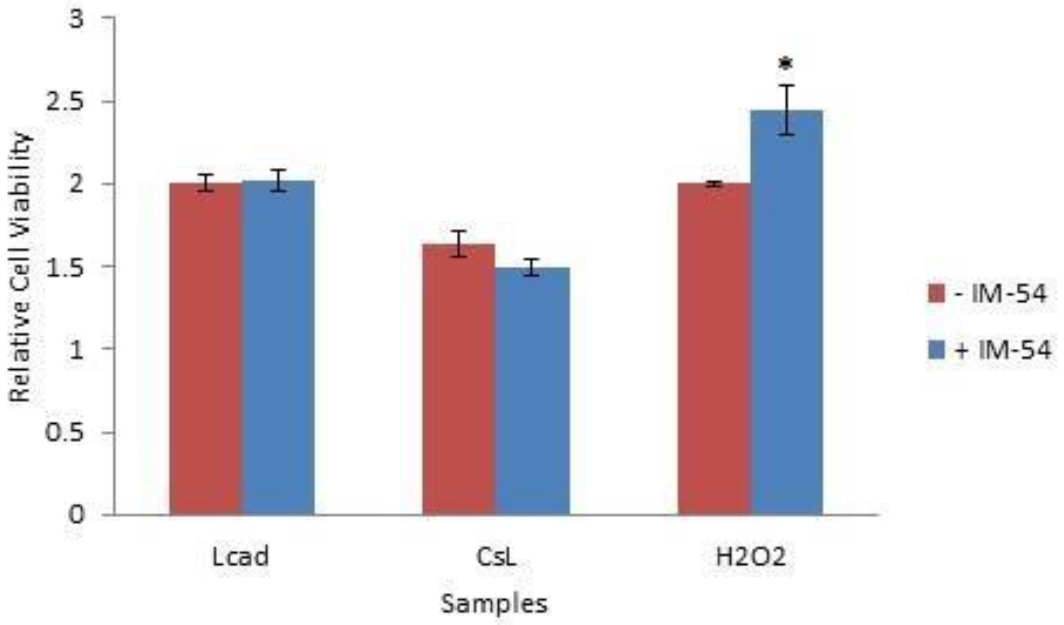

Figure 3.16: Effect of IM-54 on Lcad and CsL induced cell death: (A) A375 (5,000 cells/well) and (B) A2780 (10,000 cells/well) were treated with 10 µM of IM-54 for 2 h and then incubated with 20 µg/mL of Lcad and CsL and 1mM solution of H_2O_2 for 4h. *P=0.05 shows the significance on the cell viability compared to the untreated cells. The experiment was carried out in triplicate and data represented as mean ± SEM of the three readings compared with the negative control (n=3).

3.4.6 Effect of Lcad and CsL on intracellular ROS level

The DCDHF assay established that intracellular levels of ROS did not increase in response to 4 h treatment of Lcad and CsL (20 µg/mL). Figure 3.17 shows that only H_2O_2 (1 mM) induced a significant (P=0.05) increase in ROS levels in both A375 and A2780 cells, however, cells treated with Lcad and CsL did not demonstrate a significant increase in ROS levels compared with the negative control.

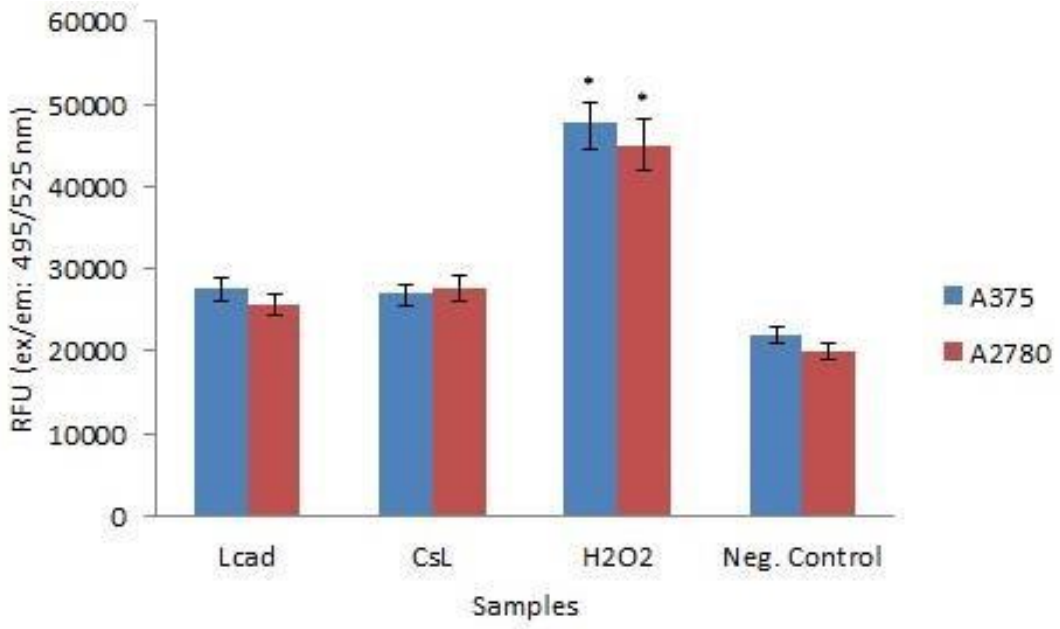

Figure 3.17: Effect of Lcad and CsL on intracellular ROS levels: A375 and A2780 cells were seeded in 96-well plate at a concentration of 5,000 and 10,000 cells/well, respectively, and treated with Lcad and CsL to a final concentration of 20 µg/mL and 1 mM H_2O_2 for 4 hours. ROS levels were detected by incubating the cell with DCDHF (10 µM). **P*=0.05 shows significant increase in the fluorescence, compared with negative control. Each point represents mean ± SEM of triplicate results compared to negative control (n=3).

3.4.7 Effect of Lcad and CsL on mitochondrial membrane potential and function

TMRE fluorescence did not decrease in A375 and A2780 cells treated with Lcad and CsL suggesting that these samples do not alter the MMP in A375 and A2780 cells upon incubation for 4 hours. The only significant (*P*<0.05) decrease in fluorescence of TMRE was observed in cells that were treated with FCCP (100 nM) (Figure 3.18), compared to the untreated control. The fluorescence imaging further verified the loss of in fluorescence of TMRE in the FCCP treated cells only, whereas the fluorescence of Lcad and CsL treated A375 (Figure 3.19) and A2780 (Figure 3.20) cells did not change relative to the negative control.

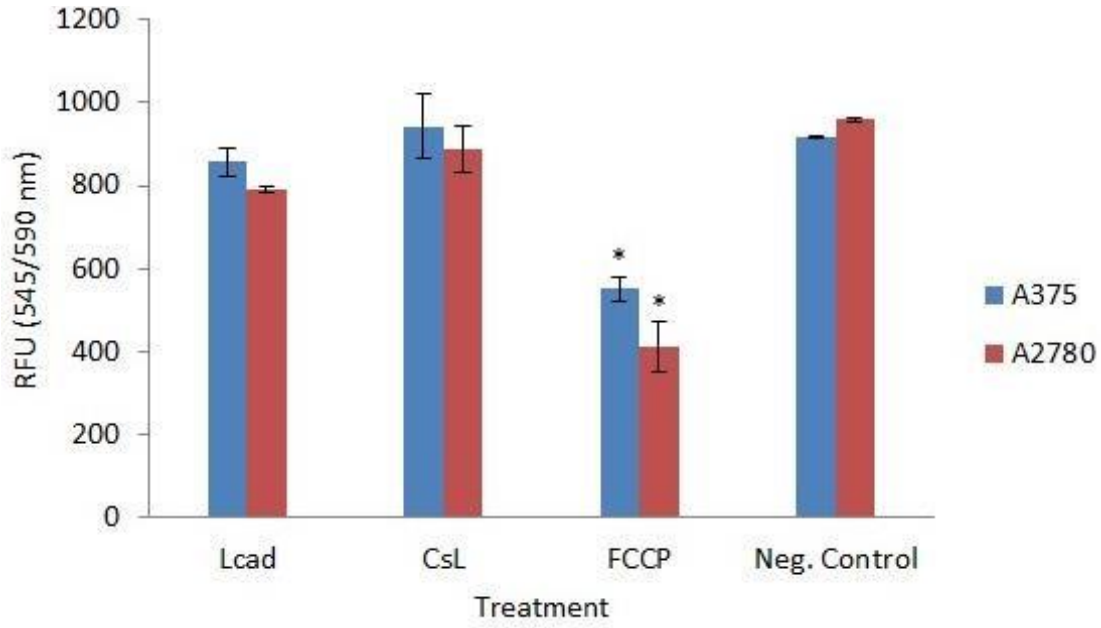

Figure 3.18: Effect of Lcad/CsL on MMP: A375 and A2780 cells were seeded at a concentration of 5,000 and 10,000 cells/well respectively and were treated with 20 µg/mL of Lcad and CsL for 4 h. FCCP (100 nM) was used as a positive control. **P*=0.05 shows a significant decrease in TMRE fluorescence after FCCP (100 nm) treatment. Each bar represents mean ± SEM of triplicate values compared to the negative control (n=3).

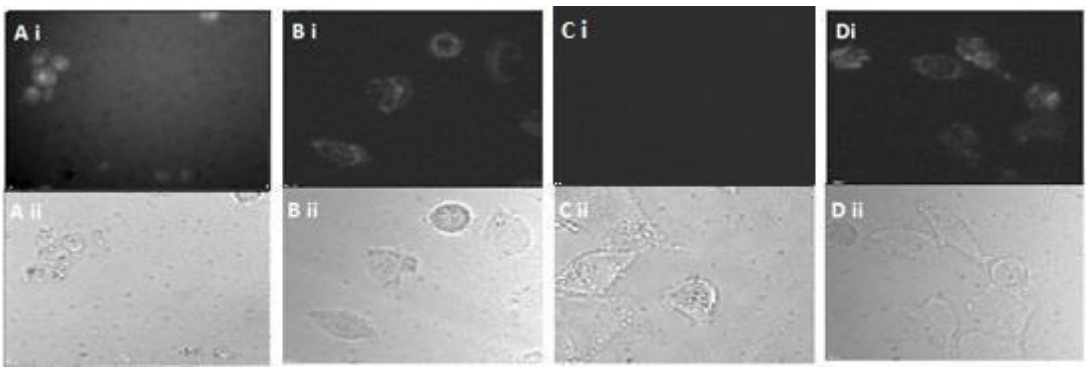

Figure 3.19: TMRE fluorescence/bright field images of A375 cells: A375 (5 x 10^5) cells were grown on cover-slips and were treated with 20 µg/mL of (Ai) Lcad, (Bi) CsL and (Ci) 100 nM FCCP for 4 h. Fluorescence images were taken with40X objective lens. Decrease in fluorescence FCCP treated cells is clear, compared to the negative control (Di). Aii, Bii, Cii and Dii are respective bright field images confirming the presence of cells in the field of view.

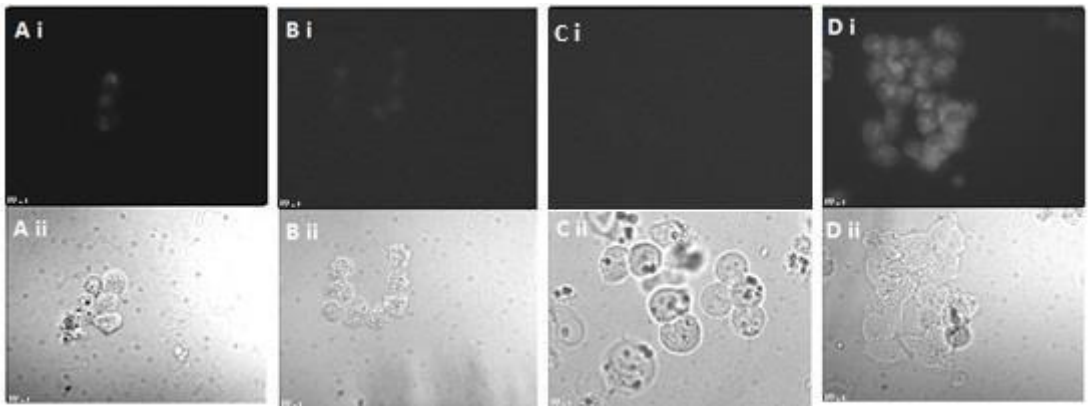

Figure 3.20: TMRE fluorescence/bright field images of A2780 cells: A2780 (10^6)cells were grown on cover-slips and were treated with 20 µg/mL of (Ai) Lcad, (Bi) CsL and (Ci) 100 nM FCCP for 4 h. Fluorescence images were taken using 40X objective lens. Decrease in fluorescence FCCP treated cells is clear, compared to the negative control. Aii, Bii, Cii and Dii are respective bright field images.

A significant (P<0.01) decrease in the metabolism of MTT by mitochondria was observed when A375 and A2780 cells were exposed to 20 µg/mL of Lcad and CsL for 4 hours. Lcad showed 44 ± 4 % and 36 ± 7 % decrease in metabolic activity of the A375 and A2780 cell lines compared to the untreated negative control cells, respectively, whereas, the inhibitory effect of CsL on the mitochondrial reduction of MTT was 38 ± 8 % and 30 ± 8 % in A375 and A2780 cells, respectively (Figure 3.21), which implies that although the mitochondrial function is affected, MPP is not compromised.

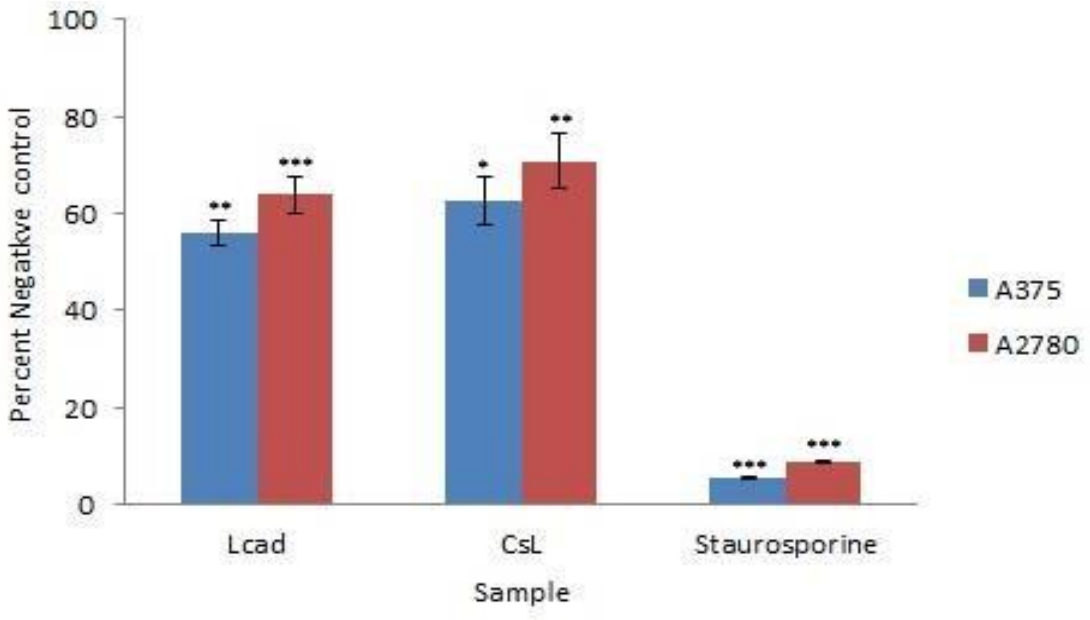

Figure 3.21: Reduction in mitochondrial metabolic activity: A375 (5,000 cells/well) and A2780 (10,000 cells/well) were seeded in 96-well and were treated with 20 µg/mL of Lcad and CsL for 4 h. Mitochondrial function was evaluated with MTT assay. **P*=0.05, ***P*=0.01, *** *P*=0.001 shows the significant effect compared with negative control on MTT metabolism. Staurosporine (5 µM) was used as a positive control. Each bar shows the mean ± SEM of triplicate readings compared with negative control (n=3).

3.4.8 Caspase 3/7 activity

The DEVD-AMC assay revealed that the effector caspases 3 and 7 are not involved in the mechanism of cell death induced in A375 and A2780 cells by Lcad and CsL. The only significant (*P*=0.001) increase in the fluorescence of the AMC (Figure 3.22), compared with the untreated control cells, was observed in the A375 and A2780 cells that were treated with Staurosporine (5 µM) for 4 hours. However, A375 and A2780 cells incubated with 20 µg/mL of Lcad and CsL for 4 hours did not show any increase in the fluorescence of the caspase 3/7 substrate confirming that caspase 3/7 were not activated in the Lcad and CsL treated cells.

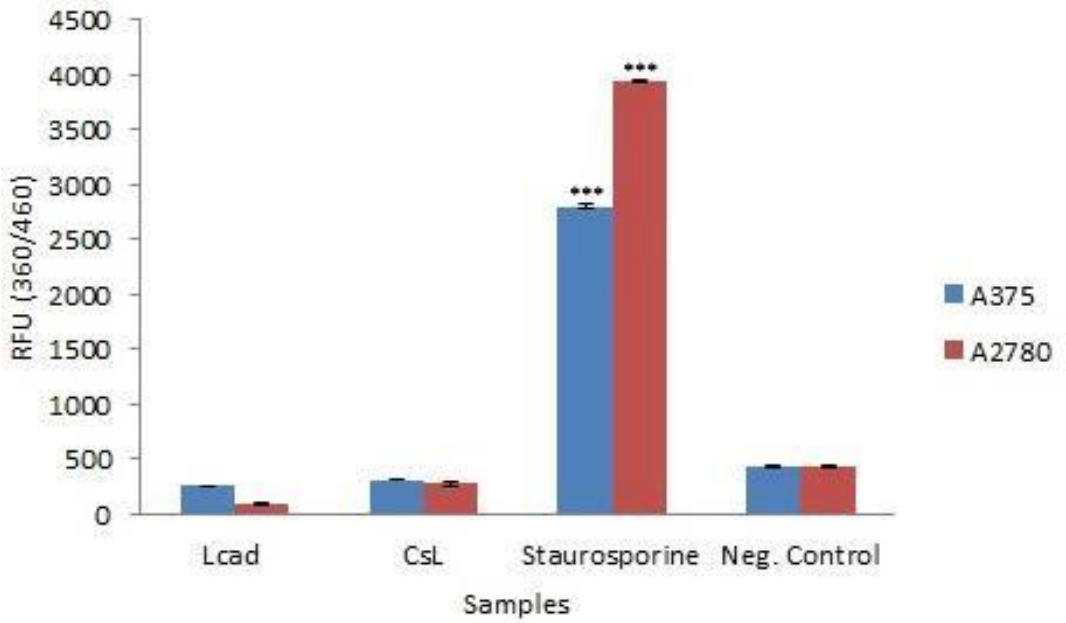

Figure 3.22: Caspase 3/7 activation in response to Lcad and CsL: A375 and A2780 cells were seeded at a concentration of 5,000 cells/well and 10,000 cells/well, respectively, in 96-well plates and incubated with Lcad (20 µg/mL), CsL (20 µg/mL) and Staurosporine (5 µM). Data is represented as mean ± SEM of triplicate results compared with the negative control (n=3).

3.4.9 Detection of AVO

AO staining was used to determine the increase in AVOs, that is, the formation of autophagolysosomes to evaluate autophagy. This assay revealed that compared with the negative control there was no increase in the intracellular acidity in the cells treated with Lcad and CsL (20 µg/mL) for 4 hours. Only the cells treated with rapamycin (1 mM) showed a significant (*P*=0.001) increase in AO fluorescence suggesting increase in intracellular acidity (Figure 3.23).

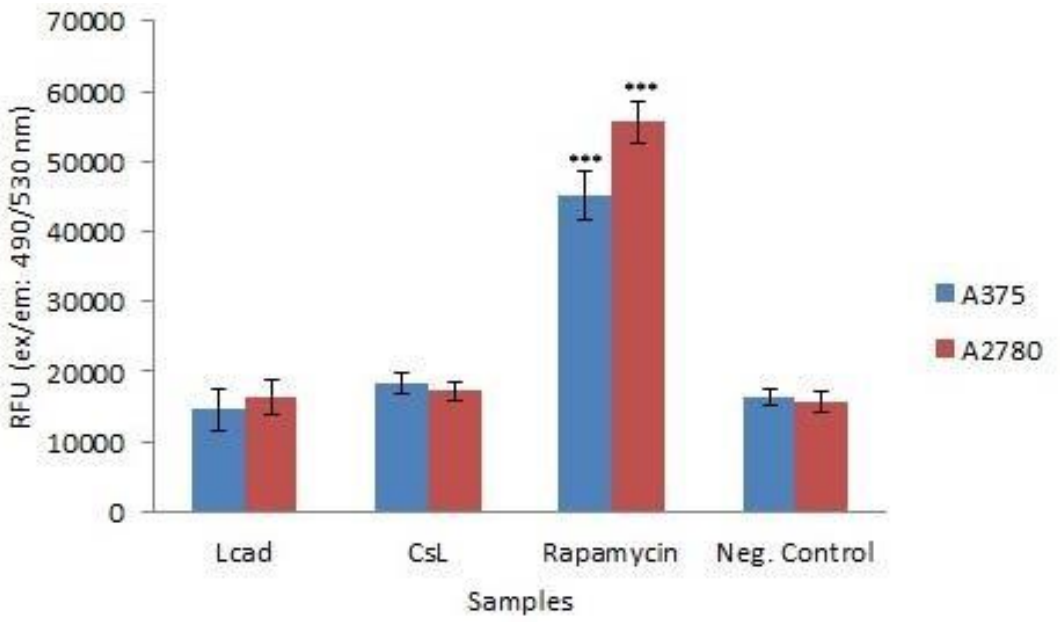

Figure 3.23: Evaluation of the formation of AVOs: A375 (5 x 10^5 cells/well) and A2780 (10^6 cells/well) were seeded in 6-well plates and were treated with of Lcad (20 µg/mL), CsL (20 µg/mL) and rapamycin (100 µg/mL) for 4 hours. ****P*=0.001 the significant increase in the AO fluorescence, compared with negative control. Each data point represents mean ± SEM of triplicate results as compared to negative control (n=3).

3.4.10 Effect on intracellular Ca^{2+} levels

The role of Ca^{2+} in the cell death process was determined with the help of Fluo-2 staining. The quantitative analysis (Figure 3.24) did not demonstrate any significant increase in Ca^{2+} flux in the Lcad/CsL treated cells, which shows that Ca^{2+} is not involved in the cell death pathways. However, A375 and A2780 cells treated with $CaCl_2$ (1 mM) showed a significant (*P*=0.001) increase in Ca^{2+} flux into the cells. These results are further supported by the fluorescence images. The intracellular compartments in A375 (Figure 3.25 Ci) and A2780 cells (Figure 3.26 Ci) that were exposed to $CaCl_2$ (1 mM) show bright fluorescence whereas Lcad (A375: Figure 3.25 Ai; A2780: Figure 3.26.Ai) and CsL (A375: Figure 3.25.Bi; A2780: Figure 3.26.Bi)

treated cells do not show increase in Fluo-2 fluorescence, as compared to the negative control cells.

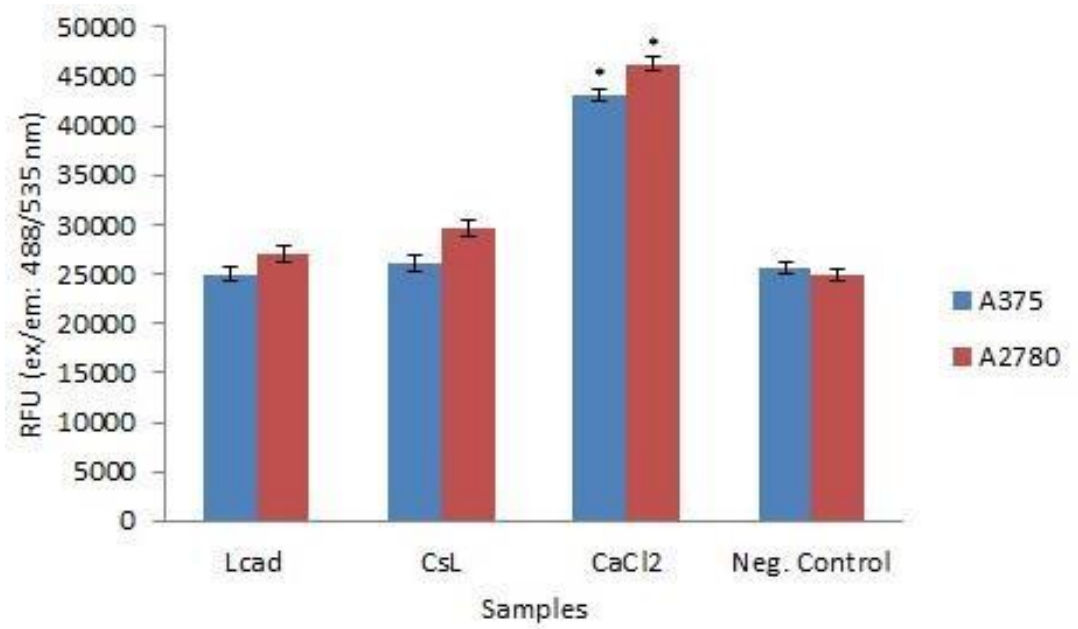

Figure 3.24: Quantitative analysis of intracellular acidic vesicles: A375 (5,000 cells/well) and A2780 (10,000 cells/well) were treated with 20 µg/mL of Lcad and CsL for 4 h. $CaCl_2$ (1 mM) to a final concentration was used as a positive control. **P*=0.05 shows a significant increase in the Fluo-2 fluorescence, compared with negative control. Each bar represents mean ± SEM of triplicate results (n=3).

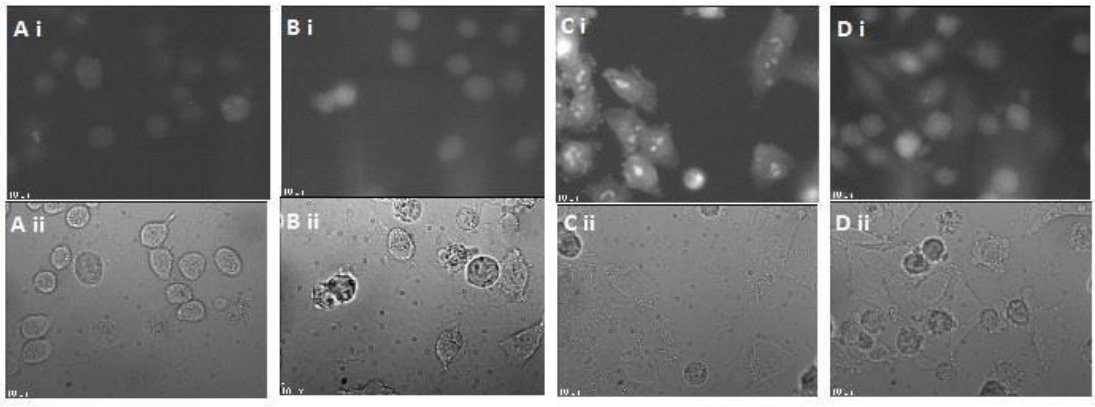

Figure 3.25: Fluo-2 fluorescence/bright field images of A375 cells: A375 cells (5×10^5) were grown on cover-slips and were treated with 20 µg/mL of (Ai) Lcad, (Bi) CsL, (Ci) $CaCl_2$ for 4 h compared with the negative control (Di). Fluorescence images were recorded with 40X lens. Aii, Bii, Cii and Dii are respective bright field images.

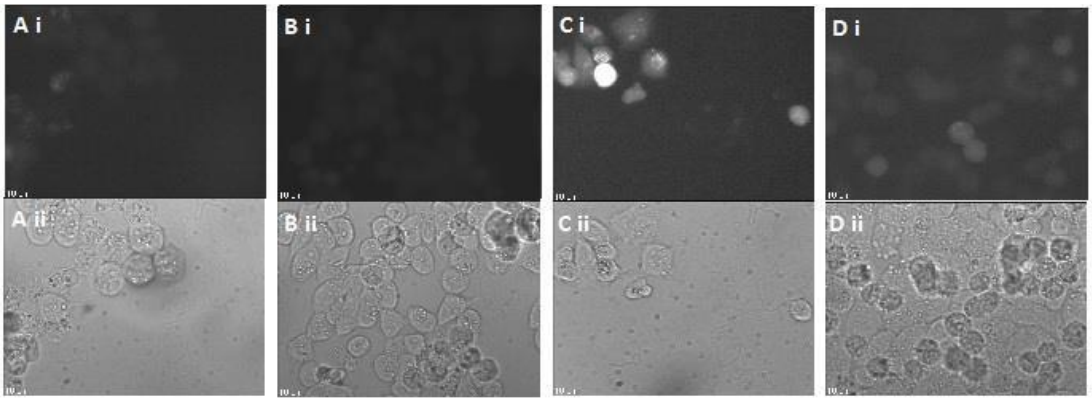

Figure 3.26: Fluo-2 fluorescence images of A375 cells: A2780 cells (10^6) were grown on cover-slips and were treated with 20 µg/mL of (Ai) Lcad and (Bi) CsL for 4 h, compared with negative control (Di). Fluorescence images were recorded with the help 40X objective lens. Aii, Bii, Cii and Dii are respective bright field images.

3.4.11 Role of caspase-8, Bid, AIF and PARP

To establish the role of the key proteins involved in the cell death pathway (apoptosis), Western blotting was carried out. It was determined that caspase-8 was activated. Pro-caspase-8 (53kDa) and the cleaved caspase-8 (18 kDa) were also confirmed. The activation of a member of BH3-only protein, Bid, which is known as translocated Bid (tBid) (MW=15 kDa) was also confirmed. The presence of AIF

translocated, tAIF (MW=57 kDa), from mitochondria to nucleus was also found with the help of this technique. Furthermore, the activation of PARP was also confirmed by detecting the activated form of PARP (89 kDa) which suggests DNA damage. GAPDH was used to confirm the equal amount of protein in all the treatments. Figure 3.27 and 3.28 shows the bands for these proteins in A375 and A2780 cells, respectively.

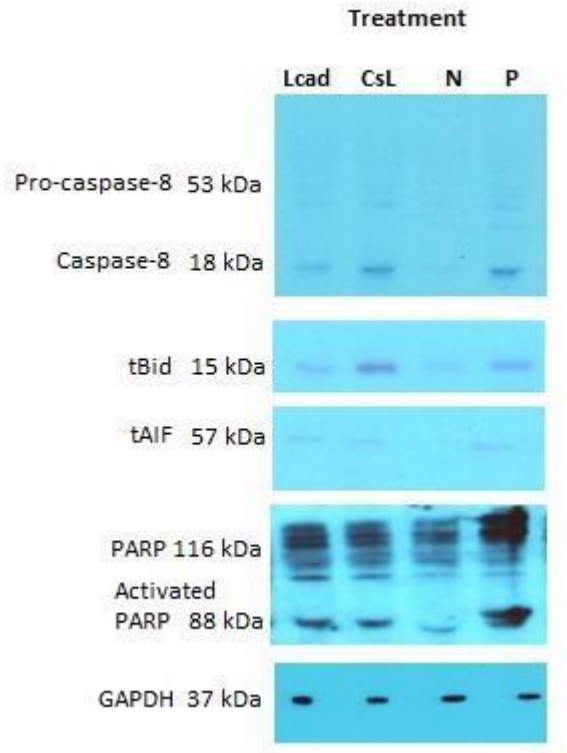

Figure 3.27: Western blot analysis of Lcad/CsL treated A375 cells: A375 cells were seeded in 6-well plate at a concentration of 5 x 10^5 and treated with Lcad and CsL to a final of 20 µg/mL for 4 h. The presence of activated forms of caspase-8, Bid, AIF and PARP was confirmed by Western blotting. GAPDH was use to normalise the levels of proteins detected by confirming equal amounts of proteins were loaded across the gel.

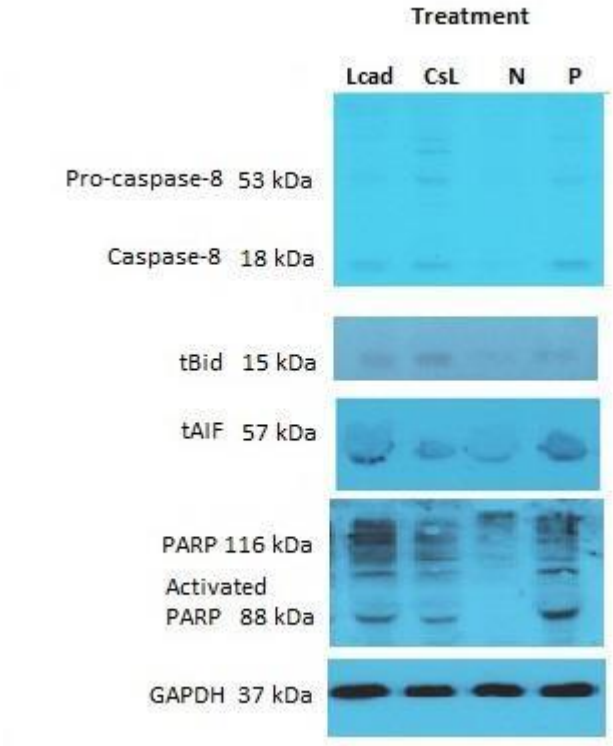

Figure 3.28: Western blot analysis of Lcad/CsL treated A2780 cells: A375 cells were seeded in 6-well plate at a concentration of 10^5 and treated with Lcad and CsL to a final of 20 µg/mL for 4 h. The presence of activated forms of caspase-8, Bid, AIF and PARP was confirmed by Western blotting. GAPDH was used to confirm that equal amount of proteins are loaded across the gel

3.5 Discussion

Snake venom has played an important role in medicine since early civilisations which is evident by the fact that a number of traditional medicines are derived from the venom of snakes (King, 2011; Harvey, 2002). From an evolutionary point of view, the purpose of venom production in snakes was to immobilise and capture a prey, with secondary use of defending against predators. Snake venom comprises of a large variety of biological molecules that perturb vital physiological systems, mainly those involving respiration, circulation and movement (Kohn and Kini, 2011). While initial efforts mostly focused on the better understanding of the biology of venom to cope with snake bite burden, the use of snake venom in medicine gained ground in the early 20th century. With recent advancements in investigational technologies, snake venom components have been thoroughly studied and it has been established that snake venom peptides have greater specificity, are highly potent and have lower toxicity which are the underlying reasons for the emergence of venom-based drug discovery as an important field on a commercial level (reviewed in Ahrens *et al*., 2012). In addition to providing potential treatments for diseases like diabetes, HIV, chronic pain (reviewed in Ahrens *et al*., 2012; King, 2011), snake venom peptides are also considered anticancer agents as snake venom peptides have shown inhibition of cell viability, since snake bites result in excessive tissue damage at the site of the bite. The antitumoral characteristic of snake venom is mostly due the effect of venom components on the metabolic activity of the cells, which is more prominent in the cancer cells than normal cells (reviewed in Calderon *et al*., 2014). Therefore,

numerous cancer research groups have focused on studying proteins obtained from snake venom and their effects and mechanism of the effects on several cancer lines (Ding *et al*., 2014; Yalcin *et al*., 2014; Park *et* al., 2012; Song *et* al., 2012).

LAAO are homodimer enzymes with a MW ranging from 110-150 kDa in the native form and are responsible for the stereospecific oxidative deamination of L-amino acids to the corresponding α-keto acid, with H_2O_2 as a by-product. Most of the biological actions related to LAAO results from oxidative stress caused by H_2O_2 produced during this process. Until the 1990s the focus of LAAO study was the enzymatic and physicochemical properties of the enzymes, however, in the last two decades the pharmacology associated with snake venom LAAO has gained the attention of researchers. Many investigations have claimed LAAO from different snake sources to have fungicidal, bactericidal, anti-leishmanitic, anti-HIV activity (Lee *et al*., 2011; Zhang *et al*., 2003; Stiles *et al*., 1991). Other *in vitro* bioactivities such as inhibition of platelet aggregation (Sakurai *et al*., 2001; Sakurai *et al*., 2001) and induction of cell death in cancer cell lines (Souza *et al*., 1999; Stabeli *et al*., 2007) have also been reported. Although the cytotoxicity mechanisms for LAAO from snake venom have not been completely clarified, both the intrinsic and extrinsic pathways of apoptosis induction, including ROS dependent cell death, activation of cell death receptors and release of AIF from the mitochondria have been suggested (Ding *et al*., 2014). Binding of LAAO to the outer membrane of cells has been established by Suhr and Kim (1996). They labelled the LAAO from *Agkistrodon halys* (Korean snake) with FITC and visualised bright spots on the surface of mouse lymphocytic leukemia cells

(L1210) with a fluorescence microscope. This binding leads to an increase in H_2O_2 levels by denaturation of local L-amino acids by LAAO. The increase of H_2O_2 levels induces cellular cytotoxicity either directly by damaging the lipids present in the cell membrane (Imlay, 2003) or indirectly by up-regulation of Fas receptors which subsequently activates caspase-8 and members of proapoptotic proteins, for example Bid (Suhara *et al*., 1998) which further act on mitochondria to carry out cell demise (extrinsic pathway). While mitochondria are widely regarded as an indispensable source of energy, they also play a role in cell death signalling and progression of cancer. Functionally, the mitochondria of cancer cells are different than normal cells, characterised by overproduction of ROS which leads to genomic instability by causing oxidative damage to DNA, resulting in cancer progression. The mitochondrial signalling pathway is triggered either by external ROS or pro-apoptotic proteins which results in secretion of mitochondrial cell death signals such as Apaf-1, Cyt.C or AIF, culminating in caspase activation or DNA fragmentation. Mitochondrial involvement in cell death as a direct consequence of high ROS concentration generated by LAAO is a widely accepted concept (Rodrigues *et al*., 2009; Wie *et al.,* 2009; Torri *et* al., 1997; Zhang and Wu, 2008). In contrast, by using ROS scavenger (catalase) concomitantly, Suhr and Kim (1996) found that cell viability was only 70% recovered in cells exposed to LAAO from *A. halys*, whereas, another study revealed 75% recovery in cell viability in the presence of *Bothrops loucurus* LAAO (Neumann *et al*., 2011), suggesting that cell death associated with snake venom LAAO cannot be solely explained on the basis of H_2O_2 production and favours the idea of direct

activation of death receptors on the cell surface. Furthermore, de Melo *et al*., (2011) reported that in the presence of catalase, LAAO from *Bothrops atrox* did not have any significant effect on the viability of human promyelocytic cell line (HL-60), leaving the role of ROS produced by the snake venom LAAO in cell death open to further debate. The cell death pathway, downstream from mitochondrial damage, proceeds either through caspase dependent or independent (AIF) mechanism. Caspases are a group of endoproteases that help maintain tissue homeostasis by regulating cell death which are wither activators (caspase-2/8) that activate other capases or effectors (caspase-3/7) that bring about the damage to cellular protein causing cell death. Upon the reception of the apoptotic signal, mitochondria release Cyt.C which leads to the subsequent activation of executioner caspases-3/7 and are responsible for the cell-dismantling events marking apoptosis. Caspase activation has been reported to be the case with LAAO from numerous snake venoms (Susin *et* al., 1999; Du *et al*., 2000; Sharma *et al*., 2000). Taken together, these reports imply that snake venom LAAO do not activate one particular pathway of cellular destruction. The pathway leading to cell death depends on the source of LAAO and type of cancer cell line.

Keeping in view the aforementioned different cell death mechanisms described for other snake venom LAAO, this study focussed on the investigation of cytotoxicity and the mechanism of cytotoxicity induced in A375 and A2780 cells by Lcad and CsL.

The initial cell viability assays confirmed the cytotoxic affinity towards A375 and A2780 cell lines. Lcad had an IC_{50} of 1.11.1±0.1 µg/mL and 1.95±0.2 µg/mL on A375 and A2780 cells, respectively. Similarly, CsL showed an IC_{50} of 2.46±0.2 µg/mL and

3.6±0.6 μg/mL, respectively, for A375 and A2780. The inhibitory effects of Lcad and CsL on cancer cells at such small concentrations prove these proteins to be highly cytotoxic. Table 3.2 presents IC_{50} values of LAAO from different snake species for various cancer cell lines, comparison of IC_{50} of Lcad and CsL to these values further verifies the high cytotoxicity of Lcad/CsL on A375 and A2780 cells lines.

Source	Tested cancer cell line (Code)	IC_{50} (µg/mL)	Reference
Ophiophagus Hannah	stomach cancer cells (SNU-1)	20	Ahn *et al*. 1997
Agkistrodon acutus	A549 cells (lung adenocarcinoma),	20	Zhang and Wu, 2003
Bungarus fasciatus	A549 cells (lung adenocarcinoma),	20	Wei *et al*., 2009
Bothrops atrox	Human promelocytic leukemia cells (HL-60)	50	Alves *et al*., 2008
Bothrops atrox	Rat adrenal gland Pheochromocytoma (PC12)	25	Alves *et al*., 2008
Bothrops atrox	murine melanoma (B16F10)	25	Alves *et al*., 2008
Bothrops atrox	JURKAT	25	Alves *et al*., 2008
Lachesis muta	gastric adenocarcinoma (AGS)	22.7	Bregge-Silva *et al*. 2012
Lachesis muta	Breast tumor (MCF-7)	1.41	Bregge-Silva *et al*., 2012
Crotalus atrox	Human promelocytic leukemia cells (HL-60)	10	Torii *et al*. 1997
Crotalus atrox	A2780 (human ovarian carcinoma)	10	Torii *et al*. 1997

Table 3.2: IC_{50} of LAAO from various snake venom: IC_{50} values showing the cytotoxicity of LAAO from different snake sources on various cancer lines. Comparing the IC_{50} values of Lcad and CsL, shows that these two proteins are one of the most cytotoxic agents.

The sensitivity of both the cancer cell lines to cisplatin was confirmed and the potency of Lcad and CsL was established by comparing the cytotoxic activity of Lcad/CsL with chemotherapeutic agent, cisplatin. Treating the A375 and A2780 cells with the same concentrations (20 µg/mL) of Lcad, CsL and cisplatin for 4 hours revealed that cisplatin had no significant effect on the viability of the treated cells whereas Lcad/CsL inhibited the cell viability by more than 97%, establishing that Lcad/CsL are highly potent. Moreover, the non-significant effect of Lcad and CsL on the viability of PNT2a confirms the cancer specificity of these proteins as is the case with LAAO from other snake sources presented in Table 3.3.

Source	**Tested non-cancer cells**	**Concentration (µg/mL)**	**Reference**
Ophiophagus hannah	Chinese hamster ovary cells	20	Ahn *et al*., 1997
Bothrops pirajai	Peritoneal macrophages	1-4	Izidoro *et al*., 2006
Bothrops atrox	Macrophages	5-50	Alves *et al*., 2008
Bothrop pirajai	Peripheral blood mononuclear cells	3-50	Burin *et al*., 2013

Table 3.3: Cancer-specific snake venom LAAO: Examples of LAAOs from different snake venom which, according to the respective studies, did not have any significant effect on the viability of non-cancer cells as compared to the cancer cell lines used, referring to the cancer-specific cytotoxicity of these proteins.

In order to investigate the mode of cell death, firstly the morphological changes in the treated cells were studied. Reduction in cellular volume was observed which is a

hallmark of apoptosis as opposed to the fragmentation of cells, which takes place in the later stages of necrosis. Furthermore, the Sytox Green® assay confirmed that the structure and permeability of cell membranes that were exposed to Lcad/CsL were intact and thus nullified the disruption of cell membrane, a characteristic of necrosis. Moreover, IM-54, a selective inhibitor of necrosis, did not have any significant effect on the recovery of cell viability of the cells exposed to Lcad/CsL which showed that necrotic pathways were not triggered in 4 h. Autophagy was excluded on the basis of no proof of increase in AVOs or autophagosomes. The acidic vesicles contain lysosomal enzymes which are responsible for the selfdestruction sequence of autophagy. AO staining did not show any significant increase in intracellular acidity of the cells exposed to Lcad/CsL. All these findings favour the concept of apoptosis to be the most likely mode of cell death that is induced in A375/A2780 by Lcad/CsL. In order to investigate the intrinsic pathway of apoptosis, the role of ROS was evaluated. DCDHF assay did not detect any significant increase in ROS levels in the cells treated with Lcad and CsL. The treated A375/A2780 cells showed only a slight and non-significant increase in ROS generation as compared to the basal ROS levels which implies that ROS did not play a role in the progression of cell death. In addition, it was also confirmed that the amino acid contained in the cell culture media, including L-Leu, is not metabolised by Lcad/CsL to produce extracellular ROS that could trigger cell death. Furthermore, it was also established that mitochondria were not affected during the cell death process. The integrity of the mitochondrial membrane as well as mitochondrial function was not influenced by Lcad/CsL, which was confirmed by

TMRE and MTT assays, respectively. MMP drops in response to ROS generation or when signalled by pro-apoptotic proteins (Bid, Bax, Bad) which results in the loss of mitochondrial function. However, this was found to be not the case with A375 and A2780 cells treated with Lcad and CsL. Also, Caspase-3/7 assay confirmed that the execution of apoptosis in A375/A2780 cells triggered by Lcad/CsL is not caspase-driven.

Therefore it is evident that the intrinsic pathway of apoptosis was not activated. Western blot analysis showed that the mode of apoptosis induced in the tested A375 and A2780 cells by Lcad/CsL is initiated via the extrinsic pathway. The detection of the activated caspase-8 (15 kDa) in both, A375 and A2780 cells, proves that procaspase-8 (51 kDa) is activated which was signalled by the death receptors. The activated caspase-8 led to the translocation of Bid to mitochondria. tBid was also detected by the western blotting technique. The outcome of interaction of tBid with the mitochondria was the release of the AIF without altering MMP. AIF is translocated to nucleus to bring about DNA damage. The detection of PARP confirmed the DNA damage, a hallmark of apoptosis. Figure 3.29 shows the initiation and progression of the extrinsic pathway of apoptosis as suggested by findings in this study.

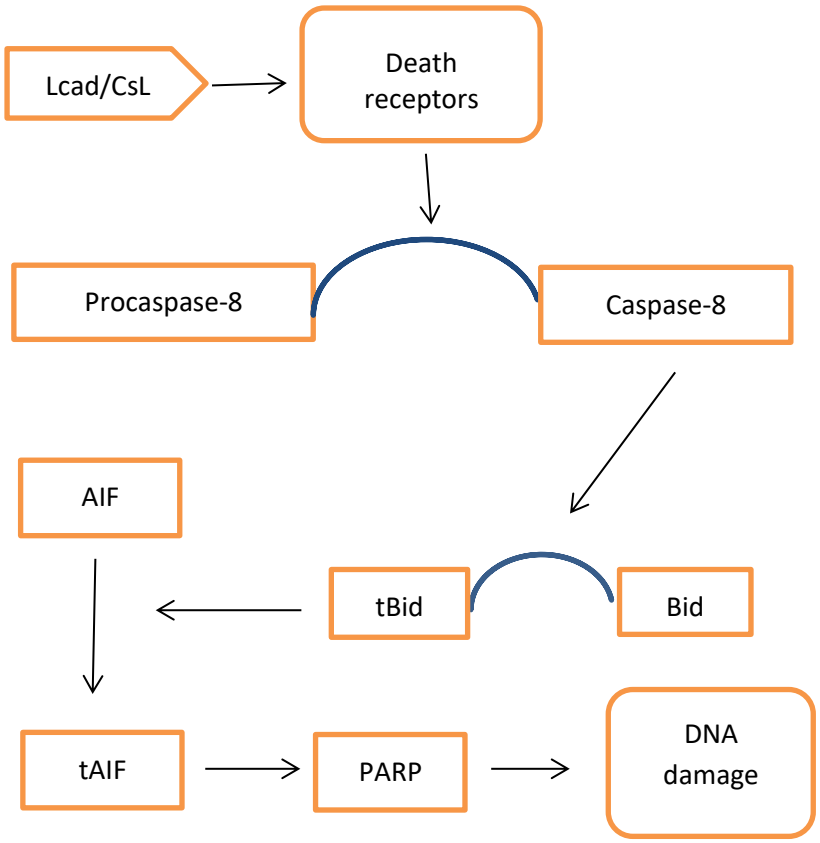

Figure 3.29: Cell death pathway triggered by Lcad/CsL in A375/A2780 cells: The flow chart shows the initiation and execution of extrinsic apoptotic pathway in A375 and A2780 cells in response to Lcad and CsL treatment as elaborated by this study.

An important question arising from this study is the mode of cancer selectivity of Lcad and CsL. It would be interesting to see if there is a difference in cell death receptors expressed by the cancer and non-cancer cell lines used in this study or to see if there

are structural differences in the receptor structure expressed by both types of cell lines. The former would highlight the cellular target for Lcad/CsL which could be further exploited for cancer targeting by Lcad/CsL, while the later would give some more detailed insight into structural modification of protein during tumorigenesis.

Despite the limitations, this study provides a detailed account of LAAO from Cad and CsL in terms of the physicochemical properties of the enzymes and pharmacology associated with the cell death induced by Lcad and CsL in A375/A2780 cancer cell lines. This study establishes that AIF can be released from mitochondria without any changes in MMP which is new information regarding snake venom LAAO related cytotoxicity and calls for further attention from researchers for potential targeted cancer treatment.

5. Conclusion and future work

5.1 Conclusion

Reports published over the last decade indicate the severity of health hazards related to snake bites. The published data estimate that there are up to 2.4 million snake bite cases globally, out of which 100,000 proved fatal (Kasturiratne *et al*., 2008; Koh *et al*., 2005). Understanding the components of snake venom is not only helpful in relieving the healthcare burden related to envenomation but has also significantly contributed to the development of treatments for other diseases, development of ACE inhibitors being the prime example. Around a billion people around the world are estimated to suffer from hypertension and the majority of these patients are treated with ACE inhibitors; the class of antihypertensive drugs originated from snake venom (reviewed by Koh and Kini, 2012). In the US alone,

27% of hypertensive patients are prescribed ACE inhibitors (Smith and Ashiya, 2007), inferring how life threatening snake venom toxins can be exploited to obtain lifesaving therapeutics. Recent advancements in screening techniques have facilitated the examination of venoms for selective bioactivities and have immensely increased the prospects of finding pharmaceutical leads from snake venom (Heus *et al*., 2013). Some ~~the~~ drug leads obtained or developed on the basis of snake venom toxins are in preclinical and clinical trials and only a few will be successful which reflects the complex and time consuming aspects of drug discovery (reviewed in Samy *et at*., 2016; Vyas *et al*., 2013; Koh and Kini, 2012). The success of the drug development relies on factors other than simple identification and application in

clinics. Other factors that are important in drug discovery mainly involve innovations steps such as pharmacophore identification, establishment of structure activity relationship followed by extensive chemical modification and, in most cases, devising a special delivery system (King, 2015; Harvey, 2014). Therefore, the development of drugs needs interdisciplinary knowledge as well as
collaborations.

In this study, whole venom of Cad and Css were examined for cytotoxic effects on two human cancer cell lines, namely, human ovarian carcinoma and human skin melanoma. The extraction of the active component, LAAO, was easy and SEC and CEC techniques sufficed to produce a LAAO of high purity. However, the downside to these techniques is that a considerable amount of salts dries down with the fractions rendering low protein content of the separated active fractions, which was established by a Bradford assay. Another challenge associated with the purification of LAAO is the deactivation of the enzymes during the process of lyophilisation which takes place due to the conformational changes in the prosthetic group of the enzymes. The lyophilised fractions were heated at 37°C at pH 5 for at least 30 min for reactivation with the ramification of loss in enzymatic activity. The active fractions were always stored at acidic pH and heated at 37°C for 30 min prior to any bioactivity assay. The amino acid sequencing of the isolated proteins could not be determined at this instance because of the desiccation of the samples during the transportation to our collaborators' lab.

The mechanism of cytotoxicity of Lcad and CsL was determined on A375 and A2780 cells lines using different cell based assays. Microscopy analysis of the cells treated with Lcad and CsL revealed loss in the cellular volume which is indicative of apoptosis and was further supported by the AO and IM-54 assays. Various assays were carried out to determine the mechanism of cell death induced by Lcad and CsL which was established to be caspase-independent and AIF mediated. The pharmacology associated with Lcad and CsL is interesting and novel in a way that the resultant cell death is independent of ROS as has been claimed for LAAO from other snake species as well as LAAO from other resources (Ande *et al*., 2006; Suhr and Kim, 1999; Torri *et* al., 1997). This study establishes that there were no external or internal ROS detected in the treated with Lcad/CsL which concludes that these proteins initiate the cell death pathway by interacting with the cell surface death receptors.

5.2 Future work

Although this study establishes that apoptosis induced in A375 and A2780 cell lines is independent of ROS-generation which is indicative of the fact that cell death was initiated by activating death receptors on the cell lines. The cell death receptors profile of A375 and A2780 cell lines is well established (Wang *et* al., 2015; Petrucci *et* al., 2007; Chawla-Sarkar *et al*., 2001; Bellarosa *et* al., 2001; Zhang *et al*., 2000) and it is very important to see which cell surface death receptors (Fas, Dr-4/5) are activated by Lcad and CsL which can be established using western blotting.

In order to have further insight into cancer selectivity of Lcad and CsL, it is necessary to determine if the target receptor of Lcad/CsL is expressed on PNT2a. As previously

discussed (section 3.5), the bioactivity of the snake venom enzymes is related to their amino acid sequence, it is crucial to determine the amino acid sequence of the extracted Lcad/CsL to further investigate the difference in the pharmacology, cancer selectivity and, also, high potency of Lcad and CsL as compared to LAAO from other resources.

This study concludes that MMP was not compromised in order for AIF to be translocated to the nucleus for PARP activation, however, for better understanding of the molecular process involved, it is necessary to directly investigate if calpains and cathepsins have a role in AIF release from mitochondria, although the lack of AVOs and Ca^{2+} favour that AIF release is not dependant on calpains and cathepsins. As calpains and cathepsins are proteases, *in vivo* substrate assays can be used to determine the activity of these enzymes as described elsewhere (Gocheva *et al*., 2010; Milacic *et al*., 2006).

In the future, it will be beneficial to answer all these questions which will make a stronger case for having more insight into the anti-tumour activity of Lcad and CsL.

5. References

Aapro, M.S., Schmoll, H.J., Jahn, F., Carides, A.D. and Webb, R.T., (2013). Review of the efficacy of aprepitant for the prevention of chemotherapy-induced nausea and vomiting in a range of tumor types. *Cancer treatment reviews*; *39*(1): 113-117.

Abou-Dunia Mohamed B., 2003. Organophosphorus ester-induced chronic Neurotoxicity. Archives of environmental health, 58 (8), 484-497.

Adams E., Boulton M.G., Horne A., Rose P.W., Durrant L., Collingwood M., Oskrochi R., Davidson S.E., Watson E.K. (2014). The Effects of Pelvic Radiotherapy on Cancer Survivors: Symptom Profile, Psychological Morbidity and Quality of Life. Clinical Oncology; 26 (1): 10-17.

Agarwala S. S., Kirkwood J.M. (2000). Temozolomide, a Novel Alkylating Agent with Activity in the Central Nervous System, May Improve the Treatment of Advanced Metastatic Melanoma. The Oncologist; 5 (2): 144-151.

Ahn, M.Y., Lee, B.M. and Kim, Y.S., 1997. Characterization and cytotoxicity of Lamino acid oxidase from the venom of king cobra (Ophiophagus hannah). *The international journal of biochemistry & cell biology*, *29*(6), pp.911-919.

Ahrens, V.M., Bellmann-Sickert, K. and Beck-Sickinger, A.G., 2012. Peptides and peptide conjugates: therapeutics on the upward path. *Future medicinal chemistry*, *4*(12), pp.1567-1586.

Aldunate R., Casar J.C., Brandan E., Inestrosa N.C., 2004. Structural and functional organization of synaptic acetylcholinesterase. Brain Res. Brain Res. Rev.,47, 96–104.

Alix-Panabières, C. and Pantel, K., 2013. Circulating tumor cells: liquid biopsy of cancer. *Clinical chemistry*, *59*(1), pp.110-118.

Al-Lazikani, B., Banerji, U. and Workman, P., 2012. Combinatorial drug therapy for cancer in the post-genomic era. *Nature biotechnology*, *30*(7), pp.679-692.

Alves, R.M., Antonucci, G.A., Paiva, H.H., Cintra, A.C.O., Franco, J.J., MendonçaFranqueiro, E.P., Dorta, D.J., Giglio, J.R., Rosa, J.C., Fuly, A.L. and Dias-Baruffi, M., 2008. Evidence of caspase-mediated apoptosis induced by L-amino acid oxidase isolated from Bothrops atrox snake venom.*Comparative Biochemistry and Physiology Part A: Molecular & Integrative Physiology*, *151*(4), pp.542-550.

Ambrosini G., Adida C., Altieri D. C. (1997). A novel anti-apoptosis gene, survivin, expressed in cancerand lymphoma. Nature Medicine; 3: 917–921.

Ande, S.R., Kommoju, P.R., Draxl, S., Murkovic, M., Macheroux, P., Ghisla, S. and Ferrando-May, E., 2006. Mechanisms of cell death induction by L-amino acid oxidase, a major component of ophidian venom. *Apoptosis*,*11*(8), pp.1439-1451.

Ande, S.R., Kommoju, P.R., Draxl, S., Murkovic, M., Macheroux, P., Ghisla, S. and Ferrando-May, E., 2006. Mechanisms of cell death induction by L-amino acid oxidase, a major component of ophidian venom. *Apoptosis*,*11*(8), pp.1439-1451.

Ansari AF, Shaikh DM, Seehar GM, Jamali AG, Jokhio R., 1989. Influence of crude snake venom on electrolyte levels and sodium potassium ATPase activity in erythrocytes, liver and heart cells. Pak J Pharm Sci,2,19-28.

Aparicio, O.M., Weinstein, D.M. and Bell, S.P., 1997. Components and dynamics of DNA replication complexes in S. cerevisiae: redistribution of MCM proteins and Cdc45p during S phase. *Cell*, *91*(1), pp.59-69.

Arcamone F., Cassinelli G., Fantini G., Grein A., Orezzi P., Pol C., Spalla C. (1969). Adriamycin, 14-hydroxydaunomycin, a new antitumor antibiotic from *S. peucetius* var. *caesius.* Biotechnology and Bioengineering; 11: 1101–1110.

Aredia, F., Guamán Ortiz, L.M., Giansanti, V. and Scovassi, A.I., 2012. Autophagy and cancer. *Cells*, *1*(3), 520-534.

Arentson, E., Faloon, P., Seo, J., Moon, E., Studts, J.M., Fremont, D.H. and Choi, K., 2002. Oncogenic potential of the DNA replication licensing protein CDT1. *Oncogene*, *21*(8), 1150-1158.

Assaraf, Y.G., Leamon, C.P. and Reddy, J.A., 2014. The folate receptor as a rational therapeutic target for personalized cancer treatment. *Drug Resistance Updates*, *17*(4), 89-95.

Assinger, A., Volf, I. and Schmid, D., 2015. A Novel, Rapid Method to Quantify Intraplatelet Calcium Dynamics by Ratiometric Flow Cytometry.*PloS one*, *10*(4), p.e0122527.

Backer, J.M., 2008. The regulation and function of Class III PI3Ks: novel roles for Vps34. *Biochemical Journal*, *410*(1), pp.1-17.

Bailey P. Wilce., 2001.Venom as a source of useful biologically active molecules. Emerg Med (Fremantle), 28-36.

Baldo Cristiani, Jamora Colin, Yamanouye Norma, Zorn Telma M., Moura-da Silva Ana M., 2010. Mechanisms of Vascular Damage by Hemorrhagic Snake Venom

Metalloproteinases: Tissue Distribution and In Situ Hydrolysis; PLOS neglegted tropical diseases, 4 (6), 1-10.

Barramova E.N., Shannon J.D., Bjarnason J.B., Fox J.W., 1989. Degradation of extracellular matrix proteins by hemorrhagic metalloproteinases. Arch. Biochem. Biophy., 275, 63–71.

Bartek, J., Lukas, C. and Lukas, J., 2004. Checking on DNA damage in S phase. *Nature reviews Molecular cell biology*, *5*(10), 792-804.

Barth, S., Glick, D. and Macleod, K.F., 2010. Autophagy: assays and artifacts. *The Journal of pathology*, *221*(2), pp.117-124.

Basak S. K., Zinabadi A., Venkatesan N., Duarte V. M., Dalgard C. L., Srivastava M., Wang M. B., Sarkar F. H., Srivatsan E. S., 2014. Cisplatin resistant head and neck cancer cells are susceptible to growth inhibition by CDF curcumin. Cancer Research;*74:* 3909.

Beghini, D.G., Toyama, M.H., Hyslop, S., Sodek, L.C. and Marangoni, S., 2000. Enzymatic characterization of a novel phospholipase A2 from Crotalus durissus cascavella rattlesnake (maracambóia) venom. *Journal of protein chemistry*, *19*(8), pp.679-684.

Bidère, N., Lorenzo, H.K., Carmona, S., Laforge, M., Harper, F., Dumont, C. and Senik, A., 2003. Cathepsin D triggers Bax activation, resulting in selective apoptosisinducing factor (AIF) relocation in T lymphocytes entering the early commitment phase to apoptosis. *Journal of Biological Chemistry*, *278*(33), pp.31401-31411.

Bock, C. and Lengauer, T., 2012. Managing drug resistance in cancer: lessons from HIV therapy. *Nature Reviews Cancer*, *12*(7), pp.494-501.

Bodó, E., Tobin, D.J., Kamenisch, Y., Bíró, T., Berneburg, M., Funk, W. and Paus, R., 2007. Dissecting the impact of chemotherapy on the human hair follicle: a pragmatic in vitro assay for studying the pathogenesis and potential management of hair follicle dystrophy. *The American journal of pathology*, *171*(4), pp.1153-1167.

Boland, C.R. and Ricciardiello, L., 1999. How many mutations does it take to make a tumor?. *Proceedings of the National Academy of Sciences*, *96*(26), pp.14675-14677.

Bonfoco E., Krainc D., Ankarcrona M., Nicotera P., Lipton S. A., 1995. Apoptosis and necrosis: Two distinct events induced, respectively,by mild and intense insults with N-methyl-D-aspartate or nitric oxide/superoxide in cortical cell cultures. Proc. Natl. Acad. Sci., 92, 7162-66.

Boveri, T. (2008). Concerning the origin of malignant tumours. Cell Science; 121 (1): 1–84.

Bradford, M.M., 1976. A rapid and sensitive method for the quantitation of microgram quantities of protein utilizing the principle of protein-dye binding.*Analytical biochemistry*, *72*(1-2), pp.248-254.

Bradley J, Thorstad W. L., Mutic S., Miller T. R., Dehdashti F., Siegel B. A., Bosch W., Bertrand R. J.,2004. Impact of FDG-PET on radiation therapy volume delineation in non-small-cell lung cancer International Journal of Radiation Oncology; 59: 78–86.

Brubacher, J.L. and Bols, N.C., 2001. Chemically de-acetylated 2', 7'dichlorodihydrofluorescein diacetate as a probe of respiratory burst activity in mononuclear phagocytes. *Journal of immunological methods*, *251*(1), pp.81-91.

Bruce A. Chabner & Thomas G. Roberts. Chemotherapy and the war on cancer. *Nature Reviews Cancer* 5, 65-72.

Burke J. E., Dennis E. A., 2009. Phospholipase A2 biochemistry. Cardiovasc. Drugs Ther., 23, 49-59.

Burke, J.E. and Dennis, E.A., 2009. Phospholipase A2 structure/function, mechanism, and signaling. *Journal of lipid research*, *50*(Supplement), pp.S237-S242.

Byzova T.V., Goldman C.K., Pampori N. et al., 2000. A mechanism for modulation of cellular responses to VEGF: Activation of the integrins. Mol. Cel., 6, 851–860.

Calderon, L.A., Sobrinho, J.C., Zaqueo, K.D., de Moura, A.A., Grabner, A.N., Mazzi, M.V., Marcussi, S., Nomizo, A., Fernandes, C.F., Zuliani, J.P. and Carvalho, B., 2014. Antitumoral activity of snake venom proteins: new trends in cancer therapy. *BioMed research international*, *2014*.

Calvete, J.J., Marcinkiewicz, C., Monleón, D., Esteve, V., Celda, B., Juárez, P. and Sanz, L., 2005. Snake venom disintegrins: evolution of structure and function. *Toxicon*, *45*(8), pp.1063-1074.

Cantley, L.C., Auger, K.R., Carpenter, C., Duckworth, B., Graziani, A., Kapeller, R. and Soltoff, S., 1991. Oncogenes and signal transduction. *Cell*,*64*(2), 281-302.

Cao, G., Xing, J., Xiao, X., Liou, A.K., Gao, Y., Yin, X.M., Clark, R.S., Graham, S.H. and Chen, J., 2007. Critical role of calpain I in mitochondrial release of apoptosisinducing factor in ischemic neuronal injury. *The Journal of Neuroscience*, *27*(35), pp.9278-9293.

Carmeliet P. (2005). VEGF as a key mediator of angiogenesis in cancer. Oncology;, 69 (3): 4-10.

Carrato A. (2008). Adjuvant treatment of colorectal cancer. Gastrointestinal Cancer Research; 2(4): 42-46.

Casewell, N.R., Wagstaff, S.C., Wüster, W., Cook, D.A., Bolton, F.M., King, S.I., Pla, D., Sanz, L., Calvete, J.J. and Harrison, R.A., 2014. Medically important differences in snake venom composition are dictated by distinct postgenomic mechanisms. *Proceedings of the National Academy of Sciences*, *111*(25), 9205-9210.

Chang, J., Musser, J.H. and McGregor, H., 1987. Phospholipase A2: function and pharmacological regulation. *Biochemical pharmacology*, *36*(15), pp.2429-2436.

Chen, Y. and Klionsky, D.J., 2011. The regulation of autophagy–unanswered questions. *Journal of cell science*, *124*(2), 161-170.

Coles, C., Edmondson, D. and Singer, T., 1977. Reversible inactivation of L-amino acid oxidase. *J. Biol. Chem*, *252*, pp.8035-8039.

Coller, H.A., Sang, L. and Roberts, J.M., 2006. A new description of cellular quiescence. *PLoS Biol*, *4*(3), p.e83.

Costa, T.R., Burin, S.M., Menaldo, D.L., de Castro, F.A. and Sampaio, S.V., 2014. Snake venom L-amino acid oxidases: an overview on their antitumor effects. *Journal of Venomous Animals and Toxins including Tropical Diseases*, *20*(1), 1

Curti, B., Massey, V. and Zmudka, M., 1968. Inactivation of snake venom L-amino acid oxidase by freezing. *Journal of Biological Chemistry*, *243*(9), pp.2306-2314.

Cushman, D.W. and Ondetti, M.A., 1991. History of the design of captopril and related inhibitors of angiotensin converting enzyme. *Hypertension*, *17*(4), pp.589592.

Cushman, D.W. and Ondetti, M.A., 1999. Design of angiotensin converting enzyme inhibitors. *Nature medicine*, *5*(10), 1110-1112.

Cushman, D.W., Pluščec, J., Williams, N.J., Weaver, E.R., Sabo, E.F., Kocy, O., Cheung, H.S. and Ondetti, M.A., 1973. Inhibition of angiotensin-converting enzyme by analogs of peptides fromBothrops jararaca venom.*Experientia*, *29*(8), 1032-1035.

Dahl C., Abildgaard C., Riber-Hansen R., Steiniche T., Lade-Keller J., Guldberg P. (2015). KIT Is a Frequent Target for Epigenetic Silencing in Cutaneous Melanoma. Journal of Investigative Dermatology; 135 (2): 516-524.

Danial N. N., Korsmeyer S. J., 2004. Cell death: critical control points. Cell ,116 (2), 205-19.

Darby, S.C., Ewertz, M., McGale, P., Bennet, A.M., Blom-Goldman, U., Brønnum, D., Correa, C., Cutter, D., Gagliardi, G., Gigante, B. and Jensen, M.B., 2013. Risk of ischemic heart disease in women after radiotherapy for breast cancer. *New England Journal of Medicine*, *368*(11),987-998.

Darzynkiewicz, Z., Li, X. and Gong, J., 1994. Assays of cell viability: discrimination of cells dying by apoptosis. *Methods in cell biology*, *41*, 15-38.

Daugas, E., Nochy, D., Ravagnan, L., Loeffler, M., Susin, S.A., Zamzami, N. and Kroemer, G., 2000. Apoptosis-inducing factor (AIF): a ubiquitous mitochondrial oxidoreductase involved in apoptosis. *FEBS letters*, *476*(3), 118-123.

Daugas, E., Susin, S.A., Zamzami, N., Ferri, K.F., Irinopoulou, T., Larochette, N., Prévost, M.C., Leber, B., Andrews, D., Penninger, J. and Kroemer, G., 2000. Mitochondrio-nuclear translocation of AIF in apoptosis and necrosis. *The FASEB Journal*, *14*(5), 729-739.

David, Crowley John J., Coltman Charles A., 2004. Prevalence of prostate cancer among men with a prostate-specific antigen level ≤4.0 ng per millilitre. The New England journal of medicine, 350 (22), 2239-2246.

Davis, P.K., Ho, A. and Dowdy, S.F., 2001. Biological methods for cell-cycle synchronization of mammalian cells. *Biotechniques*, *30*(6), 1322-1331.

de Gramont A, Figer A, Seymour M, 2000. Leucovorin and fluorouracil with or without oxaliplatin as first-line treatment in advanced colorectal cancer. Journal of Clinical Oncolongy ;18: 2938-2947.

De Mesquita, L.C., Selistre, H.S. and Giglio, J.R., 1991. The hypotensive activity of Crotalus atrox (western diamondback rattlesnake) venom: identification of its origin. *The American journal of tropical medicine and hygiene*, *44*(3), 345-353.

Dennis Edward A., 1994. Diversity of group types, regulation, and function of Phospholipase A_2, The Journal of Biological Chemistry. Vol. 269., 13057-13060

Dennis, E.A., 1987. Phospholipase A2 mechanism: inhibition and role in arachidonic acid release. *Drug Development Research*, *10*(4), 205-220.

Deter RL, De Duve C. Influence of glucagon, an inducer of cellular autophagy, on some physical properties of rat liver lysosomes. *J Cell Biol* 1967; 33: 437–449.

Dimova I., Popivanov G., Djonov V. (2014). Angiogenesis in cancer – general pathways and their therapeutic implications. Journal of Balkan Union Oncology; 19(1): 15-21.

Ding, J., Bay, B.H. and Gopalakrishnakone, P., 2014. L-amino acid oxidase from Crotalas adamanteus venom induces caspase-independent apoptosis in human NUGC-3 gastric cancer cells. *Cancer Research*, *74*(19 Supplement), pp.5425-5425.

Dmytriw, A.A., Morzycki, W. and Green, P.J., 2015. Prevention of alopecia in medical and interventional chemotherapy patients. *Journal of cutaneous medicine and surgery*, *19*(1), 11-16.

Du, C., Fang, M., Li, Y., Li, L. and Wang, X., 2000. Smac, a mitochondrial protein that promotes cytochrome c–dependent caspase activation by eliminating IAP inhibition. *Cell*, *102*(1), 33-42.

Du, X.Y. and Clemetson, K.J., 2002. Snake venom L-amino acid oxidases.*Toxicon*, *40*(6), pp.659-665.

Early Breast Cancer Trialists' Collaborative Group, 2006. Effects of radiotherapy and of differences in the extent of surgery for early breast cancer on local recurrence and 15-year survival: an overview of the randomised trials. *The Lancet*, *366*(9503), 2087-2106.

Early Breast Cancer Trialists' Collaborative Group, 2006. Effects of radiotherapy and of differences in the extent of surgery for early breast cancer on local recurrence and 15-year survival: an overview of the randomised trials. *The Lancet*, *366*(9503), 2087-2106.

Early Breast Cancer Trialists' Collaborative Group, 2011. Effect of radiotherapy after breast-conserving surgery on 10-year recurrence and 15-year breast cancer death: meta-analysis of individual patient data for 10 801 women in 17 randomised trials. *The Lancet*, *378*(9804), 1707-1716.

Early Breast Cancer Trialists' Collaborative Group (EBCTCG). (2005). Effects of radiotherapy and of differences in the extent of surgery for early breast cancer on local recurrence and15-year survival: an overview of the randomised trials. Lancet ; 366: 2087–2106.

Edinger A., Thompson C. B., 2004. Death by design: apoptosis, necrosis and autophagy. Current opinion in cell biology, 16 (6), 663-69.

Eikelboom, J.W. and Hirsh, J., 2007. Combined antiplatelet and anticoagulant therapy: clinical benefits and risks. *Journal of Thrombosis and Haemostasis*, *5*(s1), 255-263.

Ekwall, E.M., Nygren, L.M., Gustafsson, A.O. and Sorbe, B.G., 2013. Determination of the most effective cooling temperature for the prevention of chemotherapy-induced alopecia. *Molecular and clinical oncology*, *1*(6), 1065-1071.

Escoubas, P., 2006. Molecular diversification in spider venoms: a web of combinatorial peptide libraries. Mol. Divers. 10, 545–554.

Evans P. M. (2008). Anatomical imaging for radiotherapy. Physics in Medicine and Biology; 53: 151–191.

Falzacappa M. V. V, Ronchini C., Reavie L. B., Pelicci P. G. (2012). Regulation of selfrenewal in normal and cancer stem cells. FEBS Journal; 279: 3559–3572.

Farber, J.L., 1981. The role of calcium in cell death. *Life sciences*, *29*(13), 1289-1295.

Farkas, D.L., Wei, M.D., Febbroriello, P., Carson, J.H. and Loew, L.M., 1989. Simultaneous imaging of cell and mitochondrial membrane potentials.*Biophysical Journal*, *56*(6), pp.1053-1069.

Feldstein Ariel E. , Gores Gregory J., 2005. Apoptosis in alcoholic and nonalcoholic steatohepatitis, Frontiers in Bioscience, 10, 3093-99.

Ferlay J., Soerjomataram I., Dikshit R., Eser S., Mathers C., Rebelo M., Parkin M. D., Forman D., Bray F. (2015). Cancer incidence and mortality worldwide: Sources, methods and major patterns in GLOBOCAN 2012. International Journal Cancer; 136: 359–386.

Fernandez-Ortega, P., Caloto, M.T., Chirveches, E., Marquilles, R., San Francisco, J., Quesada, A., Suarez, C., Zorrilla, I., Gómez, J., Zabaleta, P. and Nocea, G. (2012). Chemotherapy-induced nausea and vomiting in clinical practice: impact on patients' quality of life. *Supportive Care in Cancer*;*20*(12): 3141-3148.

Ferreira, S.H., 1965. A bradykinin-potentiating factor (BPF) present in the venom of Bothrops jararaca. *British Journal of Pharmacology and Chemotherapy*, *24*(1), 163169.

Ferri, K.F., Jacotot, E., Blanco, J., Esté, J.A., Zamzami, N., Susin, S.A., Xie, Z., Brothers, G., Reed, J.C., Penninger, J.M. and Kroemer, G., 2000a. Apoptosis Control in Syncytia Induced by the HIV Type 1–Envelope Glycoprotein Complex Role of Mitochondria and Caspases. *The Journal of experimental medicine*, *192*(8), 1081-1092.

Ferri, K.F., Jacotot, E., Leduc, P., Geuskens, M., Ingber, D.E. and Kroemer, G., 2000b. Apoptosis of Syncytia Induced by the HIV-1–Envelope Glycoprotein Complex: Influence of Cell Shape and Size. *Experimental cell research*, *261*(1), 119-126.

Festjens N., Cornelis S., Lamkanfi M., Vandenabeele P., 2006. Caspase-containing complexes in the regulation of cell death and inflammation. Biological chemistry, 387 (8), 1005-16.

Folkman J.,2002. Role of angiogenesis in tumour growth and metastasis. Semin. Oncol., 29, 15-18.

Fox J.W., & Serrano S.M., 2008. Insights into and speculations about snake venom metalloproteinase (SVMP) synthesis, folding and disulfide bond formation and their contribution to venom complexity. F.E.B.S. J., 275, 3016–3030.

Fox J.W., Serrano S.M., 2005. Structural considerations of the snake venom metalloproteinases, key members of the M12 reprolysin family of metalloproteinases. Toxicon,45, 969–985.

Frobert Y., Creminon C., Cousin X., Remy M.H., Chatel J.M., Bon S., Bon C., Grassi J., 1997. Acetylcholinesterases from Elapidae snake venoms: biochemical, immunological and enzymatic characterization. Biochimca et Biophysica Acta 1339, 253–267.

Fry, B.G., Roelants, K., Champagne, D.E., Scheib, H., Tyndall, J.D., King, G.F., Nevalainen, T.J., Norman, J.A., Lewis, R.J., Norton, R.S. and Renjifo, C., 2009. The toxicogenomic multiverse: convergent recruitment of proteins into animal venoms. *Annual review of genomics and human genetics*, *10*, 483-511.

Funk C. D., 2001. Prostaglandins and leukotrienes: advances in eicosanoid biology. Science, 294, 1871–1875.

Galan J. A., Sanchez E. E., Rodringuez-Acosta A., Soto J. G., Bashir S., McLane M. A., Paquette-Straub C., Perez J. C., 2008. Inhibition of lung tumor colonization and cell migration with the disintegrin crotatroxin isolated from the venom of *Crotalus atrox. Toxicon, 51 (7), 1186-96.*

Galluzzi, L., Vitale, I., Abrams, J.M., Alnemri, E.S., Baehrecke, E.H., Blagosklonny, M.V., Dawson, T.M., Dawson, V.L., El-Deiry, W.S., Fulda, S. and Gottlieb, E., 2012. Molecular definitions of cell death subroutines: recommendations of the Nomenclature Committee on Cell Death 2012. *Cell Death & Differentiation*, *19*(1), 107-120.

Gama, J.B., Ohlmeier, S., Martins, T.G., Fraga, A.G., Sampaio-Marques, B., Carvalho, M.A., Proença, F., Silva, M.T., Pedrosa, J. and Ludovico, P., 2014. Proteomic analysis of the action of the Mycobacterium ulcerans toxin mycolactone: targeting host cells cytoskeleton and collagen. *PLoS Negl Trop Dis*, *8*(8), 3066-3080.

Gan, Z.R., Gould, R.J., Jacobs, J.W., Friedman, P.A. and Polokoff, M.A., 1988. Echistatin. A potent platelet aggregation inhibitor from the venom of the viper, Echis carinatus. *Journal of Biological Chemistry*, *263*(36), 19827-19832.

Geiger, T.R. and Peeper, D.S., 2009. Metastasis mechanisms. *Biochimica et Biophysica Acta (BBA)-Reviews on Cancer*, *1796*(2), pp.293-308.

Genini, D., Sheeter, D., Rought, S., Zaunders, J.J., Susin, S.A., Kroemer, G., Richman, D.D., Carson, D.A., Corbeil, J. and Leoni, L.M., 2001. HIV induces lymphocyte apoptosis by a p53-initiated, mitochondrial-mediated mechanism. *The FASEB Journal*, *15*(1), 5-6.

Georgieva Dessislava, Ohler Michaela, Seifert Jana, Bergen Martin von, Arni Raghuvir K., Genov Nicolay, Betzel Christian, 2010. Snake venomic of *crotalus durissus terrificuss* correlation with pharmacological activities. Journal of Proteome Research, 9, 2302–2316.

Georgiou, K.R., Hui, S.K. and Xian, C.J. (2012). Regulatory pathways associated with bone loss and bone marrow adiposity caused by aging, chemotherapy, glucocorticoid therapy and radiotherapy. *Am J Stem Cells*,*1*(3),205-224.

Ghavami S., Hashemi M., Ande, S., Yeganeh, B., Xiao, W., Eshraghi, M., Bus, C., Kadkhoda, K., Wiechec, E.. Halayko, A. (2009). Apoptosis and cancer: Mutations within caspase genes; 46: 497-510

Giancotti F., G. (2014). Deregulation of cell signalling in cancer. FEBS Letters; 588: 2558–2570.

Gillet, J.P. and Gottesman, M.M., 2010. Mechanisms of multidrug resistance in cancer. *Multi-drug resistance in cancer*, 47-76.

Glimelius B., Hoffman K., Graf W.,Pahlman L., Sjoden P. O., 1994. Quality of life during chemotherapy in patients with symptomatic advanced colorectal cancer. Cancer;73:556-62.

Goldstein , Galski H, Fojo AT, Willingham, MC, Lai S-L, 1989. Expression of a multidrug resistance gene in human cancers . J . Natl. Cancer In st., 81, 116-20.

Golstein P., Kroemer G., 2006. Cell death by necrosis: towards a molecular definition. TRENDS in Biochemical Sciences, 32 (1), 37-43.

Gomes A., Bhattacharjee P., Mishra R., Biswas A. K., Dasgupta S. C., Giri B., 2010. Anticancer potential of animal venoms and toxins. Indian Journal of Experimental Biology, 48, 93-103.

Gottesman M. M,. Ambudkar S.V., Ni B., Aran J.M., Sugimoto Y., 1994. Exploiting multidrug resistance to treat cancer. Quant. Biol., 59, 677-78.

Gottesman M. M., Hrycyna C. A., 1995. Genetic analysis of the Multidrug transporter, Anmt Rev, Genct., 29:607-49

Gray's Anatomy, 40th Edition By Susan Standring, PhD, DSc, FKC.

Green D. R., Reed J. C., 1998. Mitochondria and apoptosis. Science, 281, 1309-12

Greenhalgh T. A., Symonds R P. (2014). Principles of chemotherapy and radiotherapy. Obstetrics, Gynaecology And Reproductive Medicine; 24 (9): 259-265.

Grégoire V., Jeraj R., Lee J. A., O'Sullivan B. (2012). Radiotherapy for head and neck tumours in 2012 and beyond: conformal, tailored, and adaptive? The lancet oncology; 13 (7): 292-300.

Greider, C.W., 1990. Telomeres, telomerase and senescence. *Bioessays*,*12*(8), pp.363-369.

Guo, C., Liu, S., Yao, Y., Zhang, Q. and Sun, M.Z., 2012. Past decade study of snake venom L-amino acid oxidase. *Toxicon*, *60*(3), 302-311.

Hajdu S.I., 2004. Greco-Roman thought about cancer. Cancer. ;100:2048-2051.

Hajdu S.I., 2005. 2000 years of chemotherapy of tumours. Cancer, 103, 1097-1102.

Hanahan D., Weinberg R. A., 2000. A Note From History: Landmarks in History of Cancer, Part 1. Cell, 100, 57-70.

Hanahan, D. and Weinberg, R.A., 2000. The hallmarks of cancer. *cell*,*100*(1), pp.57-70.

Hanahan, D. and Weinberg, R.A., 2011. Hallmarks of cancer: the next generation. *cell*, *144*(5), pp.646-674.

Hannani D., Locher C., Yamazaki T., Colin-Minard V., Vetizou M., Aymeric L., Viaud S., Sanchez D., Smyth M. J., Bruhns P., Kroemer G., Zitvogel L. (2014). Contribution of humoral immune responses to the antitumor effects mediated by anthracyclines. Cell Death and Differentiation; 21: 50–58.

Harlozinska, A., 2005. Progress in molecular mechanisms of tumor metastasis and angiogenesis. *Anticancer research*, *25*(5), pp.3327-3333.

Hartvvell, L.H. and Weinert, T., 1989. Checkpoints: controls that ensure the order of cell cycle events. Science, 246: 629–634.

Hartwell, L.H. and Kastan, M.B., 1994. Cell cycle control and cancer.*Science*, *266*(5192), 1821-1828.

Harvey, A.L., 2002. Toxins 'R'Us: more pharmacological tools from nature's superstore. *Trends in pharmacological sciences*, *23*(5),201-203.

Hassett, M.J., O'Malley, A.J., Pakes, J.R., Newhouse, J.P. and Earle, C.C., 2006. Frequency and cost of chemotherapy-related serious adverse effects in a population sample of women with breast cancer. *Journal of the National Cancer Institute*, *98*(16), 1108-1117.

Hastie, N.D., Dempster, M., Dunlop, M.G., Thompson, A.M., Green, D.K. and Allshire, R.C., 1990. Telomere reduction in human colorectal carcinoma and with ageing. *Nature*, *346*(6287), pp.866-868.

Hati, R., Mitra, P., Sarker, S. and Bhattacharyya, K.K., 1999. Snake venom hemorrhagins. *Critical reviews in toxicology*, *29*(1), 1-19.

Hayashi-Nishino, M., Fujita, N., Noda, T., Yamaguchi, A., Yoshimori, T. and Yamamoto, A., 2009. A subdomain of the endoplasmic reticulum forms a cradle for autophagosome formation. *Nature cell biology*, *11*(12), 1433-1437.

Heinrikson, R.L., Krueger, E.T. and Keim, P.S., 1977. Amino acid sequence of phospholipase A2-alpha from the venom of Crotalus adamanteus. A new classification of phospholipases A2 based upon structural determinants.*Journal of Biological Chemistry*, *252*(14), 4913-4921.

Henrik G., 2003. Prostate cancer epidemiology. Lancet, 361, 859–64.

Hess J. A, Khasawneh M. K. (2015). Cancer metabolism and oxidative stress: Insights into carcinogenesis and chemotherapy via the non-dihydrofolate reductase effects of methotrexate bBBA. Clinical; 3: 152–161.

Heus, F., Vonk, F., Otvos, R.A., Bruyneel, B., Smit, A.B., Lingeman, H., Richardson, M., Niessen, W.M. and Kool, J., 2013. An efficient analytical platform for on-line microfluidic profiling of neuroactive snake venoms towards nicotinic receptor affinity. *Toxicon*, *61*, 112-124.

Hilarius, D.L., Kloeg, P.H., van der Wall, E., van den Heuvel, J.J., Gundy, C.M. and Aaronson, N.K. (2012). Chemotherapy-induced nausea and vomiting in daily clinical practice: a community hospital-based study.*Supportive Care in Cancer*; *20*(1):107117.

Hoeflich K. P., Gray D. C., Eby M. T., Tien J. Y., Wong L., Bower J., Gogineni A., Zha J., Cole M. J., Stern H. M., Murray L. J., Davis D. P., Seshagiri S., 2006. Oncogenic BRAF is

required for tumour growth and maintenance in melanoma models. Cancer Res., 66, 999-1006

Holle L., Song W., Holle E., Wei Y., Wagner T., Yu X., 2003. A matrix metalloproteinase 2 cleavable melittin/avidin conjugate specifically targets tumor cells in vitro and in vivo. Int. J. Oncol., 22, 93–98.

Holzer M., Mackessay, 1996. An aqueous endpoint assay of snake venom phospholipase A_2. Toxicon, 34 (10), 1149-55.

Holzer, M. and Mackessy, S.P., 1996. An aqueous endpoint assay of snake venom phospholipase A 2. *Toxicon*, *34*(10), 1149-1155.

Hong, S.J., Dawson, T.M. and Dawson, V.L., 2004. Nuclear and mitochondrial conversations in cell death: PARP-1 and AIF signaling. *Trends in pharmacological sciences*, *25*(5), 259-264.

Høyer-Hansen, M., Bastholm, L., Szyniarowski, P., Campanella, M., Szabadkai, G., Farkas, T., Bianchi, K., Fehrenbacher, N., Elling, F., Rizzuto, R. and Mathiasen, I.S., 2007. Control of macroautophagy by calcium, calmodulin-dependent kinase kinaseβ, and Bcl-2. *Molecular cell*,*25*(2), 193-205.

Igney F.H., Krammer P.H., 2002. Death and anti-death: Tumour resistance to apoptosis. Natural Review Cancer;2: 277–288.

Imlay, J.A., 2003. Pathways of oxidative damage. *Annual Reviews in Microbiology*, *57*(1), 395-418.

Iqbal J., Sanger W. G., Horsman D. E., Rosenwald A., Pickering D.L., Dave B., Dave S., Xiao L., Cao K., Zhu Q. (2004). Bcl-2 translocation defines a unique tumor subset within the germinal center B-cell-like diffuse large B-cell lymphoma. *American Journal of Pathology;165:* 159–166.

Izidoro, L.F.M., Ribeiro, M.C., Souza, G.R., Sant'Ana, C.D., Hamaguchi, A., HomsiBrandeburgo, M.I., Goulart, L.R., Beleboni, R.O., Nomizo, A., Sampaio, S.V. and Soares, A.M., 2006. Biochemical and functional characterization of an L-amino acid oxidase isolated from Bothrops pirajai snake venom. *Bioorganic & medicinal chemistry*, *14*(20), 7034-7043.

Jackson, C.M. and Nemerson, Y., 1980. Blood coagulation. *Annual review of biochemistry*, *49*(1), 765-811.

Jackson, D.A. and Pombo, A., 1998. Replicon clusters are stable units of chromosome structure: evidence that nuclear organization contributes to the efficient activation

and propagation of S phase in human cells. *The Journal of cell biology*, *140*(6), 1285-1295.

Jacob A. Gala´n, Elda E. Sa´nchez,, Alexis Rodrı´guez-Acosta, Julio G. Soto, Sajid Bashir, Mary Ann McLane, Carrie Paquette-Straub, John C. Pe´rez., 2008. Inhibition of lung tumor colonization and cell migration with the disintegrin crotatroxin 2 isolated from the venom of Crotalus atrox, Toxicon 51, 1186–1196;

Jemal A., Bray F., Center M. M., Ferlay J., Ward E., Forman D., 2011. Global Cancer Statistics. CANCER J. CLIN.,61, 69–90.

Jemal A., Siegel R., Ward E., Murray T., Xu J., Smigal C., Thun M.J. (2006). Cancer Statistics. Cancer Journal for clinicians;56: 106–130.

Jemal, A., Bray, F., Center, M.M., Ferlay, J., Ward, E. and Forman, D., 2011. Global cancer statistics. *CA: a cancer journal for clinicians*, *61*(2), pp.69-90.

Jemal, A., Center, M.M., DeSantis, C. and Ward, E.M., 2010. Global patterns of cancer incidence and mortality rates and trends. *Cancer Epidemiology Biomarkers & Prevention*, *19*(8), pp.1893-1907.

Jiang, W., Zhang, Y.J., Kahn, S.M., Hollstein, M.C., Santella, R.M., Lu, S.H., Harris, C.C., Montesano, R. and Weinstein, I.B., 1993. Altered expression of the cyclin D1 and retinoblastoma genes in human esophageal cancer. *Proceedings of the National Academy of Sciences*, *90*(19), 9026-9030.

Jin Y., Lee W.H., Zeng L., Zhang Y., 2007. Molecular characterization of l-amino acid oxidase from king cobra venom. Toxicon, 50, 479–489.

Jin, Y., Lee, W.H., Zeng, L. and Zhang, Y., 2007. Molecular characterization of Lamino acid oxidase from king cobra venom. *Toxicon*, *50*(4), 479-489.

Jones, L.J. and Singer, V.L., 2001. Fluorescence microplate-based assay for tumor necrosis factor activity using SYTOX Green stain. *Analytical biochemistry*, *293*(1), 8-15.

Jordan M. A., Thrower D., Wilson L. (1991). Mechanism of Inhibition of Cell Proliferation by Vinca Alkaloids. Cancer Research; 51: 2212-2222.

Joseph, J.K., 2014. Viperidae Envenomation in India. In *Clinical Toxinology*(pp. 1-15). Springer Netherlands.

Kalyanaraman, B., Darley-Usmar, V., Davies, K.J., Dennery, P.A., Forman, H.J., Grisham, M.B., Mann, G.E., Moore, K., Roberts, L.J. and Ischiropoulos, H., 2012.

Measuring reactive oxygen and nitrogen species with fluorescent probes: challenges and limitations. *Free Radical Biology and Medicine*, *52*(1), 1-6.

Kanashiro, M.M., Rita de Cássia, M.E., Petretski, J.H., Prates, M.V., Alves, E.W., Machado, O.L., da Silva, W.D. and Kipnis, T.L., 2002. Biochemical and biological properties of phospholipases A 2 from Bothrops atrox snake venom. *Biochemical pharmacology*, *64*(7), 1179-1186.

Kanavos, P., 2006. The rising burden of cancer in the developing world.*Annals of oncology*, *17*(suppl 8), pp.viii15-viii23.

Kang T. S., Georgieva D., Genov N., Murakami M. T., Sinha M., Kumar R. P., Kaur P., Kumar S., Dey S., Sharma S., Vrielink A., Betzel C., Takeda S., Arni R. K., Singh T. P., Kini R. M., 2011. Enzymatic toxins from snake venom: structural characterization and mechanism of catalysis. The FEBS journal, 278, 4544-76.

Kang, T.S., Georgieva, D., Genov, N., Murakami, M.T., Sinha, M., Kumar, R.P., Kaur, P., Kumar, S., Dey, S., Sharma, S. and Vrielink, A., 2011. Enzymatic toxins from snake venom: structural characterization and mechanism of catalysis. *FEBS Journal*, *278*(23), 4544-4576.

Kasturiratne, A., Wickremasinghe, A.R., de Silva, N., Gunawardena, N.K., Pathmeswaran, A., Premaratna, R., Savioli, L., Lalloo, D.G. and de Silva, H.J., 2008. The global burden of snakebite: a literature analysis and modelling based on regional estimates of envenoming and deaths. *PLoS Med*, *5*(11), 1591-1604.

Kearney, E.B. and Singer, T.P., 1951. The L-amino acid oxidases of snake venom. V. Mechanism of the reversible inactivation. *Archives of biochemistry and biophysics*, *33*(3), 414-426.

Kekre, N., Griffin, C., McNulty, J., Pandey, S., 2005. Pancratistatin causes early activation of caspase-3 and the flipping of phosphatidyl serine followed by rapid apoptosis specifically in human lymphoma cells. Cancer Chemother. Pharmacol. 56, 29–38.

Kerns, S.L., Ostrer, H. and Rosenstein, B.S., 2014. Radiogenomics: using genetics to identify cancer patients at risk for development of adverse effects following radiotherapy. *Cancer discovery*, *4*(2), 155-165.

Khong A., Cleaver A. L., Alatas M. F., Wylie B. C., Connor T., Fisher S. A., Broomfield S., Lesterhuis W. J., Currie A. J., Lake R. A., Robinson B. W. (2014). The efficacy of tumor debulking surgery is improved by adjuvant immunotherapy using imiquimod and anti-CD40. Bio Medical Central Journal of Cancer;14: 969-978.

Kim J., Hong S., Park H., Kim D., Lee W., 2005. Structure and function of RGD peptides derived fromdisintegrin proteins. Mol. Cells, 19, 205–211.

Kim You-Sun, Morgan M. J., Choksi S., Liu Zheng-gang, 2007. TNF-Induced Activation of the Nox1 NADPH Oxidase and Its Role in the Induction of Necrotic Cell Death. Molecular Cell, 26 (5), 769-771.

Kim, G.T., Chun, Y.S., Park, J.W. and Kim, M.S., 2003. Role of apoptosis-inducing factor in myocardial cell death by ischemia–reperfusion.*Biochemical and biophysical research communications*, *309*(3), 619-624.

King, G.F., 2011. Venoms as a platform for human drugs: translating toxins into therapeutics. *Expert opinion on biological therapy*, *11*(11), 1469-1484.

King, G.F., 2011. Venoms as a platform for human drugs: translating toxins into therapeutics. *Expert opinion on biological therapy*, *11*(11), 1469-1484.

Kini, R.M. and Evans, H.J., 1992. Structural domains in venom proteins: evidence that metalloproteinases and nonenzymatic platelet aggregation inhibitors (disintegrins) from snake venoms are derived by proteolysis from a common precursor. *Toxicon*, *30*(3), 265-293.

Kinnunen, P.A.I.V.I., Vuolteenaho, O.L.L.I. and Ruskoaho, H.E.I.K.K.I., 1993. Mechanisms of atrial and brain natriuretic peptide release from rat ventricular myocardium: effect of stretching. *Endocrinology*, *132*(5), 1961-1970.

Kirkin, V., McEwan, D.G., Novak, I. and Dikic, I., 2009. A role for ubiquitin in selective autophagy. *Molecular cell*, *34*(3), 259-269.

Klaunig, J.E., Xu, Y., Isenberg, J.S., Bachowski, S., Kolaja, K.L., Jiang, J., Stevenson, D.E. and Walborg Jr, E.F., 1998. The role of oxidative stress in chemical carcinogenesis. *Environmental Health Perspectives*, *106*(Suppl 1), 289-295

Klemm, F. and Joyce, J.A., 2015. Microenvironmental regulation of therapeutic response in cancer. *Trends in cell biology*, *25*(4), pp.198-213.

Knappskog, S. and Lønning, P.E., 2012. P53 and its molecular basis to chemoresistance in breast cancer. *Expert opinion on therapeutic targets*,*16*(sup1), S23-S30.

Koh D. C. I., Armugam A., Jeyaseelan K., 2006. Snake venom components and their applications in biomedicine. Cell. Mol. Life Sci., 63, 3030–41.

Koh, C.Y. and Kini, R.M., 2012. From snake venom toxins to therapeutics–cardiovascular examples. *Toxicon*, *59*(4), 497-506.

Köhler, C., Orrenius, S. and Zhivotovsky, B., 2002. Evaluation of caspase activity in apoptotic cells. *Journal of immunological methods*, *265*(1), 97-110.

Koizumi W., Narahara H. , Hara T., Takagane A, Akiya T., Takagi M., Miyashita K, Nishizaki T, Kobayashi O., Takiyama W, Toh Yasushi , Nagaie T , Takagi S., Yamamura Y., Yanaoka K., Orita H., Takeuchi M. (2008). S-1 plus cisplatin versus S-1 alone for first-line treatment of advanced gastric cancer (SPIRITS trial): a phase III trial. The Lancet oncology; 9 (3): 215-221.

Kominami K., Nakabayashi J., Nagai T., Tsujimura Y., Chiba K., Kimura H., Miyawaki A., Sawasaki T., Yokota H., Manabe N., Sakamaki., 2012. The molecular mechanism of apoptosis upon caspase-8 activation: Quantitative experimental validation of a mathematical model. Biochimica et Biophysica Acta, 1823, 1825-40.

Kroemer G., El-Deiry WS, Golstein P., Peter M. E., Vaux D., Vendenabeele P., Zhivotovsky B., Blagosklonny., Malorni W., Knight R. A., Piacentini M., Nagata S., Melino G.,2005. Classification of cell death: recommendations of the nomenclature committee on cell death. Cell Death Differ, 12, 1463–1467.

Kroemer G., Galluzzi L., Brenner C., 2007. Mitochondrial membrane permeabilisation in cell death. Physiol Rev,, 87(1), 99-163.

Krysko, D.V., D'Herde, K. and Vandenabeele, P., 2006. Clearance of apoptotic and necrotic cells and its immunological consequences.*Apoptosis*, *11*(10), pp.1709-1726.

Kuroda K., Brown E. J., Telle W. B., Russell D. G., Ratliff T. L., 1993. Characterization of the internalization of Bacillus Calmetter-Guerin by human bladder tumour cells. J Clin. Invest., 91, 69-76.

LaCasse E. C., Mahoney D. J., Cheung H. H., Plenchette S., Baird S., Korneluk R.G. (2008).

Lahtz C., Pfeifer G. P. (2011) Epigenetic changes of DNA repair genes in cancer . Journal of molecular cell biology ; 3 (1): 51-58.

Lawrence M. S., Stojanov P., Mermel C. H., Robinson J. T., Garraway L. A., Golub T. R.,Lebaron, P., Catala, P. and Parthuisot, N., 1998. Effectiveness of SYTOX Green stain for bacterial viability assessment. *Applied and environmental microbiology*, *64*(7), 2697-2700.

Lee, M.L., Tan, N.H., Fung, S.Y. and Sekaran, S.D., 2011. Antibacterial action of a heat-stable form of L-amino acid oxidase isolated from king cobra (Ophiophagus hannah) venom. *Comparative Biochemistry and Physiology Part C: Toxicology & Pharmacology*, *153*(2), 237-242.

Leonhartsberger N., Pichler R., Stoehr B., Horninger W., August H. S. (2014). Organsparing surgery is the treatment of choice in benign testicular tumors. The World Journal of Urology; 32 (4): 1087-1091.

Levine, B. and Kroemer, G., 2008. Autophagy in the pathogenesis of disease. *Cell*, *132*(1),27-42.

Levine, B., 2007. Cell biology: autophagy and cancer. *Nature*, *446*(7137), pp.745747.

Levy, M.Z., Allsopp, R.C., Futcher, A.B., Greider, C.W. and Harley, C.B., 1992. Telomere end-replication problem and cell aging. *Journal of molecular biology*, *225*(4), pp.951-960.

Li J., Yen C., Liaw D., Podsypanina K., Bose S., Wang S.I., Puc J., Miliaresis C., Rodgers L, McCombie R., 1997. *PTEN*, a putative protein tyrosine phosphatase gene mutated in human brain, breast, and prostate cancer. Science, 275**,** 1943–47.

Li L., Neaves W.B. (2006). Normal stem cells and cancer stem cells: the niche matters. Cancer Res; 66: 4553-4557.

Li, J., Kim, S.G. and Blenis, J., 2014. Rapamycin: one drug, many effects.*Cell metabolism*, *19*(3), 373-379.

Li, X., Lewis, M.T., Huang, J., Gutierrez, C., Osborne, C.K., Wu, M.F., Hilsenbeck, S.G., Pavlick, A., Zhang, X., Chamness, G.C. and Wong, H., 2008. Intrinsic resistance of tumorigenic breast cancer cells to chemotherapy. *Journal of the National Cancer Institute*, *100*(9), 672-679.

Liang, X.J., Chen, C., Zhao, Y. and Wang, P.C., 2010. Circumventing tumor resistance to chemotherapy by nanotechnology. *Multi-Drug Resistance in Cancer*, 467-488.

Lima D. C. de, Abreu P. A., Freitas C. C. de, Santos D. O., Borges R. O., Santos T. C. dos, Cabral L. M., Rodrigues C. R., Helena C. C., 2005. Snake venom: any clue for antibiotics and CAM? Evid Based Complement Alternat. Med., 2(1), 39–47.

Lindahl, T., Satoh, M.S., Poirier, G.G. and Klungland, A., 1995. Post-translational modification of poly (ADP-ribose) polymerase induced by DNA strand breaks. *Trends in biochemical sciences*, *20*(10), 405-411.

Lipps B. V., 1999. Novel snake venom proteins cytolytic to cancer cells *in vitro* and *in vivo* systems, J. Venom. Anim.. Toxins, 5, 121-130.

Liu, L., Xing, D. and Chen, W.R., 2009. μ-Calpain regulates caspase-dependent and apoptosis inducing factor-mediated caspase-independent apoptotic pathways in cisplatin-induced apoptosis. *International Journal of Cancer*, *125*(12),2757-2766.

Lloyd K. (2007). The resurgence of platinum-based cancer chemotherapy. Nature Reviews Cancer; 7: 573-584.

Lockshin, R.A. and Zakeri, Z., 2004. Apoptosis, autophagy, and more. *The international journal of biochemistry & cell biology*, *36*(12), pp.2405-2419.

Longatti, A. and Tooze, S.A., 2009. Vesicular trafficking and autophagosome formation. *Cell Death & Differentiation*, *16*(7),956-965.

Lowe S. W., Lin A. W., 2000. Apoptosis in cancer. Carcinogenesis, 21 (3), 485-95.

Lozano, G. and Elledge, S.J., 2000. Cancer: p53 sends nucleotides to repair DNA. *Nature*, *404*(6773), 24-25.

Lu L. (2013). Dose calculation algorithms in external beam photon radiation therapy. Editorial. International Journal in Cancer Therapeutics in Oncology; 1(2): 01025.

Lu, Q.M., Wei, Q., Jin, Y., Wei, J.F., Wang, W.Y. and Xiong, Y.L., 2002. L-amino acid oxidase from Trimeresurus jerdonii snake venom: purification, characterization, platelet aggregation-inducing and antibacterial effects.*Journal of natural toxins*, *11*(4), 345-352.

Lucena S., Sanchez E. E., Pere J. C., 2011. Anti-metastatic activity of the recombinant disintegrin, r-mojastin 1, from the Mohave rattlesnake. Toxicon, 57, 794-802.

Lucena, S., Sanchez, E.E. and Perez, J.C., 2011. Anti-metastatic activity of the recombinant disintegrin, r-mojastin 1, from the Mohave rattlesnake.*Toxicon*, *57*(5), pp.794-802.

Luengo-Fernandez, R., Leal, J., Gray, A. and Sullivan, R., 2013. Economic burden of cancer across the European Union: a population-based cost analysis. *The lancet oncology*, *14*(12), 1165-1174.

Lundblad, V. and Szostak, J.W., 1989. A mutant with a defect in telomere elongation leads to senescence in yeast. *Cell*, *57*(4), 633-643.

Luo, X., Budihardjo, I., Zou, H., Slaughter, C. and Wang, X., 1998. Bid, a Bcl2 interacting protein, mediates cytochrome c release from mitochondria in response to activation of cell surface death receptors. *Cell*, *94*(4), 481-490.

Lyman, G.H., 2012. Weight-based chemotherapy dosing in obese patients with cancer: back to the future. *Journal of Oncology Practice*, *8*(4),62-e64.

Lyons, P. and Shelton, M.M., 2012. Psychosocial impact of cancer in low-income rural/urban women: Phase II. *Online Journal of Rural Nursing and Health Care*, *4*(2), pp.6-24.

Ma Y., Huang D., Liu L., Xiang M., Oghagbon E. K., Zhai S. (2014). Surgical treatment of carotid body tumour: a report of 39 cases and a new classification of carotid body tumour: Our Experience. *Clinical Otolaryngology;* 39 (4): 254-25.

Macht D. I., 1936. Experimental and clinical study of cobra venom as an analgesic. PNAS, 22, 61-71.

Majno G., Joris I., 1995. Apoptosis, oncosis, and necrosis. An overview of cell death. Am. J. Pathol., 146 (1), 3-15.

Malumbres, M. and Barbacid, M., 2006. Is Cyclin D1-CDK4 kinase a bona fide cancer target?. *Cancer cell*, *9*(1), pp.2-4.

Malumbres, M. and Barbacid, M., 2009. Cell cycle, CDKs and cancer: a changing paradigm. *Nature Reviews Cancer*, *9*(3), pp.153-166.

Marco A. D., Gaetani M. (1969) Scarpinato Adriamycin (NSC-123,127): a new antibiotic with antitumor activity Cancer Chemotherapy Reports;53: 33–37.

Mariette, C., Piessen, G. and Triboulet, J.P., 2007. Therapeutic strategies in oesophageal carcinoma: role of surgery and other modalities. *The lancet oncology*, *8*(6), pp.545-553.

Mariotto, A.B., Yabroff, K.R., Shao, Y., Feuer, E.J. and Brown, M.L., 2011. Projections of the cost of cancer care in the United States: 2010–2020.*Journal of the National Cancer Institute*.

Markland F. S., Zhou Q., 2002. Snake venom disintegrins: an effective inhibitor of breast cancer growth and dissemination. In: Tu AT, Gaffield W (eds). Natural and synthetic toxins, biological implications. American chemical society, 262-82.

Markland, F.S. and Swenson, S., 2010. Fibrolase and its evolution to clinical trials: a long and winding road. In *Toxins and Hemostasis* (pp. 409-427). Springer Netherlands.

Markman M., Gordon A. N., McGuire W. P., Muggia F. M. (2004). Liposomal anthracycline treatment for ovarian cancer. Seminars in oncology; 31 (31):91–105.

Marsh N., Williams V., 2005. Practical applications of snake venom toxins in haemostasis. Toxicon, 45, 1171– 1181.

Marsh, N. and Whaler, B., 1978. The effects of snake venoms on the cardiovascular and haemostatic mechanisms. *International Journal of Biochemistry*, *9*(4), pp.217220.

Martinou, J.C. and Green, D.R., 2001. Breaking the mitochondrial barrier.*Nature Reviews Molecular Cell Biology*, *2*(1), pp.63-67.

Massague, J. (2008). TGFbeta in cancer. Cell; 134: 215–230.

Massey, D.J., Calvete, J.J., Sánchez, E.E., Sanz, L., Richards, K., Curtis, R. and Boesen, K., 2012. Venom variability and envenoming severity outcomes of the Crotalus scutulatus scutulatus (Mojave rattlesnake) from Southern Arizona. *Journal of proteomics*, *75*(9), pp.2576-2587.

Massey, D.J., Calvete, J.J., Sánchez, E.E., Sanz, L., Richards, K., Curtis, R. and Boesen, K., 2012. Venom variability and envenoming severity outcomes of the Crotalus scutulatus scutulatus (Mojave rattlesnake) from Southern Arizona. *Journal of proteomics*, *75*(9), pp.2576-2587.

Massey, V. and Curti, B., 1967. On the reaction mechanism of Crotalus adamanteus l-amino acid oxidase. *Journal of Biological Chemistry*, *242*(6), pp.1259-1264.

Mathew, R., Karantza-Wadsworth, V. and White, E., 2007. Role of autophagy in cancer. *Nature Reviews Cancer*, *7*(12), pp.961-967.

Matthew R. Ritter, Qing Zhou, and Francis S. Markland, Jr. Contortrostatin., 2000. A snake venom disintegrin, induces avb3-mediated tyrosine phosphorylation of CAS and FAK in tumor cells, Journal of Cellular Biochemistry, 79, 28–37.

Maxwell P. D. (2001). Global cancer statistics in the year 2000. Lancet oncology: 2 (9): 533–543

McLane, M.A., Vijay-Kumar, S., Marcinkiewicz, C., Calvete, J.J. and Niewiarowski, S., 1996. Importance of the structure of the RGD-containing loop in the disintegrins echistatin and eristostatin for recognition of αIIbβ3 and αvβ3 integrins. *FEBS letters*, *391*(1-2), pp.139-143.

Mesri M., Wall N. R., Li J., Kim R. W., Altieri D. C., 2001. Cancer gene therapy using a surviving mutant adenovirus. Journal of Clinical Investigation; 108: 981–990.

Minta, A., Kao, J.P. and Tsien, R.Y., 1989. Fluorescent indicators for cytosolic calcium based on rhodamine and fluorescein chromophores.*Journal of Biological Chemistry*, *264*(14), pp.8171-8178.

Mizushima, N., 2007. Autophagy: process and function. *Genes & development*, *21*(22), pp.2861-2873.

Mizushima, N., Levine, B., Cuervo, A.M. and Klionsky, D.J., 2008. Autophagy fights disease through cellular self-digestion. *Nature*, *451*(7182), pp.1069-1075.

Modjtahedi, N., Giordanetto, F., Madeo, F. and Kroemer, G., 2006. Apoptosisinducing factor: vital and lethal. *Trends in cell biology*, *16*(5), pp.264-272.

Moody T. W., Chan D., Fahrenkrug J., Jensen R. T., 2003. Neuropeptides as autocrine growth factors in cancer cells. Current pharmaceutical design, 15, 495-509.

Moon D.O., Park, S.Y., Heo, M.S., Kim, K.C., Park, C., Ko, W.S., Choi, Y.H., Kim, G.Y., 2006. Key regulators in bee venom-induced apoptosis are Bcl-2 and caspase-3 in human leukemic U937 cells through downregulation of ERK and Akt. Int. Immunopharmacol. 6, 1796–1807.

Moustafa I.M., Foster S., Lyubimov A.Y., Vrielink A., 2006. Crystal structure of LAAO from *Calloselasma rhodostoma* with an L-phenylalanine substrate: Insights into structure and mechanism. J. Mol. Biol., 364, 991-1002.

Murray, J.M. and Hunt, T., 1993. The cell cycle: an introduction: Oxford University Press.

Muss, H.B., Berry, D.A., Cirrincione, C., Budman, D.R., Henderson, I.C., Citron, M.L., Norton, L., Winer, E.P. and Hudis, C.A., 2007. Toxicity of older and younger patients treated with adjuvant chemotherapy for node-positive breast cancer: the Cancer and Leukemia Group B Experience. *Journal of Clinical Oncology*, *25*(24), pp.36993704.

Nakada T., Okumura S., Kuroda H., Uehara H., Mun M, Sakao Y, Nakagawa K. (2014) Outcome of Radical Surgery for Pulmonary Metastatic Osteosarcoma with Secondary Spontaneous Pneumothorax: Case Series Report. Annals of Thoracic and Cardiovascular Surgery; Supplement p: 574–577.

Nakatogawa, H., Suzuki, K., Kamada, Y. and Ohsumi, Y., 2009. Dynamics and diversity in autophagy mechanisms: lessons from yeast. *Nature reviews Molecular cell biology*, *10*(7), pp.458-467.

Nathan, C. and Cunningham-Bussel, A., 2013. Beyond oxidative stress: an immunologist's guide to reactive oxygen species. *Nature Reviews Immunology*, *13*(5), pp.349-361.

Naumann, G.B., Silva, L.F., Silva, L., Faria, G., Richardson, M., Evangelista, K., Kohlhoff, M., Gontijo, C.M., Navdaev, A., de Rezende, F.F. and Eble, J.A., 2011. Cytotoxicity and inhibition of platelet aggregation caused by an L-amino acid oxidase from Bothrops leucurus venom.*Biochimica et Biophysica Acta (BBA)-General Subjects*, *1810*(7), pp.683-694.

Neurath H., 1984. Evolution of proteolytic enzymes. Science, 224, 350–357.

Newhauser W. D., Durante M. (2011). Assessing the risk of second malignancies after modern radiotherapy. *Nature Reviews Cancer;* 11: 438-448.

Newmann D. J., Cragg G. M., 2007. Natural products as sources of new drugs over the last 25 years. J. Nat. Prod., 70 (3), 461-77.

Nget-Hong, T. and Saifuddin, M.N., 1991. Substrate specificity of king cobra (Ophiophagus hannah) venom L-amino acid oxidase. *International journal of biochemistry*, *23*(3), pp.323-327.

Niault T. S., Baccarini M., 2010. Targets of Raf in tumorigenesis. Carcinogenesis 2010, 31, 1165–74.

Nicholls, D.G. and Ward, M.W., 2000. Mitochondrial membrane potential and neuronal glutamate excitotoxicity: mortality and millivolts. *Trends in neurosciences*, *23*(4), pp.166-174.

Nigg, E.A., 2001. Mitotic kinases as regulators of cell division and its checkpoints. *Nature reviews Molecular cell biology*, *2*(1), pp.21-32.

Nikjoo H. , O'Neill P. , Terrissol M. , Goodhead D. T. , 1999. Quantitative modelling of DNA damage using Monte Carlo track structure method. May, Radiation and Environmental Biophysics; 38 (1): 31-38.

Nishida N., Yano H., Nishida T., Kamura T., Kojiro M. (2006). Angiogenesis in cancer Vascular Health and Risk Management; 2(3): 213–219.

Noble R. L. (1990). The discovery of the vinca alkaloids—chemotherapeutic agents against cancer. Biochemistry and Cell Biology; 68(12): 1344-1351.

Norberg, E., Gogvadze, V., Ott, M., Horn, M., Uhlen, P., Orrenius, S. and Zhivotovsky, B., 2008. An increase in intracellular Ca2+ is required for the activation of mitochondrial calpain to release AIF during cell death. *Cell Death & Differentiation*, *15*(12), pp.1857-1864.

Norberg, E., Gogvadze, V., Vakifahmetoglu, H., Orrenius, S. and Zhivotovsky, B., 2010a. Oxidative modification sensitizes mitochondrial apoptosis-inducing factor to calpain-mediated processing. *Free Radical Biology and Medicine*, *48*(6), pp.791-797.

Norberg, E., Orrenius, S. and Zhivotovsky, B., 2010. Mitochondrial regulation of cell death: processing of apoptosis-inducing factor (AIF). *Biochemical and biophysical research communications*, *396*(1), pp.95-100.

NSCLC Meta-Analyses Collaborative Group. (2008). Chemotherapy in addition to supportive care improves survival in advanced non-small-cell lung cancer: a systematic review and meta-analysis of individual patient data from 16 randomized controlled trials. Journal of Clinical Oncolongy;26: 4617-25.

O'Brien M. A, Kirby R., 2008. Apoptosis: a review of pro-apoptotic and antiapoptotic pathways and dysregulation in disease. J. Vet. Emerg. Crit. Care, 18 (6), 572-85.

O'Flaherty, J.D., Gray, S., Richard, D., Fennell, D., O'Leary, J.J., Blackhall, F.H. and O'Byrne, K.J., 2012. Circulating tumour cells, their role in metastasis and their clinical utility in lung cancer. *Lung Cancer*, *76*(1), pp.19-25.

Okines, A., Verheij, M., Allum, W., Cunningham, D., Cervantes, A. and ESMO Guidelines Working Group. (2010). Gastric cancer: ESMO Clinical Practice Guidelines for diagnosis, treatment and follow-up. *Annals of Oncology*;*21*(5):50-54.

Oliveira R. L. de, Hamm A., Mazzone M. (2011). Growing tumor vessels: More than one way to skin a cat – Implications for angiogenesis targeted cancer therapies. Molecular Aspects of Medicine; 32: 71–87.

Orrenius, S., Gogvadze, V. and Zhivotovsky, B., 2015. Calcium and mitochondria in the regulation of cell death. *Biochemical and biophysical research communications*, *460*(1), pp.72-81.

Orrenius, S., Zhivotovsky, B. and Nicotera, P., 2003. Regulation of cell death: the calcium–apoptosis link. *Nature reviews Molecular cell biology*,*4*(7), pp.552-565.

Otera, H., Ohsakaya, S., Nagaura, Z.I., Ishihara, N. and Mihara, K., 2005. Export of mitochondrial AIF in response to proapoptotic stimuli depends on processing at the intermembrane space. *The EMBO journal*, *24*(7), pp.1375-1386.

Packham, M.A. and Mustard, J.F., 1986, January. The role of platelets in the development and complications of atherosclerosis. In *Seminars in hematology* (Vol. 23, No. 1, pp. 8-26).

Padmanabhan A., Gosc E. B., Bieberich C. J., 2013. Stabilization of the prostatespecific tumor suppressor NKX3.1 by the oncogenic protein kinase pim-1 in prostate cancer cells. Journal of Cellular Biochemistry, 114, 1050–57.

Paiva, R.D.M.A., de Freitas Figueiredo, R., Antonucci, G.A., Paiva, H.H., Bianchi, M.D.L.P., Rodrigues, K.C., Lucarini, R., Caetano, R.C., Pietro, R.C.L.R., Martins, C.H.G. and de Albuquerque, S., 2011. Cell cycle arrest evidence, parasiticidal and bactericidal properties induced by L-amino acid oxidase from Bothrops atrox snake venom. *Biochimie*, *93*(5), pp.941-947.

Pal S. K., Gomes A., Dasgupta S. C., 2002. Snake venom as therapeutic agents: From toxin to drug development. Indian Journal of Experiment Biology, 40, 1353-1358.

Panina S, Stephan A, JM la Cour, Jacobsen K *et al*., 2012. Significance of calcium binding, tyrosine phosphorylation, and lysine trimethylation for the essential function of calmodulin in vertebrate cells analyzed in a novel gene replacement system. Journal of Biological chemistry, 22:287; 18173-18181.

Papetti M., Herman I., 2002. Mechanisms of normal and tumor-derived angiogenesis, Am J Physiol Cell Physiol, 282,947–70.

Pardee, A.B., 1989. G1 events and regulation of cell proliferation. *Science*,*246*(4930), pp.603-608.

Paredes, R.M., Etzler, J.C., Watts, L.T., Zheng, W. and Lechleiter, J.D., 2008. Chemical calcium indicators. *Methods*, *46*(3), pp.143-151.

Park, M.H., Jo, M., Won, D., Song, H.S., Han, S.B., Song, M.J. and Hong, J.T., 2012. Snake venom toxin from Vipera lebetina turanica induces apoptosis of colon cancer cells via upregulation of ROS-and JNK-mediated death receptor expression. *BMC cancer*, *12*(1), p.228.

Patel, L.R., Camacho, D.F., Shiozawa, Y., Pienta, K.J. and Taichman, R.S., 2011. Mechanisms of cancer cell metastasis to the bone: a multistep process. *Future Oncology*, *7*(11), pp.1285-1297.

Pattingre, S., Tassa, A., Qu, X., Garuti, R., Liang, X.H., Mizushima, N., Packer, M., Schneider, M.D. and Levine, B., 2005. Bcl-2 antiapoptotic proteins inhibit Beclin 1dependent autophagy. *Cell*, *122*(6), pp.927-939.

Pawelek P., Cheah J., Coulombe R., Macheroux P., Ghisla S., Vrielink A., 2000. The structure of l-amino acid oxidase reveals the substrate trajectory into an enantiomerically conserved active site. The EMBO journal, 19 (16), 4204-15.

Payne G. S., Leach M. O., 2006. Applications of magnetic resonance spectroscopy in radiotherapy treatment planning British Journal of Radiology; 79: 16–26.

Peetla, C., Vijayaraghavalu, S. and Labhasetwar, V., 2013. Biophysics of cell membrane lipids in cancer drug resistance: implications for drug transport and drug delivery with nanoparticles. *Advanced drug delivery reviews*, *65*(13), pp.1686-1698.

Peinado, H., Lavotshkin, S. and Lyden, D., 2011, April. The secreted factors responsible for pre-metastatic niche formation: old sayings and new thoughts. In *Seminars in cancer biology* (Vol. 21, No. 2, pp. 139-146). Academic Press.

Pierzyńska-Mach, A., Janowski, P.A. and Dobrucki, J.W., 2014. Evaluation of acridine orange, LysoTracker Red, and quinacrine as fluorescent probes for long-term tracking of acidic vesicles. *Cytometry Part A*, *85*(8), pp.729-737.

Pietras, K. and Östman, A., 2010. Hallmarks of cancer: interactions with the tumor stroma. *Experimental cell research*, *316*(8), pp.1324-1331.

Pillay, C.S., Elliott, E. and Dennison, C., 2002. Endolysosomal proteolysis and its regulation. *Biochemical Journal*, *363*(3), pp.417-429.

Planas-Silva, M.D. and Weinberg, R.A., 1997. The restriction point and control of cell proliferation. *Current opinion in cell biology*, *9*(6), pp.768-772.

Polster, B.M., Basañez, G., Etxebarria, A., Hardwick, J.M. and Nicholls, D.G., 2005. Calpain I induces cleavage and release of apoptosis-inducing factor from isolated mitochondria. *Journal of Biological Chemistry*, *280*(8), pp.6447-6454.

Ponnudurai G., Chung M.C.M., Tan N-H., 1994. Purification and properties of the lamino acid oxidase from Malayan pit viper (*Calloselasma rhodostoma*) venom. Arch. Biochem. Biophy., 313, 373–378.

Ponnudurai, G., Chung, M.C. and Tan, N.H., 1994. Purification and properties of the L-amino acid oxidase from Malayan pit viper (Calloselasma rhodostoma) venom. *Archives of biochemistry and biophysics*, *313*(2), pp.373-378.

Potten, C.S. and Loeffler, M., 1990. Stem cells: attributes, cycles, spirals, pitfalls and uncertainties. Lessons for and from the crypt. *Development*,*110*(4), pp.1001-1020.

Prevarskaya Natalia, Skryma Roman , Shuba Yaroslav, 2010. Ion channels and hallmark of cancer. Trends in molecular chemistry, 16, 107-121.

Putz, T., Ramoner, R., Gander, H., Rahm, A., Bartsch, G., Thurnher, M., 2006. Antitumor action and immune activation through cooperation of bee venom secretory phospholipase A2 and phosphatidylinositol-(3,4)-bisphosphate. Cancer Immunol. Immunother. 55, 1374–1383.

Pyo, J.O., Nah, J. and Jung, Y.K., 2012. Molecules and their functions in autophagy. *Experimental & molecular medicine*, *44*(2), pp.73-80.

Radhakrishnan K., Lee A., Harrison L. A., Morris E., Shen V., Gates L., Wells R. J., Wolff J. E., Garvin J. H., Cairo M.S. (2015). A Novel Trial of Topotecan, Ifosfamide, and Carboplatin (TIC) in Children With Recurrent Solid Tumors. Pediatric Blood Cancer;62: 274–278.

Raghunand, N., Gatenby, R.A. and Gillies, R.J., 2014. Microenvironmental and cellular consequences of altered blood flow in tumours. *The British journal of radiology*.

Rai B., Basnel A., Patel F. D., Sherma S. C., 2014. Radiotherapy for ovarian cancers. Redefining the role. Asian Pacific Journal of Cancer Prevention; 15 (12): 4759-4763.

Raibekas, A.A. and Massey, V., 1998. Primary Structure of the Snake Venom LAmino Acid Oxidase Shows High Homology with the Mouse B Cell Interleukin 4InducedFig1Protein. *Biochemical and biophysical research communications*, *248*(3), pp.476-478.

Rampersad, S.N., 2012. Multiple applications of Alamar Blue as an indicator of metabolic function and cellular health in cell viability bioassays. *Sensors*,*12*(9), pp.12347-12360.

Raso E., Tovari J., Toth K., Paku S., Trikha M., Honn K. V., Timar J., 2001. Ectopic alphaIIbbeta3 integrin signaling involves 12-lipoxygenase- and PKC-mediated serine hosphorylation events in melanoma cells. Thromb. Haemostasis, 85, 1037–42.

Re A., Aiello, A., Nann S., Grasselli I. A., Benvenuti V., Pantisano V., Strigari L., Colussi C., Ciccone S., Mazzetti A. P., Pierconti F., Pinto F., Bassi P., Gallucci M., Sentinelli S., Rebecca S., Naishadham D., Jemal A., 2012. Cancer Statistics. Cancer Journal for clinicians ; 62: 10–29.

Reed J. C., 1998. Bcl-2 familiy proteins. Oncogene, 17, 3225-36

Reuter S., Eifes S., Dicato M., Aggarwal B. B., Diederich M., 2008. Modulation of anti-apoptotic and survival pathways by curcumin as a strategy to induce apoptosis in cancer cells. Biochemical Pharmacology, 76, 1340–51.

Roach H. I., Clarke N. M. P., 2000. Physiological cell death of chondrocytes in vivo is not confined to apoptosis. New observations on the mammalian growth plate. J Bone Joint Surg [Br], 82-B (4), 601-13.

Rocha A. B., Lopes R. M., Schwartsmann G. (2001). Natural products in anticancer therapy .Current Opinion in Pharmacology; 1: 364–369.

Rockenfeller, P., Koska, M., Pietrocola, F., Minois, N., Knittelfelder, O., Sica, V., Franz, J., Carmona-Gutierrez, D., Kroemer, G. and Madeo, F., 2015. Phosphatidylethanolamine positively regulates autophagy and longevity. *Cell Death & Differentiation*, *22*(3), pp.499-508.

Rodrigues R.S., da Silva J.F., Boldrini Franca J., Fonseca F.P., Otaviano A.R., Henrique Silva F., Hamaguchi A., Magro A.J., Braz A.S., dos Santos J.I. et al., 2009. Structural and

functional properties of Bp-LAAO, a new l-amino acid oxidase isolated from Bothrops pauloensis snake venom. Biochimie, 91, 490–501.

Rodrigues, R.S., da Silva, J.F., França, J.B., Fonseca, F.P., Otaviano, A.R., Silva, F.H., Hamaguchi, A., Magro, A.J., Braz, A.S.K., dos Santos, J.I. and Homsi-Brandeburgo, M.I., 2009. Structural and functional properties of Bp-LAAO, a new L-amino acid oxidase isolated from Bothrops pauloensis snake venom. *Biochimie*, *91*(4), pp.490501.

Saberi, B., Shinohara, M., Ybanez, M.D., Hanawa, N., Gaarde, W.A., Kaplowitz, N. and Han, D., 2008. Regulation of H2O2-induced necrosis by PKC and AMP-activated kinase signaling in primary cultured hepatocytes.*American Journal of Physiology-Cell Physiology*, *295*(1), pp.C50-C63.

Sakakibara, K., Eiyama, A., Suzuki, S.W., Sakoh-Nakatogawa, M., Okumura, N., Tani, M., Hashimoto, A., Nagumo, S., Kondo-Okamoto, N., Kondo-Kakuta, C. and Asai, E., 2015. Phospholipid methylation controls Atg32-mediated mitophagy and Atg8 recycling. *The EMBO journal*, *34*(21), pp.2703-2719.

Sakurai, Y., Shima, M., Matsumoto, T., Takatsuka, H., Nishiya, K., Kasuda, S., Fujimura, Y. and Yoshioka, A., 2003. Anticoagulant activity of M-LAO, l-amino acid oxidase purified from Agkistrodon halys blomhoffii, through selective inhibition of factor IX. *Biochimica et Biophysica Acta (BBA)-Proteins and Proteomics*, *1649*(1), pp.51-57.

Sakurai, Y., Takatsuka, H., Yoshioka, A., Matsui, T., Suzuki, M., Titani, K. and Fujimura, Y., 2001. Inhibition of human platelet aggregation by L-amino acid oxidase purified from Naja naja kaouthia venom. *Toxicon*, *39*(12), pp.1827-1833.

Sakurai, Y., Takatsuka, H., Yoshioka, A., Matsui, T., Suzuki, M., Titani, K. and Fujimura, Y., 2001. Inhibition of human platelet aggregation by L-amino acid oxidase purified from Naja naja kaouthia venom. *Toxicon*, *39*(12), pp.1827-1833.

Sánchez, E.E., Rodríguez-Acosta, A., Palomar, R., Lucena, S.E., Bashir, S., Soto, J.G. and Pérez, J.C., 2009. Colombistatin: a disintegrin isolated from the venom of the South American snake (Bothrops colombiensis) that effectively inhibits platelet aggregation and SK-Mel-28 cell adhesion.*Archives of toxicology*, *83*(3), pp.271-279.

Sankaranarayanan R, Ferlay J., 2006. Worldwide burden of gynaecological cancer: the size of the problem. Best Pract. Res. Clin. Obstet. & Gynaecol, 20, 207–25.

Sartorelli A. C. (1988) Therapeutic Attack of Hypoxie Cells of Solid Tumors. Cancer Research; 48: 775-778.

Saudek, V., Atkinson, R.A. and Pelton, J.T., 1991. Three-dimensional structure of echistatin, the smallest active RGD protein. *Biochemistry*,*30*(30), pp.7369-7372.

Scarborough, R.M., Naughton, M.A., Teng, W., Rose, J.W., Phillips, D.R., Nannizzi, L., Arfsten, A., Campbell, A.M. and Charo, I.F., 1993. Design of potent and specific integrin antagonists. Peptide antagonists with high specificity for glycoprotein IIbIIIa. *Journal of Biological Chemistry*, *268*(2), pp.1066-1073.

Scarborough, R.M., Rose, J.W., Hsu, M., Phillips, D.R., Fried, V.A., Campbell, A.M., Nannizzi, L. and Charo, I.F., 1991. Barbourin. A GPIIb-IIIa-specific integrin antagonist from the venom of Sistrurus m. barbouri. *Journal of Biological Chemistry*, *266*(15), pp.9359-9362.

Schneider P., Tschopp J., 2000. Apoptosis induced by death receptors. Pharmacochemistry Library, 31, 281-86.

Schulz W.A., Burchardt M., 2006. Cronauer M.V. Molecualr human reproduction, 9 (8), 437-48.

Schwartz D. L., Garden A. S., Shah S. J., Chronowski G., Sejpal S., Rosenthal D.I., Chen Y., Zhang Y., Zhang L., Wong P., Garcia J. A., Ang K. K., Dong L. (2013). Adaptive radiotherapy for head and neck cancer—Dosimetric results from a prospective clinical trial. Radiotherapy and Oncology; 106: 80–84.

Schweitz, H., Vigne, P., Moinier, D., Frelin, C. and Lazdunski, M., 1992. A new member of the natriuretic peptide family is present in the venom of the green mamba (Dendroaspis angusticeps). *Journal of Biological Chemistry*,*267*(20), pp.13928-13932.

Sclafani, R.A. and Holzen, T.M., 2007. Cell cycle regulation of DNA replication. *Annual review of genetics*, *41*, 237-280.

Seguin, L., Desgrosellier, J.S., Weis, S.M. and Cheresh, D.A., 2015. Integrins and cancer: regulators of cancer stemness, metastasis, and drug resistance. *Trends in cell biology*, *25*(4), pp.234-240.

Shao, Y.H.J., Kim, S., Moore, D.F., Shih, W., Lin, Y., Stein, M., Kim, I.Y. and Lu-Yao, G.L., 2014. Cancer-specific survival after metastasis following primary radical prostatectomy compared with radiation therapy in prostate cancer patients: results of a population-based, propensity score–matched analysis. *European urology*, *65*(4), pp.693-700.

Sharma, K., Wang, R.X., Zhang, L.Y., Yin, D.L., Luo, X.Y., Solomon, J.C., Jiang, R.F., Markos, K., Davidson, W., Scott, D.W. and Shi, Y.F., 2000. Death the Fas way: regulation and pathophysiology of CD95 and its ligand.*Pharmacology & therapeutics*, *88*(3), pp.333-347.

Sharpless N. E., Chin L., 2003. The *INK4A/ARF* locus and melanoma. Oncogene, 22, 3092-98.

Shebuski, R.J., Ramjit, D.R., Bencen, G.H. and Polokoff, M.A., 1989. Characterization and platelet inhibitory activity of bitistatin, a potent arginine-glycine-aspartic acidcontaining peptide from the venom of the viper Bitis arietans. *Journal of Biological Chemistry*, *264*(36), pp.21550-21556.

Shintani, T. and Klionsky, D.J., 2004. Autophagy in health and disease: a doubleedged sword. *Science*, *306*(5698), pp.990-995.

Shipolini, R.A., Callewaert, G.L., Cottrell, R.C. and Vernon, C.A., 1974. The AminoAcid Sequence and Carbohydrate Content of Phospholipase A2 from Bee Venom. *European Journal of Biochemistry*,*48*(2), pp.465-476.

Siddik Z. H. (2003). Cisplatin: mode of cytotoxic action and molecular basis of resistance *Oncogene*; 22: 7265–7279.

Siegel, R., DeSantis, C. and Jemal, A., 2014. Colorectal cancer statistics, 2014. *CA: a cancer journal for clinicians*, *64*(2), pp.104-117.

Silman, I. and Sussman, J.L., 2008. Acetylcholinesterase: How is structure related to function?. *Chemico-biological interactions*, *175*(1), pp.3-10.

Silva, E.F., Richradson, M., Gomes, M.V. and Sanchez, E.F., 2007. 23.6. Biochemical properties of a l-amino acid oxidase from Bothrops leucurus (white-tailed jararaca) snake venom. *Comparative Biochemistry and Physiology Part A: Molecular & Integrative Physiology*, *148*, p.S105.

Six, D.A. and Dennis, E.A., 2000. The expanding superfamily of phospholipase A 2 enzymes: classification and characterization. *Biochimica et Biophysica Acta (BBA)Molecular and Cell Biology of Lipids*, *1488*(1), pp.1-19.

Sleeman, J.P., Christofori, G., Fodde, R., Collard, J.G., Berx, G., Decraene, C. and Rüegg, C., 2012, June. Concepts of metastasis in flux: the stromal progression model. In *Seminars in cancer biology* (Vol. 22, No. 3, pp. 174-186). Academic Press.

Smith, R.E. and Ashiya, M., 2007. Antihypertensive therapies. *Nature Reviews Drug Discovery*, *6*(8), pp.597-598.

Smith, T.J. and Hillner, B.E., 2011. Bending the cost curve in cancer care.*New England Journal of Medicine*, *364*(21), pp.2060-2065.

Smulson, M.E., Simbulan-Rosenthal, C.M., Boulares, A.H., Yakovlev, A., Stoica, B.,

Iyer, S., Luo, R., Haddad, B., Wang, Z.Q., Pang, T. and Jung, M., 2000. Roles of poly (ADP-ribosyl) ation and PARP in apoptosis, DNA repair, genomic stability and functions of p53 and E2F-1. *Advances in enzyme regulation*, *40*(1), pp.183-215.

Sodeoka, M. and Dodo, K., 2010. Development of selective inhibitors of necrosis. *The Chemical Record*, *10*(5), pp.308-314.

Soltysik, S., Byron, C.M., Einarsdottir, G.H. and Stankovich, M.T., 1987. The effects of reversible freezing inactivation and inhibitor binding on redox properties of Lamino-acid oxidase. *Biochimica et Biophysica Acta (BBA)-Protein Structure and Molecular Enzymology*, *911*(2), pp.201-208.

Solyanik, G.I., 2010. Multifactorial nature of tumor drug resistance. *Exp Oncol*, *32*(3), pp.181-5.

Son, D.J., Park, M.H., Chae, S.J., Moon, S.O., Lee, J.W., Song, H.S., Moon, D.C., Kang, S.S., Kwon, Y.E., Hong, J.T., 2007. Inhibitory effect of snake venom toxin from Vipera lebetina turanica on hormonerefractory human prostate cancer cell growth: induction of apoptosis through inactivation of nuclear factor kappab. Mol. Cancer Ther. 6, 675–683.

Son, J.W., Kang, H.K., Chae, M.H., Choi, J.E., Park, J.M., Lee, W.K., Kim, C.H., Kim, D.S., Kam, S., Kang, Y.M. and Park, J.Y., 2006. Polymorphisms in the caspase-8 gene and the risk of lung cancer. *Cancer genetics and cytogenetics*, *169*(2), pp.121-127.

Song, J.K., Jo, M.R., Park, M.H., Song, H.S., An, B.J., Song, M.J., Han, S.B. and Hong, J.T., 2012. Cell growth inhibition and induction of apoptosis by snake venom toxin in ovarian cancer cell via inactivation of nuclear factor κB and signal transducer and activator of transcription 3. *Archives of pharmacal research*, *35*(5), pp.867-876.

Souza, D.H., Eugenio, L.M., Fletcher, J.E., Jiang, M.S., Garratt, R.C., Oliva, G. and Selistre-de-Araujo, H.S., 1999. Isolation and structural characterization of a cytotoxic L-amino acid oxidase from Agkistrodon contortrix laticinctus snake venom: preliminary crystallographic data.*Archives of biochemistry and biophysics*, *368*(2), pp.285-290.

Souza, D.H., Eugenio, L.M., Fletcher, J.E., Jiang, M.S., Garratt, R.C., Oliva, G. and Selistre-de-Araujo, H.S., 1999. Isolation and structural characterization of a cytotoxic L-amino acid oxidase from Agkistrodon contortrix laticinctus snake venom: preliminary crystallographic data.*Archives of biochemistry and biophysics*, *368*(2), pp.285-290.

Stábeli, R.G., Marcussi, S., Carlos, G.B., Pietro, R.C., Selistre-de-Araújo, H.S., Giglio, J.R., Oliveira, E.B. and Soares, A.M., 2004. Platelet aggregation and antibacterial

effects of an L-amino acid oxidase purified from Bothrops alternatus snake venom. *Bioorganic & medicinal chemistry*, *12*(11), pp.2881-2886.

Stábeli, R.G., Sant'Ana, C.D., Ribeiro, P.H., Costa, T.R., Ticli, F.K., Pires, M.G., Nomizo, A., Albuquerque, S., Malta-Neto, N.R., Marins, M. and Sampaio, S.V., 2007. Cytotoxic L-amino acid oxidase from Bothrops moojeni: biochemical and functional characterization. *International journal of biological macromolecules*, *41*(2), pp.132140.

Stiles, B.G., Sexton, F.W. and Weinstein, S.A., 1991. Antibacterial effects of different snake venoms: purification and characterization of antibacterial proteins from Pseudechis australis (Australian king brown or mulga snake) venom. *Toxicon*, *29*(9), pp.1129-1141.

Suhr, S.M. and Kim, D.S., 1996. Identification of the snake venom substance that induces apoptosis. *Biochemical and biophysical research communications*, *224*(1), pp.134-139.

Suhr, S.M. and Kim, D.S., 1999. Comparison of the apoptotic pathways induced by Lamino acid oxidase and hydrogen peroxide. *Journal of biochemistry*, *125*(2), pp.305309.

Susin, S.A., Lorenzo, H.K., Zamzami, N., Marzo, I., Snow, B.E., Brothers, G.M., Mangion, J., Jacotot, E., Costantini, P., Loeffler, M. and Larochette, N., 1999. Molecular characterization of mitochondrial apoptosis-inducing factor. *Nature*, *397*(6718), pp.441-446.

Swenson, S., Costa, F., Minea, R., Sherwin, R.P., Ernst, W., Fujii, G., Yang, D. and Markland, F.S., 2004. Intravenous liposomal delivery of the snake venom disintegrin contortrostatin limits breast cancer progression.*Molecular Cancer Therapeutics*, *3*(4), pp.499-511.

Szegezdi E., Logue S. E., Gorman A. M., Samali A., 2006. Mediators of endoplasmic reticulum stress-induced apoptosis. EMBO reports, 7 (9), 880-85.

Takatsuka, H., Sakurai, Y., Yoshioka, A., Kokubo, T., Usami, Y., Suzuki, M., Matsui, T., Titani, K., Yagi, H., Matsumoto, M. and Fujimura, Y., 2001. Molecular characterization of L-amino acid oxidase from Agkistrodon halys blomhoffii with special reference to platelet aggregation. *Biochimica et Biophysica Acta (BBA)Protein Structure and Molecular Enzymology*,*1544*(1), pp.267-277.

Takeda S., Takey H., Iwanaga S., 2012. Snake venom metalloproteinases: structure, function and relevance to the mammalian ADAM/ADAMTS family proteins. Biochimica et Biophysica Acta, 1824, 164–76.

Tan N. H., 1998. L-Amino acid oxidases and lactate dehydrogenases. In: Bailey GS ed. Enzymes from snake venom. Fort Collins: Alaken Inc. 1998; Chapter 19, 579-598.

Tan Nget-Hong, Fung Shin-Yee, 2008. Snake Venom L-Amino Acid Oxidases and Their Potential Biomedical Applications. Malaysian Journal of Biochemistry and Molecular Biology, 16(1), 1-10.

Tan, N.H. and Choy, S.K., 1994. The edema-inducing activity of Ophiophagus hannah (king cobra) venom L-amino acid oxidase. *Toxicon*,*32*(5), p.539.

Tan, N.H. and Saifuddin, M.N., 1989. Isolation and characterization of an unusual form of L-amino acid oxidase from King cobra (Ophiophagus hannah) venom. *Biochemistry international*, *19*(4), pp.937-944.

Tang, G., Gudsnuk, K., Kuo, S.H., Cotrina, M.L., Rosoklija, G., Sosunov, A., Sonders, M.S., Kanter, E., Castagna, C., Yamamoto, A. and Yue, Z., 2014. Loss of mTORdependent macroautophagy causes autistic-like synaptic pruning deficits. *Neuron*, *83*(5), pp.1131-1143.

Temkin V., Huang Q., Liu H., Osada H., Pope R. M., 2006. Inhibition of ADP/ATP Exchange in Receptor-Interacting Protein-Mediated Necrosis. Mol. Cell. Biol., 26 (6), 2215-25.

Tew W. P., Muss H. B., Kimmick G. G. , Gruenigen V. E. V., Lichtman S. M. (2014). Breast and Ovarian Cancer in the Older Woman. Journal of clinical oncology; 32 (24): 2553-2561.

Text book of medical physiology, eleventh edition, arthur c. guyton, m.d., john e. hall, ph.d. p. 999, ISBN 0-7216-0240-1

The EMBO Journal vol.6 no.11 pp.3341-3351, 1987 Human proto-oncogene c-kit: a new cell surface receptor tyrosine kinase for an unidentified ligand Yosef Yarden"14, Wun-Jing Kuang', Teresa Yang-Feng2, Lisa Coussens', Susan Munemitsul, Thomas J.Dull', Ellson Chen', Joseph Schlessinger3, Uta Francke2 and Axel Ullrichl

Thorburn A., 2004. Death receptor-induced cell killing. Cellular Signalling, 16, 139-44.

Thornberry N. A., Lazebnik Y., 1998. Caspases: Enemies Within. Science, 281 (5381), 1312-16.

Tiago Elias Heinen, Ana Beatriz Gorini da Veiga, C.L., Powell, J.R., Jiang, M.S., Fletcher, J.E., 1997. Melittin and phospholipase A2 from bee (Apis mellifera) venom cause necrosis of murine skeletal muscle in vivo. Toxicon 35, 67–80.

Tibballs, J., 1998. The cardiovascular, coagulation and haematological effects of tiger snake (Notechis scutatus) venom. *Anaesthesia and intensive care*, *26*(5), p.529535

Timmer, J.C. and Salvesen, G.S., 2007. Caspase substrates. *Cell Death & Differentiation*, *14*(1), pp.66-72.

Tomlinson, I.P., Lambros, M.B., Roylance, R.R. and Cleton-Jansen, A.M., 2002. Loss of heterozygosity analysis: practically and conceptually flawed?.*Genes, Chromosomes and Cancer*, *34*(4), pp.349-353.

Tõnismägi, K., Samel, M., Trummal, K., Rönnholm, G., Siigur, J., Kalkkinen, N. and Siigur, E., 2006. L-amino acid oxidase from Vipera lebetina venom: isolation, characterization, effects on platelets and bacteria. *Toxicon*, *48*(2), pp.227-237.

Torii, S., Naito, M. and Tsuruo, T., 1997. Apoxin I, a novel apoptosis-inducing factor with L-amino acid oxidase activity purified from Western diamondback rattlesnake venom. *Journal of Biological Chemistry*, *272*(14), pp.9539-9542.

Torre, L.A., Bray, F., Siegel, R.L., Ferlay, J., Lortet-Tieulent, J. and Jemal, A., 2015. Global cancer statistics, 2012. *CA: a cancer journal for clinicians*,*65*(2), pp.87-108.

Toyama, M.H., Toyama, D.D.O., Passero, L.F., Laurenti, M.D., Corbett, C.E., Tomokane, T.Y., Fonseca, F.V., Antunes, E., Joazeiro, P.P., Beriam, L.O. and Martins, M.A.C., 2006. Isolation of a new L-amino acid oxidase from Crotalus durissus cascavella venom. *Toxicon*, *47*(1), pp.47-57.

Toyama, M.H., Toyama, D.D.O., Passero, L.F., Laurenti, M.D., Corbett, C.E., Tomokane, T.Y., Fonseca, F.V., Antunes, E., Joazeiro, P.P., Beriam, L.O. and Martins, M.A.C., 2006. Isolation of a new L-amino acid oxidase from Crotalus durissus cascavella venom. *Toxicon*, *47*(1), pp.47-57.

Tran, D., Sinclair, R.D., Schwarer, A.P. and Chow, C.W., 2000. Permanent alopecia following chemotherapy and bone marrow transplantation.*Australasian journal of dermatology*, *41*(2), pp.106-108.

Travis, L.B., Ng, A.K., Allan, J.M., Pui, C.H., Kennedy, A.R., Xu, X.G., Purdy, J.A., Applegate, K., Yahalom, J., Constine, L.S. and Gilbert, E.S., 2012. Second malignant neoplasms and cardiovascular disease following radiotherapy. *Journal of the National Cancer Institute*.

Trikha M., Zhou Z., Timar J., Raso E., Kennel M., Emmell E., M. Nakada T., 2002. Multiple GPIIb/IIIa and alphavbeta3 integrins in tumor growth, angiogenesis, and metastasis. Cancer Res., 62, 2824–33.

Trimarchi F., Bacchetti S., Pontecorvi A., Bello M. L., Farsetti A., 2011. Silencing of *GSTP1*, a prostate cancer prognostic gene, by the estrogen receptor and endothelial nitric oxide synthase complex. Mol Endocrinol, 25(12), 2003–16.

Trimmer E. E, Essigmann J. M. (1999). Ciplatin. Essays in Biochemistry; 34: 191-211.

Trüeb, R.M., 2007. Chemotherapy-induced anagen effluvium: diffuse or patterned?. *Dermatology*, *215*(1), pp.1-2.

Trüeb, R.M., 2009, March. Chemotherapy-induced alopecia. In *Seminars in cutaneous medicine and surgery* (Vol. 28, No. 1, pp. 11-14).

Trüeb, R.M., 2010. Chemotherapy-induced alopecia. *Current opinion in supportive and palliative care*, *4*(4), pp.281-284.

Valdez-Cruz, N.A., Batista, C.V. and Possani, L.D., 2004. Phaiodactylipin, a glycosylated heterodimeric phospholipase A2 from the venom of the scorpion Anuroctonus phaiodactylus. *European Journal of Biochemistry*,*271*(8), pp.14531464.

van den Hurk, C.J.G., Winstanley, J., Young, A. and Boyle, F., 2015. Measurement of chemotherapy-induced alopecia—time to change.*Supportive Care in Cancer*, *23*(5), pp.1197-1199.

van Loo, G., Saelens, X., Van Gurp, M., MacFarlane, M., Martin, S.J. and Vandenabeele, P., 2002. The role of mitochondrial factors in apoptosis: a Russian roulette with more than one bullet. *Cell death and differentiation*,*9*(10), pp.10311042.

Vargas, L.J., Quintana, J.C., Pereañez, J.A., Núñez, V., Sanz, L. and Calvete, J., 2013. Cloning and characterization of an antibacterial L-amino acid oxidase from Crotalus durissus cumanensis venom. *Toxicon*, *64*, pp.1-11.

Vigny M., Bon S., Massoulie J., Leterrier F., 1978. Active-site catalytic efficiency of acetylcholinesterase molecular forms in Electrophorus, Torpedo, rat and chicken. Eur. J. Biochem., 85, 317–323.

Vilmar, A. and Sørensen, J.B., 2009. Excision repair cross-complementation group 1 (ERCC1) in platinum-based treatment of non-small cell lung cancer with special emphasis on carboplatin: a review of current literature. *Lung Cancer*, *64*(2), pp.131139.

Vyas, V.K., Brahmbhatt, K., Bhatt, H. and Parmar, U., 2013. Therapeutic potential of snake venom in cancer therapy: current perspectives. *Asian Pacific journal of tropical biomedicine*, *3*(2), pp.156-162.

Walters C. L., Arend R. C., Armstrong D. K., R. Naumann W., Alvarez R. D. (2013). Folate and folate receptor alpha antagonists mechanism of action in ovarian cancer. Gynecological Oncology ;131: 493–498.

Wang, Y., Probin, V. and Zhou, D., 2006. Cancer therapy-induced residual bone marrow injury-Mechanisms of induction and implication for therapy.*Current cancer therapy reviews*, *2*(3), pp.271-279.

Webb, J.L., Ravikumar, B. and Rubinsztein, D.C., 2004. Microtubule disruption inhibits autophagosome-lysosome fusion: implications for studying the roles of aggresomes in polyglutamine diseases. *The international journal of biochemistry & cell biology*, *36*(12), pp.2541-2550.

Wei, J.F., Wei, Q., Lu, Q.M., Tai, H., Jin, Y., Wang, W.Y. and Xiong, Y.L., 2003. Purification, characterization and biological activity of an L-amino acid oxidase from Trimeresurus mucrosquamatus venom. *ACTA BIOCHIMICA ET BIOPHYSICA SINICACHINESE EDITION-*, *35*(3), pp.219-228.

Wei, J.F., Yang, H.W., Wei, X.L., Qiao, L.Y., Wang, W.Y. and He, S.H., 2009. Purification, characterization and biological activities of the L-amino acid oxidase from Bungarus fasciatus snake venom. *Toxicon*, *54*(3), pp.262-271.

Wei, J.F., Yang, H.W., Wei, X.L., Qiao, L.Y., Wang, W.Y. and He, S.H., 2009. Purification, characterization and biological activities of the L-amino acid oxidase from Bungarus fasciatus snake venom. *Toxicon*, *54*(3), pp.262-271.

Wei, M.C., Zong, W.X., Cheng, E.H.Y., Lindsten, T., Panoutsakopoulou, V., Ross, A.J., Roth, K.A., MacGregor, G.R., Thompson, C.B. and Korsmeyer, S.J., 2001. Proapoptotic BAX and BAK: a requisite gateway to mitochondrial dysfunction and death. *Science*, *292*(5517), pp.727-730.

Wei, X.L., Wei, J.F., Li, T., Qiao, L.Y., Liu, Y.L., Huang, T. and He, S.H., 2007. Purification, characterization and potent lung lesion activity of an L-amino acid oxidase from Agkistrodon blomhoffii ussurensis snake venom.*Toxicon*, *50*(8), pp.1126-1139.

Wei, Y., Pattingre, S., Sinha, S., Bassik, M. and Levine, B., 2008. JNK1-mediated phosphorylation of Bcl-2 regulates starvation-induced autophagy.*Molecular cell*, *30*(6), pp.678-688.

Weidberg, H., Shvets, E. and Elazar, Z., 2011. Biogenesis and cargo selectivity of autophagosomes. *Annual review of biochemistry*, *80*, pp.125-156.

Weinert, T.A. and Hartwell, L.H., 1993. Cell cycle arrest of cdc mutants and specificity of the RAD9 checkpoint. *Genetics*, *134*(1), pp.63-80.

Weinert, T.A., Kiser, G.L. and Hartwell, L.H., 1994. Mitotic checkpoint genes in budding yeast and the dependence of mitosis on DNA replication and repair. *Genes & development*, *8*(6), pp.652-665.

Welch, D.R., Bisi, J.E., Miller, B.E., Conaway, D., Seftor, E.A., Yohem, K.H., Gilmore, L.B., Seftor, R.E.B., Nakajima, M. and Hendrix, M.J., 1991. Characterization of a highly invasive and spontaneously metastatic human malignant melanoma cell line. *International journal of cancer*, *47*(2), pp.227-237.

Wellner, D., 1966. Evidence for Conformational Changes in L-Amino Acid Oxidase Associated with Reversible Inactivation*. *Biochemistry*, *5*(5), pp.1585-1591.

West C. M., Davidson S. E. (2009). Measurement tools for gastrointestinal symptoms in radiation oncology. Current Opinions in Support and Palliative Care;3(1): 36e40

Williams, G.H. and Stoeber, K., 2007. Cell cycle markers in clinical oncology. *Current opinion in cell biology*, *19*(6), pp.672-679.

Wilson I.B., Harrison M.A., 1961. Turnover number of acetyl-cholinesterase. J. Biol. Chem., 236, 2292–2295.

Wilting, R.H. and Dannenberg, J.H., 2012. Epigenetic mechanisms in tumorigenesis, tumor cell heterogeneity and drug resistance. *Drug Resistance Updates*, *15*(1), pp.21-38.

Wong R. S. Y., 2011. Apoptosis in cancer: from pathogenesis to treatment. Journal of Experimental and Clinical cancer research, 30 (80), 1-14.

Xie Q., Lan G., Zhou Y., Huang J., Liang Y., Zheng W., Fu X., Fan C., Chen T. (2014). A Strategy to enhance the anticancer efficacy of X-ray radiotherapy in melanoma cells by platinum complexes, the role of ROS-mediated signalling pathways. Cancer Letters; 354: 58–67.

Yalcın, H.T., Ozen, M.O., Gocmen, B. and Nalbantsoy, A., 2014. Effect of Ottoman viper (Montivipera xanthina (Gray, 1849)) venom on various cancer cells and on microorganisms. *Cytotechnology*, *66*(1), pp.87-94.

Yang, Z., Wilkie-Grantham, R.P., Yanagi, T., Shu, C.W., Matsuzawa, S.I. and Reed, J.C., 2015. ATG4B (Autophagin-1) phosphorylation modulates autophagy. *Journal of Biological Chemistry*, *290*(44), pp.26549-26561.

Yilmaz, M., Christofori, G. and Lehembre, F., 2007. Distinct mechanisms of tumor invasion and metastasis. *Trends in molecular medicine*, *13*(12), pp.535-541.

Ylä-Anttila, P., Vihinen, H., Jokitalo, E. and Eskelinen, E.L., 2009. 3D tomography reveals connections between the phagophore and endoplasmic reticulum. *Autophagy*, *5*(8), pp.1180-1185.

Yousefi, S., Perozzo, R., Schmid, I., Ziemiecki, A., Schaffner, T., Scapozza, L., Brunner, T. and Simon, H.U., 2006. Calpain-mediated cleavage of Atg5 switches autophagy to apoptosis. *Nature cell biology*,*8*(10), pp.1124-1132.

Yu, S.W., Wang, H., Poitras, M.F., Coombs, C., Bowers, W.J., Federoff, H.J., Poirier, G.G., Dawson, T.M. and Dawson, V.L., 2002. Mediation of poly (ADP-ribose) polymerase-1-dependent cell death by apoptosis-inducing factor. *Science*, *297*(5579), pp.259-263.

Zetterberg, A. and Larsson, O., 1985. Kinetic analysis of regulatory events in G1 leading to proliferation or quiescence of Swiss 3T3 cells. *Proceedings of the National Academy of Sciences*, *82*(16), pp.5365-5369.

Zhang, L. and Wu, W.T., 2008. Isolation and characterization of ACTX-6: a cytotoxic L-amino acid oxidase from Agkistrodon acutus snake venom.*Natural product research*, *22*(6), pp.554-563.

Zhang, Y.J., Wang, J.H., Lee, W.H., Wang, Q., Liu, H., Zheng, Y.T. and Zhang, Y., 2003. Molecular characterization of Trimeresurus stejnegeri venom L-amino acid oxidase with potential anti-HIV activity. *Biochemical and biophysical research communications*, *309*(3), pp.598-604.

Zhivotovsky, B. and Orrenius, S., 2011. Calcium and cell death mechanisms: a perspective from the cell death community. *Cell calcium*,*50*(3), pp.211-221.

Zhou Q., Nakada M. T., Brooks P. C., Swenson S. D., Ritter M. R., Argounova, Arnod C., Markland F. S., 2000. Contortrostatin, a Homodimeric Disintegrin, Binds to Integrin αvβ5. Biochemical and Biophysical Research Communications**,** 267 (1), 350–55

Zitvogel, L., Casares, N., Péquignot, M.O., Chaput, N., Albert, M.L. and Kroemer, G., 2004. Immune response against dying tumor cells. *Advances in immunology*, *84*, pp.131-180.

Zor, T. and Selinger, Z., 1996. Linearization of the Bradford protein assay increases its sensitivity: theoretical and experimental studies. *Analytical biochemistry*, *236*(2), pp.302-308.

Zuloaga D.,G., Puts D.,A., Jordan C.,L., Breedlove S.,M., 2008. The role of androgen receptors in the masculinization of brain and behavior: what we've learned from the testicular feminization mutation. Horm Behav, 53(5),613–26.